


12-2015

THE TUMOR SUPPRESSOR NOTCH INHIBITS HEAD AND NECK SQUAMOUS CELL CARCINOMA (HNSCC) TUMOR GROWTH AND PROGRESSION BY MODULATING PROTO-ONCOGENES AXL AND CTNNAL1 (α -CATULIN)

Shhyam Moorthy

Shhyam Moorthy

Follow this and additional works at: https://digitalcommons.library.tmc.edu/utgsbs_dissertations

 Part of the [Biochemistry, Biophysics, and Structural Biology Commons](#), [Cancer Biology Commons](#), [Cell Biology Commons](#), and the [Medicine and Health Sciences Commons](#)

Recommended Citation

Moorthy, Shhyam and Moorthy, Shhyam, "THE TUMOR SUPPRESSOR NOTCH INHIBITS HEAD AND NECK SQUAMOUS CELL CARCINOMA (HNSCC) TUMOR GROWTH AND PROGRESSION BY MODULATING PROTO-ONCOGENES AXL AND CTNNAL1 (α -CATULIN)" (2015). *The University of Texas MD Anderson Cancer Center UTHealth Graduate School of Biomedical Sciences Dissertations and Theses (Open Access)*. 638.

https://digitalcommons.library.tmc.edu/utgsbs_dissertations/638

This Dissertation (PhD) is brought to you for free and open access by the The University of Texas MD Anderson Cancer Center UTHealth Graduate School of Biomedical Sciences at DigitalCommons@TMC. It has been accepted for inclusion in The University of Texas MD Anderson Cancer Center UTHealth Graduate School of Biomedical Sciences Dissertations and Theses (Open Access) by an authorized administrator of DigitalCommons@TMC. For more information, please contact digitalcommons@library.tmc.edu.

**THE TUMOR SUPPRESSOR NOTCH INHIBITS HEAD AND NECK SQUAMOUS
CELL CARCINOMA (HNSCC) TUMOR GROWTH AND PROGRESSION BY
MODULATING PROTO-ONCOGENES AXL AND CTNNAL1 (α -CATULIN)**

by

Shhyam Moorthy, B.S.

APPROVED:

Dr. Jeffrey N. Myers, M.D., Ph.D.
Advisory Professor

Dr. Gary E. Gallick, Ph.D.

Dr. Patrick A. Zweidler-McKay, M.D., Ph.D.

Dr. Paul Chiao, Ph.D.

Dr. Rick A. Wetsel, Ph.D.

APPROVED:

Dean, The University of Texas
Graduate School of Biomedical Sciences at Houston

**THE TUMOR SUPPRESSOR NOTCH INHIBITS HEAD AND NECK
SQUAMOUS CELL CARCINOMA (HNSCC) TUMOR GROWTH AND
PROGRESSION BY MODULATING THE EXPRESSION OF PROTO-
ONCOGENES, AXL AND CTNNAL1 (α -CATULIN)**

A

DISSERTATION

Presented to the Faculty of
The University of Texas
Health Science Center at Houston
and
The University of Texas
MD Anderson Cancer Center
Graduate School of Biomedical Sciences
in Partial Fulfillment
of the Requirements
for the Degree of

DOCTOR OF PHILOSOPHY

by

Shhyam Moorthy, B.S.
Houston, Texas

December, 2015

Abstract

**THE TUMOR SUPPRESSOR NOTCH INHIBITS HEAD AND NECK
SQUAMOUS CELL CARCINOMA (HNSCC) TUMOR GROWTH AND
PROGRESSION BY MODULATING THE EXPRESSION OF PROTO-
ONCOGENES, AXL AND CTNNAL1 (α -CATULIN)**

Shhyam Moorthy, B.S.

Advisory Professor: Dr. Jeffrey N. Myers, M.D., Ph.D.

Background: Head and Neck Squamous Cell Carcinoma (HNSCC) is the sixth most common malignancy worldwide, with roughly 300,000 cancer related deaths occurring globally each year. The survival of patients with HNSCC has not changed significantly over the past decade, leading investigators to search for promising molecular targets. To identify new treatment targets and biomarkers that could better guide therapy, we previously characterized the genomic alterations from primary HNSCC patient samples. We were among the first to discover that NOTCH1 is one of the most frequently mutated genes in this cancer type. The spectrum of inactivating NOTCH1 mutations in HNSCC suggested a tumor suppressive role for this protein; however, the mechanism of its function is currently unknown.

Procedure: We used Sanger sequencing and immunoblotting to characterize 50 well-established HNSCC cell lines as being wild-type or mutant for NOTCH1. We cloned the full length NOTCH1 receptor to restore the NOTCH signaling function in mutant cell lines and activated this pathway by culturing cells on immobilized NOTCH ligand, Jagged1,

coated plates. Clonogenic assays and competitive cell proliferation assays was used to evaluate cell growth and proliferation. CRISPR-Cas9 system was used to knock out NOTCH1 and/or NOTCH2 in wild-type cells. Tumor growth was evaluated *in vivo* in a mice orthotopic model of oral cancer. An unbiased gene expression analysis was performed to identify potential downstream targets of the NOTCH pathway. RNA-Seq data was obtained from HNSCC TCGA data and was correlated with the 120 gene expression signature obtained from cell lines. Flag-tagged constructs were used to overexpress HES2 and HES5, while shRNA's was used to knock down AXL and catulin in mutant cell lines to evaluate tumor growth.

Results: We show here that restoration of full length NOTCH1 in mutant HNSCC cell lines and activation of NOTCH signaling in wild-type cell lines significantly decreases cell growth *in vitro* and tumor growth *in vivo*. CRISPR-Cas9 knock out of NOTCH1 and NOTCH2 in wild-type HNSCC cells accelerated cell growth that was reversed by restoration of NOTCH1 in the same cell line. To evaluate the mechanism of NOTCH induced growth inhibition, we performed an unbiased microarray analysis and observed suppression of two proto-oncogenes, AXL and CTNNAL1 (α -catulin) after NOTCH1 activation, but not in its absence. In addition, genes modulated by NOTCH activation in cell lines correlated with RNA-Seq data from 498 TCGA patient tumors. Restoration of NOTCH1 in mutant cell lines significantly decreased protein expression levels of AXL and α -catulin, while CRISPR-Cas9 knock out of NOTCH1 and NOTCH2 in wild-type cells increased expression of these proto-oncogenes. Knock down of AXL and α -catulin using shRNA's abrogated tumor growth. Lastly, we show that HES2 and HES5, transcriptional

regulatory proteins induced by NOTCH signaling might be sufficient to inhibit protein expression levels of AXL and α -catulin and suppress growth.

Conclusions: For the first time, we are attributing a tumor suppressive function of NOTCH in HNSCC. We conclude that reactivation of NOTCH signaling in HNSCC inhibits tumor growth and progression. In addition, we are also providing a possible mechanism linking NOTCH1 to the decreased expression of proto-oncogenes, AXL and CTNNAL1 (α -catulin) that potentially abrogates tumor growth. This underscores the need to understand the clinical significance of the NOTCH pathway and its downstream targets, which could then be exploited for potential therapeutic strategies.

Contents	
APPROVED:	i
Abstract	iii
Dedication	xix
Acknowledgments	xx
CHAPTER 1: HEAD AND NECK SQUAMOUS CELL CARCINOMA (HNSCC) .	1
Anatomy and incidence	2
Pathogenesis	6
Treatment	8
Field cancerization	9
Sequencing studies in HNSCC.....	10
CHAPTER 2: NOTCH SIGNALING	18
Structure of NOTCH receptor	19
Structure of NOTCH ligands.....	21
NOTCH activation and regulation	24
NOTCH signaling in differentiation	29
NOTCH in cancer.....	31
NOTCH as an oncogene.....	31
NOTCH as a tumor suppressor	33
NOTCH in HNSCC.....	34
CHAPTER 3: AXL AND α-CATULIN	36
AXL.....	37
AXL in cancers.....	40
AXL in Non-small cell lung carcinoma (NSCLC).....	40
AXL in breast cancer	41
AXL in Acute Myeloid Leukemia (AML)	43
AXL in HNSCC	43
AXL inhibitors	44
CTNNAL1: α -catulin	47
CHAPTER 4: MATERIALS AND METHODS	49
Cell lines.....	50
Western Blots	51

Plasmids	52
Intracellular NOTCH1 (ICN1).....	52
CRISPR-Cas9 plasmids.....	53
NOTCH1 Full Length (NFL1)	53
Short Hairpin RNA's for AXL and α -catulin.....	54
HES2 and HES5	54
Transfections	55
Retroviral infections	56
Lentiviral infections	56
Clonogenic assays	56
Quantitative Real Time PCR (qRT-PCR)	57
Jagged1 and Fc immobilization.....	58
Competitive Cell Proliferation Assay	59
Cell Cycle Analysis	60
Senescence	60
Orthotopic Mice injections	60
Unbiased gene expression analysis	61
Antibodies	63
Statistical Analysis	63
CHAPTER 5: ACTIVATION OF NOTCH SIGNALING INHIBITS GROWTH ..	64
Chapter 5.1: NOTCH1 mutational status in HNSCC cell lines	65
Chapter 5.2: Activation of NOTCH1 in mutant HNSCC cell lines is detrimental to cell growth.....	68
Chapter 5.3: NOTCH1 activation appears to induce senescence and G1 growth arrest	73
Chapter 5.4: NOTCH1 or NOTCH2 is possibly sufficient to inhibit cell growth	77
Chapter 5.5: Restoration of full-length NOTCH1 is sufficient to inhibit cell growth ..	79
Chapter 5.5: Activation of the NOTCH signaling pathway in wild-type cell lines inhibits cell growth.....	88
Chapter 5.6: Restoration of NOTCH signaling in mutant HNSCC cell lines inhibits <i>in vivo</i> tumorigenicity	101
Chapter 5.7: Inhibition of NOTCH signaling enhances tumor growth <i>in vivo</i>	105
Discussion	109

CHAPTER 6: DOWNSSTREAM EFFECTORS OF NOTCH MEDIATED GROWTH INHIBITION	112
Chapter 6.1: AXL and CTNNAL1 (α -catulin) are downstream of NOTCH signaling 113	
Chapter 6.2: NOTCH1 modulates AXL and CTNNAL1 (α -catulin) at the protein level	125
Chapter 6.3: HES2 and HES5 may be sufficient to modulate AXL and α -catulin	131
Chapter 6.4: The 120 <i>in vitro</i> gene signature corresponds with NOTCH activation status in patients	136
Discussion	150
CHAPTER 7: INHIBITION OF AXL AND α-CATULIN MODULATES CELL GROWTH.....	153
Chapter 7.1: Knocking down AXL and α -catulin inhibits cell growth and tumor formation	154
Chapter 7.2: HES2 and HES5 might be sufficient to inhibit cell growth	163
Discussion	166
CHAPTER 8: DISCUSSION AND FUTURE DIRECTIONS	168
Activation of NOTCH signaling inhibits growth.....	172
NOTCH and senescence.....	172
NOTCH and differentiation	173
Roles of NOTCH1 and NOTCH2	175
Identification of downstream effectors of the NOTCH signaling pathway	179
Non-canonical NOTCH signaling	185
Canonical transcriptional modulation of NOTCH targets	186
Gene expression in TCGA HNSCC patient tumors	193
Inhibition of AXL and α -catulin modulates cell growth.....	195
HES2 and HES5 inhibit cell growth.....	197
CHAPTER 9: CONCLUSIONS	201
Appendix	204
Bibliography	255
Vita	297

List of figures

Figure 1: Anatomy of Head and Neck Squamous Cell Carcinoma (HNSCC). Permission obtained from Algiris, A., Karamouzis, M.V., Raben, D., and Ferris, R.L. (2008). Lancet. 371 (9625): 1695-709. (Argiris et al., 2008).....	4
Figure 2: Molecular pathogenesis of HNSCC. Permission obtained from Califano, J., van der Riet, P., Westra, W., Nawroz, H., Clayman, G., Piantadosi, S., Corio, R., Lee, D., Greenberg, B., Koch, W., and Sidransky, D. (1996). Cancer Research. 56(11): 2488-92. (Califano et al., 1996)	6
Figure 3: Frequent somatic mutations in HNSCC by whole exome sequencing. Permission obtained from Agrawal, N., Frederick, M. J., Pickering, C. R., Bettegowda, C., Chang, K., Li, R. J., Myers, J. N. (2011). Science, 333(6046), 1154-1157. (Agrawal et al., 2011).	13
Figure 4: Frequent somatic mutations in HNSCC. Permission obtained from Stransky, N., et al., (2011) Science.. 333(6046): p. 1157-60 (Stransky et al., 2011)	14
Figure 5: Structure of NOTCH family receptors in drosophila and mammalian systems. Permission obtained from Kopan, R. and M.X. Ilagan. (2009). Cell. 137(2): p. 216-33. (Kopan & Ilagan, 2009)	20
Figure 6: Structure of NOTCH ligands in drosophila and mammalian systems. Permission obtained from Kopan, R. and M.X. Ilagan. (2009). Cell. 137(2): p. 216-33. (Kopan & Ilagan, 2009)	23
Figure 7: NOTCH signaling pathway. Permission obtained from Kopan, R. and M.X. Ilagan. (2009). Cell. 137(2): p. 216-33. (Kopan & Ilagan, 2009).....	27
Figure 8: NOTCH1 protein expression levels in HNSCC cell lines	67

Figure 9: Retroviral constructs of ICN1, ICN2 and NFL1	70
Figure 10: Intracellular NOTCH1 is disadvantageous to the growth of mutant HNSCC cells.	71
Figure 11: ICN1 infected mutant HN31 cells are smaller and rounder and some have a flattened package-like morphology compared to cells infected with the empty vector MigR1.	72
Figure 12: Mutant HNSCC cells HN31 undergoes senescence after restoring the activated form of NOTCH1 (ICN1).....	74
Figure 13: Induction of p21 (a marker for senescence and cell cycle arrest) in HN31 cells infected with ICN1 but not MigR1 at two different time points (D3= Day 3 post infection and D5=Day 5 post infection)	75
Figure 14: Activated NOTCH1 or NOTCH2 is sufficient to inhibit growth of HNSCC cell lines	78
Figure 15: The fraction of mutant cells restored with NFL1 decreases progressively compared to cells infected with the empty vector. UM47 mutant cells infected with NFL1 is selected against a mixed population of NFL1 and non-NFL1 expressing cells while cells infected with MigR1 remains steady through the 23 day time period.....	82
Figure 16: The fraction of mutant cells restored with NFL1 decreases progressively compared to cells infected with the empty vector. HN4 mutant cells infected with NFL1 is selected against a mixed population of NFL1 and non-NFL1 expressing cells while cells infected with MigR1 remains steady through the 23 day time period.....	83
Figure 17: The fraction of mutant cells restored with NFL1 decreases progressively compared to cells infected with the empty vector. HN31 mutant cells infected with NFL1	

is selected against a mixed population of NFL1 and non-NFL1 expressing cells while cells infected with MigR1 remains steady through the 23 day time period.....	84
Figure 18: Restoration of NOTCH1 inhibits cell growth. Inhibition in the number of colonies of mutant cells after restoration with NFL1 and culture on Jagged1. (a: quantitation of clonogenic assay, b: crystal violet staining of colonies)	85
Figure 19: NOTCH1 is activated only in mutant cells infected with NFL1 but not MigR1. Restoration of NFL1 in mutant cell lines induces cleavage of NOTCH1 when cultured on Jagged1 but not on Fc or uncoated plates.	86
Figure 20: HN31, HN4 and UMSCC22A mutant HNSCC cells undergo senescence after restoring NFL1 and culturing on Jagged1	87
Figure 21: Morphology change and senescence when NOTCH1 wild-type are cultured on Jagged1. Culture of wild-type cell lines on Jagged1 shows small, rounded and growth inhibited colonies, some of which undergo senescence compared to cells cultured on Fc.	92
Figure 22: Protein expression of Total-NOTCH1 and cleaved NOTCH1: Western blot depicting total NOTCH1 (Tm-NOTCH1) in wild-type and mutant cell lines and cleaved NOTCH1 (cl-NOTCH1) expression in wild-type cell lines cultured on Jagged1	93
Figure 23: Wild-type cell lines cultured on Jagged1 are significantly growth inhibited ..	94
Figure 24: Inhibition of NOTCH signaling using γ -secretase inhibitor reverses NOTCH mediated growth suppression.	95
Figure 25: dnMAML1 reversed Jagged1 mediated growth inhibition	96
Figure 26: CRISPR-Cas9 knockout of NOTCH1 (NOTCH1 KO), NOTCH2 (NOTCH2 KO) or both	97

Figure 27: Knocking out both NOTCH and NOTCH2 relieves Jagged1 mediated growth suppression. KO: Knockout	98
Figure 28: Restoration of NFL1 in the double knock out cell line activates NOTCH signaling: CRISPR-Cas9 double knockout cell line PJA34 shows activation of NOTCH signaling after restoration with NFL1 and culturing cells on Jagged. KO: Knockout	99
Figure 29: NOTCH signaling is necessary and sufficient to modulate cell growth. CRISPR-Cas9 NOTCH1 and NOTCH2 double knockout cell line PJA 34 promotes growth on Jagged1 and Fc that is inhibited after restoration with NFL1.	100
Figure 30: Restoration of NOTCH signaling in mutant HNSCC cell lines inhibits tumor growth (a) and increases overall survival (b) in a xenograft orthotopic model of oral cancer	103
Figure 31: NFL1 infected UM47 tumor xenografts appear more differentiated. Mutant UM47 infected with NFL1 (a, c) grew slowly in mouse tongues compared to UM47 infected with control MigR1. (b, d). Anti-total NOTCH 1 staining (brown) of NFL1-infected (a) or MigR1 infected (b) tumors. Growth of NFL1-infected tumors was more organized (c) and had keratin pearls (arrows) compared to MigR1 infected tumors, apparent after H&E stain.....	104
Figure 32: NOTCH signaling may be necessary for inhibiting tumor growth.	107
Figure 33: Possibility of cis-inhibition when PJA34 and 183 cells are overexpressed with Jagged1	108
Figure 34: Heat-map of 277 differentially expressed genes having treatment effects but not cell lines effects. Top green bar: control samples. Top orange bar: Jagged1 treated samples.....	123

Figure 35: Heat map of 1571 differentially expressed genes that have both treatment and cell line effects. Top green bar: control samples. Top orange bar: Jagged1 treated samples	124
Figure 36: Activated NOTCH1 (ICN1) is sufficient to suppress AXL and α -catulin. ..	127
Figure 37: Restoration of full length NOTCH1 (NFL1) in the mutant cell lines: HN31, UM22A and UMSCC47 after activation with Jagged1 suppress AXL and α -catulin	128
Figure 38: Inhibition of NOTCH signaling using dnMAML1 reverses Jagged1 induced suppression of AXL and α -catulin.	129
Figure 39: NOTCH signaling is necessary and sufficient to inhibit AXL and catulin: Knocking out NOTCH signaling using the CRISPR-Cas9 system induces AXL and α -catulin which is reversed when the same cell line is restored with NFL1.	130
Figure 40: Modulation of HES and HEY members after restoration of NOTCH signaling in HN31 cells and culturing on Jagged1 for 20h	133
Figure 41: HES2 and HES5 might be sufficient to modular protein expression of AXL, p-AXL, Gad6 and α -catulin. Overexpressing HES2 and HES5 using Flag tagged constructs in the mutant cell line HN31 inhibits protein expression of proto-oncogenes AXL and α -catulin.	134
Figure 42: Relative expression levels of Flag-Tag, HES5, AXL, p-AXL, α -catulin and Gas6 from the western blot shown in Figure 41	135
Figure 43: Heat-map of the 120 in vitro gene signature in Oral Cavity TCGA tumors .	140
Figure 44: Heat-map of the 120 in vitro gene signature in Laryngeal/Hyopharyngeal TCGA tumors.....	142

Figure 45: Unsupervised clustering of 498 TCGA Oral Cavity (OC) tumors based on 20,000 genes.....	144
Figure 46: Unsupervised clustering of 498 TCGA Laryngeal/Hypopharyngeal (LH) tumors based on 20,000 genes	145
Figure 47: Knockdown of AXL and α -catulin in wild-type cell lines 183 and PJA34 using shRNA's.....	157
Figure 48: Knockdown of AXL and α -catulin in mutant cell lines UM22A and HN31 using shRNA's	158
Figure 49: Quantitation of the western blots after knocking out AXL and catulin in wild-type cell lines 183 (above) and PJA 34 (below).	159
Figure 50: Quantitation of the western blots after knocking out AXL and catulin in mutant cell lines UM22A (above) and HN31 (below).	160
Figure 51: Clonogenic assay in wild-type (PJA34 and 183) and mutant cell lines (UM22A and HN31). Knocking down AXL (shAXL) and α -catulin (shCAT) inhibits cell growth in a colony forming clonogenic assay	161
Figure 52: AXL and α -catulin modulates in vivo tumor formation and overall survival. Knocking down AXL and α -catulin using shRNA's in a mutant cell line significantly inhibits tumor growth and increases overall survival	162
Figure 53: HES2 and HES5 are sufficient to inhibit cell growth	165
Figure 54: Basal NUMB expression in wild-type and mutant HNSCC cell line.....	171
Figure 55: Jagged1 expression in wild-type and mutant HNSCC cell lines	171
Figure 56: ICN1 inhibits p63 expression	182

Figure 57: Activation of NOTCH signaling by Jagged1 slightly inhibits protein expression of Δ NP63	183
Figure 58: NOTCH1 and TP63 mutations tend to be mutually exclusive	184
Figure 59: Activated NOTCH1 increases gene expression of HES5	188
Figure 60: HES2 and HES5 don't seem to transcriptionally modulate levels of AXL or CTNNAL1.	190
Figure 61: Promoter sequence of AXL lacks N-box or E-box motifs suggesting that HES and HEY might not directly transcriptionally regulate AXL gene expression.	191
Figure 62: Promoter sequence of CTNNAL1 lacking N-box and E-box binding sites. .	192
Figure 63: Possible mechanistic model of NOTCH mediated growth suppression.....	200

List of Appendices

Appendix 1: Differentially expressed genes after activation of NOTCH signaling in PJA34 and 183 cells. Green highlighted "Significance" cells show genes modulated based on treatment, independent of cell lines. Orange highlighted "Significance" cells show genes modulated based on treatment and cell lines	205
Appendix 2: Correlation heat-map in the Oral Cavity group	247
Appendix 3: Histogram of p-values testing Cluster 1 versus Cluster 2 in the Oral Cavity group	248
Appendix 4: Ingenuity Pathway Analysis of significantly modulated pathways after NOTCH activation by Jagged1 in cell lines	249

List of Tables

Table 1: Core components of the NOTCH signaling pathway in Drosophila and mammals.	28
Table 2: HNSCC cell lines. LN: Lymph Node, OC: Oral Cancer, HP: Hypopharyngeal, OP: Oropharyngeal, L: Lungs	51
Table 3: Sample description.....	61
Table 4: Antibodies description	63
Table 5: NOTCH1 status in HNSCC cell lines	67
Table 6: ICN1 cells are arrested in the G1 phase of the cell cycle.	76
Table 7: Top 120 genes modulates when NOTCH signaling is activated. (Red= upregulates, Green= Downregulated when treated with Jagged1)	121
Table 8: Ingenuity Pathway Analysis of significantly modulated pathways when NOTCH is activated in wild-type cell lines PJA34 and 183. (Red= Genes Upregulated by NOTCH, Green= Genes Downregulated by NOTCH).	122
Table 9: Total number of Oral Cavity (OC) patients in each cluster corresponding to NOTCH1 mutational status. Shown in parenthesis are expected numbers based on Chi-Squared test.....	141
Table 10: Total number of genes in each cluster of Oral Cavity (OC) patients corresponding to modulation by Jagged1 in cell lines. Shown in parenthesis are expected numbers based on Chi-Squared test.	141

Table 11: Total number of Laryngeal/Hypopharyngeal (LH) patients in each cluster corresponding to NOTCH1 mutational status. Shown in parenthesis are expected numbers based on Chi-Squared test	143
Table 12: Total number of Laryngeal/Hypopharyngeal (LH) patients in each cluster corresponding to NOTCH1 mutational status. Shown in parenthesis are expected numbers based on Chi-Squared test	143
Table 13: Clustering of genes modulated in both tumor sites corresponding to the genes clustered in cell lines	149

Dedication

This thesis is dedicated to my Mom and Dad who have always showered me with their unconditional love and have been a source of tremendous determination and will power, supporting me in all my endeavors.

Acknowledgments

Five years of graduate school wouldn't have been possible without the support and blessings of mentors, advisors, family and friends

First and foremost, I'd like to thank the University of Texas Graduate School of Biomedical Sciences and M.D. Anderson Cancer Center for accepting me giving me all the support during my journey through the Ph.D. program.

My heartfelt and deepest gratitude goes to Dr. Jeffrey Myers who humbly opened the doors of his lab for my training. Dr. Myers has not only been a great mentor, but also a role model from whom I am often motivated to pursue cancer research for the greater cause of curing patients. I was very fortunate to be mentored by one of the most well accomplished physician-scientists in the country. I not only learned the fundamentals of bench work, but Dr. Myers often steered me in a way that during every experiment I performed, I had in mind the bigger picture of how we as scientists impact the clinical realm of therapy.

I am also indebted to Dr. Mitchell Frederick who has guided me through every step of my training. His dedication and hard work towards research has often motivated me as a graduate student. Dr. Frederick taught me how to raise from downfalls and how to modestly embrace the highs and lows of research work. His composure and patience has always inspired me during the different stages of my training. There have been times of excitement and frustrations during which I have often barged into Dr. Frederick's office and was always greeted by his calm and modest nature.

I was fortunate to have a great committee who always supported and guided me through all my committee meetings in the past five years. I sincerely thank Dr. Gary Gallick, Dr. Patrick Zweidler-McKay, Dr. Paul Chiao and Dr. Rick Wetsel for being excellent mentors and guiding me through my projects with their constructive feedback. Dr. Rick Wetsel and Dr. Gary Gallick kindly allowed me to rotate in their respective labs when I first started graduate school giving me a warm welcome into the research realm. During my first week of graduate school, it was Dr. Rick Westel's lab that give me exposure to the basics of stem cells and induced pluripotent stem cells that drove my passion to research and stabilized my decision to pursue a Ph.D. Dr. Gallick was not only my rotation mentor and committee member, but he also taught me the fundamentals of cancer biology and cancer metastasis in his classes/seminars. His lab gave me the first exposure to research in cancer therapy by targeting the IGF receptors in prostate cancer that motivated me to further my education in targeted therapy. Dr. Patrick Zweidler-McKay was not only a committee member, but also our closest collaborator and often called "NOTCH expert" having guided us at every step of investigating the role of NOTCH signaling in Head and Neck Cancers through his expertise in hematopoietic malignancies. Special thanks to members of Dr. Zwediler-McKay's lab; Drs. Sankarnarayan Kannan and Ritta Nolo for readily providing me with cells and plasmids whenever needed. Dr. Paul Chiao often welcomed me to his office with open doors and has many times given me positive feedback during my candidacy exam and my committee meetings. His guidance during my candidacy exam made me cross one of the major milestone of the Ph.D. program.

Members of the Myers lab whom I often call the lab family have been great support during my training. Special thanks to current and former Myers lab members that include: Samar Jasser, Ameeta Patel, Mei Zhao, Rami Saade, Qiuli Li, Jiping Wang, Noriaki Tanaka, Curtis Pickering and David Neskey. In addition, I want to thank all the visiting scientists and former lab members who have kept the lab environment light and happy during times of stress.

I don't have words to express my gratitude to my Dad and Mom for their unconditional love and support throughout my education. My Dad, Mr. Srinivasan Moorthy and Mom, Mrs. Padma Moorthy are my greatest role models. I have learned to work hard and push myself beyond limits from my Dad. My Dad always taught me not to succumb to failures but to raise and face them to emerge successfully. My Mom has been great support in pursuing whatever dream I had. I often regard my Mom as my best friend with whom I have poured all my stress, frustrations, happiness and joy at all stages of my education from primary to graduate school. I thank my Dad and Mom for all the freedom they give me to achieve anything I want.

Finally, I thank God for the will power and confidence through this educational journey in molding me into a successful doctorate

CHAPTER 1: HEAD AND NECK SQUAMOUS CELL CARCINOMA (HNSCC)

Chapter 1: Head and Neck Squamous Cell Carcinoma (HNSCC)

Anatomy and incidence

Head and Neck cancers is a broad term encompassing cancers that arise in the upper aerodigestive tract and are usually localized to the oral cavity, oropharynx, larynx, hypopharynx, nasopharynx, paranasal sinuses and nasal cavity (Argiris, Karamouzis, Raben, & Ferris, 2008) (Figure 1). These cancers usually arise from the squamous epithelial cells that reside in the moist surfaces of the mucosal areas of the head and neck region. Thus, most head and neck cancers are squamous in nature giving it the term Head and Neck Squamous Cell Carcinomas (HNSCC). Head and neck cancers can also arise from different cell types, 90% of head and neck cancers are squamous cell carcinomas. Approximately 650,000 new cases and 350,000 HNSCC related deaths occur each year (Torre et al., 2015). HNSCC's in the oral cavity is very common worldwide. Regions of high prevalence of oral cancers include Melanesia, South-central Asia, Eastern and Western Europe, and Southern Africa (F. Bray, Sankila, Ferlay, & Parkin, 2002). In the United States alone, 45,780 new cases and 8,650 head and neck cancer-related deaths occurred this year (Argiris et al., 2008). The approximate age for diagnosis is in a patient's early 60's. These cancers are predominant in the male population. According to the Surveillance Epidemiology and End Results (SEER) database, the 5-year survival for all stages combined is about 60%.

Tobacco and alcohol consumption have been attributed as the major risk factors of HNSCC that is exacerbated when combined (Blot et al., 1988; Hashibe et al., 2006; Tuyns et al., 1988). Increased risk of HNSCC has been associated with polymorphisms in certain enzymes that have the ability to metabolize alcohol and tobacco (Hashibe et al.,

2006). In parts of Southeast Asia, there is high incidence of oral cancers associated with chewing of betel quid (Proia, Paszkiewicz, Nasca, Franke, & Pauly, 2006).

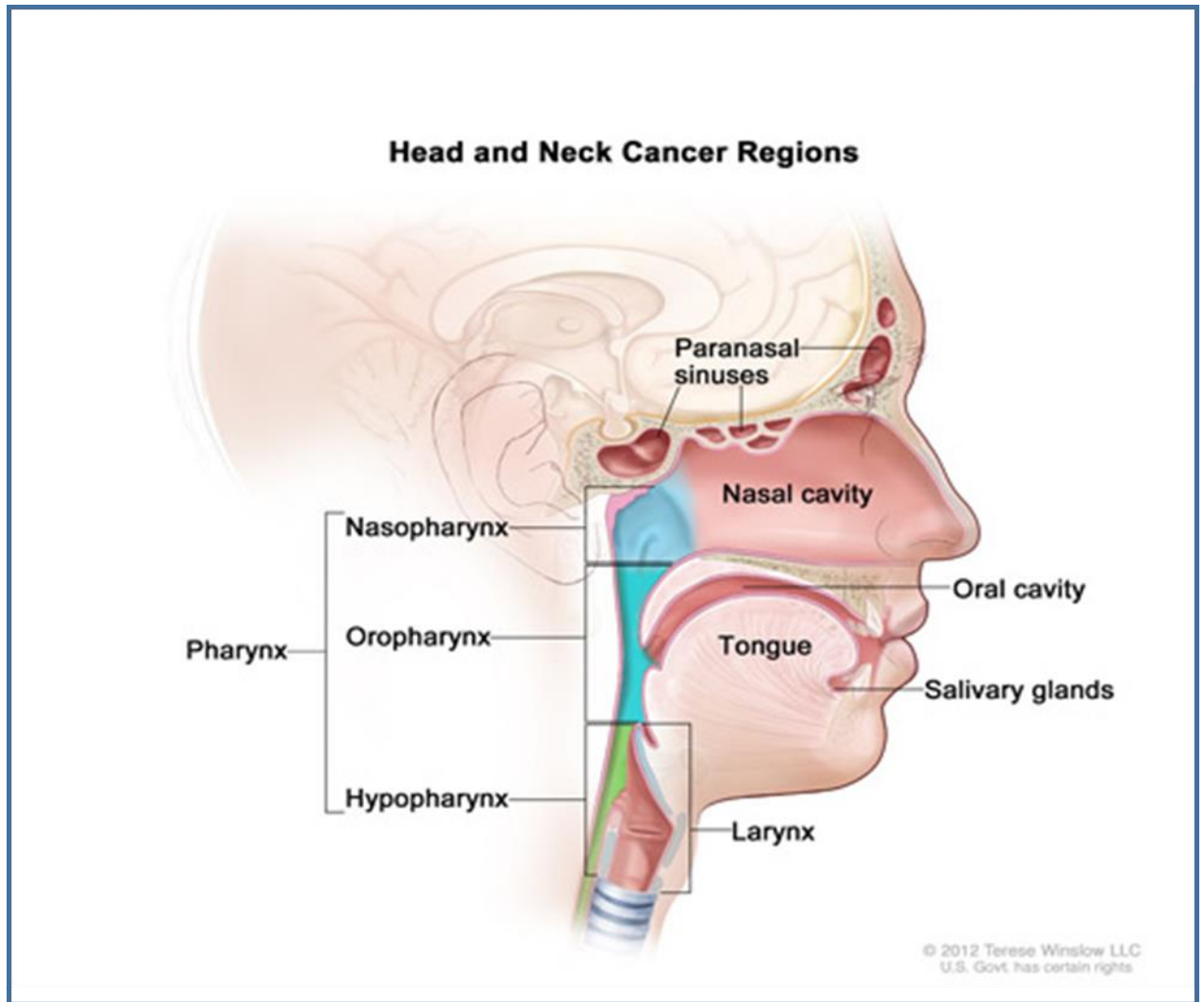


Figure 1: Anatomy of Head and Neck Squamous Cell Carcinoma (HNSCC). Permission obtained from Argiris, A., Karamouzis, M.V., Raben, D., and Ferris, R.L. (2008). Lancet. 371 (9625): 1695-709. (Argiris et al., 2008)

The risk of HNSCC in individuals with certain cancer susceptibility has shown to be increased. These include hereditary non-polyposis colorectal cancer, Li-Fraumeni syndrome, Fanconi's anaemia, and ataxia telangiectasia (Foulkes et al., 1996; Trizna & Schantz, 1992). Besides tobacco and alcohol, recently, the Human Papilloma Virus (HPV)- HPV16 and HPV18 has been identified as causal factor for HNSCC (G. D'Souza et al., 2007). It has been reported that approximately 25% of HNSCC's contain HPV genomic DNA (Kreimer, Clifford, Boyle, & Franceschi, 2005). In terms of anatomic regions HPV causes HNSCC predominantly in the tonsils and base of tongue within the oropharynx and much less in the oral cavity and larynx (Hobbs et al., 2006). Although not completely mutually exclusive, HPV related HNSCC has been observed frequently in individuals without exposure to tobacco or alcohol and individuals who are immunosuppressed. HNSCC of this type is poorly differentiated and have the tendency to exhibit a basal cell histology (G. D'Souza et al., 2007). E6 and E7 viral oncoproteins have the ability to inactivate tumor suppressor genes such as p53 and pRb thus mediating their carcinogenic effects (Munger & Howley, 2002). HPV positive and negative tumors show differences in their gene expression patterns (Slebos et al., 2006). HPV status can be an important biomarker for prevention, treatment and prognosis. HPV positive tumors have better response to therapy than HPV negative tumors (Califano et al., 1996). Furthermore, they are more susceptible to immune surveillance than HPV negative tumors. Lastly, vaccination against HPV has shown efficacy in preventing cervical cancer. This might also prove useful for HPV positive HNSCC (G. D'Souza & Dempsey, 2011).

Pathogenesis

HNSCC is a heterogeneous disease whose development is governed by diverse genetic events leading to inactivation of tumor-suppressor genes and/or activation of proto-oncogenes (Figure 2).

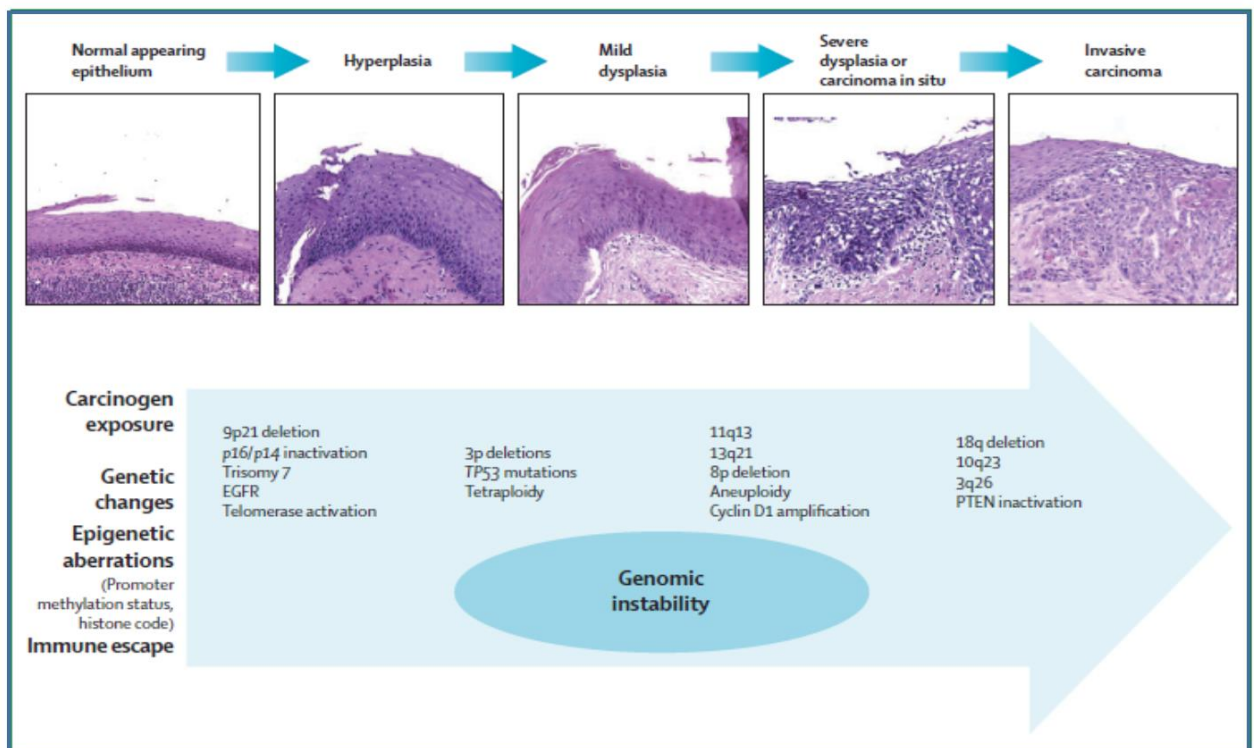


Figure 2: Molecular pathogenesis of HNSCC. Permission obtained from Califano, J., van der Riet, P., Westra, W., Nawroz, H., Clayman, G., Piantadosi, S., Corio, R., Lee, D., Greenberg, B., Koch, W., and Sidransky, D. (1996). *Cancer Research*. 56(11): 2488-92. (Califano et al., 1996)

HNSCC's arise from a premalignant progenitor after which certain clonal populations accumulate genetic alterations that progress to invasive malignancy (Califano et al., 1996; Califano et al., 2000). These genetic alterations include somatic mutations, insertions, deletions, promoter methylation and gene amplifications that result in loss of tumor suppressor genes and/or activation of oncogenes. Califano et al. (Califano et al., 2000) used PCR based microsatellite analysis to identify genetic alterations at different histopathological stages of progression of the lesion. The most common genetic alteration seen in HNSCC is the loss of 9p21, which is found in 70-80% of the cases seen in squamous dysplasia and HNSCC (Califano et al., 2000; van der Riet et al., 1994). Loss of Heterozygosity (LOH) of 9p21 is an early event in squamous neoplasia and has also been in pre-neoplastic lesions (van der Riet et al., 1994). The CDKN2A gene located at 9p21 encodes p16 and p14^{ARF}, which are responsible for G1 cell cycle regulation and MDM2-mediated degradation of p53. Promoter methylation and homozygous deletions often inactivate p16 (Reed et al., 1996). Although the highest LOH frequency in benign squamous neoplastic lesions is 9p21, there is also LOH at 3p21 and 17p13 to a lesser extent (Califano et al., 1996). The loss of 3p is considered another major event that allows the benign hyperplasia to progress towards dysplasia (Hogg et al., 2002). For example, in the region 3p14, the exomic deletion of the FHIT gene (fragile histidine triad gene), a tumor suppressor gene, has been shown in HNSCC and other tumor types (Boyle et al., 1993; Hogg et al., 2002; Mao, Fan, Lotan, & Hong, 1996). The most frequently mutated gene TP53, located on 17p is mutated in over 80% of HNSCC ("TCGA Releases Head and Neck Cancer Data," 2015). These mutations begin to appear during the progression of hyperplasia to dysplasia but most of these mutations occur late in the

progression towards invasive carcinoma (Boyle et al., 1993). Overexpression of cyclin D1 is often due to amplification of 11q13 has been seen in 30-60% of HNSCC and has been associated with lymph node metastasis and poor overall survival (Meredith et al., 1995; Michalides et al., 1995). Most transcriptional alterations in head and neck cancer pathogenesis occur during the transition from normal mucosa to premalignant lesions rather than premalignant lesions to invasive carcinomas (Ha et al., 2003). Amplification of the epidermal growth factor receptor (EGFR) is seen 90% of cases of HNSCC (Grandis & Tweardy, 1993). The EGFR, a receptor tyrosine kinase, binds to its ligand EGF and activates a molecular cascade that involves modulation of molecules involved with cell proliferation, growth, angiogenesis, apoptosis and metastatic potential (Rubin Grandis et al., 1998). Many studies have shown poor prognosis of cases with overexpression of EGFR. Targeting this receptor has been exploited and been successful for therapeutic purposes (Karamouzis, Grandis, & Argiris, 2007).

Treatment

Surgery is used as a conventional treatment strategy for HNSCC. This, however, is limited by tumor volume and cosmetic and functional concerns. For small tumors located in the oral cavity or pharynx, surgical excision is preferred with preservation of the functionality of the organ and good overall prognosis. Techniques such as microsurgical treatment or robotic techniques have shown significant progress. These techniques integrated with high-resolution magnified optics will likely have significant benefit (Ambrosch, 2007; Lefebvre, 2006).

In addition to surgery, radiotherapy is an integral part of primary or adjuvant HNSCC treatment. Radiation therapy for HNSCC is typically administered daily at a 2.0

Gy dose for 5 days for a total of 70 Gy over a 7-week period. Post-operatively, radiation doses varying from 60-65 Gy are typically prescribed (Argiris et al., 2008). Clinical results from radiation therapy are very promising, and this is a major standard of care for tumors of the oropharynx, hypopharynx, and larynx. Nevertheless, but its use is associated with significant sequelae and occasional complications in the peri-treatment period and many years later due to the progressive effects on tissue vasculature and fibrosis.(Konski et al., 2006).

Chemotherapy plays an important role in HNSCC treatment. Platinum compounds, anti-metabolites, and taxanes have shown effectiveness in treating HNSCC. Cisplatin, a platinum based compound is regarded as the standard chemotherapeutic agent in combination with surgery and/or radiation. Like cisplatin, carboplatin is also used but is less effective as a combination regimen (Colevas, 2006). Taxane based combinations have been tested successfully in induction and/or concomitant treatment of locally advanced HNSCC. Cetuximab, an antibody against EGFR, was the first targeted agent introduced in chemotherapy (Grandis & Tweardy, 1993). The combination of EGFR inhibitors and other target agents (such as angiogenesis inhibitors) has surfaced as novel treatment strategies and their effectiveness in combination with surgery and/or radiotherapy is under investigation.

Field cancerization

Slaughter and colleagues first described the concept of field cancerization when they observed multiple independent tumors surrounding the mucosa adjacent to the HNSCC (Slaughter, Southwick, & Smejkal, 1953). Slaughter suggested that there are large areas in the aerodigestive tract mucosa affected by long term exposure to

carcinogens that results in genetic events independent of the primary tumor site resulting in genetically altered fields. Techniques such as chromosome X inactivation, microsatellite analysis and p53 mutational status have confirmed the presence of these alterations neighboring the primary HNSCC site, confirming Slaughter's concept of field cancerization (Califano et al., 1996). Although these independent genetic lesions result in satellite tumor sites, there is evidence that tumors arising in these fields are clonally related and arise from a common neoplastic progenitor. It is possible that these transformed cells might have micro-metastasized across the aerodigestive tract. The clinical implication of a field is that it may be a potential source of local recurrence and second primary tumors after surgical resection of the primary tumor. The genetic constitution of the field is currently not completely understood but in recent studies that stained for p53, genetic changes at chromosome 9p, decreased Keratin 4 expression and decreased cornulin expression are potential biomarkers with this regard (Karamouzis et al., 2007).

Sequencing studies in HNSCC

Cancer, in general, arises through accumulation of genetic and epi-genetic changes often caused due to carcinogen exposure. This induces alterations in signaling pathways that result in cancer related phenotypes such as unlimited replicative potential, self-sufficiency in growth signals, insensitivity to anti-growth signals, ability to evade apoptosis, invasion and metastasis, and angiogenesis which has been well summarized by Hanahan and Weinberg (Hanahan & Weinberg, 2011). The accumulation of these aberrant pathways is often secondary to a lifetime of environmental exposure to carcinogens such as tobacco and alcohol that results in enhanced proliferation,

dedifferentiation, immortalization and loss of cell death of epithelial cells in the mucosa. Therefore, a deeper understanding of the molecular biology of HNSCC is needed to enhance the development of therapeutic approaches. Investigators have identified several critical genes important in HNSCC progression. These include TP53(Poeta et al., 2009), CDKN2A(Demokan et al., 2012), Cyclin D1(Papadimitrakopoulou et al., 2001), PIK3CA(Murugan, Hong, Fukui, Munirajan, & Tsuchida, 2008), HRAS and EGFR(Bonner et al., 2010). The approaches used for the identification of these genes involved fluorescence in situ hybridization (FISH), immunohistochemistry (IHC), promoter methylation studies, histone modification analysis and copy number variations from extracted tumors compared to the surrounding normal tissues. Despite efforts to identify biomarkers in HNSCC, no prognostic marker has been able to predict the response to treatments. On the contrary, other tumor types have drug-able targets and specific genetic alterations predictive of treatment outcomes (Rothenberg & Ellisen, 2012). These include HER2 amplifications in breast cancers, BRAF mutations in melanoma, and JAK2 in hematopoietic malignances. In breast cancers, PIK3CA is mutated at a frequency of 30%, while FGFR2, which is mutated in 20% of endometrial and lung cancers, has been investigated as a target in clinical trials (Thariat et al., 2015). Until 2011, the mutational status in HNSCC was not completely understood. Identification of targetable genes by next generation sequencing (NGS) opened new avenues for personalized cancer therapy.

In order to gain a better understanding of the genetic alterations in HSNCC, Aggarwal and colleagues (Agrawal et al., 2011) (Figure 3) and Stransky and colleagues (Stransky et al., 2011) (Figure 4) used high throughput next generation sequencing to

analyze the genomic alterations found in HNSCC. Both groups performed whole exome sequencing from 32 and 74 primary tumors, respectively and compared the sequence to the corresponding normal DNA of the same patient (Figures 3 and 4). Agarwal and colleagues (Agrawal et al., 2011) used the Illumina or SOLiD platform to sequence the DNA with coverage of 77 or 40-fold respectively and approximately 90% of the targeted bases were represented by at least 10 reads in these platforms. They identified 911 somatic mutations in 725 genes among the 32 tumors. Furthermore, Sanger and/or 454 sequencing was used to validate these findings.

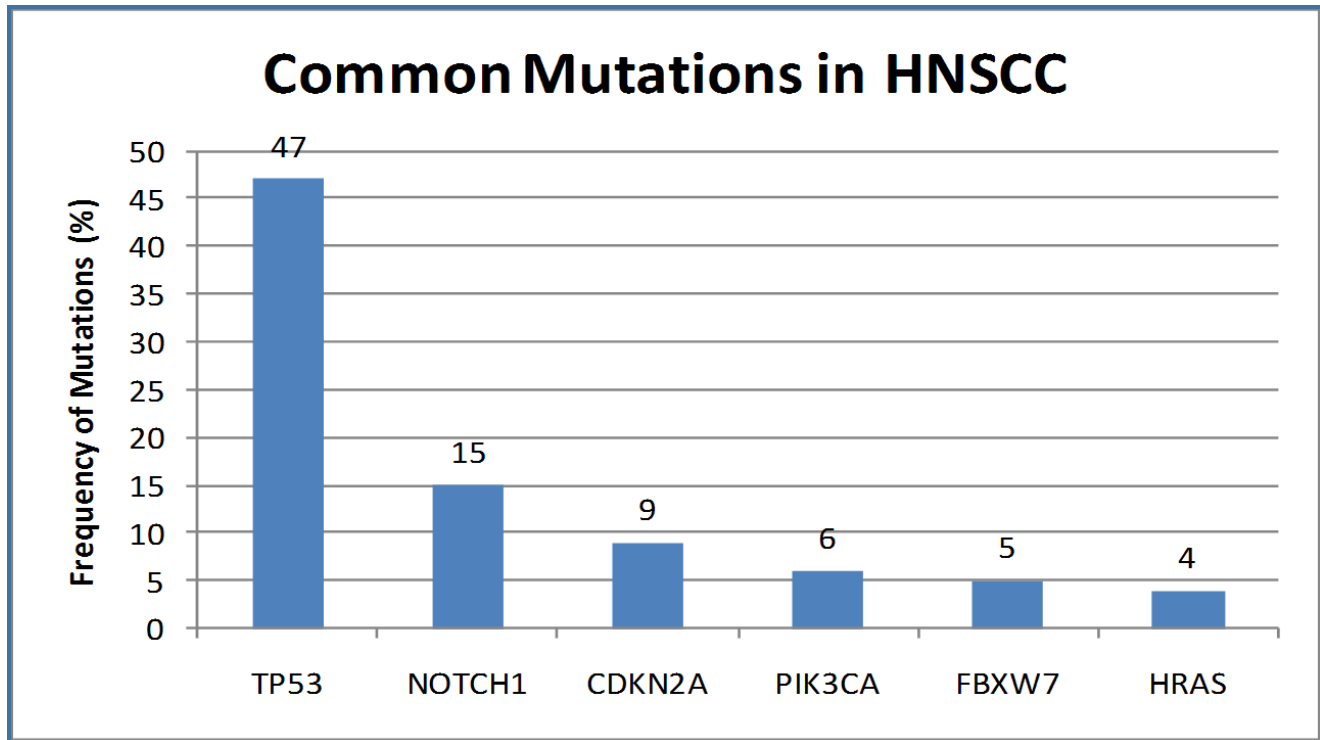


*Figure 3: Frequent somatic mutations in HNSCC by whole exome sequencing.
Permission obtained from Agrawal, N., Frederick, M. J., Pickering, C. R., Bettegowda, C., Chang, K., Li, R. J., Myers, J. N. (2011). Science, 333(6046), 1154-1157. (Agrawal et al., 2011).*

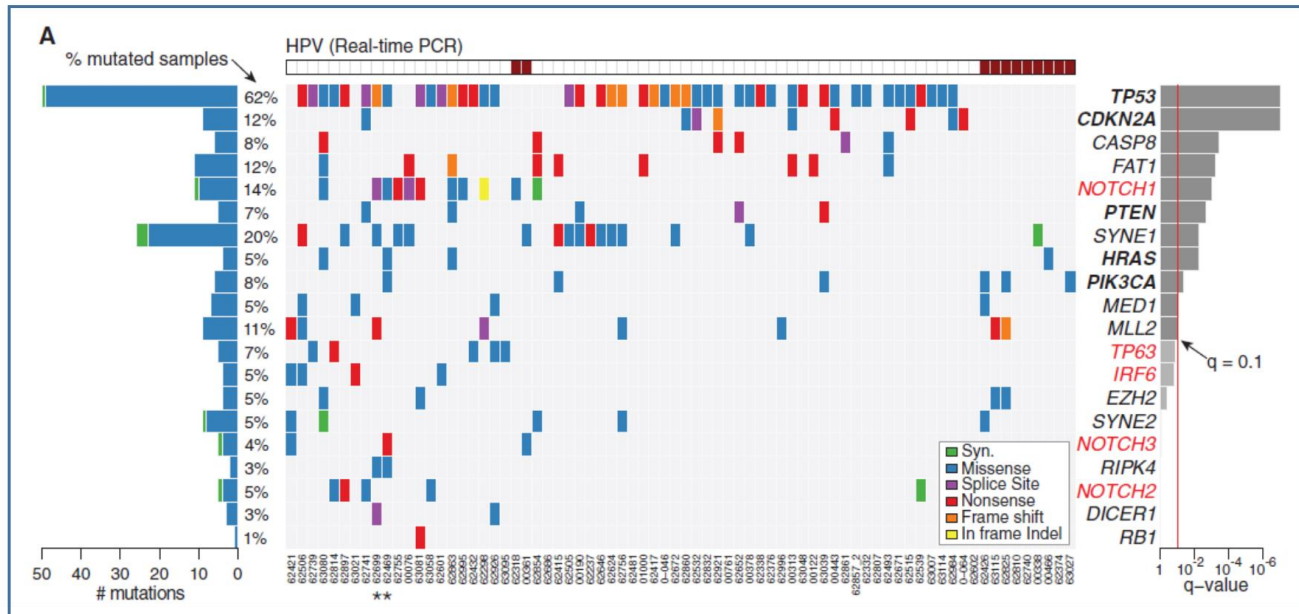


Figure 4: Frequent somatic mutations in HNSCC. Permission obtained from Stransky, N., et al., (2011) Science.. 333(6046): p. 1157-60 (Stransky et al., 2011)

Mutations identified from these studies confirmed previous reports of alterations in TP53, CDKN2A, PIK3CA, PTEN and HRAS. In both studies, novel inactivating mutations in NOTCH1 were found. This was the first time mutations in NOTCH1 in solid tumors were reported. NOTCH signaling is involved in the development of multicellular organisms. Maintenance of stem cells and differentiation are two processes by which NOTCH signaling regulates development. NOTCH signaling in cancer was first highlighted in T-cell Acute Lymphoblastic Leukemia (T-ALL) in which constitutive activation of NOTCH signaling promotes tumorigenesis. The role of NOTCH1 in T-ALL was found as a result of translocation of the NOTCH1 gene from chromosome 7 to chromosome 9 adjacent to the T-cell Receptor β enhancer/promoter (Reynolds, Smith, & Sklar, 1987). However such translocations was found in less than 1% of all human T-ALL. Weng et al. (Weng et al., 2004) published that more than 50% of all T-ALL have activating mutations in NOTCH1, revealing an oncogenic function of this protein in T-ALL. Pear et al. (W. Pear et al., 1999) showed that mice when reconstituted with hematopoietic progenitor cells expressing the human intracellular NOTCH1 (ICN1) develop T-cell leukemia.

NOTCH1 acts as a tumor suppressor or oncogene (Egloff & Grandis, 2012) depending on cancer type. In HNSCC, both Agarwal et al. (Agrawal et al., 2011), and Stransky et al. (Stransky et al., 2011) have shown loss of function mutations consistent with a tumor suppressor role. Targeting NOTCH signaling with gamma secretase inhibitors in T-ALL has shown pre-clinical activity in inhibiting tumorigenesis and currently being evaluated clinically. In contrast, the role of NOTCH signaling as a tumor

suppressor has been difficult to target in certain cancers due to loss of this pathway and a lack of NOTCH agonists.

Evidence of NOTCH as a tumor suppressor comes from studies in keratinocytes. NOTCH1 signaling in murine keratinocytes upregulates early differentiation markers such as keratin 1 and involucrin as well as WAF1 allowing terminal differentiation in the suprabasal layers of the skin (Nicolas et al., 2003). Recently Pickering et al. (Pickering et al., 2013) performed whole exome sequencing from primary cutaneous cell carcinoma that identified the tumor suppressive role of NOTCH1 as a potential driver in this cancer type. The mutational landscape of cutaneous squamous cell carcinoma is similar to HNSCC. In both cancers, alterations in NOTCH1 appear to be inactivating. The missense mutations cluster in the EGF-like repeats and truncating mutation are distributed throughout the gene except the PEST domain, which in contrast is found in T-ALL. More than 30% to 50% tumors with NOTCH1 mutations in cSCC have inactivating NOTCH1 mutations, further supporting the role of this gene as a tumor suppressor. Recently, Mao et al. (Song et al., 2014) sequenced 52 Chinese patients with HNSCC and detected NOTCH1 mutations in 43% of the tumors. Although, this group confirmed previous reports of inactivating mutations in the EGF domain, interestingly, 29% of the mutations were localized to the NOTCH1 the LNR domain. This is a domain is located close to the heterodimerization domain that harbors activating mutations in hematologic malignancies, however, the functional impact of these mutations remains unclear. Califano et al. (Sun et al., 2014) evaluated copy number variations, gene expression, methylation and mutations from 44 HNSCC primary tumors. They found a bimodal pattern of NOTCH signaling pathway expression in which a smaller set of mutants

exhibited inactivating NOTCH1 mutations, whereas a larger subset exhibited overexpression or increased gene copy number of the NOTCH receptor, ligands or downstream pathway activations. Although this group found significant upregulation of the NOTCH ligands, JAG1 and JAG2, it is unclear whether their overexpression within the same tumors would contribute to cis-inhibition or activation of the pathway. Moreover, copy number gains in NUMB, an inhibitor of the NOTCH pathway, were also found with JAG1 gains. This might argue that both cis-inhibition and inhibition by NUMB might downregulate the NOTCH signaling pathway in tumors. Whether overexpression of ligands in the same tumor contributes to cis-inhibition should be further investigated. Over the past 4 years, several efforts have been made to identify frequent somatic mutations in HNSCC, however few have offered insights into the mechanistic role of NOTCH as an oncogene or tumor suppressor. Recent TCGA data showed that inactivating mutations in FAT1 and NOTCH1 are not mutually exclusive. FAT sequesters β -catenin and inhibits the Wnt signaling cascade. These findings touch upon the mechanistic insights into the essential interplay between NOTCH signaling and the Wnt pathway. So far, we know that in a subset of HNSCC tumors, NOTCH might act as a tumor-suppressor and in the others it might play the role of an oncogene. This might depend on tumor type, stage, extracellular factors or the microenvironment, but is not completely understood. The main objective of this thesis is to provide data that support a tumor suppressor role for NOTCH1 in a subset of HNSCC through functional and mechanistic studies. In addition, we offer insights into how these tumors might be targeted by identification of the association of NOTCH signaling with two potential proto-oncogenes AXL and α -catulin that are suppressed after NOTCH activation.

CHAPTER 2: NOTCH SIGNALING

Chapter 2: NOTCH signaling

Structure of NOTCH receptor

NOTCH is family of transmembrane receptors that are involved in cell-cell interaction. Mammals have four NOTCH (NOTCH 1-4) paralogs that have both unique and redundant functions. The NOTCH receptor can be broadly structured into 4 regions: extracellular domain, transmembrane domain, intracellular domain and PEST domain (Figure 5) (Kopan & Ilagan, 2009).

The extracellular domain of all NOTCH receptors contain 29-36 tandem epidermal growth factor (EGF) – like repeats which are involved in binding to the NOTCH receptor of the adjacent cell. Interactions between the receptor of one cell and the ligand of a neighboring cell are called *trans* activation. This occurs by the binding of the EGF repeats 11-12 on the NOTCH receptor. On the contrary, binding of the NOTCH receptor and ligand on the same cell results in inhibition of the pathway called *cis*-inhibition. This includes EGF repeats 24-29 on the NOTCH receptors that bind to the ligand expressed by the same cell. Calcium ions play an important role in ligand-receptor binding. The EGF repeats binding to calcium ions can determine structure and affinity of binding. The extracellular region is composed of a Negative Regulatory Region (NRR) which has three cysteine-rich Lin12-NOTCH repeats (LNR) in addition to a heterodimerization domain (Figure 3). This NRR is important as it prevents activation of the NOTCH pathway without ligand binding. The region below the heterodimerization (HD) domain contains a cleavage site called S1, which is the site for furin-like convertases.

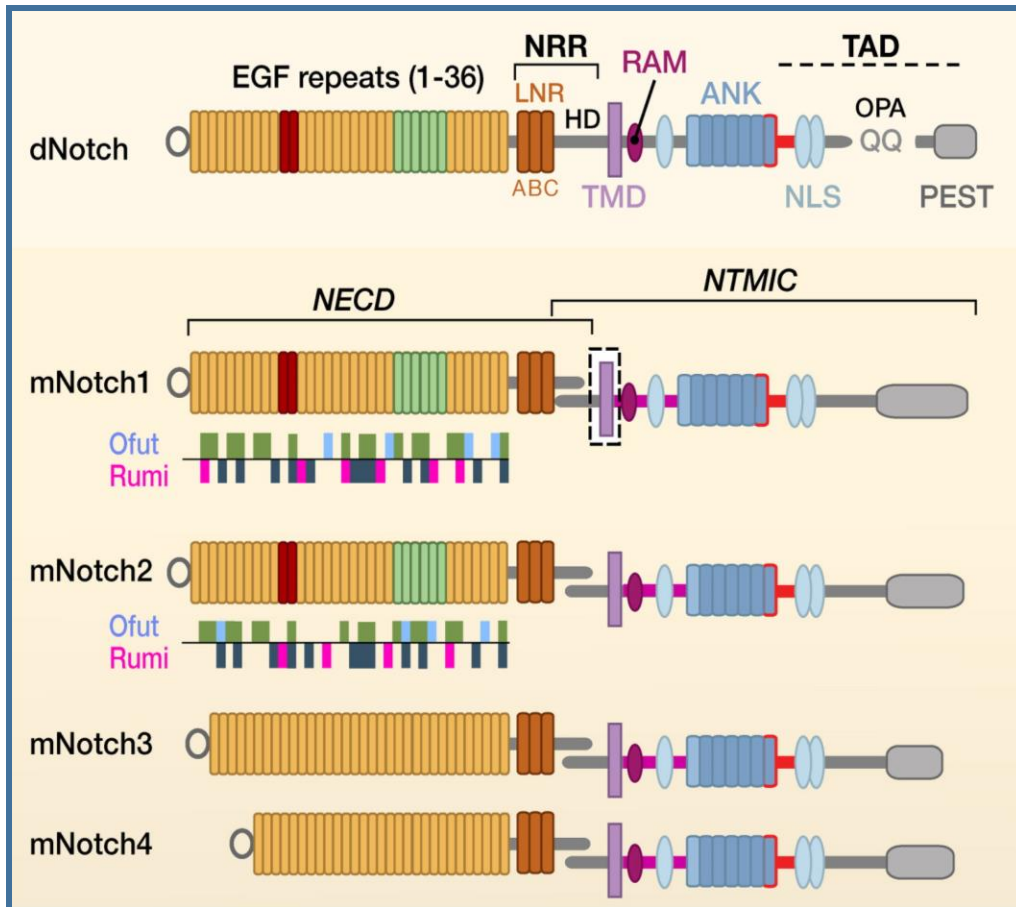


*Figure 5: Structure of NOTCH family receptors in drosophila and mammalian systems. Permission obtained from Kopan, R. and M.X. Ilagan. (2009). Cell. **137**(2): p. 216-33. (Kopan & Ilagan, 2009)*

Figure legend: EGF: Extracellular Growth Factor, NRR: Negative Regulatory Region, LNR: Lin12 NOTCH Repeats (LNR A, B and C), HD: Heterodimerization Domain, TMD: TransMembrane Domain, RAM: RBP-J κ Association Module, ANK: ANKyrin Repeats, NLS: Nuclear Localization Sequence, TAD: TransActivation Domain, OPA: glutamine rich repeat, QQ: Glutamine repeats, PEST: Proline/Glutamic acid/Serine/Threonine rich motif, Ofut: fucosylation motifs (green: common, light blue: unique), Rumi: glycosylation motifs (dark blue: common, magenta: unique), NECD: NOTCH ExtraCellular Domain, NTMIC: NOTCH TransMembrane and Intracellular Domain.

Cleavage at S1 converts full length NOTCH into a NECD-NTMIC (NOTCH extracellular domain- NOTCH transmembrane Intracellular domain) that is bound by covalent interactions between the N and C- terminus of the HD domain. The furin-like cleavage at S1 is part of the secretory pathway that occurs in the golgi before NOTCH receptor gets translocated to the plasma membrane. The transmembrane domain (TMD) contains a “stop translocation” signal that has 3-4 Arg/Lys residues that regulates translocation of the receptor. After the TMD, begins the intracellular domain. The domain near the N-terminus of the intracellular region contains a RAM domain (RBPjκ association module), with 12-20 amino acids centered around a conserved WxP motif (Lubman, Koroley, & Kopan, 2004). RAM is linked to several ankyrin repeats (ANK) by one nuclear localization sequence (NLS). Following the ANK, are more NLS and a transactivation domain (TAD). The end C-terminus contains proline/glutamic acid/serine/threonine (PEST) motifs that governs the stability of NICD.

Structure of NOTCH ligands

NOTCH ligands may be present in the same cell or adjacent cells that bind to the extracellular domains of the NOTCH receptor. Most NOTCH ligands are also type 1 transmembrane proteins and are membrane bound like the receptors. Cordle and colleagues (Cordle et al., 2008) employed X-ray and NMR techniques to study the structure of the NOTCH receptor. These receptors are characterized by three related structural motifs: N-terminal DSL (Delta/Serrate/LAG-2), EGF repeats called the DOS domain (Delta and OSM-11 like proteins) and EGF like repeats (Figure 6). The DSL and DOS domains are both involved in binding to the NOTCH receptor. Mammals have two types of NOTCH ligands, Jagged1/Jagged2 and Delta like ligand 1, 3 and 4 (DLL1, 3, 4).

Both Jagged ligands have a cysteine rich domain, which is absent from DLL1. Additional proteins that lack DSL or DOS domains have been reported as non-canonical ligands for the NOTCH receptor. For example, F3/Contactin1, NB-3/Contactin6 DNER and MAGP1 have been reported in the central nervous system and in cultured cells (B. D'Souza, Miyamoto, & Weinmaster, 2008). These non-canonical receptors have been unexplored and their physiological functions in the NOTCH signaling pathway hasn't been elucidated. After binding of the ligand to the receptor, endocytosis of the ligand is triggered by the cell expressing the ligand. E3 ubiquitin ligases like Neuralized and Mindbomb monoubiquitinate the ligand that is followed by degradation of the ligand. After endocytosis, in a process that is not completely understood, cells produce more active surface ligands (Le Borgne, 2006).

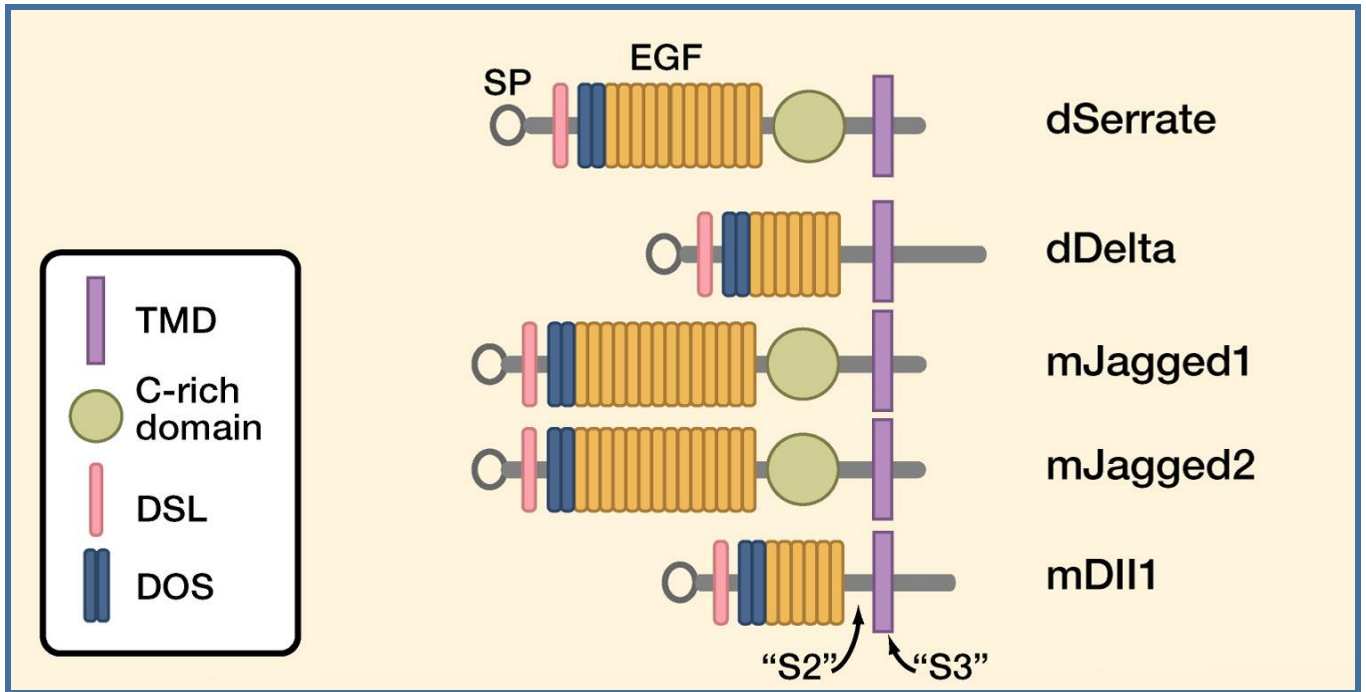


Figure 6: Structure of NOTCH ligands in drosophila and mammalian systems.
 Permission obtained from Kopan, R. and M.X. Ilagan. (2009). *Cell*. **137**(2): p. 216-33.
 (Kopan & Ilagan, 2009)

NOTCH activation and regulation

The binding of the NOTCH ligand to its receptor results in a sequence of proteolytic events. The first proteolytic cleavage occurs at site S2 (located just before the TMD and in the NRR) by ADAM metalloproteases (Figure 7). S2 cleavage is one of two key proteolytic cleavages that is often mediated by ADAM17/TACE. After S2 cleavage, an intermediate receptor called NOTCH Extracellular Truncation (NEXT) is formed that is still tethered to the plasma membrane. The S2 cleavage exposes the receptor to another key cleavage site called site 3, S3 that is located within the transmembrane domain. The enzyme that cleaves the NOTCH receptor at S3 is called γ -secretase. This enzyme belongs to a class of intermembrane cleaving proteases (i-CLiPs) (Wolfe & Kopan, 2004). Only after cleavage by γ -secretase, the NOTCH intracellular domain (NICD) (also called Intracellular NOTCH (ICN) or activated NOTCH) is released from the plasma membrane and translocates to the nucleus. In the nucleus, it interacts with DNA binding proteins CSL (CBF1/RBPjk) via its RAM domain. The ANK domain associates with CSL, which then recruits a co-activator called Mastermind-like 1 (MAML1). This complex then binds to the promoter regions of their targets and regulate diverse phenotypes. Canonically, these targets belong to the HES and HEY family of genes that are known transcriptional repressors.

The NOTCH ligand, meanwhile, is endocytosed by E3 Ubiquitin ligase in the neighboring cell. Mindbomb and Neuralized are E3 Ubiquitin ligases that recognize Jagged and Delta ligands respectively. After endocytosis, the process by which NOTCH ligands re-surface to the plasma membrane is not completely understood. Ligand

clustering, post-translational modifications and/or recycling ligands to specific membrane microdomains are some potential explanations (Pfister et al., 2003).

Just like the NOTCH ligand, several processes also regulate the NOTCH receptor. E3 ubiquitin ligases such as Deltex, Nedd4, and Cbl1 either recycle the receptors or target them for lysosomal degradation (S. J. Bray, 2006; Le Borgne, 2006). Another key molecule involved in regulation of the NOTCH receptor is NUMB, which in association with the AP2 component α -adaptin promotes NOTCH degradation. NUMB is a membrane-associated phosphotyrosine binding (PTB) protein that was first discovered as a cell fate determinant in *Drosophila melanogaster* (M. Park, Yaich, & Bodmer, 1998; Uemura, Shepherd, Ackerman, Jan, & Jan, 1989). The antagonistic effect on NUMB on NOTCH signaling has drawn attention to the role of NUMB in several cancers (Flores, McDermott, Meunier, & Marignol, 2014). The exact mechanism of NUMB inhibiting NOTCH signaling is not completely understood, but two models have been suggested for such inhibition. Endosomal trafficking of NOTCH is essential for its activation, regulation and degradation (Yamamoto, Chang, & Bellen, 2010). NUMB associates with AP2 adapter complex via α -adaptin in clathrin coated pits and is involved in endocytic trafficking (Santolini et al., 2000). This model suggests the possibility of NOTCH being endocytosed and thus inhibited by NUMB. On the other hand, NUMB can also directly bind to ICN and prevent its translocation to the nucleus. This was shown by Frise et al., (Frise, Knoblich, Younger-Shepherd, Jan, & Jan, 1996) by co-expressing NOTCH and NUMB that prevented translocation of ICN. Both these models suggest an inhibitory role of NUMB in regulating NOTCH signaling.

Besides E3 ubiquitin ligases and NUMB, post-translational modifications, particularly glycosylation (the process of adding glycans to proteins), at the EGF repeats of the NOTCH receptor is another mechanism of regulation. The NOTCH receptors have been thought of as large glycoproteins. Two forms of O-glycosylation; O-glucose and O-fucose modify the EGF repeats of the receptor (Haines & Irvine, 2003; Rampal, Luther, & Haltiwanger, 2007; Stanley, 2007). Post-translation, NOTCH receptor is fucosylated by O-fucosyltransferase. O-fucosylation facilitates proper folding of the receptor in the endoplasmic reticulum. The addition of O-fucose and/or O-glucose determines specificity of ligand binding. For example, fringe mediated addition of N-glucosamine on EGF repeat 12 enhances binding of the receptor to Delta but reduces its binding to Serrate in *Drosophila melanogaster* (Wu & Bresnick, 2007). In mammals, multiple fringe proteins (Lunatic, Manic and Radical fringes) regulate fucosylation of NOTCH receptors and their ligands. For example, lunatic fringe modifies NOTCH signaling in T-cells such that it enhances binding to Delta like ligand but not Jagged1 (Tsukumo, Hirose, Maekawa, Kishihara, & Yasutomo, 2006; Visan et al., 2006). Although the mechanistic contribution of these saccharides to NOTCH biology is not completely understood, the development of improved methods to detect glycosylation and the generation o-glycosylation deficient NOTCH alleles will be important contributors to NOTCH biology. Table 1 summarizes the core components of the NOTCH signaling pathway in *Drosophila* and mammalian systems.

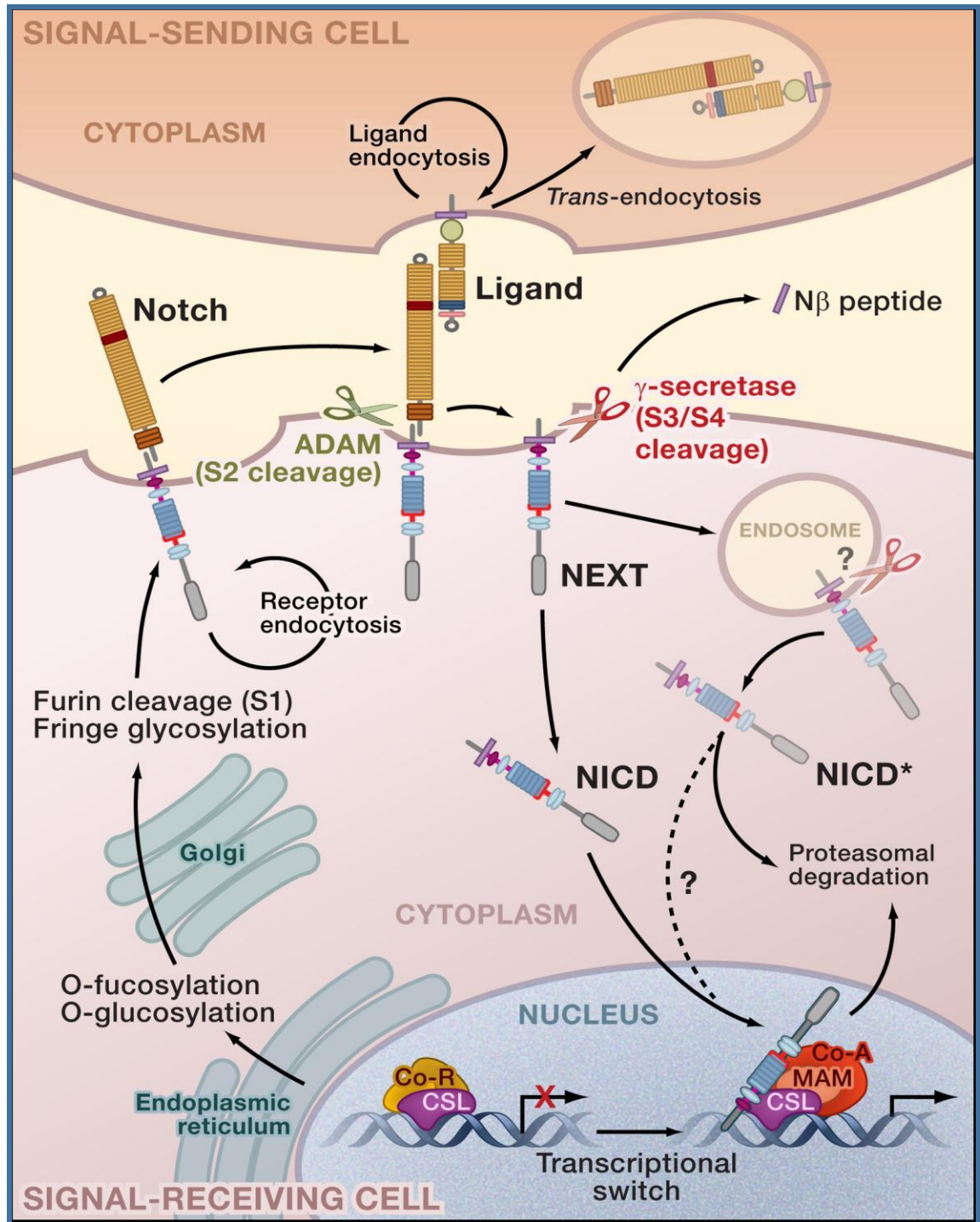


Figure 7: NOTCH signaling pathway. Permission obtained from Kopan, R. and M.X. Ilagan. (2009). *Cell*. 137(2): p. 216-33. (Kopan & Ilagan, 2009)

Type	Drosophila	Mammals
	Notch	Notch 1–4
DSL/DOS	Delta, Serrate	Dll1, Jagged1 and 2
DSL only		Dll3 and 4
DOS Coligands		DLK-1, DLK-2/EGFL9
Noncanonical		DNER, MAGP-1 and -2, F3/Contactin1, NB-3/Contactin6
CSL DNA-binding transcriptionfactor	Su(H)	RBPjk/CBF-1
Transcriptional Coactivator	Mastermind	MAML1-3
Transcriptional Corepressors	Hairless, SMRTR	Mint/Sharp/SPEN, NCoR/SMRT, KyoT2
Furin convertase (site 1 cleavage)	?	PC5/6, Furin
Metalloprotease (site 2 cleavage)	Kuzbanian, Kuzbanian-like, TACE	ADAM10/Kuzbanian, ADAM17/TACE
γ -secretase (site 3/site 4 cleavage)	Presenilin, Nicastrin, APH-1, PEN-2	Presenilin 1 and 2, Nicastrin, APH-1a-c, PEN-2
O-fucosyl-transferase	OFUT-1	POFUT-1
O-glucosyl-transferase	RUMI	
β 1, 3-GlcNAc-transferase	Fringe	Lunatic, Manic, and Radical Fringe
Ring Finger E3 Ubiquitin ligase (ligand endocytosis)	Mindbomb 1–2, Neuralized	Mindbomb, Skeletrophin, Neuralized 1–2
Ring Finger E3 Ubiquitin ligase (receptor endocytosis)	Deltex	Deltex 1–4
HECT Domain E3 Ubiquitin ligase (receptor endocytosis)	Nedd4, Su(Dx)	Nedd4, Itch/AIP4
Negative regulator	Numb	Numb, Numb-like, ACBD3
Neuralized Inhibitors	Bearded, Tom, M4	
Other endocytic modifiers	sanpodo	
F-Box Ubiquitin ligase	Archipelago	Fbw-7/SEL-10
Canonical Targets (bHLH repressor genes)	E(spl)	HES/ESR/HEY

Table 1: Core components of the NOTCH signaling pathway in Drosophila and mammals.

NOTCH signaling in differentiation

The NOTCH signaling pathway is an evolutionarily conserved pathway from invertebrates to vertebrates. NOTCH signaling is critical to the maintenance and renewal of several organs that include skin, blood, intestine, liver and muscle. NOTCH plays an important role in stem cells, in that it determines whether stem cells continue to proliferate and maintain their stemness or promote the differentiation of stem cells to progenitors or terminally differentiated cells. Embryonic stem (ES) cells are derived from the early embryonic stages and are pluripotent (Thomson et al., 1998). These cells express NOTCH1, however the progenitor cells from which these ES cells are derived do not express NOTCH1 (Hadland et al., 2001). The activation of NOTCH signaling at different stages of ES cell differentiation has been shown to enhance the generation of particular precursor cells (P. M. Chen et al., 2008; Kobayashi et al., 2009). Schroeder et al. (Schroeder & Just, 2000) have shown that activation of NOTCH signaling in mesodermal cells blocks the generation of endothelia, cardiac muscle, and hematopoietic cells while inhibition of NOTCH signaling in ES cells (by deletion of RBP-J κ) directs differentiation of the cardiomyocyte lineage. On the other hand, NOTCH signaling also plays an important role in the differentiation of a variety of progenitor cells. In the hematopoietic system, Delta1 ligand mediated NOTCH1 activation has shown to stimulate megakaryocytic development from hematopoietic stem cells (Mercher et al., 2009). In T-cell progenitors, it has been shown that NOTCH gain of function induced by overexpression of NOTCH1 or stimulation with DLL1 and DLL4 ligands led to aberrant proliferation and differentiation (de La Coste et al., 2005; Hozumi, Abe, Chiba, Hirai, & Habu, 2003; Jaleco et al., 2001; Pui et al., 1999). On the contrary, loss of function studies

using inactivated NOTCH1, mutant RBP-J κ or using the γ -secretase inhibitor produced a similar phenotype in B-cell progenitor cells (Hadland et al., 2001; H. Han et al., 2002). Put together, NOTCH signaling instructs differentiation along the T-cell rather than the B-cell lineage during lymphopoiesis.

In addition to hematopoiesis, NOTCH signaling also plays an important role in skin differentiation. The epidermis has four layers: basal, spinous, granular and cornified. Each layer expresses different markers. Adult stem cells reside either in the basal layer or in the bulge of the hair follicle. Stem cells at the basal layer are unipotent and these cells commit to terminal differentiation (Blanpain & Fuchs, 2006; Fuchs & Raghavan, 2002) while the stem cells at the follicle bulge are usually quiescent and enter the proliferative stage in response to injury (Blanpain & Fuchs, 2009; L. Li & Clevers, 2010). NOTCH signaling modulates differentiation and proliferation of epidermal stem cells (Ambler & Maatta, 2009; Okuyama, Tagami, & Aiba, 2008; Watt, Estrach, & Ambler, 2008). Condition gain of function (NICD overexpression) and loss of function studies (NOTCH1 $-/-$) have shown that NOTCH signaling promotes basal to spinous differentiation (Blanpain, Lowry, Pasolli, & Fuchs, 2006; Rangarajan et al., 2001). Dotto et al. (Dotto, 2008) and others (Demehri, Turkoz, & Kopan, 2009; Nicolas et al., 2003) have shown that embryonic ablation of RBP-J κ in the epidermis causes epidermal hyperplasia. After birth, loss of NOTCH results in hyperplasia, creating a tumor-promoting microenvironment. NOTCH as a tumor suppressor in skin highlights the complex role played by NOTCH signaling in controlling epidermal differentiation and regulating exit from the proliferative stem cell niche. In the follicular bulge stem cell population, NOTCH signaling functions as a gate-keeper. In the absence of NOTCH,

stem cells can select either epidermal or follicular differentiation (Demehri & Kopan, 2009). The differences observed in the specific activities of NOTCH signaling in different stem cell populations plays a complex, context dependent role in stem cell biology.

NOTCH in cancer

NOTCH signaling plays diverse roles during the development and maintenance of normal tissues. This effect is recapitulated in several forms of cancer. NOTCH may act as a tumor suppressor or an oncogene depending on the context and exerting its effect on differentiation, growth, migration, angiogenesis and self-renewal. In this chapter, the role of NOTCH as an oncogene and tumor suppressor will be elucidated.

NOTCH as an oncogene

The best-known example of oncogenic NOTCH signaling is in T-cell acute lymphoblastic leukemia (T-ALL) that is a neoplasm of immature T-cells. The first known role of NOTCH1 in T-ALL was known because of its translocation from chromosome 7 to chromosome 9 (Ellisen et al., 1991). This translocation was found only in 1% of all T-ALL's. A much broader role of NOTCH1 was revealed after the discovery of activating mutations in this cancer type. Activating mutation in NOTCH1 was found at frequency of 60% (Weng et al., 2004). There are two types of activating mutations in T-ALL. The first occurs at the heterodimerization domain that results in ligand independent metalloprotease cleavage at the S2 site. The second consists of frame shift mutations or stop codons at the PEST degradation domain. Such mutations prevent degradation of

NOTCH and stabilize the NICD (Malecki et al., 2006). In the murine system, NOTCH1 plays a role in the early stages of T-cell development, including commitment to T-cell fate and subsequent progression to the DN3 stage of development. This suggests that the leukemogenic activity stems from exaggerated normal development function (Radtke, Wilson, Mancini, & MacDonald, 2004). Besides, T-ALL, NOTCH signaling also has oncogenic functions in other contexts, especially breast cancer, medulloblastoma, colorectal cancer, non-small cell lung carcinoma and melanoma (Ranganathan, Weaver, & Capobianco, 2011). The oncogenic function of NOTCH in solid tumors was first discovered in breast cancers, which was driven by mouse mammary tumor virus (MMTV). Integration of MMTV in the host genome resulted in the constitutively active form of NOTCH4 (Gallahan, Kozak, & Callahan, 1987). The expression of NOTCH receptors is elevated in breast cancers and the expression of NOTCH ligands such as Jagged1 correlates with more aggressive disease (Reedijk et al., 2005; Weijzen et al., 2002). Recently, activating mutations in chronic lymphocytic leukemia (CLL) has been identified. NOTCH1 activating mutations in this cancer type predicts to impair FBW7 degradation of NOTCH1 (Fabbri et al., 2011). NOTCH receptor expression and its downstream targets are up regulated in primary human melanomas (Balint et al., 2005). Forced expression of intracellular NOTCH (NICD) promotes melanoma progression. Increased NOTCH activity has been correlated with PI3K-Akt activity in melanoma cells (Z. J. Liu et al., 2006). To date, no gain of function mutations have been discovered in solid tumors suggesting the ligand activation of the receptor dominates the role of NOTCH as an oncogene (Lobry, Oh, & Aifantis, 2011). Recently, other work has implied the role of NOTCH as an oncogene in other solid tumors such as medulloblastoma

(Hallahan et al., 2004) and ovarian cancer (J. T. Park et al., 2006). It is likely that there might be other neoplasms in which the oncogenic function of NOTCH will be uncovered in the future.

NOTCH as a tumor suppressor

Although activation of NOTCH can be oncogenic, there is also sufficient evidence to show that NOTCH can be tumor suppressive. This has been shown in skin, pancreatic epithelium, hepatocyte and other hematopoietic cells. In skin keratinocytes, activation of NOTCH in the suprabasal layers results in differentiation and cell cycle arrest (Rangarajan et al., 2001). Conditional knock out of NOTCH1 in the skin resulted in increase of the basal epidermis. Loss of NOTCH1 in the skin causes spontaneous basal cell carcinoma and increased sensitization to chemically induced skin carcinogenesis (Nicolas et al., 2003). Viatour and colleagues (Viatour et al., 2011) showed that NOTCH acts a tumor suppressor in hepatocellular carcinoma (HCC). They found that inhibition of NOTCH signaling using the γ -secretase inhibitor accelerated HCC development. Furthermore, using intracellular NOTCH1 (ICN1) resulted in cell cycle arrest and apoptosis. In order to evaluate the clinical relevance, the authors looked at patient survival and its correlation with NOTCH. They found better patient survival in cohorts that had increased NOTCH related genes. Taken together, their results suggest a tumor suppressive role of NOTCH in HCC. Zweidler-McKay et al. showed that in B-cell malignancies, NOTCH is known to arrest cell growth and induce apoptosis suggesting a tumor suppressor role (Zweidler-McKay et al., 2005). This role of NOTCH has also been elucidated in neuroblastoma using the activated intracellular form of NOTCH (ICN) or activation by recombinant NOTCH ligand (Zage et al., 2012). The recently published

work in HNSCC sheds light on inactivating mutation seen in NOTCH1 which renders this protein an oncogene in this tumor type (Agrawal et al., 2011; Stransky et al., 2011; "TCGA Releases Head and Neck Cancer Data," 2015). These were initial sequencing studies that identified NOTCH as a tumor suppressor based on the mutational landscape. The functional significance of these inactivating mutations is currently unknown and is the main focus of this thesis.

The role of NOTCH as an oncogene in breast, T-ALL, and ovarian cancer versus tumor suppressor in skin, HNSCC, and HCC highlights an intriguing dual role of NOTCH that is context dependent. NOTCH either promotes stem cell maintenance of terminal differentiation. It is possible that these fundamental roles of NOTCH may contribute to its role as an oncogene or tumors suppressor. By affecting differentiation, for example, NOTCH could set the stage for accumulation of additional mutations. In myeloid-leukemia, defective NOTCH signaling promotes differentiation of stem cells to granulocytic/monocytic progenitor cells (GMP). This expands the pool of putative leukemia initiating cells driving the accumulation of oncogenic mutations in TET that then results in granulocytic/monocytic leukemia (Moran-Crusio et al., 2011). Activating mutations in NOTCH could potentially promote T-cell progenitors population, resulting in T-ALL while NOTCH could also stimulate terminal differentiation of progenitor cells preventing further accumulation of cancer initiating populations, which might be the case in HCC (Lobry et al., 2011).

NOTCH in HNSCC

Currently, very little is known about the functional role of NOTCH in HNSCC. Following whole exome sequencing studies that identified inactivating mutations in

NOTCH1, there has been growing interest in the potential role of NOTCH signaling in the development of head and neck cancers. Besides TP53, NOTCH mutations commonly occur in head and neck cancers, skin and NSCLC. NOTCH signaling is still being assessed as a tumor suppressor in squamous cell carcinomas. Prior to the sequencing studies, there have been very little studies elucidating the role of NOTCH in HNSCC most of which was in relation to aberrations in other molecules. The purpose of this thesis is to attribute a tumor suppressive role of NOTCH in HNSCC and elucidate the functional relevance of NOTCH signaling in inhibiting growth *in vitro* and *in vivo*. Here, we show for the first time, that NOTCH1 inhibits two proto-oncogenes AXL and CTNNAL1 and make a novel connection of these molecules with NOTCH1 in abrogating cell growth. Elucidating how NOTCH inactivation promotes tumorigenicity could identify new therapeutic targets that are upregulated because NOTCH signaling is lost in HNSCC. We propose that AXL and CTNNAL1 may be novel targets downstream of NOTCH that can be exploited for therapeutic intervention in tumors that have an inactive NOTCH pathway.

CHAPTER 3: AXL AND α -CATULIN

Chapter 3: AXL and α -CATULIN

AXL

AXL is a receptor tyrosine kinase (RTK) that belongs to the TAM family of transmembrane receptors (Axelrod & Pienta, 2014). This receptor gets its name from the first letter of each member of its family: Tyro3, AXL and Mer (Prasad et al., 2006). These are a structurally distinct family of orphan RTK's that was discovered after isolation of their full length cDNA's (Graham, Dawson, Mullaney, Snodgrass, & Earp, 1994; Lai & Lemke, 1991; O'Bryan et al., 1991). The TAM receptors have two ligands; growth arrest specific 6 (Gas6) and Protein S. While Gas6 can bind to all TAM receptors, Protein S can only bind to Tyro3 and Mer (Hafizi & Dahlback, 2006). The AXL gene is harbored on chromosome 19. It has 20 exons spread over a 44 kb region. The 5' upstream region of AXL is GC rich. This region does not have TATA and CAAT boxes. Using cloning and 5' deletion techniques Mudduluru and Allgayer characterized the promoter region of AXL (Mudduluru & Allgayer, 2008). In their publication, they show that a minimalistic GC-region alone is sufficient to activate the AXL promoter. In addition, there are also several binding sites for transcription factors upstream of the AXL start codon. These binding sites include five Sp binding sites (SP a- Sp e), one MZF1 and one AP1 binding site (Mudduluru & Allgayer, 2008; Mudduluru, Leupold, Stroebel, & Allgayer, 2010; Mudduluru, Vajkoczy, & Allgayer, 2010). Another feature of this promoter shown by Sayan et al. is how CpG islands control promoter activation of AXL. CpG islands are critical in gene expression and consequently the control of cell cycle, tumor differentiation and development (Bartolomei, Webber, Brunkow, & Tilghman, 1993; Carlone et al., 2005). In the CpG islands, promoter methylations is a common

epigenetic modification that is used to repress gene expression. There are 19 CpG islands within the promoter region as putative methylation sites (Mudduluru & Allgayer, 2008). The transactivation potential of Sp1 and Sp3 transcription factors is affected by methylation of these CpG sites within the Sp transcription factor binding motifs (Zhu et al., 2003). Using cell lines with varying expression levels of AXL, Mudduluru and Allgayer elucidated that CpG islands located in proximity to the Sp family binding motifs were methylated in low AXL expressing cell lines. On the contrary, cell lines which had high AXL expression that showed no methylation (Mudduluru & Allgayer, 2008).

Mouse loss of function mutants demonstrated the biological role of the TAM receptors after identification of the structure of TAM receptor and ligands (Camenisch, Koller, Earp, & Matsushima, 1999). Tyor 3 ^{-/-}, AXL ^{-/-}, and Mer ^{-/-} mice are all viable and fertile. Liu and colleagues (E. Liu, Hjelle, & Bishop, 1988) first discovered AXL from patients with Chronic Myelogenous Leukemia (CML). When this discovery was made, AXL was shown to be necessary but not sufficient for transformation. AXL is located in the “p” arm of chromosome 19 with a molecular weight of about 140 kDa.

The extracellular domain of the TAM receptors have two structural modules that are repeated in other RTK ectodomains, defining two plus two configuration. In the ectodomains, the amino terminal regions have immunoglobulin domains that facilitate binding of the ligand (Sasaki et al., 2006) that is followed by type 3 fibronectin sequences. The transmembrane domain of most TAM receptors have a protein tyrosine kinase catalytic domain. Activation of this domain results in downstream activation of the phosphoinositide 3 kinase (PI3K)/ Akt pathway. The PI3K signaling is associated through a TAM-autophosphorylated Grb2-binding site, which is located approximately

18 residues at the carboxy terminal of the kinase domain. This region is conserved across all the TAM's (Fridell et al., 1996; Ling, Templeton, & Kung, 1996). Activation of phospholipase C, ERK1/2, Ras and MAP kinase activation has also been shown before (Keating et al., 2010). The TAM ligands are large (80kDa) proteins that share the same multidomain arrangement. The carboxy terminal has an SHBG domain composed of two laminin G domains. The SHBG domain is responsible for binding to the Ig domains of the receptors. This binding induces their dimerization and kinase activation. The second domain is called Gla domain. This domain is located at the amino terminus of both ligands (Stitt et al., 1995). The Gla domain is known to be rich in glutamic acid residues. The hydroxyl groups of these residues are carboxylated post-translationally (Huang et al., 2003).

Like other RTK's, AXL can also function independent of the ligand depending upon the context. For example, in vascular smooth muscle cells (VSMC) and lens epithelial cells, ligand independent AXL activation occurs in response to hydrogen peroxide. The binding of the receptor to the ligand activates the AXL signaling cascade, which results in diverse phenotypic functions such as cell proliferation, migration, invasion, differentiation and EMT (Figure 6). Which signaling pathways are activated are regulated spatially and temporally determined by extracellular environment, cell and tissue type. When AXL was discovered in CML, PI3K signaling was the first discovered downstream cascade through which it regulates cell migration, growth, and apoptosis (Nielsen-Preiss et al., 2007; Ruan & Kazlauskas, 2013). Over the years, AXL has been shown to have diverse signaling capabilities through the PI3K, Akt, mTOR, NFκB and MAPK pathways.

Like other RTK's binding of Gas6 to AXL down regulates its expression through degradation via c-Cbl ubiquitin ligase (Valverde, 2005). AXL is also regulated post-transcriptionally by micro RNA's miR-34a and miR-199a/b. This was shown in a bioinformatics screen in NSCLC, breast and colorectal cancer cell lines (Mudduluru et al., 2011). HIF1- α , MZF1, AP1, sp1 and sp3 transcriptional factors can also regulate AXL expression transcriptionally.

AXL in cancers

AXL is overexpressed in several cancer types. Correlation studies have shown the association of AXL with motility and invasion and that the treatment with R428, an AXL inhibitor reverses this phenotype. Increased AXL expression has been evaluated as a poor prognostic factor for overall survival in colon cancer, osteosarcoma, and pancreatic cancer (Dunne et al., 2014; J. Han et al., 2013; Song et al., 2011). AXL expression is also a prognostic for increased lymph node metastasis and clinical stage in lung adenocarcinoma, breast and ovarian cancer (D'Alfonso et al., 2014; Rankin et al., 2010; Shieh et al., 2005)

AXL in Non-small cell lung carcinoma (NSCLC)

AXL overexpression has been observed in 60% of NSCLC cell lines and also in a significant fraction of primary tumors (Shieh et al., 2005; Wimmel, Glitz, Kraus, Roeder, & Schuermann, 2001). In H1299 lung cancer cell lines, it has been shown that AXL is upregulated upon loss of p53 and in part gain of function activities of mutant p53 was mediated through AXL overexpression (Vaughan et al., 2012). Zhang et al. had shown

high AXL activation in NSCLC and demonstrated evidence for epithelial-to-mesenchymal transition (EMT) in lung cancer models that were resistant to erlotinib *in vitro* and *in vivo* (Z. Zhang et al., 2012). After AXL inhibition, the sensitivity to erlotinib was restored showing that inhibition of AXL can overcome chemo resistance. They also showed low AXL expression levels in cells that have vimentin blocked. This suggests that AXL expression is higher during the process of EMT and that AXL confers resistance occurs in the process of EMT. Evaluation of AXL expression in patients before and after EGFR inhibitor treatment demonstrated that increased expression of AXL is essential for resistance to EGFR inhibitors. Around the same time, Byers et al. confirmed a 75-gene EMT signature by employing gene expression profiles (Byers et al., 2013). This was done in NSCLC cell lines and tumors from lung cancer patients, using three different arrays. This defined signature could predict resistance to EGFR and PI3K/Akt inhibitors. They suggested that AXL is a mediator of resistance to EGFR inhibitors further implicating that such resistance could be associated with a mesenchymal phenotype. Their signature strongly correlates with the mesenchymal group in which they observed upregulation of AXL but this was not seen in the epithelial group. Furthermore, they observed that inhibition of AXL in mesenchymal cells reversed resistance to the drug treatments. Taken together, AXL has two possible roles in cancer; association with an EMT phenotype and resistance to targeted agents.

AXL in breast cancer

AXL is overexpressed in highly invasive breast cancer cell lines. On the contrary, weakly invasive breast cancer cell lines express AXL at very low levels. It has also been

shown that AXL expression correlates with motility and invasiveness of breast cancer cell lines (Y. X. Zhang et al., 2008). Estrogen receptor has also been shown to induce AXL expression and this could be important in proliferation, differentiation and apoptosis of human breast epithelium (Berclaz et al., 2001). The progesterone receptor B (PRB) upregulates the AXL ligand, Gas6 (Richer et al., 2002) and Her2 is also reported to trigger AXL activation suggesting crosstalk in clinically important pathways (Bose et al., 2006). Berclaz et al. immunostained AXL and estrogen receptor (ER) in a panel of 23 normal and 111 malignant breast cancer samples (Berclaz et al., 2001). They found a high correlation between AXL and ER expression in malignant breast tissue. In addition, there was also a correlation between AXL expression and the stage of the tumor. Gjerdrum et al. had investigated AXL expression levels in 190 breast cancer patients and showed that high AXL expression negatively correlates with breast cancer survival (Gjerdrum et al., 2010). Holland et al. used RNAi to inhibit AXL and showed decreased growth of MDA-MB-231 cells in a xenograft model (Holland et al., 2005). In addition, AXL knockdown in MDA-MB-231 demonstrated that AXL was necessary for invasiveness in metastatic breast cancer cells (Gjerdrum et al., 2010). In the same cell lines, decreased AXL mRNA and protein levels correlates with cell invasion potential and decreases phosphorylation of AKT (Mackiewicz et al., 2011). Similar to NSCLC in which AXL expression was reduced when vimentin was blocked (Z. Zhang et al., 2012), Vuoriluoto et al. found that vimentin promotes EMT activation and is also necessary for AXL upregulation (Vuoriluoto et al., 2011).

AXL in Acute Myeloid Leukemia (AML)

AXL was found as a prognostic marker and therapeutic target in acute myeloid leukemia (AML). AML cells can induce expression of Gas6 from bone marrow derived stromal cells. Gas6 mediates proliferation, survival and chemo resistance of AXL expressing AML cells. This creates a chemo protective tumor cell niche. The small molecule AXL inhibitor BGB324 (R428), is able to overcome this mechanism and synergize with chemotherapy (Ben-Batalla et al., 2013). AXL overexpression also promotes migration and invasion of prostate cancer cells *in vitro* (Paccez et al., 2013; Shiozawa et al., 2010). It is also associated with higher frequency of distant metastasis in patients with pancreatic adenocarcinoma (Linger et al., 2013; Song et al., 2011). Recently performed work has shown that AXL can mediate resistance to anti-EGFR inhibitors (Byers et al., 2013; Giles et al., 2013; Ye et al., 2010; Z. Zhang et al., 2012). Patients with AML had high AXL mRNA levels and worse progression free survival (Rochlitz et al., 1999). AXL expression in drug resistance was shown by Hong et al. wherein they observed high expression of AXL in AML patients refractory to doxorubicin treatment (Hong et al., 2008). In the same study, expression of endogenous AXL was shown to be induced by chemotherapeutic drugs in a dose-dependent manner in AML cell lines.

AXL in HNSCC

Brand and colleagues evaluated if AXL is a functional molecular target in HNSCC and whether targeting AXL could enhance the efficacy of standard treatments used to treat these patients (Brand et al., 2015). They show that AXL inhibition (using siRNA's and a pharmacological inhibitor- R428) effectively reduced HNSCC cell

growth, migration and invasion. The pharmacological inhibitor of AXL, R428, has shown specificity for AXL (Holland et al., 2010) and is now being evaluated clinically in Phase 1 trials (Fleuren et al., 2014). Brand et al. (Brand et al., 2015) showed that using increasing doses of R428, all AXL expressing HNSCC cell lines were significantly growth inhibited. Furthermore, they also used patient derived xenografts (PDX) that were resistant to radiation therapy and showed higher AXL expression in these PDX models. Their study concluded that AXL is highly expressed in HNSCC and is associated with worse clinical outcomes.

AXL inhibitors

As described earlier, overexpression of AXL has been implicated in a variety of cancer types. Genetic and possibly epigenetic mechanisms potentially regulate the activation of AXL in cancers. Like other RTK's that have inhibitors such as imatinib mesylate (Gleevec), Herceptin, Tarceva and Iressa (Gschwind, Fischer, & Ullrich, 2004), AXL has also been the subject of study for therapeutic intervention. The development of AXL inhibitors could potentially improve the treatment of different cancer types in which AXL is deregulated. Recently, RNA interference (RNAi) and therapeutic agents have been used to validate the efficacy of AXL inhibition. In 2010, Ye and colleagues developed a monoclonal antibody (YW327.6S2) against AXL which has high affinity for this receptor (Ye et al., 2010). This antibody has been shown to decrease xenograft tumor growth and potentiates the effect of anti-VEGF treatment. It also enhances the effect of erlotinib in decreasing NSCLC tumor growth as well as breast cancer metastasis. The identification of 3-quinolinecarbonitrile (Keri et al., 2005) compounds demonstrated potent inhibitory activity against AXL as well as inhibition of motility and invasiveness

especially in breast cancer cell lines (Y. X. Zhang et al., 2008). NA80x1 is a compound that directly inhibits AXL phosphorylation. This compound was previously reported to display inhibitory activity against Src kinase (Boschelli, Barrios Sosa, Golas, & Boschelli, 2007; Boschelli et al., 2001). SKI-606 is a Src/Abl inhibitor that also is a potent AXL inhibitor. SKI-606 can inhibit AXL 20 times lower than NA80x1. In their publication, it was suggested that both SKI-606 and NA80x1 might be potential therapeutic targets against breast cancer growth and metastasis. However, both these compounds have many off target effects and show effects in the micro-molar range, which is clinically not a viable option.

In 2010, a small molecule AXL inhibitor called R428 ((1-(6,7-dihydro-5H-benzo[6,7]cyclohepta[1,2-c] pyridazin-3-yl)-N3-((7-pyrrolidin-1-yl)-6,7,8, 9-tetrahydro-5Hbenzo[7]annulene-2-yl)-1H-1,2,4-triazole-3,5- diamine) was identified by Holland and colleagues (Holland et al., 2010) that had effects in the nanomolar range. This small molecule inhibits AXL activity and blocks downstream events of AXL such as Akt phosphorylation, cell invasion and cytokine production. Dose dependent reduction in Snail, an EMT transcriptional regulator, inhibition of angiogenesis and tumor formation was also seen. Holland et al. also translated this *in vivo* and observed an increase in survival. Breast cancer and lung cancer models in animals after receiving R428 had a median survival of over 80 days compared to non-treated animals that had a survival of 52 days. Furthermore, R428 had a synergistic effect with cisplatin treated mice resulting in suppression of liver metastasis.

Using an *in silico* approach, Mollard et al. developed a series of compounds that potentially inhibits AXL and identified 2,4,5-trisubstituted pyrimidines as potent AXL

inhibitor in the nanomolar range (Mollard et al., 2011). Cerchia et al. employed the concept of RNA Aptamers to develop GL21.T, a potential AXL inhibitor (Cerchia et al., 2012). DNA or RNA aptamers are molecules that bind to targets with high specificity and affinity. GL21.T binds to the extracellular regions of AXL and Tyro3. The authors used a xenograft fluorescent model and demonstrated that this aptamer specifically accumulates in the tumor region and mice treated with this aptamer had close to 70% smaller tumors compared to non-treated controls.

Thus, the identification of molecules with different structures (antibodies, small molecules, and aptamers) reveals the versatility that can be exploited in the development of inhibitors against AXL. In this context, identification and development of therapies involving the inhibition of AXL as well as targeting its downstream effectors may represent novel targeted therapeutics.

CTNNAL1: α -catulin

CTNNAL1 is a gene encoding the protein α -catulin, an 82kDa vinculin/ α -catenin family protein. This gene was originally identified as a down-regulated transcript in sodium butyrate treated pancreatic cancer cells which were undergoing differentiation and apoptosis (J. S. Zhang et al., 1998). The N-terminal region of α -catulin has structural similarities to human vinculin and α -catenin thus giving it the name α -catulin (α -CATenin and vinCULIN). It contains binding sites for β -catenin, α -actinin and talin suggesting that α -catulin may be a cytoskeletal linker protein (Janssens, Staes, & van Roy, 1999). Vinculins and α -catenins are functionally and structurally related proteins. Both have analogous functions despite their low sequence similarity. Both these molecules are important for the formation of adhesion complexes since they can both bind to actin. During cell-cell contacts, α -catenin binds to either β -catenin or plakoglobin (γ -catenin) linking the transmembrane to the actin cytoskeleton (Aberle, Schwartz, & Kemler, 1996). During cell-substrate contacts, vinculin is linked to integrins via talins (transmembrane receptors for binding to the extracellular matrix) (Burrige, Chrzanowska-Wodnicka, & Zhong, 1997). The formation of adhesion complexes and its association to the actin cytoskeleton is necessary for proper differentiation and homeostasis and also for cell growth, motility, gene expression and apoptosis (Rudiger, 1998). Notwithstanding the sequence similarities of α -catulin with α -catenin and vinculin, α -catulin does not inhibit the Wnt/ β -catenin signaling pathway (Merdek, Nguyen, & Toksoz, 2004). The CTNNAL1 gene is located on chromosome 9q31-32. This is a region that is frequently lost and is a tumor suppressor marker that has been reported in many cancers (Schultz et al., 1995). This suggests that α -catulin might have a tumor

suppressive function. There are, however, conflicting reports that show evidence of α -catulin binding directly to IKK- β and Lbc (a Rho GEF) which promotes cell migration and is resistant to apoptosis (B. Park et al., 2002; Wiesner et al., 2008). This evidence suggests an oncogenic potential of α -catulin. In their publication, Wiesner et al. performed a genetic screen using the regulatory C-terminal HLH domain of IKK- β as bait and identified α -catulin as an IKK-interacting protein. α -catulin augments activation of NF- κ B after stimulation with TNF- α or IL1. Thus, α -catulin serves as a scaffold protein linking the IKK- β and Rho signaling pathways. Consequently, the biological functions are promotion of cell migration and protection of cells from undergoing apoptosis. These are the hallmarks of a gene with tumorigenic potential suggesting an oncogenic role of α -catulin. Recently, Kreisde and colleagues have shown that α -catulin is highly expressed in melanoma cells compared to melanocytes and that α -catulin is a key driver of tumor formation, growth, invasion and metastasis by upregulating E-cadherin and downregulating Snail/Snug and MMP2/MMP9. Cao et al. reported that α -catulin was highly expressed in squamous cell carcinoma and its knockdown increased migratory and invasive behavior *in vitro* and *in vivo* (Cao, Chen, Masood, Sinha, & Kobiak, 2012). Furthermore, the increase of NF- κ B expression by α -catulin elevates fibronectin and α v β 3 expression and promotes cell migration, invasion and metastasis in lung cancer cells (Liang et al., 2013). More recently, Kreisde et al. have shown that downregulation of α -catulin using shRNA's diminished NF- κ B, MAPK and AP-1 activation in melanoma cells and sensitized these cells to cisplatin treatment (Kreieder et al., 2015). Although recent studies have underscored the importance of α -catulin in tumor growth, progression, invasion and metastasis, currently there are no inhibitors targeting this

protein. Investigating the modulation of α -catulin might shed light into exploiting other molecules regulating α -catulin which may be further extended to targeted therapy.

CHAPTER 4: MATERIALS AND METHODS

Chapter 4: Materials and Methods

Cell lines

HNSCC cell lines were obtained from sources outlined in (Zhao et al., 2011) and were Short Tandem Repeat (STR) profiled for authenticity. Zhao and colleagues have described the assembly, characterization and STR profile of all these cell lines which is outlined in Table 2. All cells were cultured in DMEM complete media containing 10% FBS, Penicillin/Streptomycin, glutamate, non-essential amino acids, vitamins, pyruvate and Myco-Zap ®. Cells were incubated in a 37°C, 5% Carbon Dioxide incubator.

Cell line	Primary site	Age	Sex	TNM Stage	Primary Source
HN31	LN				Dr. John Ensley, Wayne State University
PJA34	OC	50	M		
UMSCC 47 (UM47)	OC	53	M	T3N1M0	Dr. Thomas E. Carey, University of Michigan
UMSCC 22A (UM22A)	HP	58	F	T2N1M0	Dr. Thomas E. Carey, University of Michigan
183	OP	54	M	T3N0M0	Dr. Peter G. Sacks, New York University
HN4	REC(L)	57	M	T2N0M0	Dr. D.M. Easty, Ludwig Institute of Cancer Research, London
CAL27		54	F	T2N1M0	
PCI15B	LN	69	M	T2N0M0	Dr. Theresa Whiteside, UPMC
UMSCC1	REC (OC)	73	M	T2N0M0	Dr. Thomas E. Carey, University of Michigan
JHU022	LN		M	T3N2B	Dr. David Sidransky, Johns Hopkins University

Table 2: HNSCC cell lines. LN: Lymph Node, OC: Oral Cancer, HP: Hypopharyngeal, OP: Oropharyngeal, L: Lungs

Western Blots

HNSCC cells were lysed with Radio Immune Precipitation Assay (RIPA) lysis buffer (Tris: 50mmol/L, NaCl: 150mmol/L, EDTA: 1mmol/L, NP-40: 1%, SDS: 1%, deoxycholate: 0.5%, glycerol: 10%, mercaptoethanol: 10%, NaF: 10mmol/L, orthovanadate: 1mmol/L, pyrophosphate: 2.5 mmol/L and protein inhibitors). After lysing, cells were subjected to sonification and then allowed to solubilize in the buffer for 30 min. The lysates were then centrifuged at 14,000 rpm at 4°C for 30 min after which the supernatant was collected. Protein quantitation was performed using the Pierce™ BCA protein assay kit (ThermoFisher Scientific). The protein lysate after the protein assay was mixed with 5% β-mercaptoethanol and SDS and loaded onto either 7.5% or 4-

20% gradient gels (Mini-PROTEAN[®] TGX Pre-Cast protein gels) based on the size of the protein blotted. Gels were run using 10X premixed electrophoresis buffer containing 25mM Tris, 192 mM glycine and 0.1%SDS at pH 8.3 mixed with double distilled water at 80-110 V for 2-2.5h. Gels were then transferred on nitrocellulose membranes using 10X premixed transfer buffer containing 25mM Tris, 192 mM glycine and 20% methanol at pH 8.3 either for 2h or overnight at 4⁰C at 100 V. After transfer, the membrane was blocked using 5% milk-TBST for 2 hours with constant movement. The membrane was then incubated with the primary antibody at concentrations ranging from 1:100- 1:1000 depending on the antibody overnight at 4⁰C with constant movement. After incubation, the membrane was washed for 5 min. with TSB buffer containing 0.1% Tween-20 about 5 times. Secondary antibody containing species-specific Horseradish peroxidase-conjugated antibody for 1h at room temperature with constant movement. Protein signals were developed using SuperSignal West chemiluminescent system (Pierce[®] Biotechnology) on an X-ray film.

Plasmids

Intracellular NOTCH1 (ICN1)

Plasmids encoding the activated forms of NOTCH1 and NOTCH2 were obtained from Dr. Patrick Zweidler-McKay's lab. ICN1-MigR1 was constructed by sub cloning the ICN1 region (codons 1770-2555) of the human total NOTCH1 (W. S. Pear et al., 1996) into the BgIII site of MigR1 (W. S. Pear et al., 1998). This is a bicistronic vector that co-expresses GFP after the Internal Ribosome Entry Site (IRES) providing a surrogate marker for gene expression.

CRISPR-Cas9 plasmids

CRISPR-Cas9 NOTCH1 and NOTCH2 plasmids were obtained from Santa Cruz Biotechnology (sc400167). Each plasmid contained a pool of three plasmids, encoding the Cas9 nuclease and a target specific 20 nucleotide guide RNA (gRNA) for maximum knockout efficiency. CRISPR-Cas9 plasmids for NOTCH1 and NOTCH2 were transfected into PJA34 cells and sorted to obtain a pure population of GFP positive cells. Knockout was confirmed by western blotting for total NOTCH1, Cleaved-NOTCH1 and total NOTCH2.

NOTCH1 Full Length (NFL1)

The full length NOTCH1 cDNA was obtained from Origene that was initially untagged and cloned into a pCMV6-XL6 vector. We obtained the MigR1 empty vector (6.5 kb) from Dr. Patrick Zweidler-McKay's lab. We cloned NFL1 (7.3 kb) into the MigR1 vector. The MigR1 vector was first digested with BglII and EcoR1 restriction sites to insert a Multiple Cloning Site (MCS) containing the restriction sites for MfeI and XhoI. This is because NFL1 lacked a BglII restriction site but had an MfeI site. Since MfeI and EcoR1 contain compatible cohesive ends, we swapped the MCS on MigR1 with another one that contains MfeI and XhoI restriction sites. We then cleaved the MigR1 construct with MfeI and XhoI and cleaved the NFL1 with EcoR1 and XhoI and ligated the two constructs to engineer a MigR1-NFL1 (13.8 kb) construct.

Short Hairpin RNA's for AXL and α -catulin

Several of the shRNA's were obtained from Dharmacon (GE Life Sciences) through the shRNA and ORFeome core facility at M.D. Anderson Cancer Center. We obtained four shRNA's for each gene: AXL and CTNNAL1. The mature antisense sequences for AXL are:

- 1) AACTTAGATGCTTAGGATC
- 2) TGATAGCTAAGAAGGAGAG
- 3) TGAGGATGGAGTCGTCCTG
- 4) TCTTTGAAACCTAGAACCT

The mature antisense sequences for CTNNAL1 are

- 1) ATCTTTATGATTAATAAGC
- 2) TCAATGACCTTATCCAATG
- 3) TATTTCAGAGGTTCTGTC
- 4) TCCAATGCCACTTTCATAC

Each shRNA was cloned into pGIPZ lentiviral vector driven by a human CMV promoter that also harbors a GFP construct before the IRES sequence. In addition, these lentiviral vectors carry a gene encoding N-acetyl transferase mediating puromycin resistance.

HES2 and HES5

HES2 and HES5 gene constructs were obtained from Dr. Patrick Zweidler-Mckay's lab and subcloned into a MigR1 vector.

Transfections

Retroviral transfections were performed in HEK-293GP2 cells. Cells were plated at a density of 6 million cells on the day before transfection. On the day of transfection, 10.8 µg plasmid was used with 1.2 µg of packaging plasmid, VSV-G (Dr. Zwediler-McKay's lab) suspended in Serum free DMEM media. In a separate tube, Genjet was suspended in serum free DMEM media and later mixed with the tube containing the plasmid and VSVG. The Genjet-plasmid complex was incubated at room temperature for 20 min. before addition to HEK 293-GP2 cells. After adding the complex to the cells, they were incubated at 37°C, 5% CO₂ incubator for 45 min. after which complete media was added. About 8h after incubation, the media was replaced with complete media and incubated in a 33°C 5% CO₂ incubator for 48-72h. Viral supernatants were collected at 48h and 72h time points.

Lentiviral transfections were performed using HEK 293 F17 cells. Cells were plated at a density of 6 million cells the day before transfection. On the day of transfection, 10 µg of DNA, 5µg of envelope plasmid, pMD2.G (addgene) and 5 µg of packaging plasmid pCMV-dr8.2 dvpr (addgene) were mixed in Opti-Mem Reduced Serum Media (gibco, Life technologies). In a separate tube, Lipofectamine 2000 (ThermoFischer Scientific) was mixed with Opti-Mem Reduced Serum Media and incubated at room temperature for 10 min. Plasmid-lipofectamine complex was then allowed to form for 45 min. at room temperature after which this complex was added to cells. About 8h after transfection, media was replaced with complete media with serum and incubated in a 37°C 5% CO₂ incubator for 48-72h. Viral supernatants were collected at 48h and 72h time points

Retroviral infections

Retroviral infections were performed on adherent cells plated a day before infection. Briefly, 300,000 cells were plated in each well of a six well plate before infections. On the day of the infection, 2 ml of the viral supernatant was added to the cells after removing the media. This was considered a 100% viral titer. Similar titers were made at 50%, 25%, and 12.5% by adjusting the amount of viral titer and media such that the total volume is 2ml in each well. To each well, 2 μ l of polybrene (1 mg/ml. Santa Cruz Biotechnology) was then added. The six well plates were then centrifuged at 12,000g for 1.5 hr at room temperature and incubated at 37°C for 48-72h.

Lentiviral infections

Lentiviral infections were performed on non-adherent cells on the day of infection on 10 cm tissue culture plates. Briefly, 1.5 million cells were suspended in 1ml of complete media after which 5 ml of viral supernatant was added and plated on 10 cm dishes. This was considered a 100% viral titer. Similar titers were made at 50%, 25%, and 12.5% by adjusting the amount of viral titer and media such that the total volume is 6 ml in each 10 cm plate. Each well also had 2.4 μ l of polybrene. After transduction, plates were incubated at 37°C for 12-14h before media was changed to complete media and incubated for an additional 48-72h.

Clonogenic assays

Clonogenic assays were conducted on 6-well plates. The plating efficiency was determined for each HNSCC cell line by seeding the cells at different densities in the wells and allowing them to form colonies over a 10-14 day period. Roughly, 1000-2000

cells per well were found to be good plating numbers for cell lines used in this assay. After transduction, cells were sorted for GFP positive cells by flow cytometry and allowed to recover for 48h. Post recovery, cells were plated at a density of 1000 cells per well and incubated in a 37°C, 5% CO₂ incubator. About 10-14 days after plating, cells were washed with PBS twice after removing the growth media and stained with crystal violet (0.5% w/v) for 5 min. Cells were washed again with water and colonies were observed under a microscope. A colony was marked if it contained at least 50 cells. By visual observation, we recorded one colony per well containing 50 cells and set that colony as the threshold for colony number and size. Later, using the Image J software (NIH), we measured the size of the marked colony and excluded any colonies that were smaller than the threshold. Such an analysis allowed us to measure both colony number and colony size at the same time.

Quantitative Real Time PCR (qRT-PCR)

Total RNA was extracted using RNAqueous[®] - 4PCR DNA-free RNA isolation kit (Ambion, Life technologies). Briefly, cells were scrapped using a scraper after adding the guanidinium lysis buffer solution. The sample lysate was then mixed with ethanol and applied to a silica-based filter. This filter selectively and quantitatively binds mRNA and larger rRNA. Small RNA's such as tRNA and 5S rRNA are not bound. The filter is washed to remove residual DNA, protein and other contaminants and the RNA is eluted in nuclease-free water containing EDTA. Post elution from the filter, the RNA was treated with ultra-pure DNase 1 to remove any trace amounts of DNA. Finally, using the DNase Inactivation agent, Dnase and divalent cations are removed. RNA concentration was measured using NANODROP 2000 spectrophotometer (Thermo Scientific). cDNA

was prepared by reverse transcription using SuperScript ® First-Strand synthesis (Invitrogen, Life Technologies) in a Veriti Dx 96-well thermal cycler (Applied Biosystems, Life technologies) according to the manufacturer's instructions that included temperature cycles ranging from 4⁰C to 70⁰C. FAM-MGB TaqMan PCR primers and probes specific for HES1, HES2, HES3, HES4, HES5, HEY1, HEY2 and GAPDH were purchased commercially (ThermoFisher Scientific). A total of 100ng of cDNA was used per reaction and each reaction was measured in quadruplets using a c1000 Bio-Rad Thermal Cycler (Bio-Rad). The expression of each target gene was normalized against GAPDH that was calculated by the $\Delta\Delta CT$ method ($\Delta\Delta CT = [\Delta CT \text{ of target gene}] - [\Delta CT \text{ of internal control gene (GAPDH)}]$) and the fold change of expression was calculated using the comparative CT method, $2^{(-\Delta\Delta CT)}$

Jagged1 and Fc immobilization

Recombinant human Jagged1-Fc chimera was bought from R&D Biosystems. Recombinant Jagged1 was dissolved in PBS and sterile filtered using 0.22 μm syringe driven filters (Millex ®- GV). Before coating six well plates with Jagged1 or human IgG-Fc (control), 1 mg/ml of protein G, (PROSPEC) was added to 1.5 ml of PBS in each well and incubated at room temperature overnight. Next day, plates were washed with 2ml of PBS and blocked with 1% Bovine Serum Albumin (Rockland Immunochemicals) dissolved in PBS for 2h. Plates were then washed with PBS and coated with 10 $\mu\text{g/ml}$ of recombinant Jagged1 or Fc and incubated either at room temperature for 3.5h or overnight at 4⁰C to allow immobilization of Jagged1 or Fc onto the surface after which cells were cultured on Jagged1 or Fc coated plates. Cells were plated at a density of

300,000 cells/well for western blot and harvested 72h later or 1000-2000 cells/well for a clonogenic assay.

Competitive Cell Proliferation Assay

ICN1 and MigR1: Cells were plated at a density of 300,000 cells/ well in six well plates a day before transduction with ICN1 or MigR1. Retroviral infections were performed at a low Multiplicity Of Infection (MOI) such that only 30-50% of the cells are infected with either ICN1 or MigR1. After transduction, cells were allowed to grow for 72h after which cells were trypsinized. Post trypsinizations, a fraction of the cells were analyzed for GFP by flow cytometry (100,000 cells with the use of FL1; BD FACS Calibur) while the rest were plated at a density such that they can be sequentially passaged every three days for two weeks. FlowJo Software (TreeStar Inc) was used to calculate the percentage of GFP positive cells in the mixed population.

NFL1: Cells were plated at a density of 300,000 cells per well in six well plates before transduction with NFL1. Similar to ICN1 and MigR1, cells were infected at a low multiplicity of infection such that only 30-50% of the cells are infected with NFL1. Three days post infection, cells were plated on immobilized Jagged1, Fc or uncoated plates. Seventy two hours after culturing on immobilized ligand coated plates, cells were trypsinized and a fraction of cells was analyzed by flow cytometry (100,000 cells) while the rest were replated on Jagged1, Fc or uncoated plates for another three days. FlowJo Software (TreeStar Inc) was used to calculate the percentage of GFP positive cells in the mixed population.

Cell Cycle Analysis

Cell cycle assessment was performed on XL flow cytometer or FACS Calibur or FACS Fortessa analyzer. The cell cycle data was analyzed on FlowJo software.

Senescence

After transduction and flow sorting, cells were plated at a density of 2000 cells per well in a 6-well plate and allowed to attach overnight. At day 4 or 6, cells were exposed to a fixative for 10 minutes, washed again with PBS and incubated with 1ml senescence staining solution overnight at 37°C.

Orthotopic Mice injections

The Institutional Animal Care and use Committee (IACUC) of the University of Texas MD Anderson Cancer Center approved all animal experimentation. Our orthotopic nude mouse tongue model has been previously described in the literature. Nude mice were obtained from Jackson Laboratories and acclimatized for 2 weeks prior to injections. HNSCC cell lines HN31, UM47 and PJA34 were transduced with ICN1, NFL1, MigR1 or dnMAML1 and sorted for GFP positive cells by flow cytometry. Prior to sorting, cells were optimized using variable titers for the intensity of GFP and percentage of viable cells such that all viral titers were matched equally. Cells were allowed to recover for 48h prior to mice injections. 50,000 cells were then injected in the dorsal tongue of mice in a volume of 30 ul of Serum free DMEM media. Mice were examined twice a week for 4 weeks where tumor size and weight loss were assessed and recorded. Tongue tumors were measured with microcalipers, and tumor volume calculated as $(A)(B^2)\pi/6$, where A is the longest dimension of the tumor and B is the

dimension of the tumor perpendicular to A. At the end of study, mice were euthanized by CO₂ asphyxiation when they lost more than 20% of their preinjection body weight or 30 days following the initiation of treatment. For immunohistochemical analysis, mice were sacrificed and tongue tumors were collected. Tissues were then fixed in 4% paraformaldehyde, paraffin-embedded, sectioned and stained with hematoxylin and eosin (H&E). Tumor growth and overall survival was measured until mice were sacrificed and plotted using Graphpad Prism.

Unbiased gene expression analysis

Three biological replicates of two HN cell lines, PJA34 and 183, were treated with Jagged ligand or control, Fc for 5 days. Table 3 contains detailed sample information.

Gene expression was measured by Affymetrix HuGene 2.0 ST array.

Sample	Cell line	Comment
PJA 34 on Jagged1 (A)	PJA34	Treated
PJA 34 on Jagged1 (B)	PJA34	Treated
PJA 34 on Jagged1 (C)	PJA34	Treated
PJA34 on Fc (A)	PJA34	Control
PJA34 on Fc (B)	PJA34	Control
PJA34 on Fc (C)	PJA34	Control
183 on Jagged1 (A)	183	Treated
183 on Jagged1 (B)	183	Treated
183 on Jagged1 (C)	183	Treated
183 on Fc (A)	183	Control
183 on Fc (B)	183	Control
183 on Fc (C)	183	Control

Table 3: Sample description

All the data pre-processing steps have been done by the Department of Bioinformatics at M.D. Anderson Cancer Center by Dr. Jing Wang's team. A linear model was fit to each probeset with both treatment and cell line as fixed effects. Therefore, we started with their preliminary result. Based on these raw p-values, we modeled them using a beta-uniform mixture (BUM) mode to generate different p-value cut offs based on selected false discovery rates (FDR). Based on the identified significant differentially expressed probesets using the FDR of 0.05, we assessed concordance correlation of multiple probesets that map to the same gene, and selected only one probeset for each gene if their expression is inconsistent, and averaged the expression of those probesets if their expression is consistent. Therefore, we generated one record for each gene. The RNA-seq data include 279 TCGA Head and Neck cancer patient samples. The 131 genes of interest were originated from the significant gene list from the comparison of JAG treated and control HN cells based on Affymetrix HuGene 2.0 ST array data. The TCGA RNA-seq data were downloaded from Broad firehose and have already been processed with RSEM and normalized. We read in the TCGA RNA-seq data and the genes of interest. We added 1 to the data and did log2 transformation. Then, we accumulated the data into the one with the expression of the interested genes. There were 131 genes of interest, but we can only find 118 genes that matched in the TCGA data. We then produced heat maps with Pearson distance and ward linkage based on the data with 279 samples and 118 genes.

Antibodies

The antibodies used in this project is outlined in Table 4:

Antibody	Source	Catalog number	Concentration	Diluent
Total-NOTCH1	Santa Cruz	sc 6014	1 to 750	2.5% Milk-TBST
Total-NOTCH2	Santa Cruz	sc 5545	1 to 750	2.5% Milk-TBST
Cleaved-NOTCH1	Cell Signaling	D3E8	1 to 750	2.5% Milk-TBST
P21	CalBioChem	OP64	1 to 1000	5% BSA-TBST
Δ NP63	Santa Cruz	Sc 8431	1 to 1000	2.5% Milk-TBST
AXL	Cell Signaling	C89E7	1 to 1000	2.5% Milk-TBST
Phospho-AXL	Cell Signaling	D12B2	1 to 1000	2.5% Milk-TBST
Gas6	Santa Cruz	sc 1936	1 to 1000	5% BSA-TBST
A-catulin	Santa Cruz	sc 390584	1 to 1000	2.5% Milk-TBST
Flag	Cell Signaling	2368S	1 to 1000	2.5% Milk-TBST
HES5	AbCam	Ab25374	1 to 100	5% BSA-TBST
Actin	Sigma	A1978	1 to 2000	5% BSA-TBST

Table 4: Antibodies description

Statistical Analysis

The Student t and a one-way ANOVA tests were carried out to analyze in vitro data. For mouse studies, a 2-way ANOVA test was used to compare tumor volumes between control and treatment groups. All data were expressed as mean \pm standard error, and $P < 0.05$ was considered significant

CHAPTER 5: ACTIVATION OF NOTCH SIGNALING INHIBITS GROWTH

Chapter 5: Activation of NOTCH signaling inhibits growth

Parts of this chapter are adapted from my previous co-author publication in *Cancer Discovery* in 2013 (Pickering et al., 2013). According to the journal: “**Authors** of articles published in AACR journals are permitted to use their article or parts of their article in the following ways **without** requesting permission from the AACR. All such uses must include **appropriate attribution** to the original AACR publication. Authors may do the following as applicable: Submit a copy of the article to a doctoral candidate's university in support of a doctoral thesis or dissertation”

Chapter 5.1: NOTCH1 mutational status in HNSCC cell lines

Rationale: NOTCH1 is mutated at a frequency of 15-19% (Agrawal et al., 2011; Stransky et al., 2011; "TCGA Releases Head and Neck Cancer Data," 2015). To explore the mutation rate of NOTCH1 in cells, our lab had previously sequenced a panel of 44 HNSCC cell lines that had previously been characterized for TP53 mutations and tumorigenicity (Sano et al., 2011; Zhao et al., 2011). The spectrum of homozygous mutations found in NOTCH1 closely mirrored previously sequenced tumors (Agrawal et al., 2011). Table 5 lists sequencing results for some HNSCC cell lines that included nonsense mutations (UMSCC47, UMSCC22A, PCI15B), a frame shift (HN4), and a C478F missense mutation (HN31), which corresponds to an amino acid critical for ligand binding. However, expression of NOTCH1 at the translational level was not established. In order to validate the sequencing studies, we evaluated total-NOTCH1 protein expression levels

Results: We performed a western blot to evaluate the NOTCH1 protein expression levels in wild-type and mutant cell lines based on Sanger sequencing (Figure 8). Cell lines that were wild-type for NOTCH1 (PJA34, 183, CAL27, UMSCC1 and JHU022) expressed the total-NOTCH1 protein, while cell lines mutant for NOTCH1 (HN4, UMSCC22A, UM47 and PCI15B) did not express the protein. HN31 has a C478F missense mutation and expresses total NOTCH1 but the mutation prevents NOTCH1 from being activated. The results from the western blot corroborate with sequencing studies and provided us an *in vitro* model system to manipulate the phenotypic effect of NOTCH1.

Cell Line	NOTCH1
UM47	G192X
HN4	A343Fs
HN31	C478F ms
UM22A	E1679X
PCI15B	Q1957X
PJ34	Wt
CAL27	Wt
183	Wt
UMSCC1	Wt
JHU022	Wt
NOM9	Wt

Table 5: NOTCH1 status in HNSCC cell lines

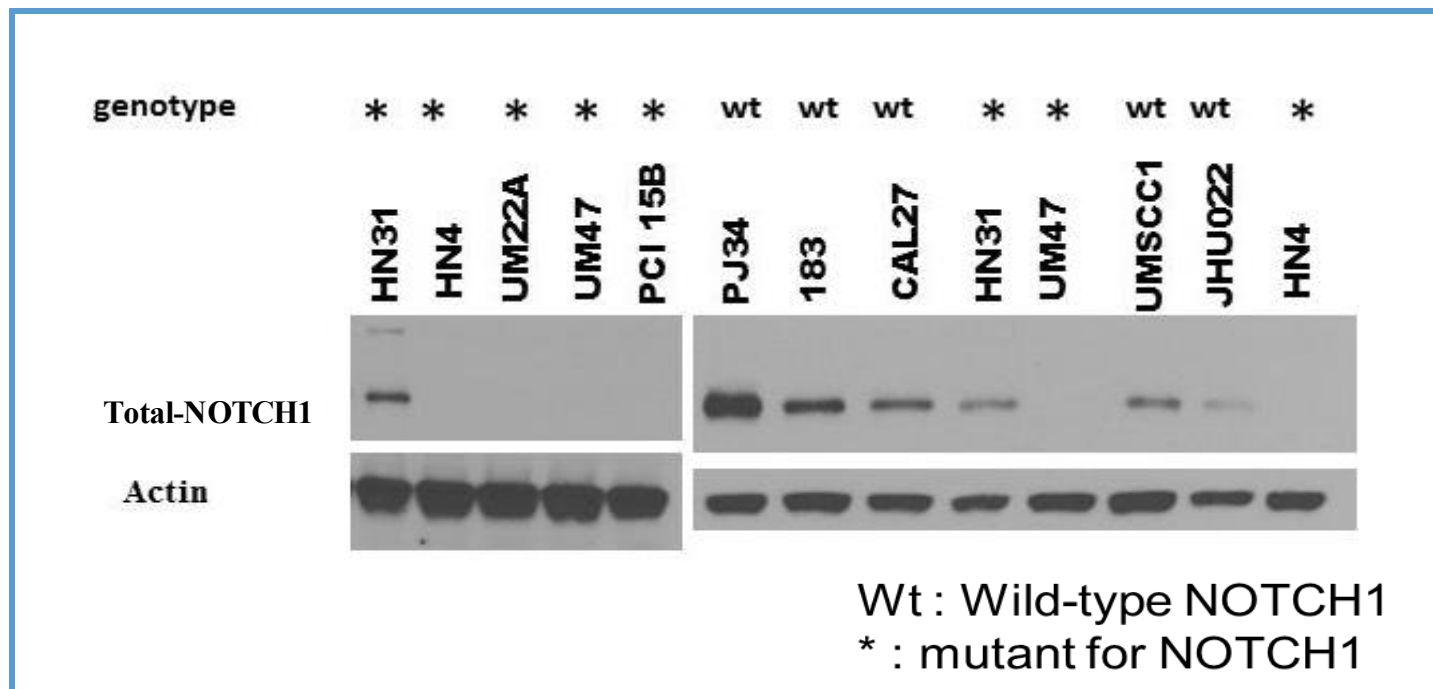


Figure 8: NOTCH1 protein expression levels in HNSCC cell lines

Chapter 5.2: Activation of NOTCH1 in mutant HNSCC cell lines is detrimental to cell growth

Rationale: NOTCH1 is mutated in about 15-19% of HNSCC (Agrawal et al., 2011; Stransky et al., 2011; "TCGA Releases Head and Neck Cancer Data," 2015). HNSCC cell lines were previously classified as being mutant or wild-type from Sanger sequencing and protein expression levels. Based on the spectrum of mutations from sequencing studies, we know that a subset of HNSCC have an inactive NOTCH pathway. The functional relevance of these mutations has not been explored. Since mutant HNSCC cell lines have inactive NOTCH1, we sought to determine the phenotypic effects of restoring a functional NOTCH signaling pathway in these cells.

Results: Retroviral constructs of the intracellular forms of NOTCH1 (ICN1) that was cloned into a Murine Stem Cell Driven Vector (MSCV) IRES driven GFP vector called MigR1 (kindly provided to us by Dr. Zweidler-McKay) was engineered to overexpress the protein. Additionally, the full-length, wild type NOTCH1 receptor (NFL1) was cloned into the same parental retroviral vector (MigR1) (Figure 9). Mutant NOTCH1 bearing HNSCC cell lines HN31, HN4, PCI15B and UMSCC47 were infected with ICN1 or MigR1 at low multiplicity of infection such that only a small fraction of the infected population (20-50%) expressed the vector. Using this method, a mixed population of green and non-green cells was obtained and a competitive cell proliferation assay (also known as "horserace" assay) was performed. The fraction of green cells in the mixed population was monitored by flow cytometry and recorded every 3 days. The cells were sequentially passaged such that some cells were evaluated for GFP by flow analysis and the rest were cultured for another three days. By doing so, the modulation in GFP

positive population could be monitored over a 15-day period. The population of cells expressing GFP was normalized to day three after infection. The fraction of cells having ICN1 (green cells) progressively declined after infection (Figure 10). At day 15, the relative fraction of ICN1 cells had been reduced to 40% of its initial value. This suggested that the population of cells having ICN1 was selected against those cells that do not express the protein, implying that the activation of NOTCH1 in mutant HNSCC cells could be disadvantageous to their growth and proliferation. Moreover, the morphology of cells infected with ICN1 was vastly different from cells infected with MigR1. Some of these cells were smaller, circular and had a flattened morphology reminiscent of senescent cells, while others were rounded and spheroid in shape that eventually detached from the substrate (Figure 11).

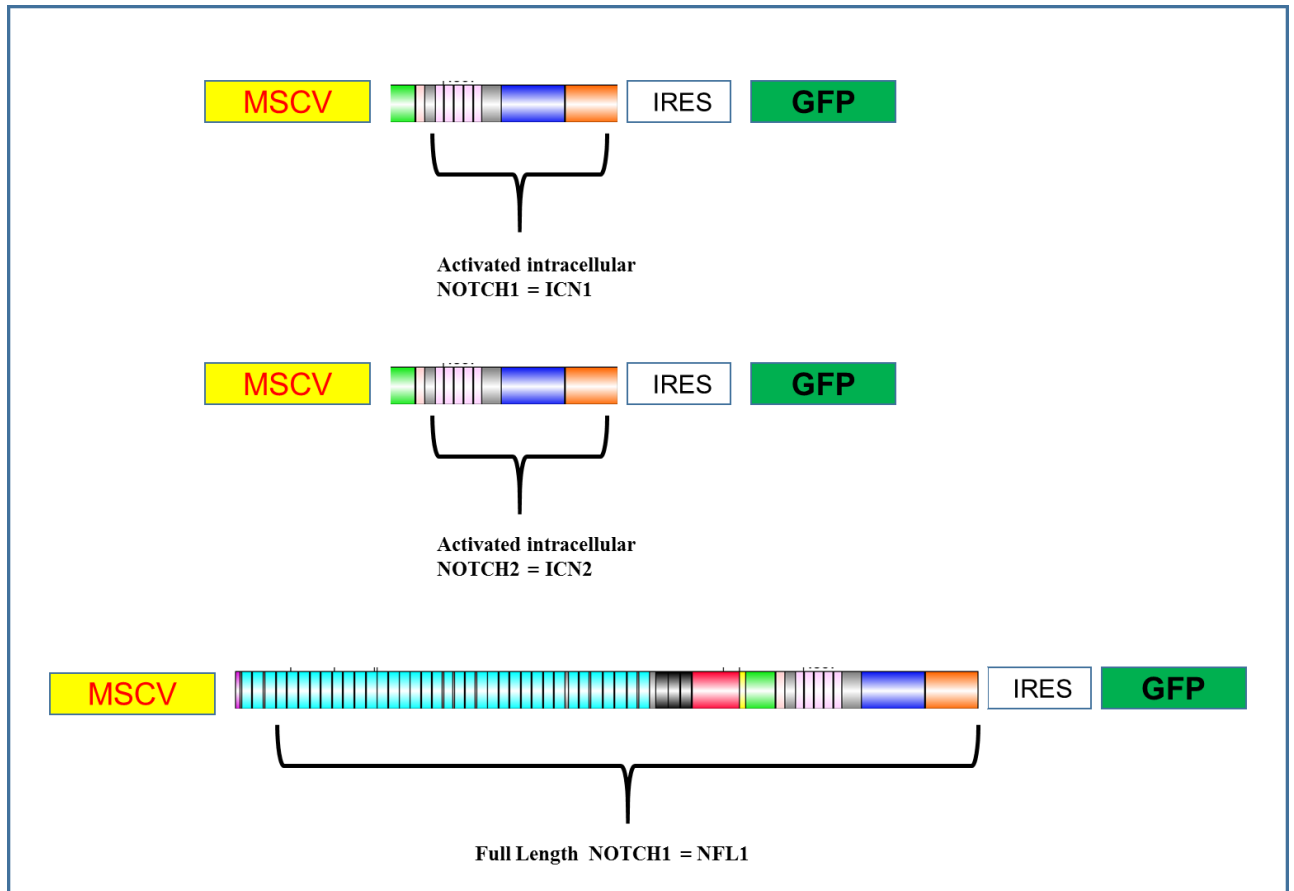


Figure 9: Retroviral constructs of ICN1, ICN2 and NFL1

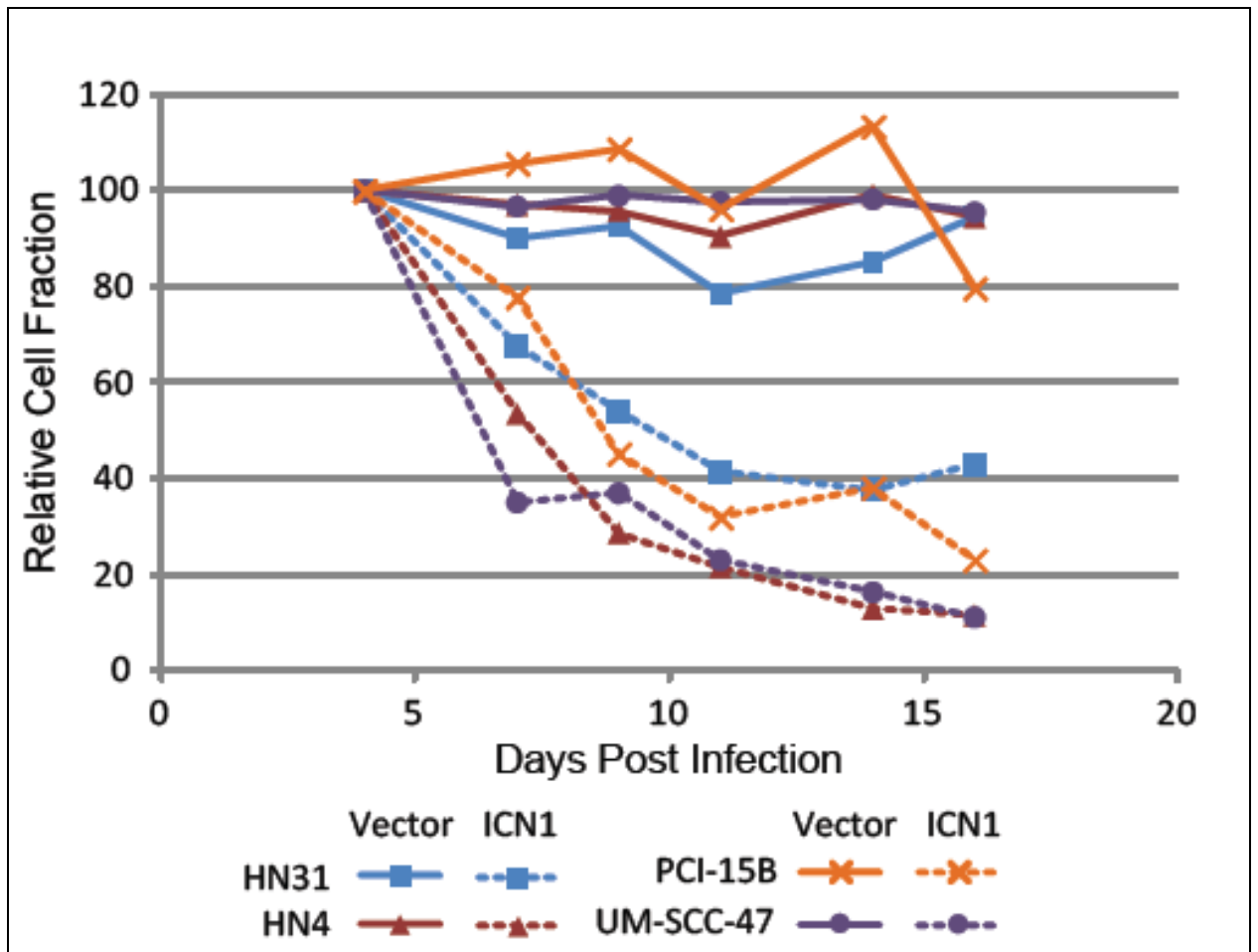


Figure 10: Intracellular *NOTCH1* is disadvantageous to the growth of mutant HNSCC cells.

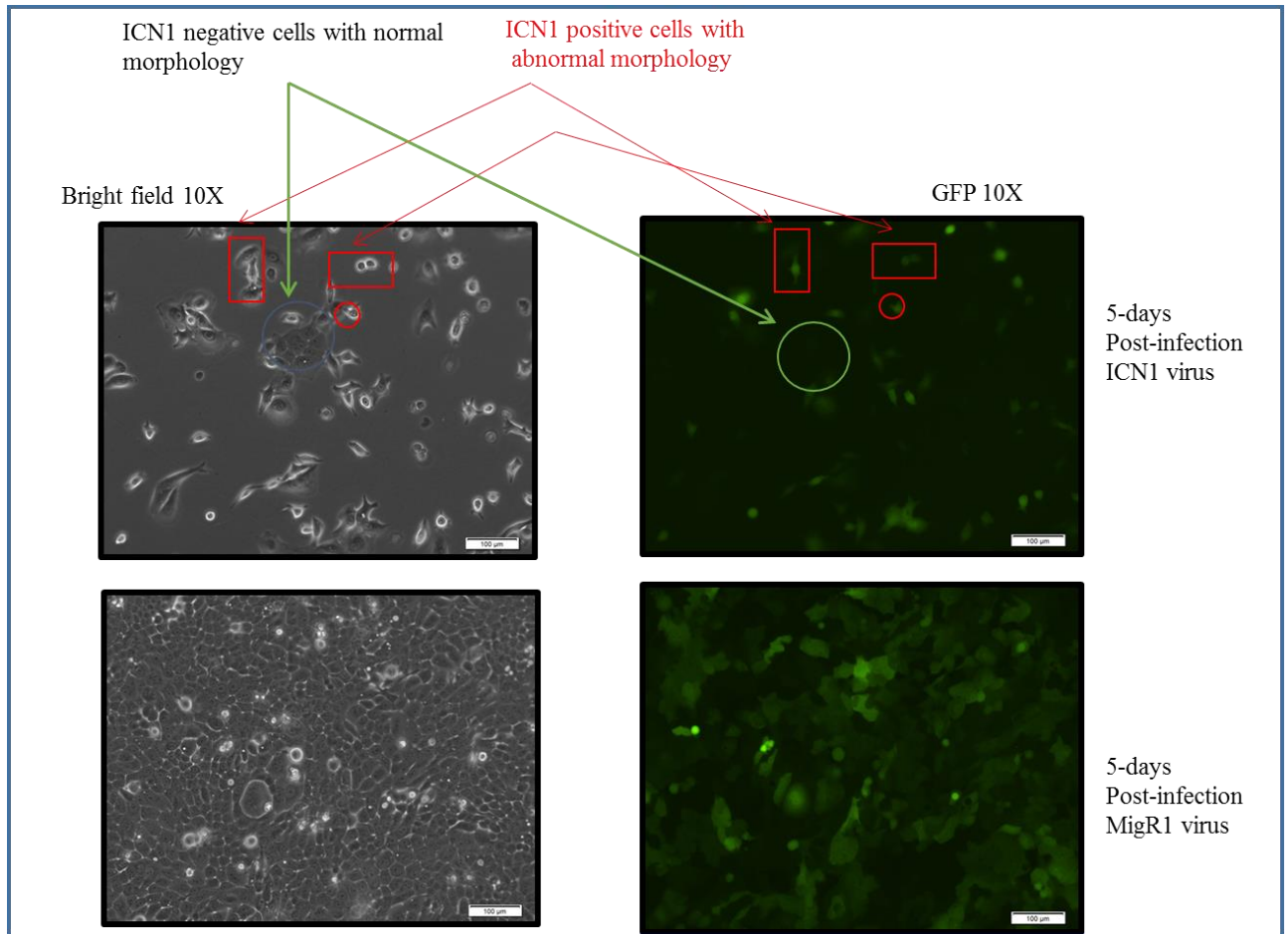


Figure 11: ICN1 infected mutant HN31 cells are smaller and rounder and some have a flattened package-like morphology compared to cells infected with the empty vector MigR1.

Chapter 5.3: NOTCH1 activation appears to induce senescence and G1 growth arrest

Rationale: Inhibition of cell growth can be attributed to various factors such as cell death (apoptosis/necrosis), senescence, cell cycle arrest or mitotic catastrophe. Since growth inhibition was found in mutant cells after restoration and activation of NOTCH1, the phenomenon governing the growth arrest was evaluated in these cells. In esophageal squamous cell carcinoma (ESCC), Kagawa et al. demonstrated that the activated form of NOTCH1 (ICN1) induced cellular senescence corroborated by G0/G1 cell cycle arrest, flat and enlarged morphology and senescence associated β -galactosidase activity (Kagawa et al., 2015). Based on morphology, some cells appeared to have an enlarged, flat, and pancake-like structure, while some cells exhibited a spheroid apoptotic-like morphology after restoring ICN1 in mutant HNSCC cell lines.

Results: To evaluate senescence, mutant cells expressing ICN1 and/or MigR1 were evaluated for β -galactosidase using immunohistochemistry. Nearly 30% of the HN31 ICN1 cells stained positively, indicating that some of these cells do undergo senescence (Figure 12). Furthermore, western blotting performed three days and five days after infection with ICN1 or MigR1 revealed increased expression of p21 (marker for senescence) only in the NOTCH1 mutant cells infected with ICN1 (Figure 13). Cell cycle analysis demonstrated that the ICN1 infected cells were arrested in the G1 phase of the cell cycle relative to the MigR1 infected cells (Table 6). In addition, a small percentage (15%) of the cells were also present at the sub-G0 phase indicating that some of these cells undergo apoptosis. Taken together, senescence, cell cycle arrest and apoptosis appear to contribute to the delayed growth in NOTCH1 infected cells.

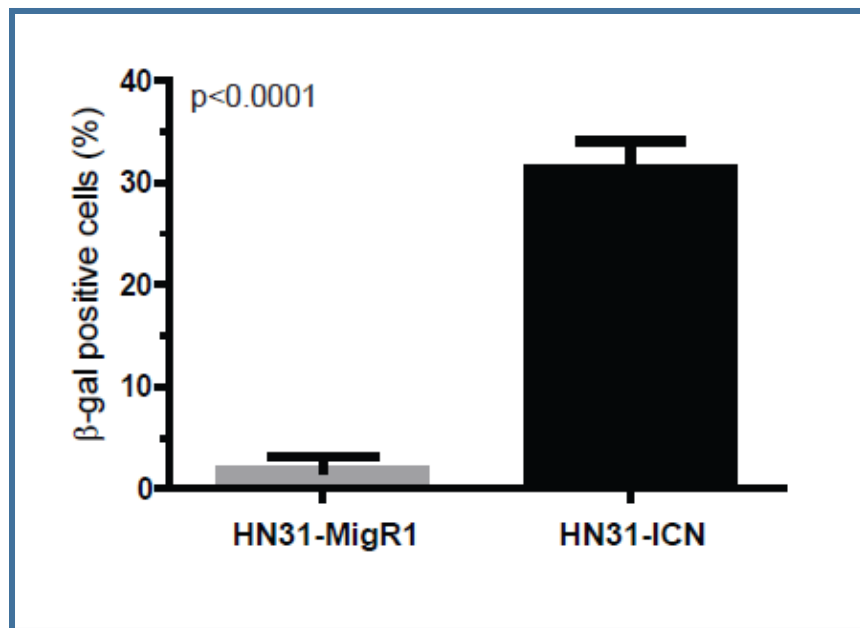
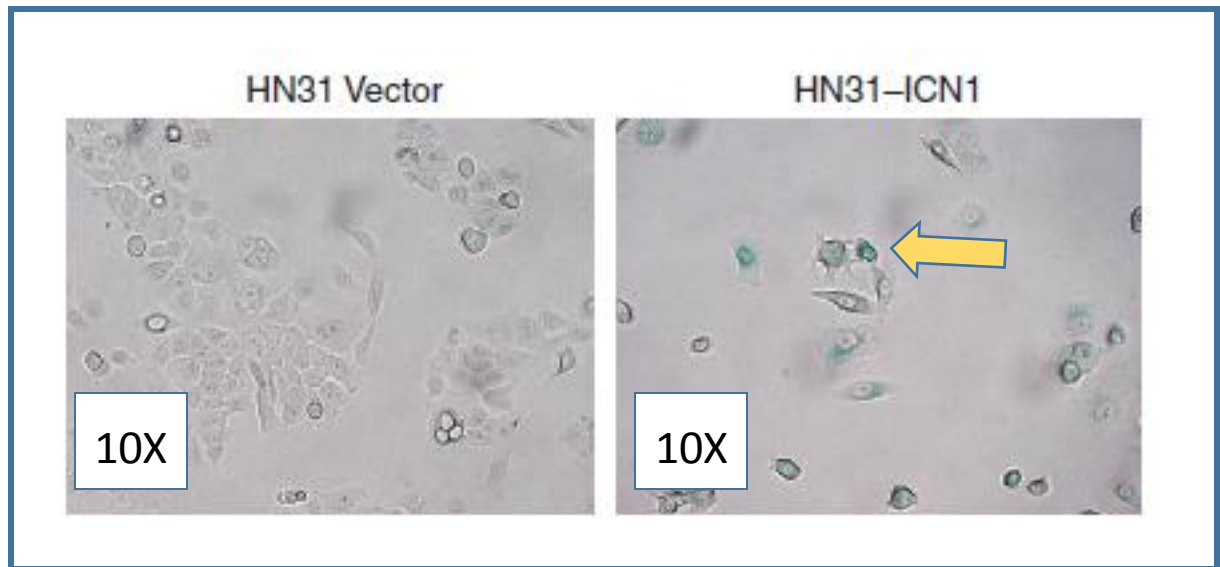


Figure 12: Mutant HNSCC cells HN31 undergoes senescence after restoring the activated form of NOTCH1 (ICN1).

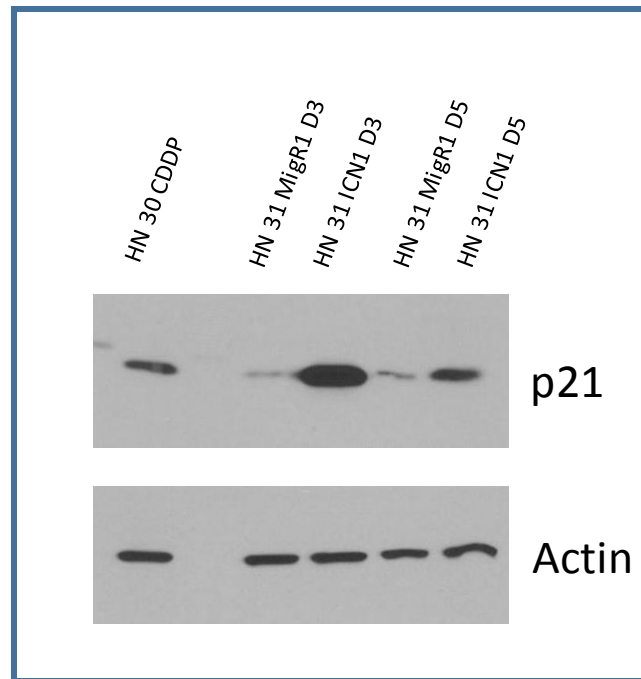


Figure 13: Induction of p21 (a marker for senescence and cell cycle arrest) in HN31 cells infected with ICN1 but not MigR1 at two different time points (D3= Day 3 post infection and D5=Day 5 post infection)

Cell-cycle phase	Vector	ICN1
G ₁	26	67
S	30	3
G ₂ -M	35	12
Sub-G ₁	0	15

Table 6: ICN1 cells are arrested in the G1 phase of the cell cycle.

Chapter 5.4: NOTCH1 or NOTCH2 is possibly sufficient to inhibit cell growth

Rationale: NOTCH has four family members; NOTCH 1-4. Among the NOTCH family members, NOTCH1 is the most frequently mutated in HNSCC (15-19%), followed by NOTCH2 (2-5%) (Agrawal et al., 2011). NOTCH1 and NOTCH2 mutations are not mutually exclusive in HNSCC cells. Li et al. demonstrated deletions in the NOTCH2 genes in HNSCC cell lines and tumors (H. Li et al., 2014). Whether NOTCH1 and NOTCH2 contribute to similar phenotypes is currently unknown. To investigate if NOTCH2 had any effect on cell growth, the NOTCH1 mutant (HN31) and NOTCH wild-type cell lines (PJA34) were infected either with the empty vector-MigR1, activated form of NOTCH1 (ICN1) or activated form of NOTCH2 (ICN2).

Results: Cells were transduced and sorted for GFP positive cells such that the percentage and intensity of GFP was similar in all conditions. Forty-eight hours after sorting, cells were seeded at 1000 cells per well in 6-well plates for a colony forming clonogenic assay. After seeding, cells were evaluated for change in morphology every two days and stained with crystal violet after colony sizes reached about 50 cells in the control MigR1 plates (12 days after seeding). ICN1 and ICN2 alone were sufficient to inhibit cell growth compared to the empty vector (MigR1) and parental controls (Figure 13). Parental and MigR1 transduced cells had similar colony number 10 days after plating, but the colony number and size in cells transduced with ICN1 or ICN2 significantly declined by more than 90%. This suggests that ICN2 may also be sufficient to inhibit cell growth.

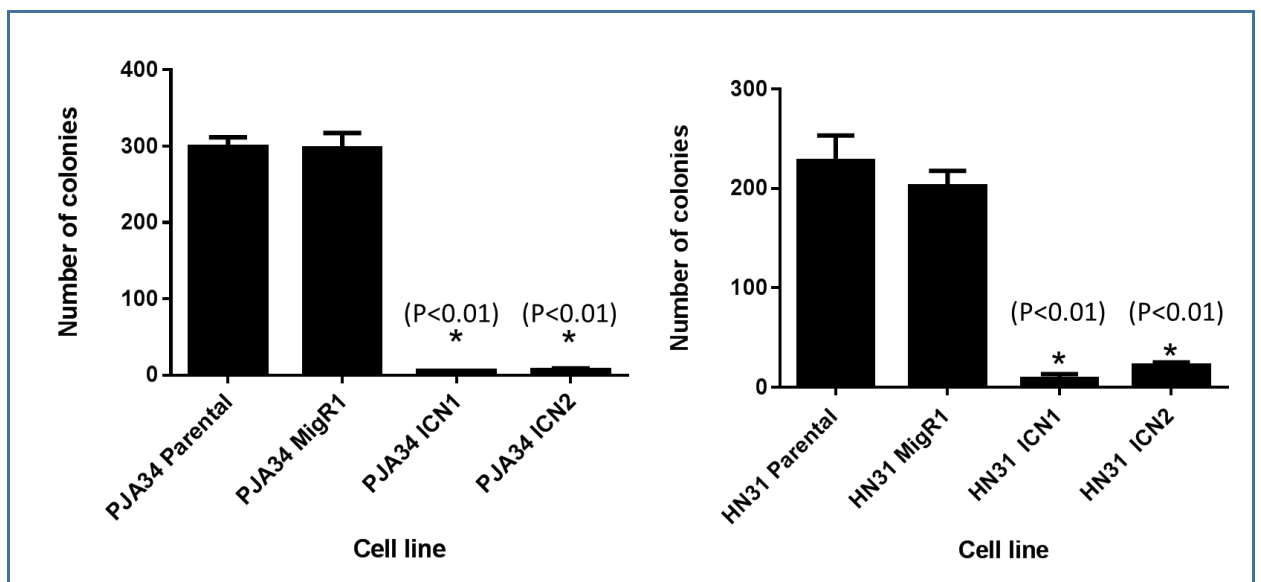


Figure 14: Activated *NOTCH1* or *NOTCH2* is sufficient to inhibit growth of HNSCC cell lines

Chapter 5.5: Restoration of full-length NOTCH1 is sufficient to inhibit cell growth

Rationale: Transducing cells with activated NOTCH1 is often not ideal since cells are subjected to non-physiological amounts of the protein. In other cancer types such as hepatocellular carcinoma (Qi et al., 2003), neuroblastoma (Zage et al., 2012) and B-ALL (Kannan et al., 2011), the activated form of NOTCH has been used to elucidate growth inhibitory phenotypes. Although such studies have demonstrated how NOTCH inhibits growth, to date, the impact of expression of the full-length NOTCH receptor on mutant NOTCH1 bearing cells has not been evaluated. To test this, the full-length NOTCH1 receptor was cloned in the retroviral system, and the impact of NOTCH1 signaling was evaluated by growing the cells on plates coated with the NOTCH ligand, recombinant Jagged1.

Results: NOTCH1 mutant cells HN31 and UMSCC 47 were infected at a low multiplicity of infection (MOI of 20% to 50%) with retrovirus bearing either full length NOTCH1 (NFL1-GFP) or the empty vector (MigR1-GFP) such that there was a mixed population of green and non-green cells. These cells were then cultured on the recombinant NOTCH ligand, Jagged1 that is fused to an Fc chimera and coated onto plastic cell culture plates. Jagged1 and Fc were coated on plates the day before seeding cells. As a control, cells were cultured on the Fc chimera coated plates that is not fused to Jagged1. Additionally, cells were also plated on plates without Jagged1 or Fc (Uncoated plates). A competitive cell proliferation assay was then performed by sequentially passaging these cells every three days on Jagged1, Fc or uncoated (UC) plates and analyzing GFP positive cell fraction by flow cytometry. The population of NFL1-GFP positive cells cultured on Jagged1 was suppressed by at least 50% relative to NFL1-GFP

cells cultured on Fc and uncoated plates (Figure 15Figure 16Figure 17). In sharp contrast, the fraction of cells infected with MigR1 remained relatively steady through the time course. Compared to MigR1 infected cells, all cells infected with NFL1 were selected against the mixed population of cells. This, in part, implies that signaling between NOTCH receptors and endogenous NOTCH ligands contributes to growth inhibition in NFL1 infected cells plated on Fc or uncoated plates. Taken together, these results suggest that restoration on NFL1 and possible activation of the NOTCH pathway by culturing these cells on Jagged1 is disadvantageous to the growth of these mutant cells. In order to investigate long-term growth of these cells, a colony forming clonogenic assay was performed in which HNSCC cells UM47, HN31 and HN4 were infected with NFL1 or MigR1 and sorted by flow cytometry to obtain a pure population of green cells. After sorting, these cells were cultured at a low density (1000 cells/well in 6-well plates) on Jagged1 or Fc coated plates for a 10-day period. The cells were then stained with crystal violet after 10 days and the number of colonies (a colony was defined as one having at least 50 cells) were counted. Mutant cells infected with NFL1 and cultured on Jagged1 were significantly growth inhibited compared to those cultured on Fc and the MigR1 infected controls (

Figure 18). Based on these findings, it was hypothesized that this inhibition in cell growth is mediated by the activation of NOTCH signaling. To test this, a western blot was performed on these mutant cell lines after infection with NFL1 or MigR1 and

culturing on Jagged1 or Fc. Mutant cell lines infected with NFL1 cultured on Jagged1 expressed high levels of cleaved (activated) NOTCH1, while cells infected with the empty vector did not induce cleavage of NOTCH1 (Figure 19). The presence of cleaved NOTCH1 only in mutant cell lines infected with NFL1 suggests that activation of the NOTCH signaling pathway contributes to the growth inhibitory phenotype. Maximal induction of cleaved NOTCH1 was observed in NFL1 infected mutant cells cultured on Jagged1, however, we also observed cleaved NOTCH1 induction in NFL1 infected cells cultured on Fc and uncoated plates as well. This confirms the phenotype previously seen in the competitive cell proliferation assays (Figure 15Figure 16Figure 17) that activation of the NOTCH pathway through endogenous ligand contributes to inhibition of growth. Previously, while using ICN1, we observed that mutant cells underwent senescence (Figure 12). We examined if a similar phenomenon also occurs after restoring the full-length NOTCH1 protein. Similar to our previous results, we observed that mutant cells with NFL1 cultured on Jagged1 stained positive for β -galactosidase indicating that restoration of NFL1 and activation of the pathway by Jagged1 in mutant cells possibly contributes to senescence mediated growth arrest. On the contrary, Jagged1 mediated senescence was not observed in MigR1 infected cells. Mutant cells infected with NFL1 cultured on Fc also did not exhibit a senescent morphology. Although these cells express modest cleaved NOTCH1 levels and are growth inhibited compared to MigR1 infected cells, it is possible that the expression levels of NOTCH1 was not strong enough to induce senescence.

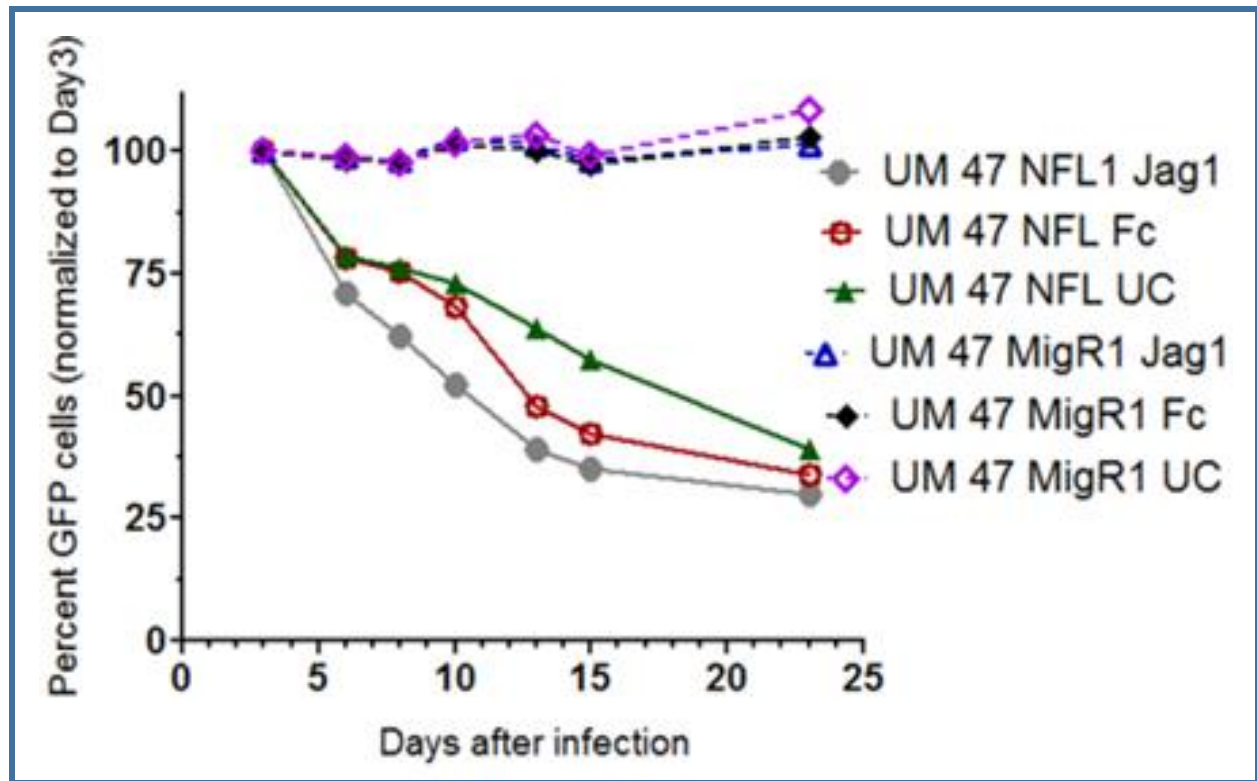


Figure 15: The fraction of mutant cells restored with NFL1 decreases progressively compared to cells infected with the empty vector. UM47 mutant cells infected with NFL1 is selected against a mixed population of NFL1 and non-NFL1 expressing cells while cells infected with MigR1 remains steady through the 23 day time period.

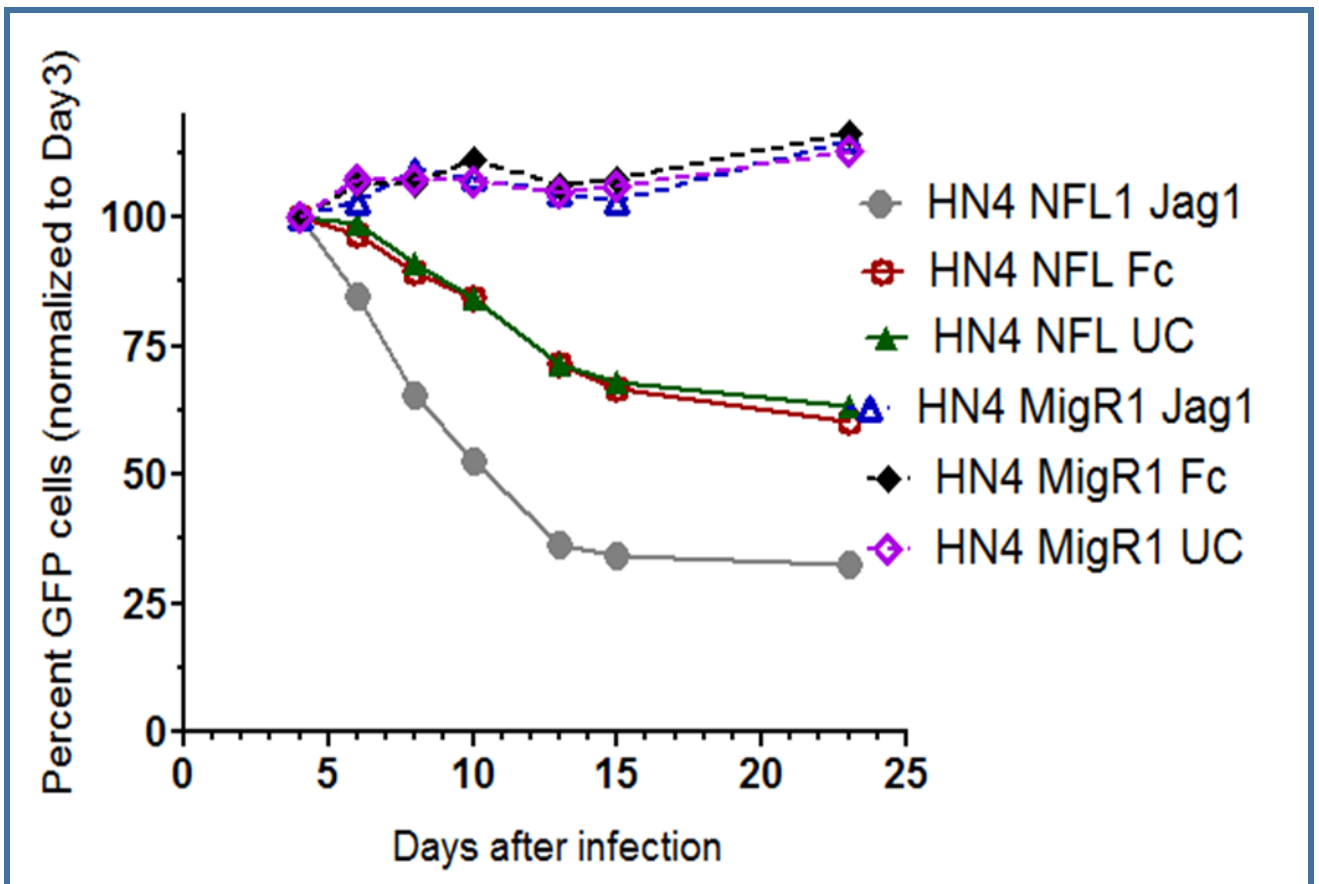


Figure 16: The fraction of mutant cells restored with NFL1 decreases progressively compared to cells infected with the empty vector. HN4 mutant cells infected with NFL1 is selected against a mixed population of NFL1 and non-NFL1 expressing cells while cells infected with MigR1 remains steady through the 23 day time period.

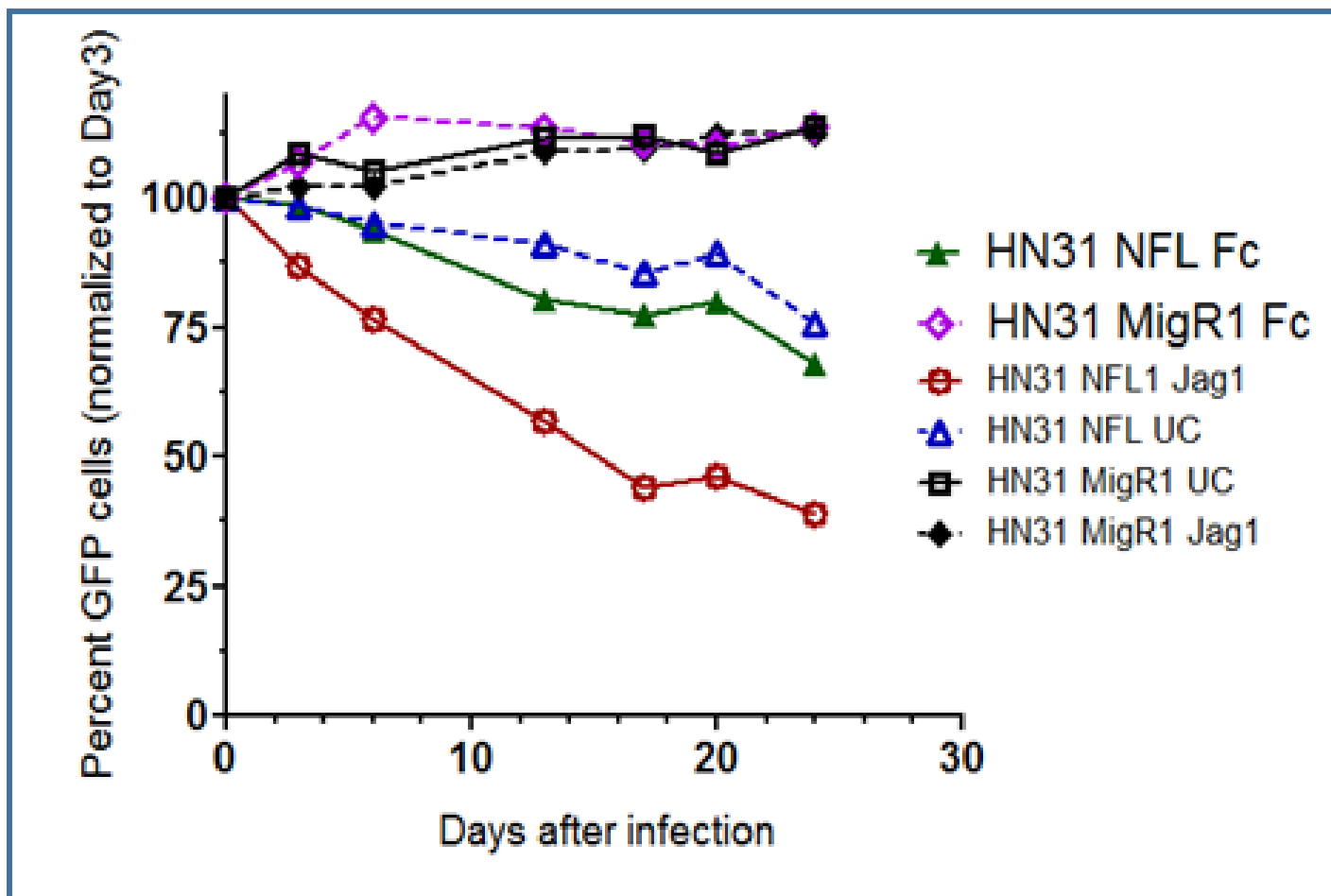


Figure 17: The fraction of mutant cells restored with NFL1 decreases progressively compared to cells infected with the empty vector. HN31 mutant cells infected with NFL1 is selected against a mixed population of NFL1 and non-NFL1 expressing cells while cells infected with MigR1 remains steady through the 23 day time period.

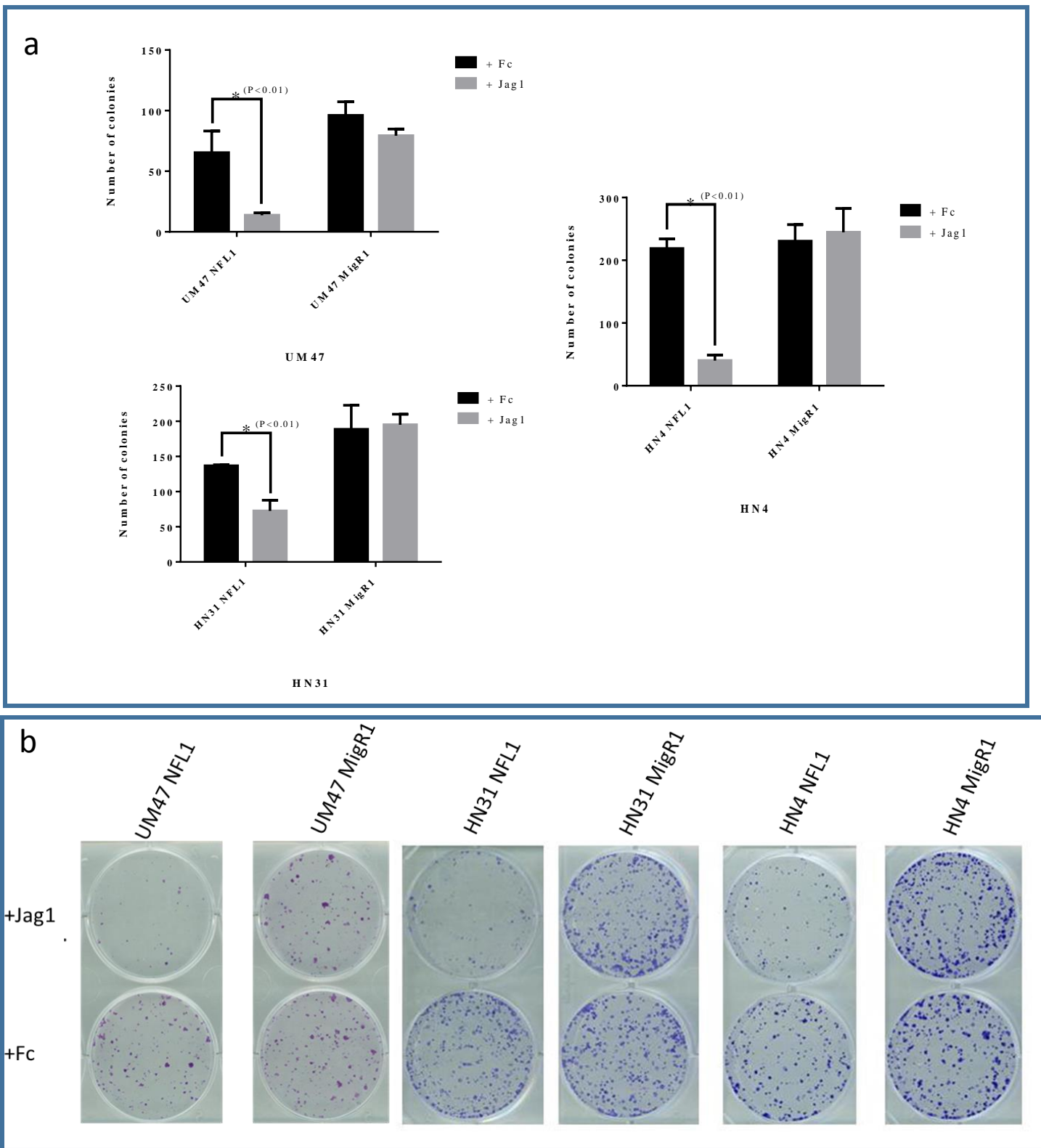


Figure 18: Restoration of NOTCH1 inhibits cell growth. Inhibition in the number of colonies of mutant cells after restoration with NFL1 and culture on Jagged1. (a: quantitation of clonogenic assay, b: crystal violet staining of colonies)

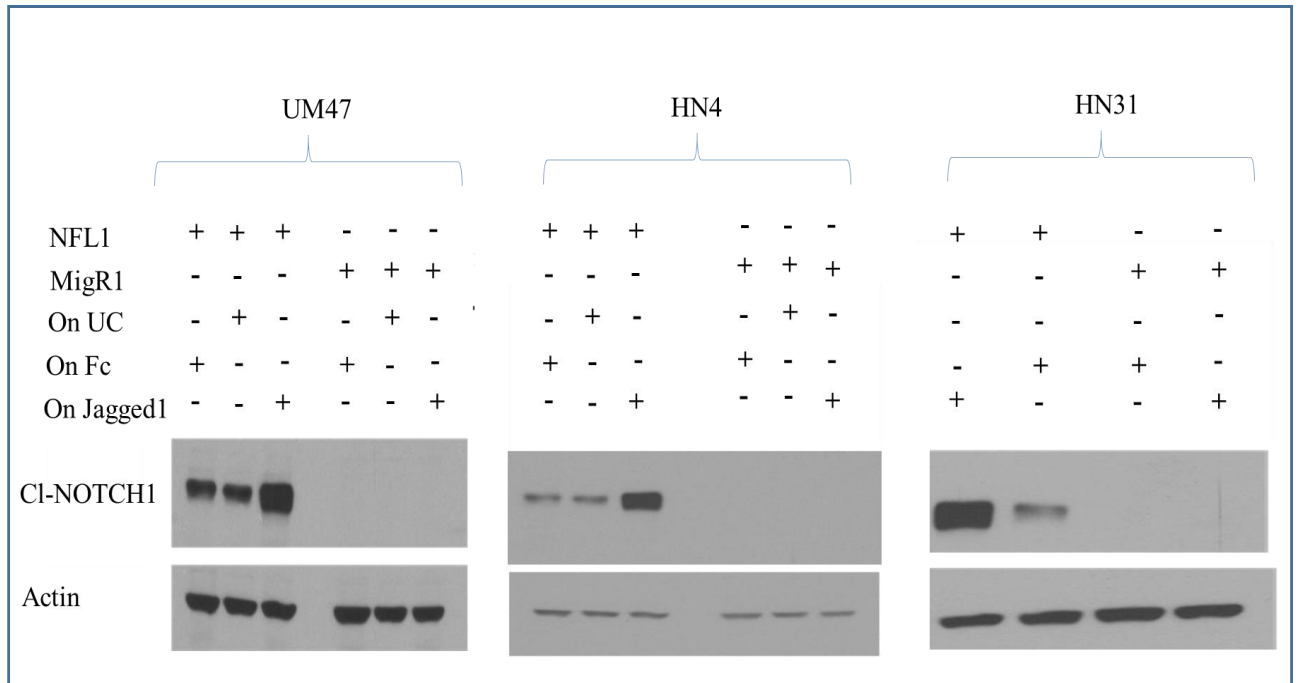


Figure 19: NOTCH1 is activated only in mutant cells infected with NFL1 but not MigR1. Restoration of NFL1 in mutant cell lines induces cleavage of NOTCH1 when cultured on Jagged1 but not on Fc or uncoated plates.

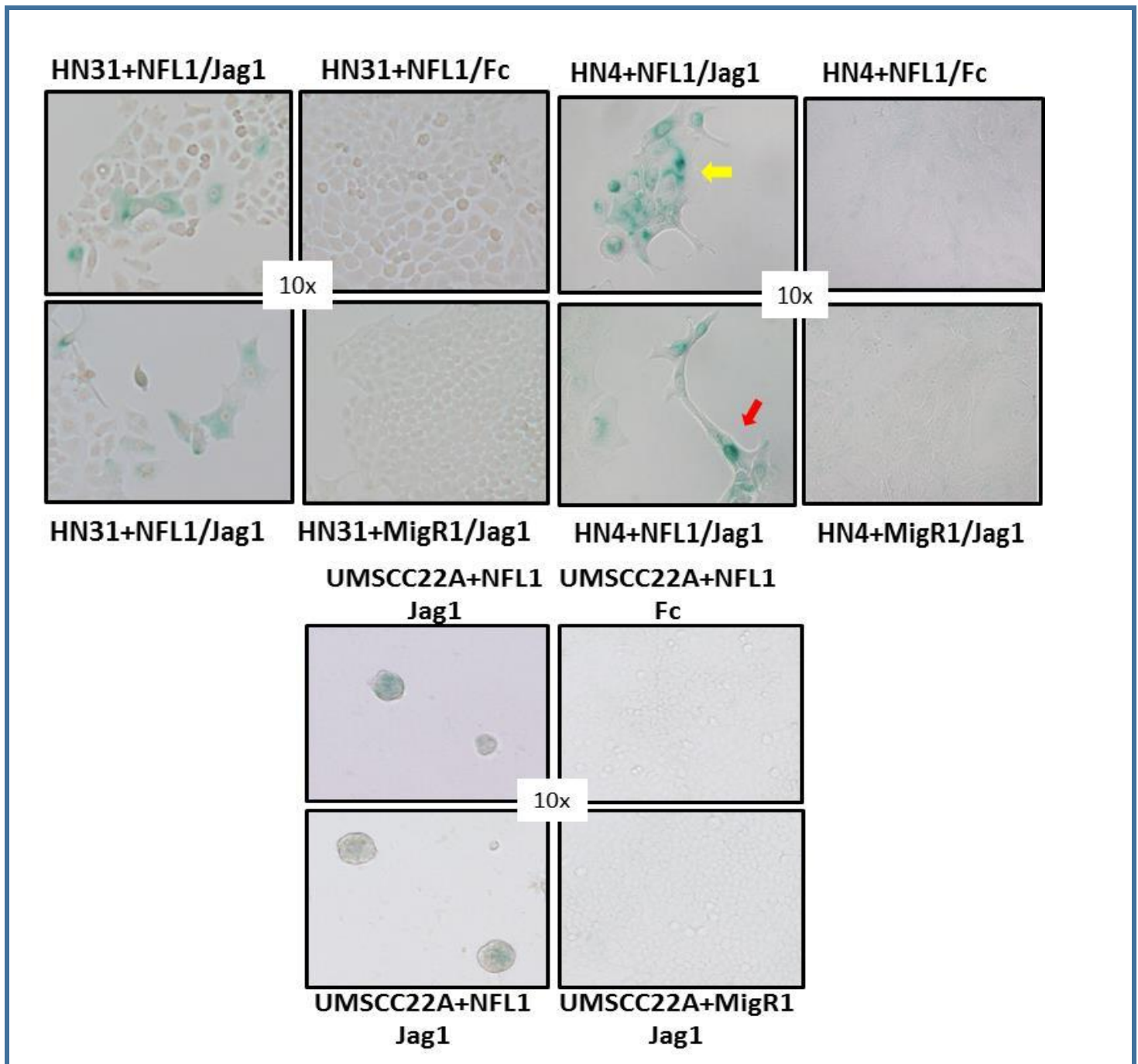


Figure 20: HN31, HN4 and UMSCC22A mutant HNSCC cells undergo senescence after restoring NFL1 and culturing on Jagged1

Chapter 5.5: Activation of the NOTCH signaling pathway in wild-type cell lines inhibits cell growth

Rationale: We previously demonstrated that restoration of NOTCH signaling in mutant HNSCC cells inhibits cell growth. NOTCH1 is mutated in about 15-19% of HNSCC (Agrawal et al., 2011; Stransky et al., 2011; "TCGA Releases Head and Neck Cancer Data," 2015), however, majority of the tumors have wild-type NOTCH1. Although these tumors express the wild-type receptor, the NOTCH pathway may not be activated due to alterations in Jagged1, overexpression of NUMB, improper glycosylation, or proteosomal degradation. Thus, we wanted to investigate the functional relevance of activating the NOTCH pathway in a wild-type setting. To activate the NOTCH pathway, wild-type cells were cultured on Jagged1 and hypothesized that Jagged1 would induce growth inhibition in wild-type cells similar to the mutant cells.

Results: PJA34 and CAL27 NOTCH1 wild-type cells were cultured on recombinant Jagged1 or Fc coated plates. Jagged1 and Fc were coated on cell culture plates the day before seeding. Both wild-type cell lines were plated at a low density to observe morphology change and colony formation. Cells cultured on Jagged1 appeared to be slower in growth, small, and spherical (Figure 21). Similar to the mutant cells, a small fraction of wild-type cells when cultured on Jagged1 appeared flattened and exhibited a pancake-like morphology. These cells stained positive for β -galactosidase indicating that NOTCH activation may result in some cells undergoing senescence (Figure 21). Moreover, when protein expression levels for cleaved NOTCH were evaluated by western blotting, activation of NOTCH signaling was observed only in cells cultured on Jagged1

but not on Fc (Figure 22). These results imply that activation of the NOTCH signaling pathway in wild-type cells might be responsible for aberrations in cell morphology. To measure the long term effects of activating NOTCH signaling in these cells, a colony forming clonogenic assay was performed in which wild-type cell lines (PJA34, 183, CAL27 and UMSCC1) were cultured on Jagged1 or Fc for a 10-day period. All wild-type cell lines were significantly growth inhibited when cultured on Jagged1 (Figure 23). Furthermore, cleaved NOTCH1 expression was observed only in cells cultured on Jagged1 but not Fc. Taken together, the change in morphology, growth inhibition and expression of cleaved NOTCH1 was evident only in wild-type cells cultured on Jagged1 suggesting that NOTCH activity induces these changes. To confirm that NOTCH signaling does indeed play a role in modulating cell growth, NOTCH activation was inhibited using the γ -secretase inhibitor DAPT (N-[N-(3,5-Difluorophenacetyl)-L-alanyl]-S-phenylglycine t-butyl ester) at two different concentrations (2 μ M and 10 μ M) in CAL27 and PJA34 wild-type cell lines after culturing them on Jagged1 or Fc. After addition of DAPT, a reversal in growth inhibition was observed when cell were cultured on Jagged1 (Figure 24). This result suggests that NOTCH activation might be necessary for growth inhibition. Since inhibition of γ -secretase may exert a dose dependent effect, the wild-type cell lines PJA34 was infected with the dominant negative form of Mastermind-like 1 (MAML1) that has a mutation that prevents MAML1 from binding to ICN, thus physiologically blocking the NOTCH pathway. After sorting infected cells to obtain a pure population of dnMAML1-GFP cells, PJA 34 dnMAML1 cells were cultured on Jagged1 or Fc using parental PJA34 cells as controls. PJA34 parental cells as observed before had suppressed levels of cell growth when cultured on Jagged1

compared to Fc. However, dnMAML1 was able to reverse the Jagged1 mediated growth inhibition (Figure 25). Both approaches to inhibit NOTCH signaling (GSI and dnMAML1) showed a reversal of Jagged1 mediated cell growth inhibition. In addition to these approaches, we also employed the CRISPR-Cas9 system to knock out NOTCH1 and NOTCH2 in PJA34 cell lines. This system was used not only to knockout both NOTCH isoforms, but also to determine which specific NOTCH member (NOTCH 1 or NOTCH 2) mediates growth inhibition. Using this technique, stable knockouts of either or both NOTCH receptors was achieved (Figure 26). To determine cell growth potential, PJA 34 parental cells, NOTCH1 knockout cells (NOTCH1 KO), NOTCH2 knockout (NOTCH2 KO) cells and NOTCH1/NOTCH2 double knockout cells (dKO) were cultured on Jagged1 or Fc in a colony forming assay. Knocking out either NOTCH1 (NOTCH1 KO) or NOTCH2 (NOTCH2 KO) in PJA34 cells did not relieve the growth inhibition relative to parental cells on Jagged1. However, knocking out both NOTCH1 and NOTCH2 (double knockout- dKO) significantly reversed Jagged1 mediated growth inhibition (Figure 27). The CRISPR-Cas9 knockout studies suggested that both NOTCH1 and NOTCH2 are required for inhibiting cell growth. To show that NOTCH signaling is sufficient to inhibit cell growth, full length NOTCH1 (NFL1) was infected in the double knockout (dKO) PJA34 cell line to evaluate cell growth in a colony forming clonogenic assay. Abrogation in protein expression levels of total NOTCH1 and cleaved NOTCH1 was observed in PJA34 dKO cells cultured on Jagged1 or Fc (Figure 28). However, after restoration of NFL1 in PJA34 dKO cells, the abrogation in protein expression levels of total-NOTCH1 and cleaved NOTCH1 was rescued (Figure 28) suggesting restoration of the pathway. Next, PJA34 parental cells, dKO cells and dKO cells after restoration of

NFL1 (dKO+NFL1) were subjected to a clonogenic assay on Jagged1 or Fc. As expected, PJA34 parental cells on Jagged1 was growth suppressed that was abrogated by PJA34 dKO cells cultured on Jagged1 and Fc. However, restoration of NFL1 in the double knockout (dKO+NFL1) cell lines suppressed growth similar to the parental cells when cultured on Jagged1 and rescued the PJA34 dKO phenotype (Figure 29). Taken together, we have shown that NOTCH activation in wild-type cells inhibits cell growth and that NOTCH1 is necessary and sufficient to inhibit cell growth *in vitro*.

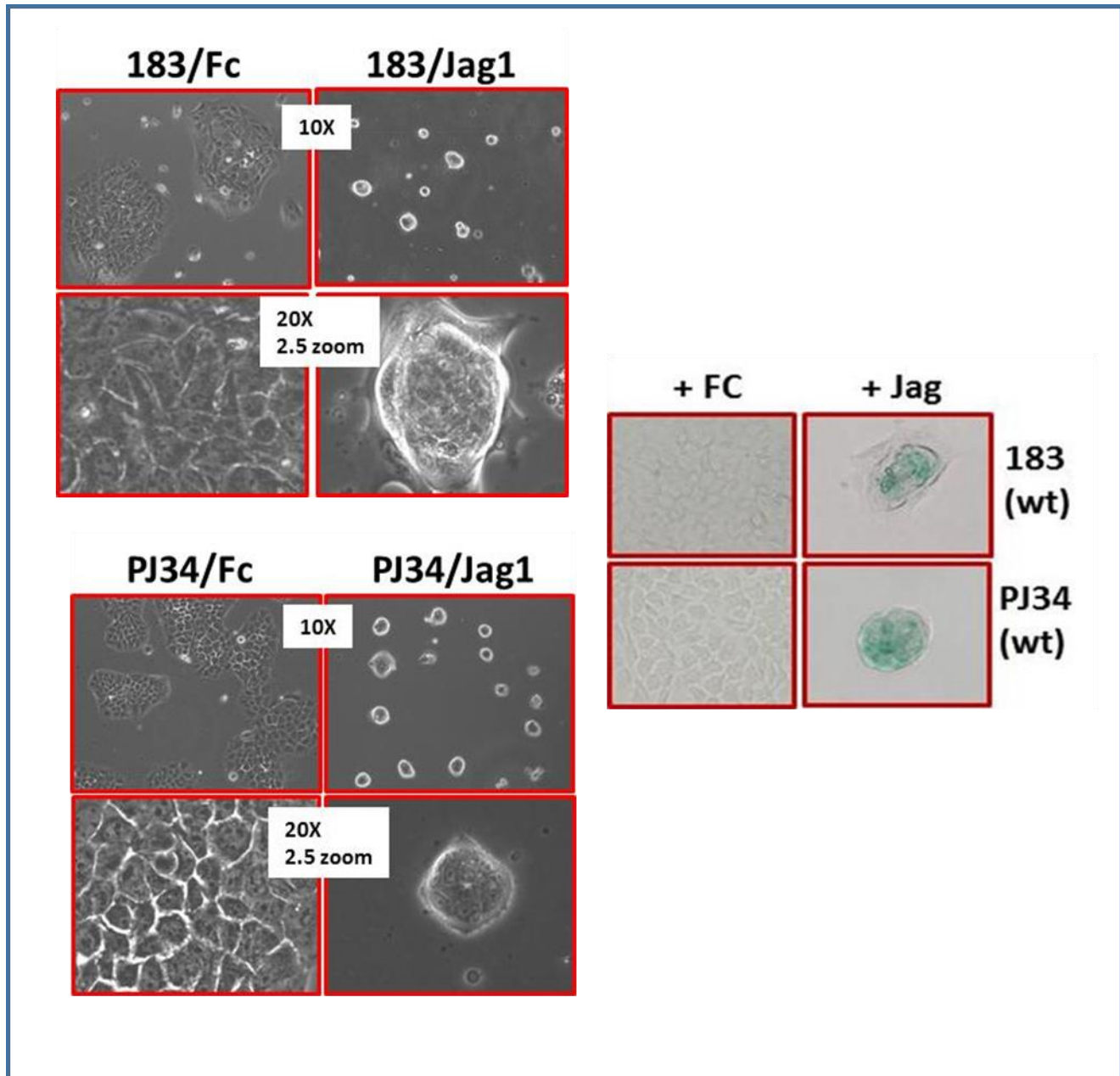


Figure 21: Morphology change and senescence when NOTCH1 wild-type are cultured on Jagged1. Culture of wild-type cell lines on Jagged1 shows small, rounded and growth inhibited colonies, some of which undergo senescence compared to cells cultured on Fc.

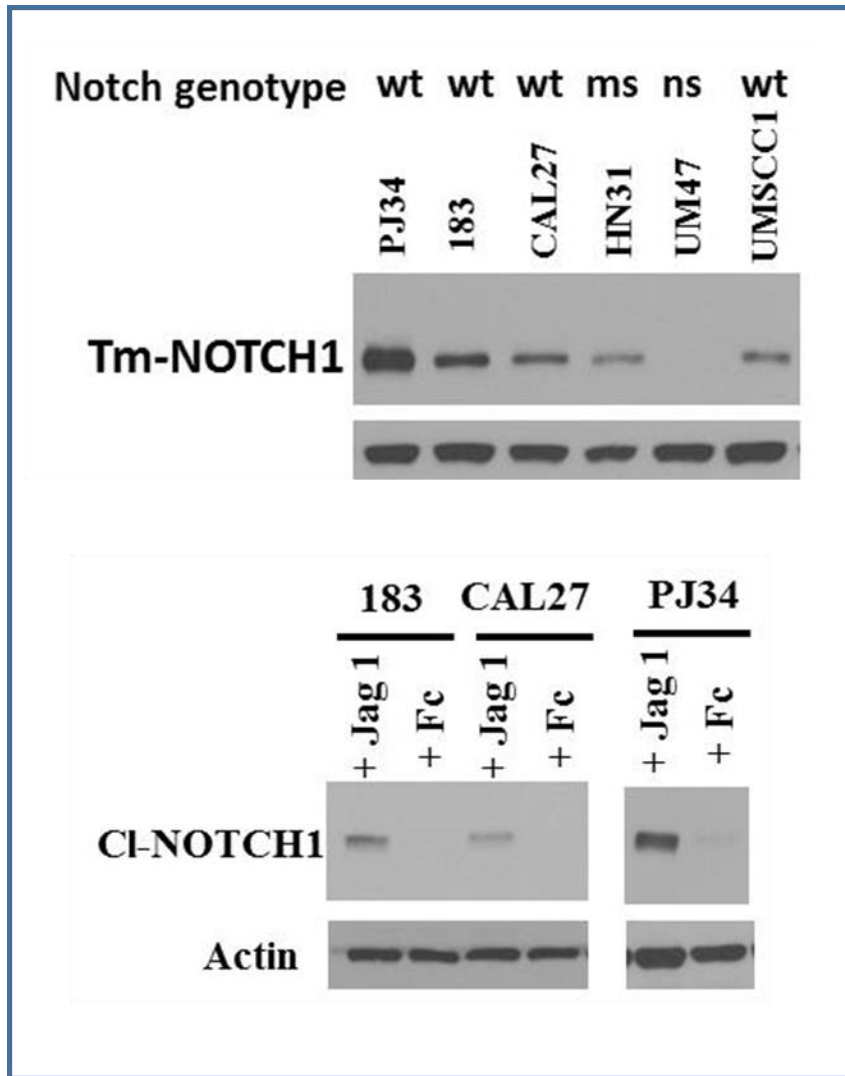


Figure 22: Protein expression of Total-NOTCH1 and cleaved NOTCH1: Western blot depicting total NOTCH1 (Tm-NOTCH1) in wild-type and mutant cell lines and cleaved NOTCH1 (cl-NOTCH1) expression in wild-type cell lines cultured on Jagged1

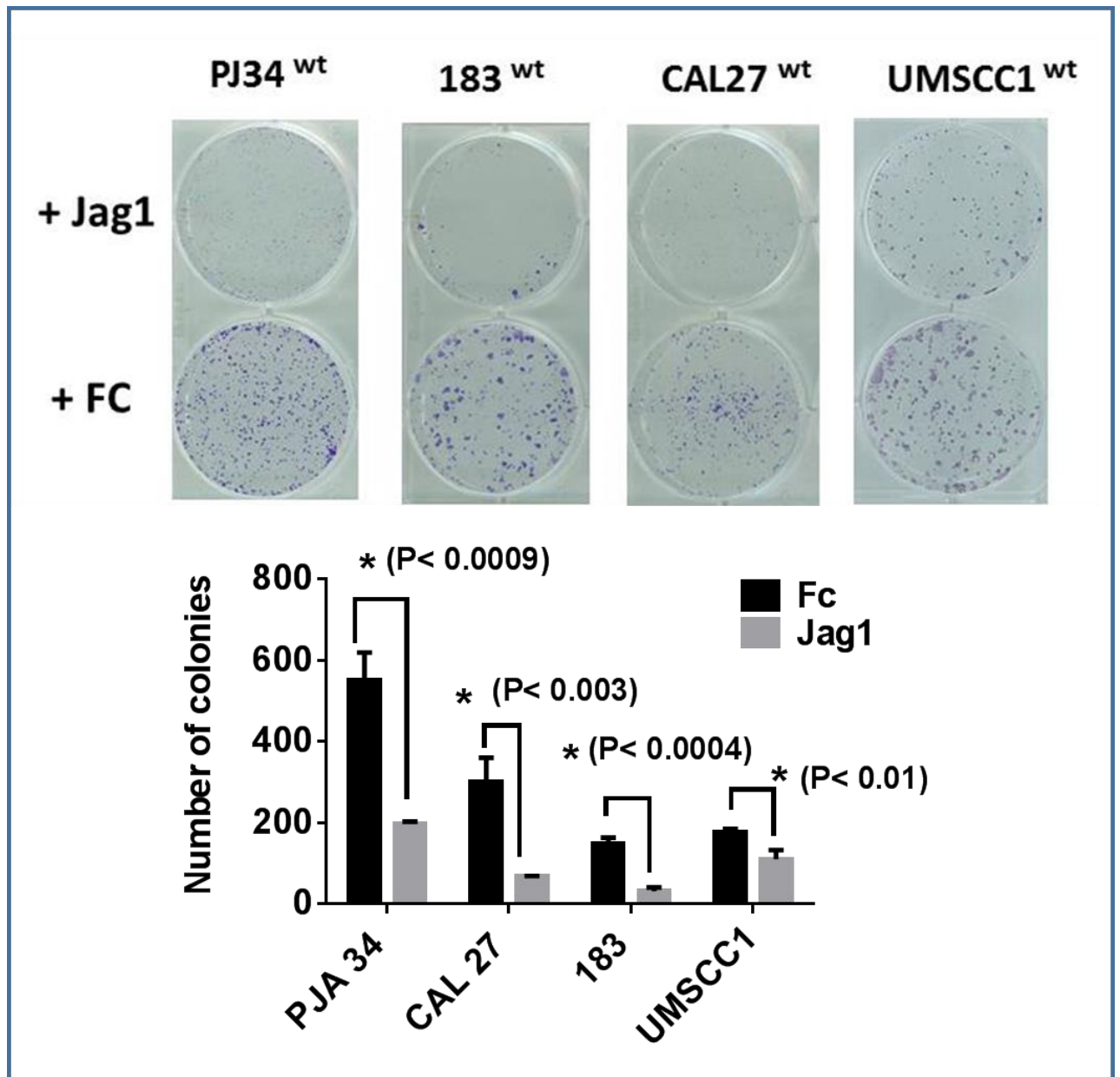


Figure 23: Wild-type cell lines cultured on Jagged1 are significantly growth inhibited

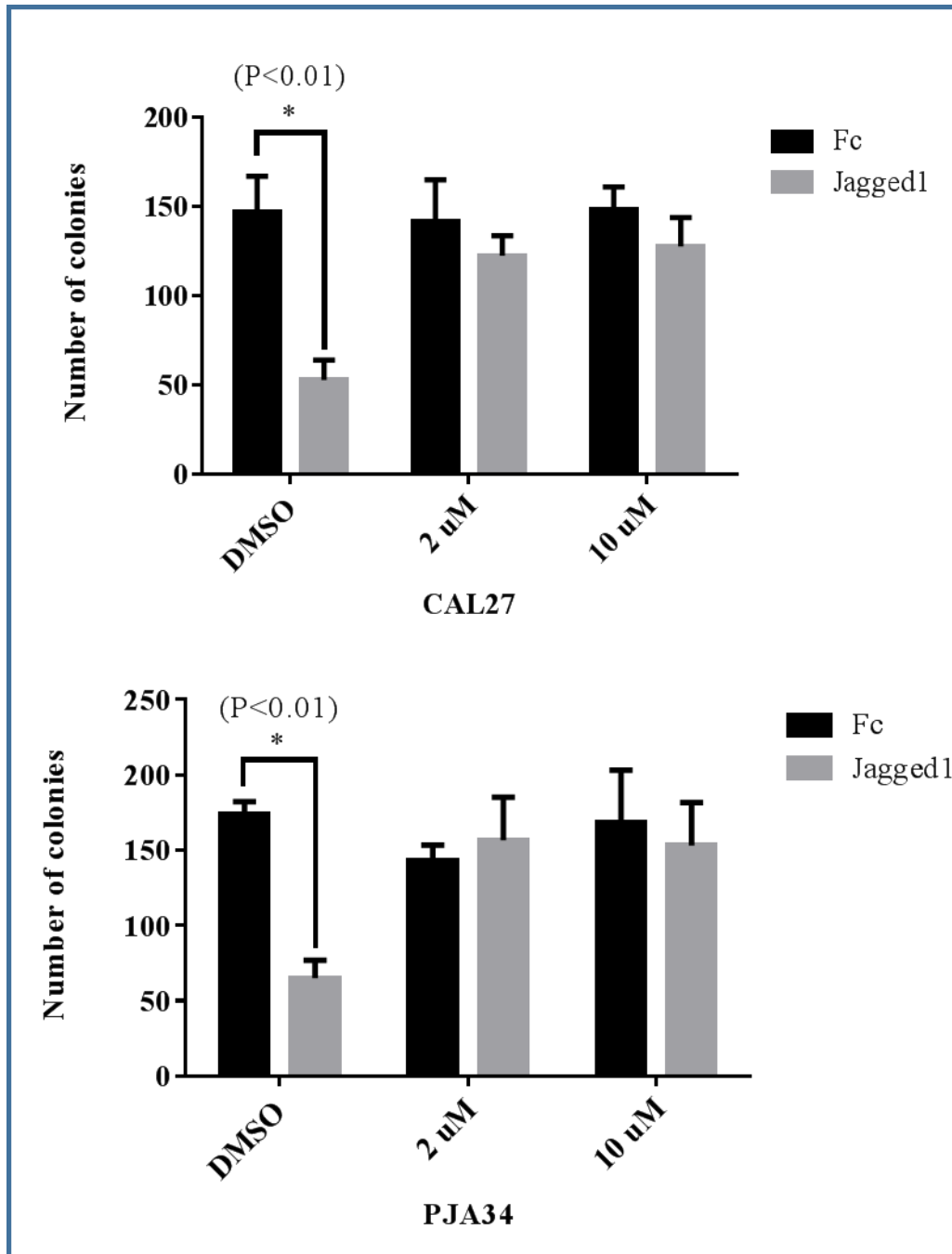


Figure 24: Inhibition of NOTCH signaling using γ -secretase inhibitor reverses NOTCH mediated growth suppression.

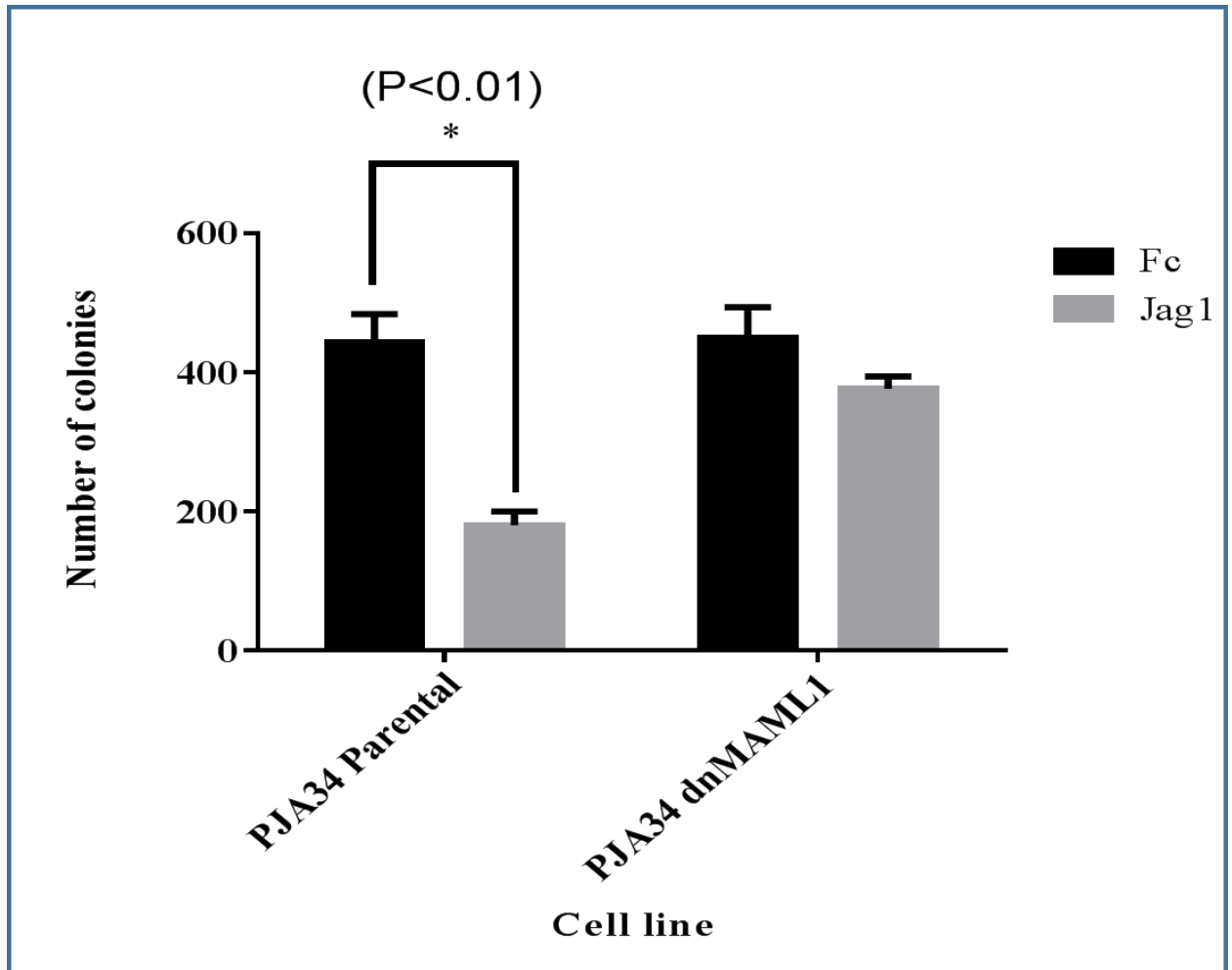


Figure 25: *dnMAML1* reversed *Jagged1* mediated growth inhibition

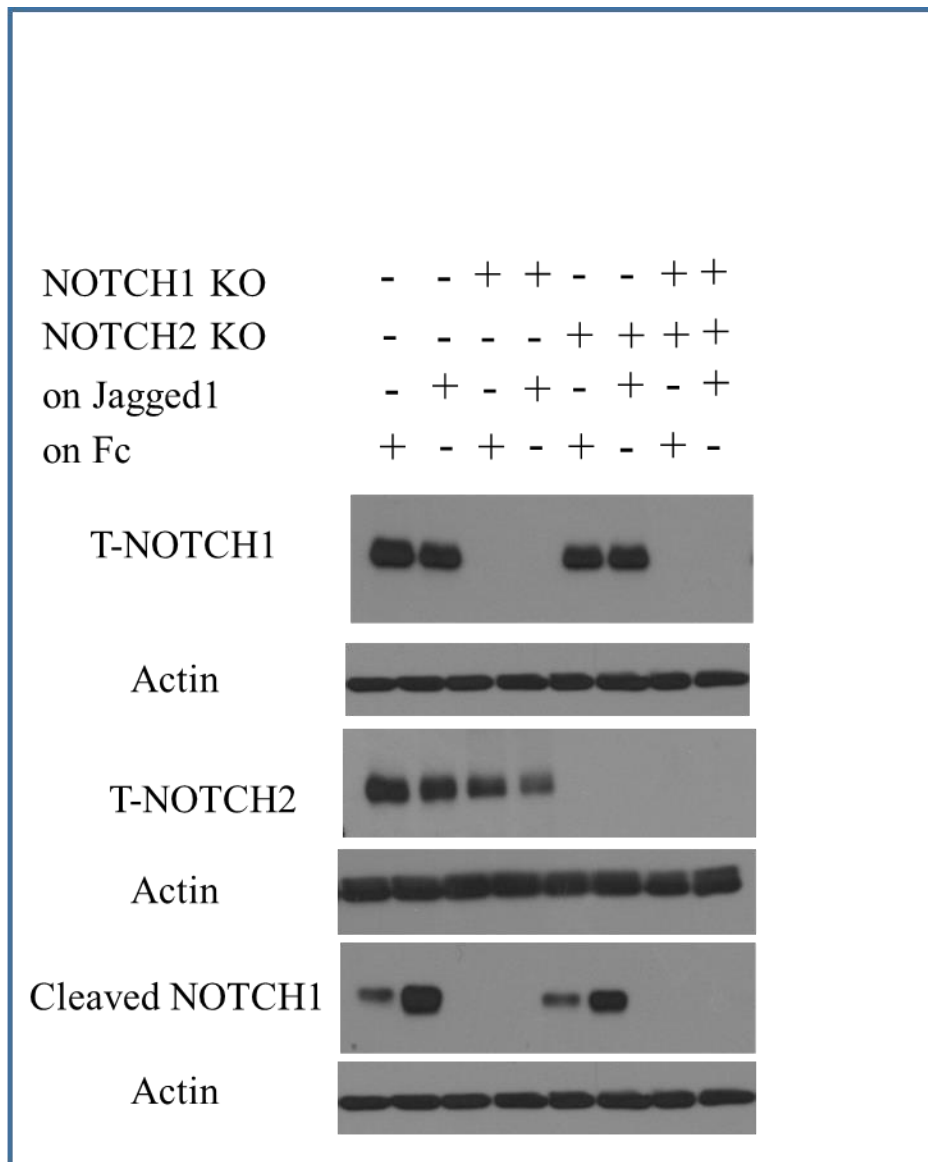


Figure 26: CRISPR-Cas9 knockout of *NOTCH1* (*NOTCH1 KO*), *NOTCH2* (*NOTCH2 KO*) or both

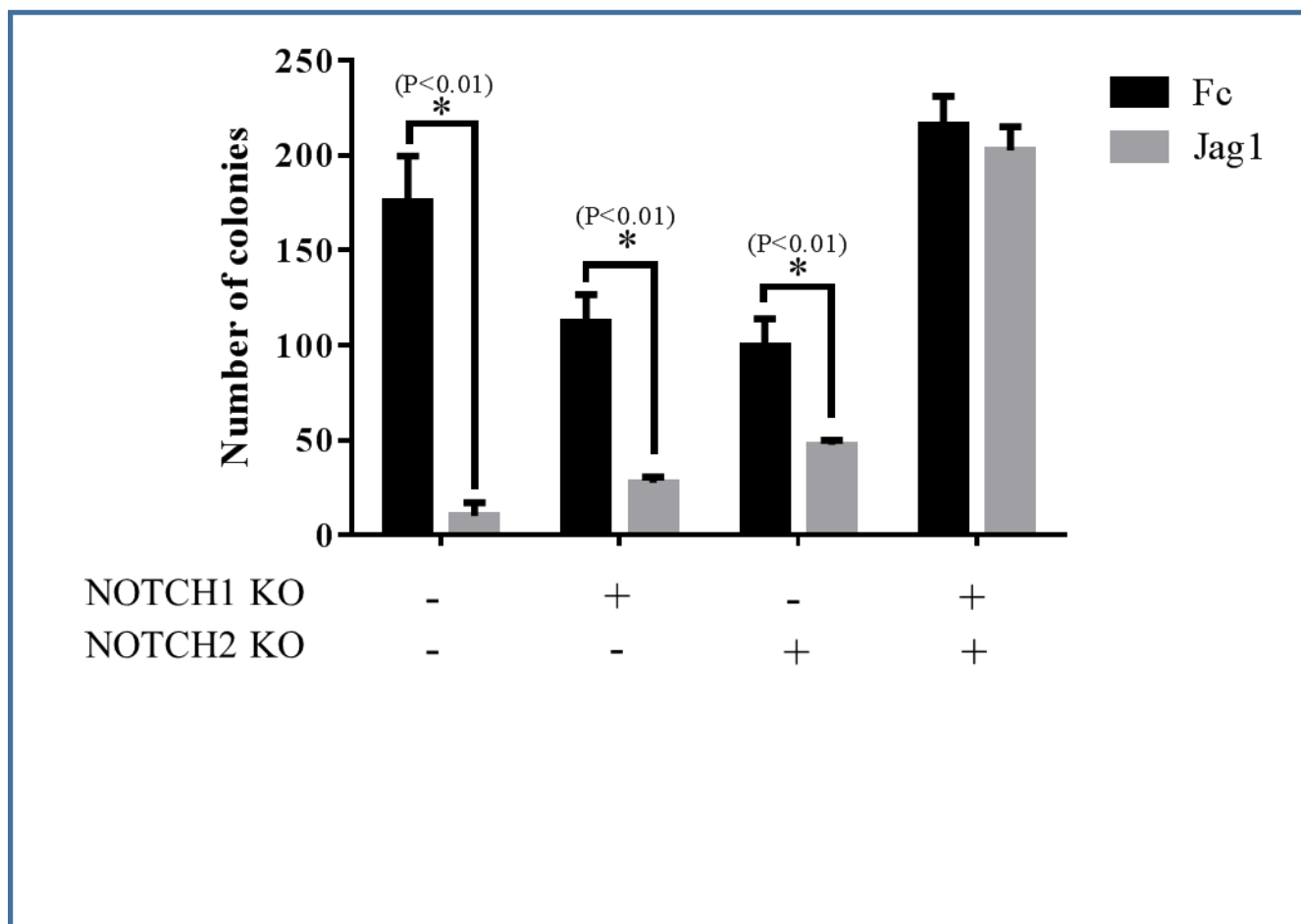


Figure 27: Knocking out both *NOTCH* and *NOTCH2* relieves *Jagged1* mediated growth suppression. KO: Knockout

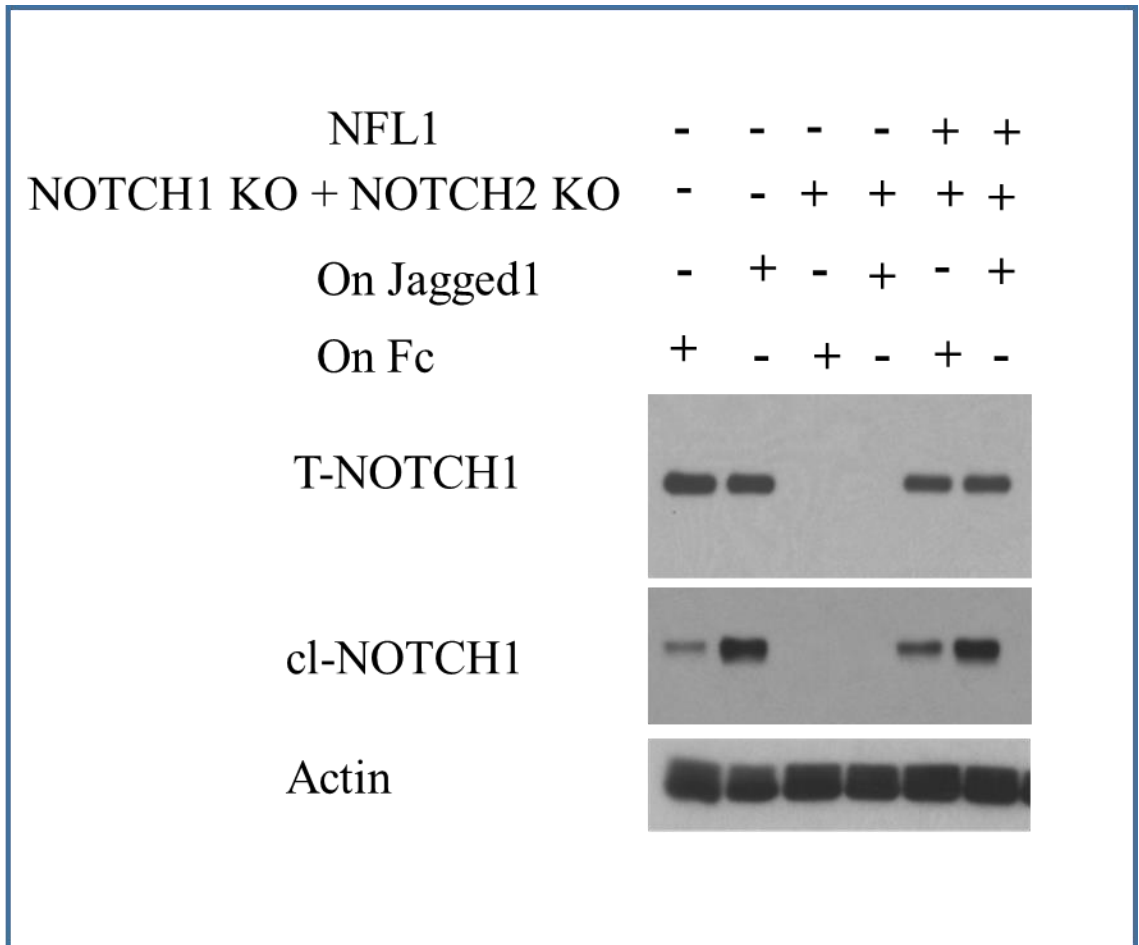


Figure 28: Restoration of NFL1 in the double knock out cell line activates NOTCH signaling: CRISPR-Cas9 double knockout cell line PJA34 shows activation of NOTCH signaling after restoration with NFL1 and culturing cells on Jagged. KO: Knockout

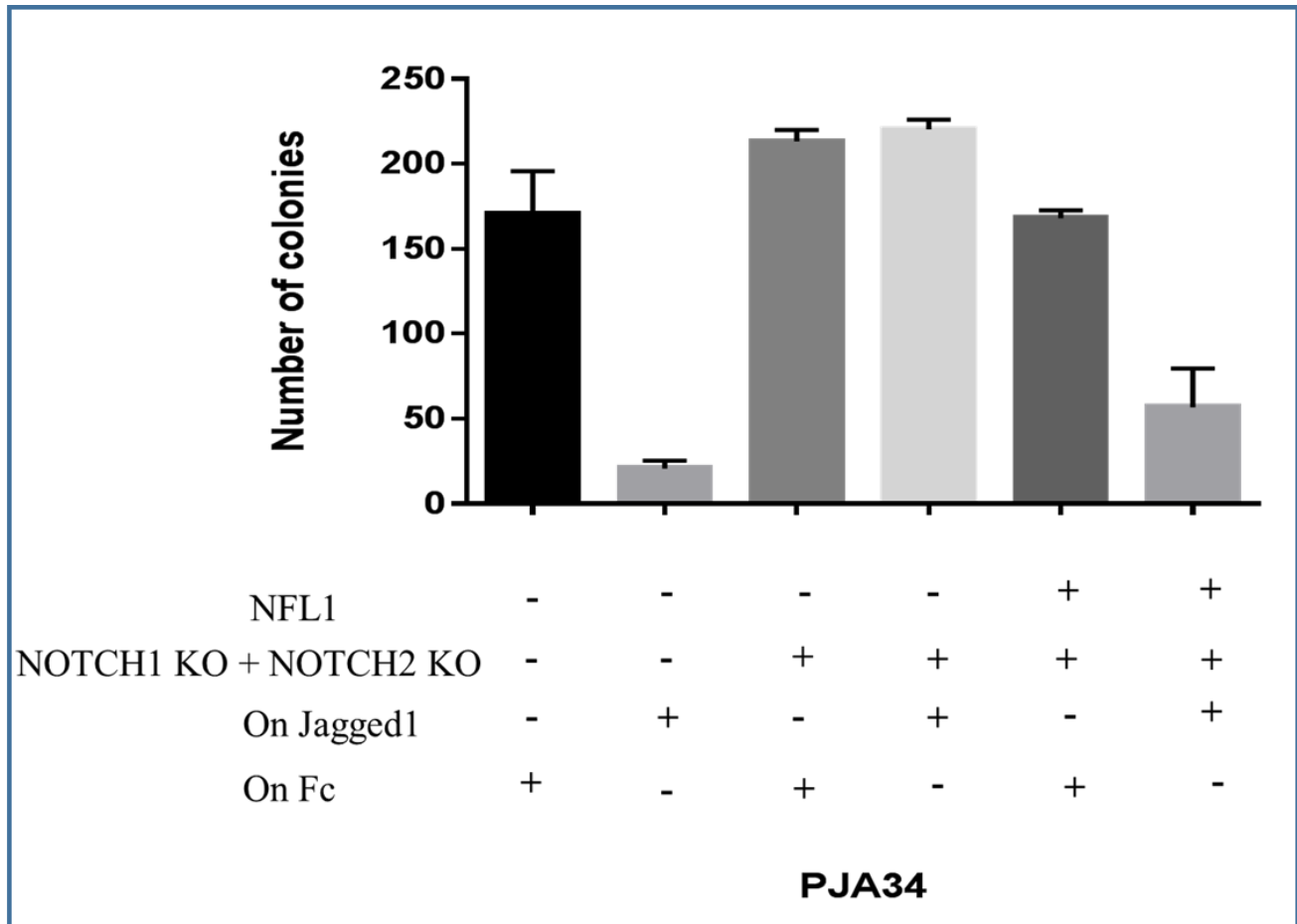


Figure 29: NOTCH signaling is necessary and sufficient to modulate cell growth. CRISPR-Cas9 NOTCH1 and NOTCH2 double knockout cell line PJA 34 promotes growth on Jagged1 and Fc that is inhibited after restoration with NFL1.

Chapter 5.6: Restoration of NOTCH signaling in mutant HNSCC cell lines inhibits *in vivo* tumorigenicity

Rationale: We have demonstrated that activation of the NOTCH signaling pathway in mutant and wild-type HNSCC cell lines inhibits *in vitro cell* growth abilities. To evaluate *in vivo* tumor growth of mutant cell lines after restoration with NOTCH1, we infected mutant cell lines HN31 and UM47 with ICN1 or NFL1 and hypothesized that restoration of NOTCH signaling would inhibit *in vivo* tumor forming ability. Tumor forming ability was evaluated in an orthotopic tongue model of oral cancer.

Results: NOTCH signaling was restored in mutant cell lines HN31 and UM47 using full-length NOTCH1 (NFL1) or the intracellular form of NOTCH1 (ICN1). The empty vector MigR1 and parental cells were used as controls. After retroviral infections with ICN1, NFL1 and MigR1, cells were sorted for GFP by flow cytometry. Forty-eight hours after sorting later, 50,000 cells were injected per mouse cells into the dorsal right region of the tongue in nude mice. Ten mice were injected in each condition. We then monitored tumor formation for a 25 day period measuring tumor size every 3 days. Mutant cells infected with NFL1 or ICN1 when injected in mice had significantly lower tumor volumes and an increase in overall survival was observed (Figure 30a and b). At the end of the 25 day period, the tumor volume in NFL1 and ICN1 injected mice was less than 50% compared to the parental and empty vector (MigR1) controls. The effect was even pronounced in cells having ICN1 (blue dashed line in the graph of Figure 30a) compared to NFL1 cells (although there was no significant difference between ICN1 and NFL1) and these mice began to form tumors only 20 days

post injection. The slow-growing *in vivo* tongue tumors derived from mutant UM47 infected with NFL1 expressed NOTCH1 (Figure 31a), grew in a more organized fashion than control MigR1 infected cells lacking NOTCH1 protein (Figure 30b), and had frequent keratin pearls (Figure 30c) suggesting increased differentiation compared to MigR1 infected tumors which had higher tumor cellularity (Figure 30d). These results suggested that in addition to inhibiting *in vivo* tumor forming ability, NOTCH activation *in vivo* can also induce differentiation, in part, explaining the reduction in cell growth.

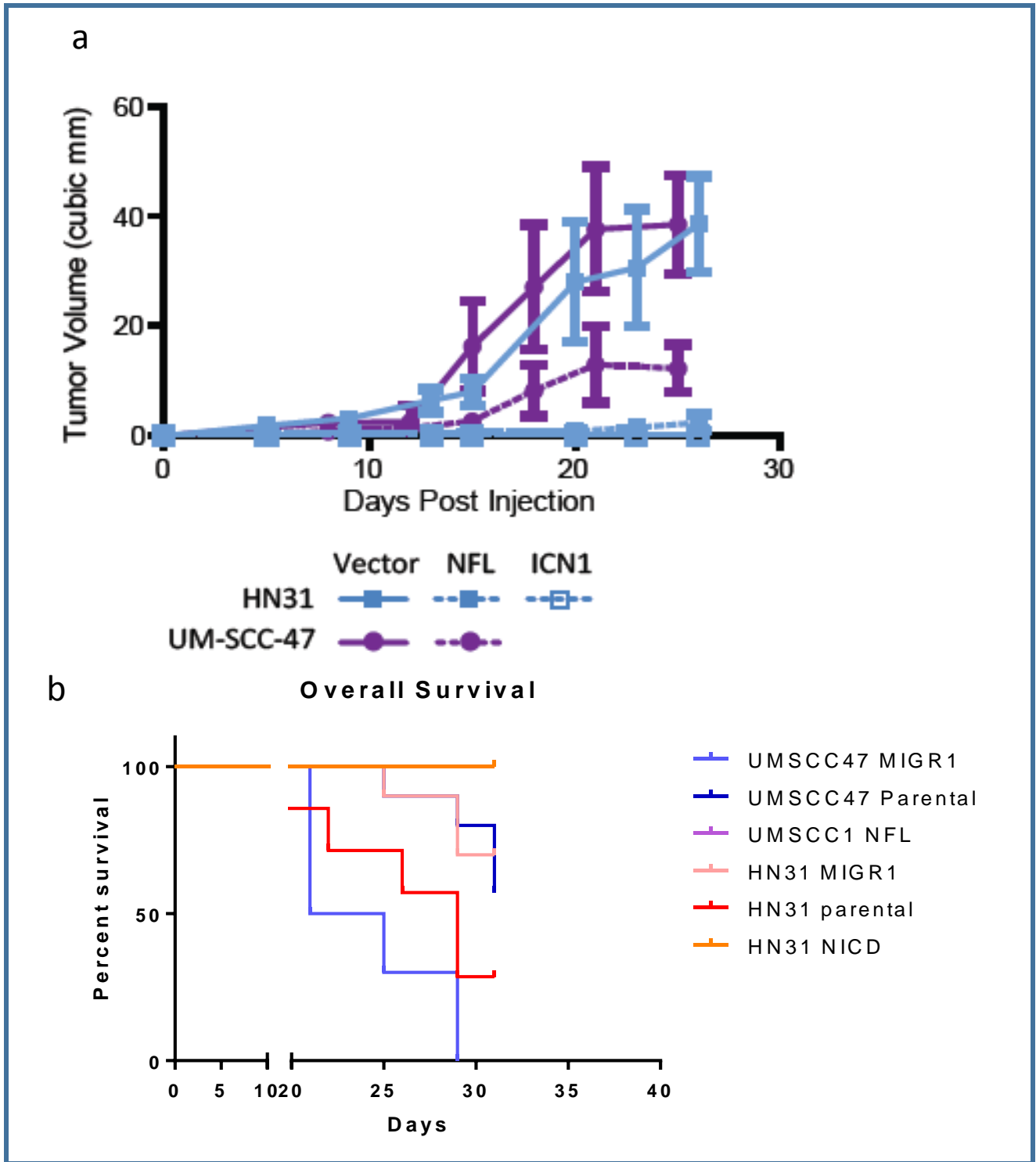


Figure 30: Restoration of NOTCH signaling in mutant HNSCC cell lines inhibits tumor growth (a) and increases overall survival (b) in a xenograft orthotopic model of oral cancer

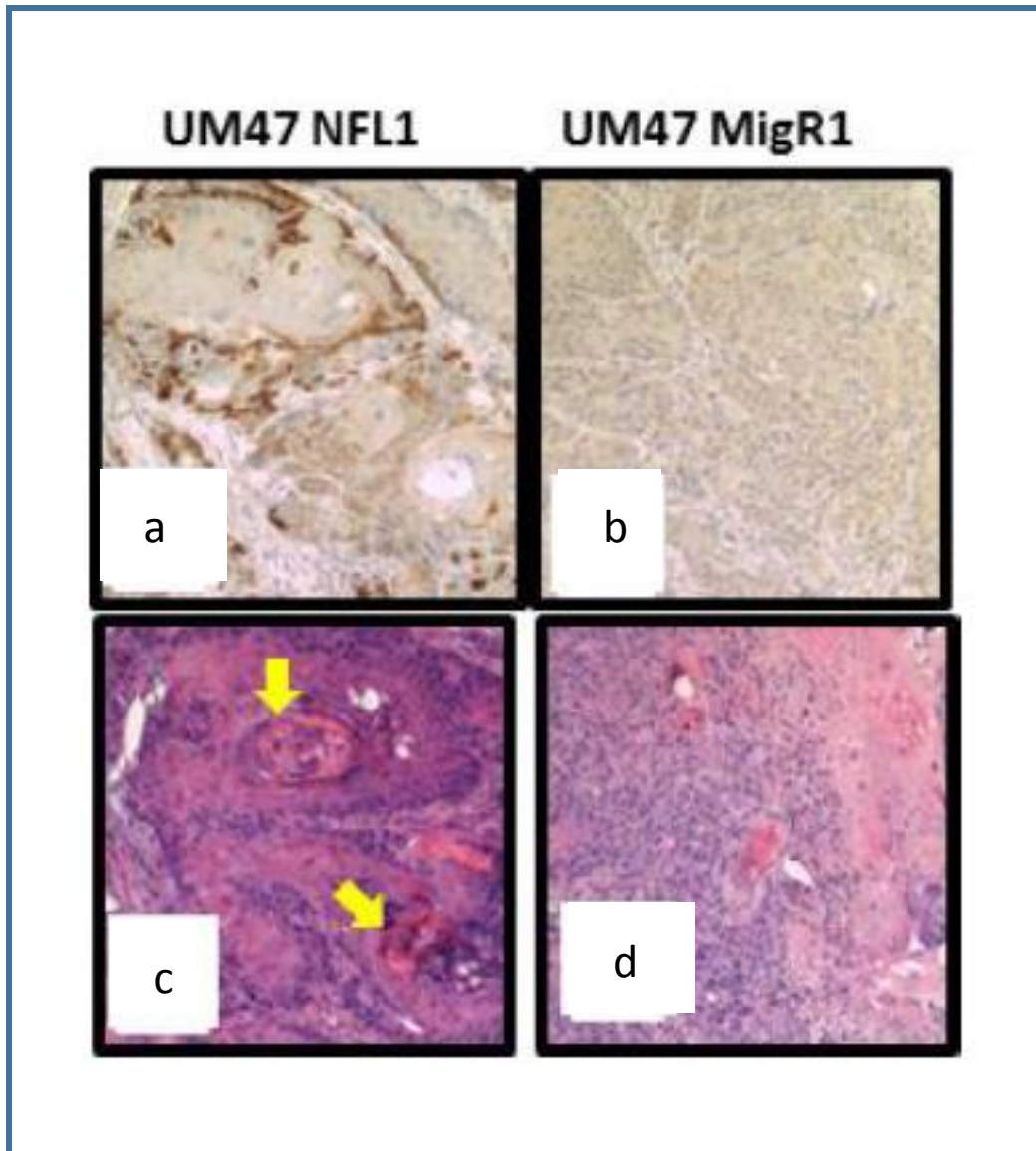


Figure 31: NFL1 infected UM47 tumor xenografts appear more differentiated. Mutant UM47 infected with NFL1 (a, c) grew slowly in mouse tongues compared to UM47 infected with control MigR1. (b, d). Anti-total NOTCH 1 staining (brown) of NFL1-infected (a) or MigR1 infected (b) tumors. Growth of NFL1-infected tumors was more organized (c) and had keratin pearls (arrows) compared to MigR1 infected tumors, apparent after H&E stain

Chapter 5.7: Inhibition of NOTCH signaling enhances tumor growth *in vivo*

Rationale: I previously showed that NOTCH1 is sufficient to inhibit tumor growth. Proweller et al. demonstrated that in mouse keratinocytes, expression of the pan-NOTCH inhibitor dominant negative Mastermind like-1 (dnMAML1) resulted in a hyperplastic epidermis and spontaneous development of cutaneous squamous cell carcinoma (cSCC) (Proweller et al., 2006). Their results imply that in tumor types wherein NOTCH acts as a tumor suppressor (such as skin cancer in this case), transcriptional inhibition of this pathway accelerates tumor growth. On the contrary, in pancreatic cancer, NOTCH acts as an oncogene. In this cancer type, it was shown that dnMAML1 delays the formation of pancreatic intraepithelial neoplasia (Thomas et al., 2014). Taken together, dnMAML1 appears accelerate or inhibit tumorigenesis in cancers in which NOTCH acts as a tumor suppressor and oncogene respectively. In HNSCC, since NOTCH1 has inactivating mutations similar to cSCC (Pickering et al., 2014), I hypothesized that abrogation of all NOTCH signaling would exacerbate tumor formation. To determine the comprehensive function of NOTCH mediated growth suppression and overcome potential redundancies between receptors, I proposed to abrogate some of canonical (LAG1-CSL- dependent) NOTCH signaling using dnMAML1 in a NOTCH wild-type cell line that is non-tumorigenic in mice.

Results: I infected PJA34 cells with dnMAML1 (MigR1-GFP-tagged) or with the empty vector MigR1 and sorted these cells to obtain a pure population GFP positive cell by flow cytometry. The transductions were performed such the percentage and intensity of GFP cells were equal in all conditions. In addition, I also transduced Jagged1, the ligand for the NOTCH receptor in the same cell line before mice injections. Twelve days

post injection in the dorsal tongue of mice, tumors in the dnMAML1 and Jag1 group began to develop. By end of 20 days, tumor volumes in the Jag1 and dnMAML1 mice were significantly larger than the control groups (Figure 26). Although only 5/10 dnMAML1 formed tumors, the growth of these tumors was significantly larger than the parental and MigR1 group. Jagged1 and NOTCH receptor in the same cell can potentially result in cis-inhibition (Cordle et al., 2008). It might be possible that cis-inhibition rather than *trans* activation in PJA34 cells overexpressing Jagged1 contributes to accelerated tumor growth. To address the issue of cis-inhibition, we co-cultured wild-type parental cells with wild-type Jagged1 overexpressing cells. We performed a western blot to evaluate expression levels of cleaved NOTCH1. Parental cells expressed very little cleaved NOTCH1, while parental cells mixed with Jagged1 overexpressing cells had higher amounts of cleaved NOTCH1 (Figure 27). Interestingly, levels of cleaved NOTCH1 was lower in Jagged1 overexpressing cells. This suggests that although there might have been some cis-inhibition in parental-Jagged1 mixed cells, there was more transactivation resulting in cleaved NOTCH1. In Jagged1 overexpressing cells, cis inhibition might have possibly resulted in lower levels of cleaved NOTCH1. In mice, when Jagged1 cells were injected, there might have been greater *cis*-inhibition than *trans*-activation resulting in increased tumor volumes. Since MAML1 exerts its effects in the nucleus, it might be possible that there was no little or nuclear localization of dnMAML1 after transduction in these cells. I did not determine the nuclear presence of dnMAML1 in these cells, thus, in 50% mice that did not form tumors in the dnMAML1 group, dnMAML1 may have not have translocated to the nucleus.

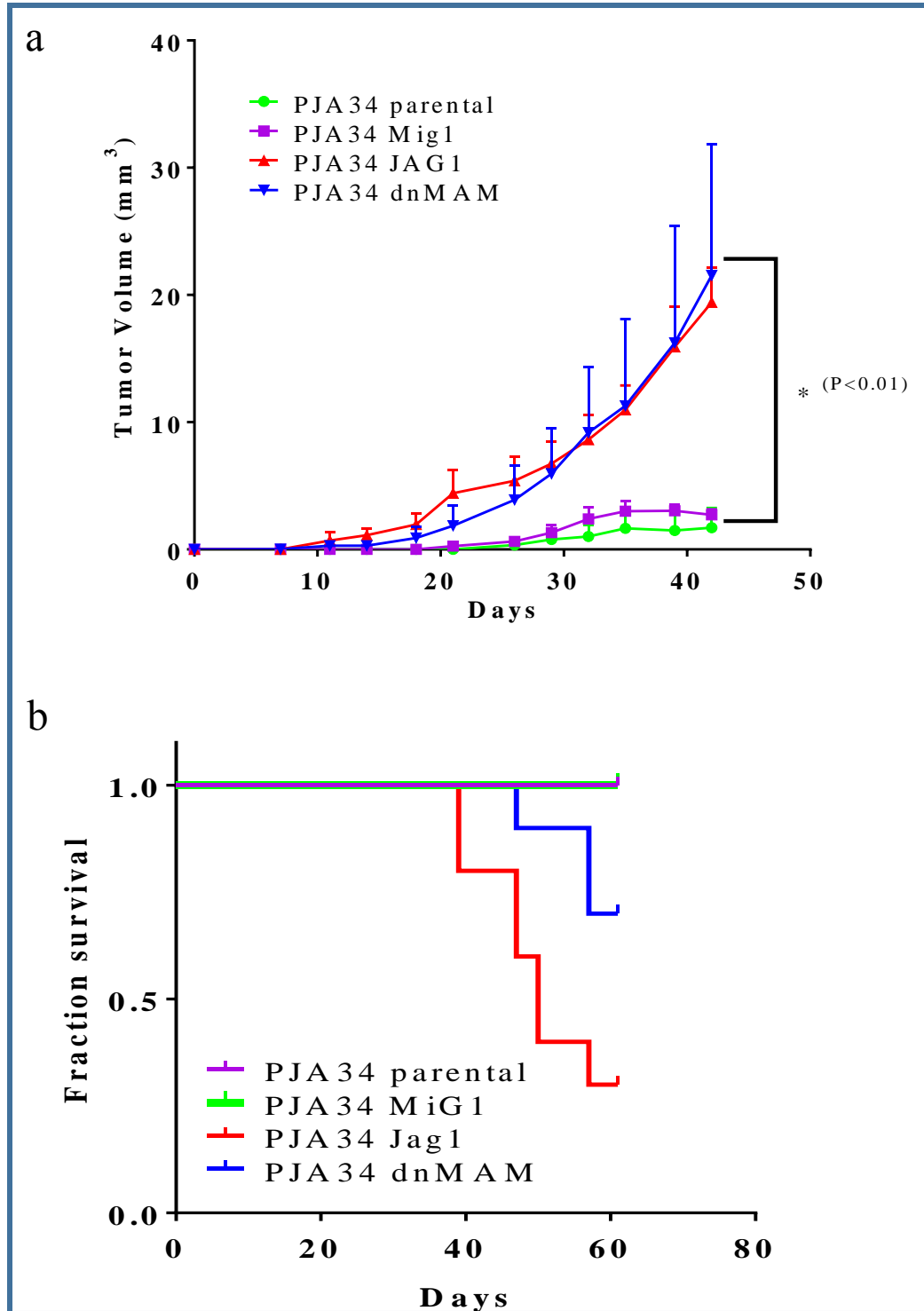


Figure 32: NOTCH signaling may be necessary for inhibiting tumor growth.

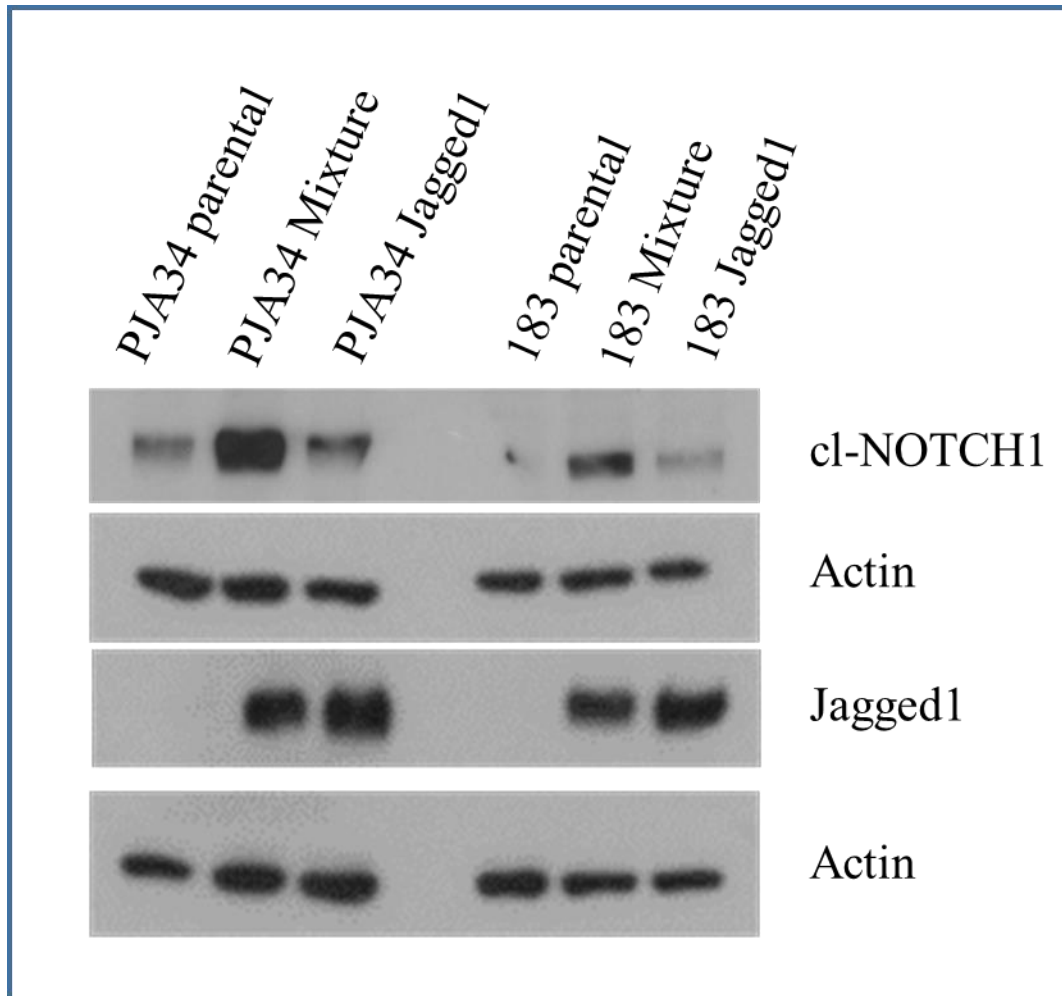


Figure 33: Possibility of cis-inhibition when PJA34 and 183 cells are overexpressed with Jagged1

Discussion

In this chapter, for the first time the growth inhibitory effects after restoration of NOTCH signaling in mutant and wild-type NOTCH1 expressing HNSCC cell lines has been demonstrated. In addition, we found that NOTCH1 is sufficient to inhibit tumorigenicity and might also be necessary for mediating inhibitory growth signals. Using the activated form of NOTCH (ICN1) and the full-length NOTCH1 (NFL1), it has been shown that NOTCH1 is sufficient to inhibit *in vitro* growth by competitive cell proliferation assays and clonogenic assays. In Acute Myeloid Leukemia (AML), Kannan et al. have shown that ICN1 induces growth arrest through a competitive cell proliferation assay (Kannan et al., 2013). Moreover they have shown arrest of cells in the G1 phase of the cell cycle, which is also consistent with our data. Since NOTCH1 acts as a tumor suppressor in AML, our results corroborate with previously reported findings. The reason for growth inhibition is not completely understood. As we have shown, senescence in part contributes to growth arrest, while a small fraction of cells also undergo cell death. Devgan et al. have shown that in keratinocytes, p21 is downstream of NOTCH1 signaling and regulates keratinocyte growth (Devgan, Mammucari, Millar, Briskin, & Dotto, 2005). Although we have also shown an induction in p21 when NOTCH1 is activated, it doesn't completely account for growth inhibition since only 30% of the cells undergo senescence. More than 60% of the cells were arrested in the G1 phase of the cell cycle and about 15% in the sub-G0 phase after transduction with activated NOTCH1 (ICN1). Kannan et al. have shown that in B-ALL, NOTCH signaling induces PARP mediated apoptosis (Kannan et al., 2011). Since only 15% of cells were arrested in the sub-G0 phase, the apoptotic mechanism was not further investigated.

When using a more physiological full-length NOTCH1 (NFL1), the growth inhibitory effects mirrored ICN1. Even in this case the percentage of senescent cells was lower suggesting that there might be other mechanisms besides senescence and cell death contributing to growth arrest. Indeed, the role of NOTCH in differentiation cannot be discounted because in mice that were injected with mutant cells having NFL1 or ICN1, the formation of keratin pearls representative of a differentiated phenotype were observed. Thus, it is possible that such induction in differentiation may contribute to growth arrest. Rangarajan and colleagues (Rangarajan et al., 2001) used a tamoxifen inducible system to delete the NOTCH1 gene in the keratinocytes of mice. They show that NOTCH1 promotes differentiation, transcriptionally up regulates p21 and inhibits keratinocyte growth (Rangarajan et al., 2001). Their results confirm our findings of NOTCH1 inducing p21, inhibiting tumor growth and possibly activating a differentiation program. Furthermore, we have shown that either the intracellular form of NOTCH1 or NOTCH2 (ICN1 or ICN2) may be sufficient to inhibit cell growth. NOTCH2 is mutated at a lower frequency compared to NOTCH1 and these mutations are not mutually exclusive. Thus, there is a possibility that in tumors that have an intact NOTCH1, mutations in NOTCH2 may contribute to tumor progression. Our findings indicate that both ICN1 and ICN2 can contribute to growth inhibition. To represent a more physiological condition, the full-length NOTCH2 needs to be cloned and experiments similar to NFL1 must be performed which is part of our future directions. NOTCH1 and NOTCH2 may be required for growth inhibition. To prove that both these isoforms may be necessary, the NOTCH signaling pathway was inhibited by expression of the pan-NOTCH inhibitor, dnMAML1. In a weakly tumorigenic NOTCH1 wild-type cell line,

inhibiting the NOTCH signaling pathway increased tumor growth but this effect was seen only in 50% of the mice injected. dnMAML1 has been shown to induce basal hyperplasia impairing squamous differentiation in mouse esophageal epithelium (Ohashi et al., 2010). In our system, we might have to evaluate the nuclear localization of dnMAML1. Since dnMAML1 suppresses the transcriptional activity of NOTCH in the nucleus, it is possible that the lack of nuclear localization after transduction in cells prevents NOTCH pathway inhibition. In light of this caveat, to better inhibit the pathway we have stably knocking out NOTCH1, NOTCH2 or both using the CRISPR-Cas9 approach. For the first time, we demonstrate the use of CRISPR technology to knock out the NOTCH gene in HNSCC cell lines and show that knocking out both NOTCH1 and NOTCH2 relieves growth suppression *in vitro*. Furthermore, we have also demonstrated that restoring NOTCH1 in double knock out cells rescues abrogation of growth inhibition, implying that NOTCH1 is necessary and sufficient to modulate cell growth. In future studies, we will examine the *in vivo* tumorigenicity after injected these cells in mice and hypothesize that knocking out both NOTCH1 and NOTCH2 would exacerbate tumor growth.

CHAPTER 6: DOWNSNTREAM EFFECTORS OF NOTCH MEDIATED GROWTH INHIBITION

Chapter 6: Downstream effectors of NOTCH mediated growth inhibition

Chapter 6.1: AXL and CTNNAL1 (α -catulin) are downstream of NOTCH signaling

Rationale: In Chapter 5, the effects of activating the NOTCH signaling pathway in wild-type and mutant cell lines was elucidated and its growth suppressive effect was demonstrated. There are several mediators of cell growth and diverse signaling cascades involved in regulating cell growth and proliferation. Previous publications have extensively detailed the oncogenic role NOTCH in breast, pancreatic cancer and T-ALL. Others have characterized NOTCH as a tumor suppressor in skin, esophageal cancer, B-ALL and hepatocellular carcinoma. For example, in B-ALL, Kannan et al. examined the role of NOTCH inducing HES1 and PARP mediated apoptosis (Kannan et al., 2011). Rangarajan and colleagues have described the role of p21 in contributing to NOTCH induced differentiation and growth arrest (Rangarajan et al., 2001). In esophageal cancer, Kagawa et al. attributed a p16 –Rb pathway or a p14-p53 pathway to senescence (Kagawa et al., 2015). To date, the mechanism of NOTCH acting as a tumor suppressor in HNSCC has not been explored. Identifying modulators downstream of the NOTCH pathway would help in targeting certain molecules that are upregulated in the absence of NOTCH signaling, and could potentially lead to better-targeted therapeutics. We had previously shown the induction of p21 as a possible potential downstream target of NOTCH1 based on the senescent morphology observed after activation with ICN1 in one mutant cell line (HN31). To identify the downstream modulators of the NOTCH signaling pathway in an unbiased fashion, we performed a microarray after activating the NOTCH pathway in two wild-type cell lines PJA34 and 183 by culturing them on

Jagged1 for 5 days. Subsequently, the Affymetrix 2.0 gene array was used to evaluate gene expression.

Results: Each condition was performed in biological triplicates and normalized before analyzing differences for expression between genes when these wild-type cells were cultured on Jagged1 compared to Fc. We used the BRB-ArrayTools in a univariate test. All the data pre-processing steps were performed by the Department of Bioinformatics (M.D. Anderson Cancer Center). Linear model was fit to each probeset using both treatment (culture on Jagged1 or Fc) and cell lines (PJA34 and 183) as fixed effects. Based on the raw p-values, they generated a model using beta-uniform mixture (BUM) to generate different p-value cut-offs based on a False Discovery Rate (FDR) of 0.05. Using this FDR, based on the identified significantly modulated probesets, concordance correlation of multiple probesets that map to the same gene was evaluated. Only one probeset for each gene was selected if their expression was inconsistent. If their expression was consistent, an average of the expression of those probesets was reported.

We found 1808 genes to be differentially regulated when comparing both treatment and cell line conditions (Appendix 1). There are 277 differentially expressed genes that have treatment effects (Jagged1 versus Fc) without cell line difference (PJA34 versus 183). Appendix 1 contains the average expression of 1808 differentially expressed genes including the p-value and the relative fold change of the treated group to the control group (relative to Fc). Out of these 1808 genes, we filtered genes that had more than a 1.4 fold difference in gene expression when these cells were cultured on Jagged1 versus Fc. Based on this filter, we narrowed the number of genes to 120 of which 50 genes were upregulated and 70 genes were downregulated by Jagged1 induced NOTCH

activation (Table 7). Some of the genes that were upregulated when NOTCH was activated are tumor suppressor genes like EPHA4, TP53INP1, PDCD 4, KRT4, KRT13 while genes that were downregulated when NOTCH was activated include AXL, MMP9, INTGA3, LAMC2 and CTNNAL1 among others. The set of 120 altered genes was then subjected to an unbiased core analysis using the Ingenuity Pathway software (IPA) to identify the most significantly altered cellular functions and pathways (Table 8). Based on the Ingenuity Pathway analysis, the three most significantly altered pathways when NOTCH is activated is cell movement ($P=2.7 \times 10^{-12}$) followed by cell growth and proliferation ($P=3.95 \times 10^{-11}$) that was followed by cell adhesion/interaction ($P=8.05 \times 10^{-10}$). Our finding that cell growth and proliferation was one of the significantly altered phenotypes validated our previous report (Chapter 5) of NOTCH significantly affecting cell growth and tumor progression. The current microarray analysis extends our earlier report to identify potential candidate genes that might be involved in modulating cell growth. Based on the significance of change (P-values), intensity of change (1.4 fold threshold) and novelty of these candidate targets with NOTCH1 (based on literature published), we identified two proto-oncogenes that were down modulated when NOTCH was activated. AXL was the most significantly altered gene in both cell lines (6.41×10^{-9}) and had approximately 3-fold downregulation when NOTCH was activated by Jagged1. CTNNAL1 (α -catulin) had the highest downregulation among all genes in the 183 wild-type cell line (24 fold). We were interested in genes suppressed by NOTCH signaling since these genes may be potentially targeted therapeutically and thus investigated the modulation of AXL and α -catulin after NOTCH activation.

Official Gene Symbol	Gene Symbol used in TCGA	Regulation by NOTCH activation	P-value	Fold change in PJ34	Fold change in 183
CAV1	CAV1	Down regulated	3.59E-09	-1.88	-2.21
AXL	AXL	Down regulated	6.41E-09	-2.74	-3.55
FHL2	FHL2	Down regulated	1.15E-07	-1.79	-2.05
CMTM8	CMTM8	Down regulated	1.64E-07	-1.47	-1.62
SERPINE1	SERPINE1	Down regulated	2.07E-07	-2.74	-2.22
PTRF	PTRF	Down regulated	3.53E-07	-2.02	-2.16
NAV3	NAV3	Down regulated	4.33E-07	-2.02	-1.84
LAMC2	LAMC2	Down regulated	5.09E-07	-2.60	-4.66
DRAM1	DRAM1	Down regulated	5.62E-07	-1.88	-2.08
AFAP1L2	AFAP1L2	Down regulated	6.00E-07	-1.49	-1.60
NETO2	NETO2	Down regulated	1.31E-06	-1.79	-1.59
TMCC3	TMCC3	Down regulated	2.29E-06	-1.72	-1.88
SEMA7A	SEMA7A	Down regulated	2.29E-06	-1.57	-1.59
ITGA5	ITGA5	Down regulated	2.34E-06	-1.55	-1.67
HOMER3	HOMER3	Down regulated	2.38E-06	-1.61	-1.46
ZBED2	ZBED2	Down regulated	2.55E-06	-1.89	-1.70
SYT16	SYT16	Down regulated	2.68E-06	-1.76	-1.62
SLC16A2	SLC16A2	Down regulated	3.34E-06	-1.80	-2.57
FGFBP1	FGFBP1	Down regulated	3.66E-06	-1.84	-2.19

FHOD1	FHOD1	Down regulated	3.75E-06	-1.44	-1.47
ITGA3	ITGA3	Down regulated	5.03E-06	-1.56	-1.88
PXN	PXN	Down regulated	5.48E-06	-1.51	-1.83
PKP2	PKP2	Down regulated	5.73E-06	-1.51	-1.54
THSD4	THSD4	Down regulated	6.42E-06	-1.50	-1.54
KLK6	KLK6	Down regulated	1.11E-05	-1.83	-1.76
SOX15	SOX15	Down regulated	1.34E-05	-1.76	-1.40
PLEK2	PLEK2	Down regulated	1.86E-05	-1.79	-1.61
MOBKL2B	MOBKL2B	Down regulated	1.94E-05	-1.58	-1.52
LOXL2	LOXL2	Down regulated	2.16E-05	-2.49	-1.63
PLAUR	PLAUR	Down regulated	2.35E-05	-1.91	-1.74
MMP9	MMP9	Down regulated	2.35E-05	-1.60	-2.53
UPP1	UPP1	Down regulated	2.80E-05	-1.43	-1.55
LOXL4	LOXL4	Down regulated	2.94E-05	-3.12	-1.80
SLC7A2	SLC7A2	Down regulated	3.00E-05	-1.50	-2.24
TMEM27	TMEM27	Down regulated	3.16E-05	-1.63	-1.48
ANKRD2	ANKRD2	Down regulated	3.72E-05	-1.67	-1.56
AP2B1	AP2B1	Down regulated	4.28E-05	-1.43	-2.22
LEPREL1	LEPREL1	Down regulated	6.37E-05	-1.63	-1.51
SLC39A14	SLC39A14	Down regulated	6.56E-05	-1.46	-2.26
CD55	CD55	Down regulated	8.36E-05	-1.42	-1.73
HEG1	HEG1	Down regulated	8.76E-05	-1.49	-1.87
PI4K2A	PI4K2A	Down regulated	9.68E-05	-1.49	-1.40

FST	FST	Down regulated	0.00010061	-1.99	-5.32
NXPE3	FAM55C	Down regulated	0.000109425	-1.52	-1.69
VEGFC	VEGFC	Down regulated	0.000109475	-2.01	-1.50
SIRPA	SIRPA	Down regulated	0.000121239	-1.80	-1.42
KIRREL	KIRREL	Down regulated	0.000126131	-1.77	-1.46
OLR1	OLR1	Down regulated	0.00013061	-6.59	-2.08
KIAA0040	KIAA0040	Down regulated	0.000150652	-1.55	-1.46
CYR61	CYR61	Down regulated	0.000154488	-1.92	-1.70
VLDLR	VLDLR	Down regulated	0.00018433	-1.58	-2.03
RAB32	RAB32	Down regulated	0.000209603	-1.48	-1.80
TIMP4	TIMP4	Down regulated	0.000261133	-1.40	-1.46
ABCG2	ABCG2	Down regulated	0.000307053	-1.84	-6.60
FAM101B	FAM101B	Down regulated	0.000374899	-2.28	-1.45
MFAP5	MFAP5	Down regulated	0.000455964	-1.48	-3.14
NT5E	NT5E	Down regulated	0.000464717	-1.48	-2.34
COL17A1	COL17A1	Down regulated	0.000479488	-1.43	-3.37
CPA4	CPA4	Down regulated	0.000582963	-1.45	-1.56
EMP3	EMP3	Down regulated	0.000688038	-2.13	-1.53
CTNNAL1	CTNNAL1	Down regulated	0.0009852	-2.12	-24.86
TIMP3	TIMP3	Down regulated	0.001204042	-1.54	-1.41
CDH13	CDH13	Down regulated	0.001276195	-1.61	-1.45
FAM46B	FAM46B	Down regulated	0.001472671	-1.41	-1.65
IL6R	IL6R	Down regulated	0.002073781	-1.61	-1.63

HBEGF	HBEGF	Down regulated	0.002619748	-1.44	-1.72
EREG	EREG	Down regulated	0.003182918	-1.93	-1.46
EPHA2	EPHA2	Down regulated	0.003589923	-1.49	-1.62
FOSL1	FOSL1	Down regulated	0.004399443	-2.54	-1.82
B4GALT6	B4GALT6	Down regulated	0.004750404	-1.46	-1.50
BCL6	BCL6	Up regulated	0.002698801	1.61	1.49
TNKS	TNKS	Up regulated	0.002485846	1.77	1.41
HLA-DRA	HLA-DRA	Up regulated	0.001875278	3.39	1.50
SCARNA9	SCARNA9	Up regulated	0.001560804	2.16	1.53
LONP2	LONP2	Up regulated	0.001107504	1.45	1.41
SCARNA17	SCARNA17	Up regulated	0.00090611	1.47	1.67
GUSBP3	GUSBP3	Up regulated	0.000559537	1.50	1.46
AKR1C3	AKR1C3	Up regulated	0.00054151	1.52	1.76
ZNF117	ZNF117	Up regulated	0.000509494	1.63	2.63
MUC16	MUC16	Up regulated	0.000431455	2.03	1.47
PGLYRP4	PGLYRP4	Up regulated	0.000373443	1.44	2.23
IKZF2	IKZF2	Up regulated	0.00033363	1.41	1.45
DLX5	DLX5	Up regulated	0.000332635	1.77	1.64
KRT4	KRT4	Up regulated	0.000263173	2.00	7.95
PRODH	PRODH	Up regulated	0.00016933	1.83	1.59
MYH14	MYH14	Up regulated	0.000141238	1.57	1.73
TXNIP	TXNIP	Up regulated	0.000124053	2.63	1.67
KLHL24	KLHL24	Up regulated	0.00010392	1.74	1.55

KRT13	KRT13	Up regulated	9.57E-05	1.77	3.60
GOLGA8A	GOLGA8A	Up regulated	7.85E-05	1.70	1.40
GLUL	GLUL	Up regulated	6.63E-05	1.67	1.43
TMEM45B	TMEM45B	Up regulated	6.02E-05	1.43	2.06
GOLGA8B	GOLGA8B	Up regulated	4.87E-05	1.76	1.43
MANSC1	MANSC1	Up regulated	4.58E-05	1.56	1.73
FAM102B	FAM102B	Up regulated	2.85E-05	1.66	1.41
DSP	DSP	Up regulated	2.46E-05	1.47	1.65
PRKX	PRKX	Up regulated	2.37E-05	1.56	1.66
PCMTD2	PCMTD2	Up regulated	2.07E-05	1.41	1.48
CNKSR3	CNKSR3	Up regulated	1.67E-05	1.41	1.92
GCLC	GCLC	Up regulated	1.57E-05	1.77	1.41
RNF138P1	RNF138P1	Up regulated	1.42E-05	2.98	2.43
FAM214A	KIAA1370	Up regulated	1.28E-05	1.41	1.46
HES5	HES5	Up regulated	1.15E-05	1.46	1.64
ST6GALNAC2	ST6GALNAC2	Up regulated	1.15E-05	1.46	1.57
ACPP	ACPP	Up regulated	9.76E-06	1.62	1.44
SLC12A2	SLC12A2	Up regulated	8.22E-06	1.57	2.29
PBX1	PBX1	Up regulated	7.54E-06	1.64	1.82
CYP1A1	CYP1A1	Up regulated	6.40E-06	1.65	2.25
PPAP2A	PPAP2A	Up regulated	4.43E-06	1.83	3.05
TNFSF10	TNFSF10	Up regulated	3.47E-06	1.41	1.63
KIAA1147	KIAA1147	Up regulated	3.24E-06	1.47	1.71

PDCD4	PDCD4	Up regulated	2.01E-06	1.72	2.08
PLD1	PLD1	Up regulated	8.95E-07	1.66	2.02
LURAP1L	C9orf150	Up regulated	7.13E-07	1.74	2.03
SLPI	SLPI	Up regulated	1.58E-07	1.44	1.56
TP53INP1	TP53INP1	Up regulated	1.21E-07	2.99	2.27
EPHA4	EPHA4	Up regulated	8.73E-08	1.65	1.94
VTCN1	VTCN1	Up regulated	2.24E-08	3.08	2.96
KRT15	KRT15	Up regulated	2.22E-08	1.90	1.69
RAB40B	RAB40B	Up regulated	1.78E-08	1.70	1.98

Table 7: Top 120 genes modulates when NOTCH signaling is activated. (Red= upregulates, Green= Downregulated when treated with Jagged1)










Genes regulated by NOTCH		Hits/total
Cell Movement (P=2.72E-12)		47/2780
Invasion (P=1.63E-10)		27/1069
Keratinocyte Migration (P=8.90E-5)		5/80
Proliferation (P=3.95E-11)		62/4110
Keratinocyte Proliferation (P=3.65E-04)		6/164
Cell Death (P=7.44E-08)		52/3946
Differentiation of cells (P=1.42E-08)		42/4286
Differentiation of skin (P=9.61E-04)		6/210
Adhesion of tumors (P=8.05E-10)		15/337

Table 8: Ingenuity Pathway Analysis of significantly modulated pathways when NOTCH is activated in wild-type cell lines PJA34 and 183. (Red= Genes Upregulated by NOTCH, Green= Genes Downregulated by NOTCH).

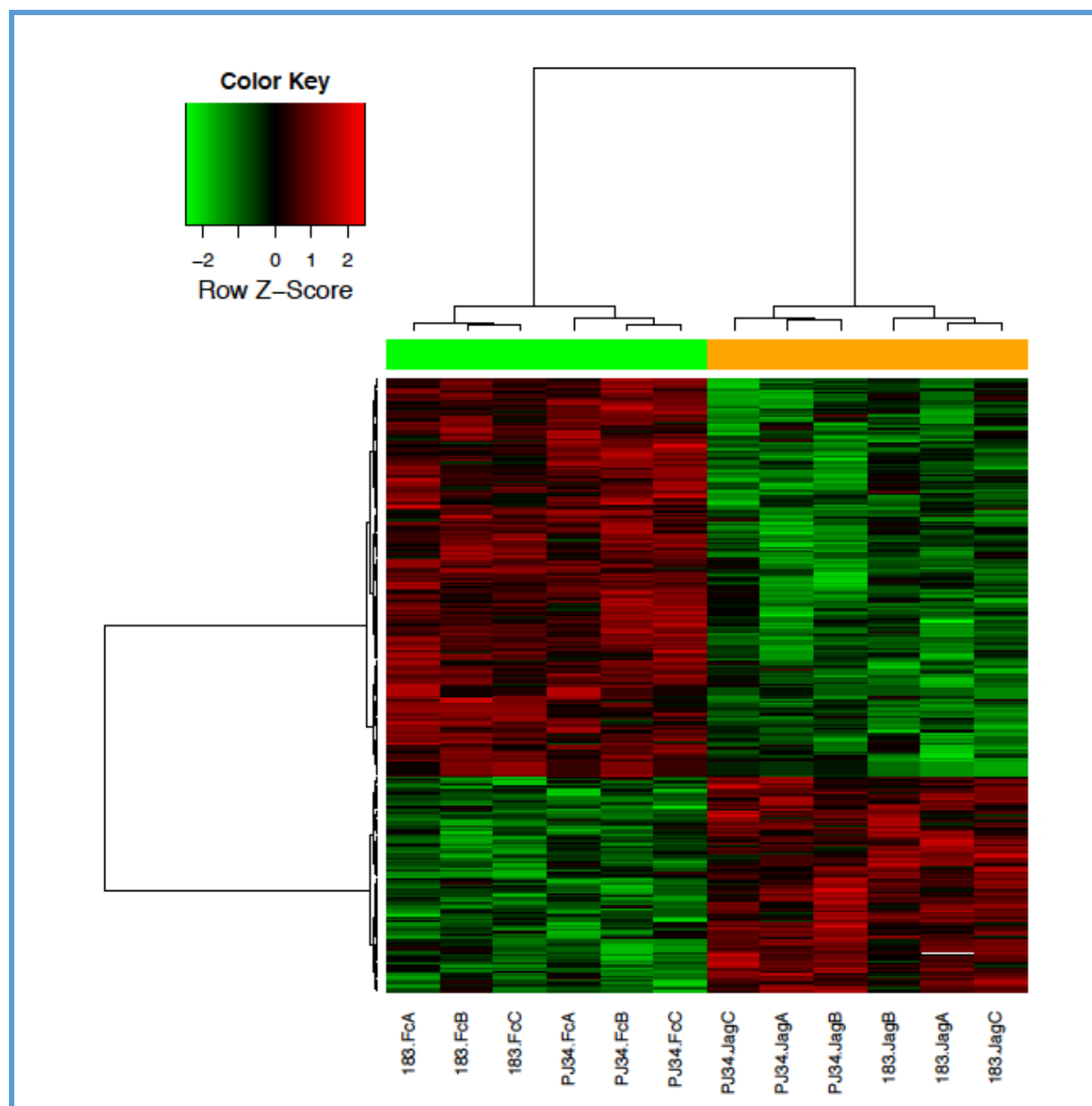


Figure 34: Heat-map of 277 differentially expressed genes having treatment effects but not cell lines effects. Top green bar: control samples. Top orange bar: Jagged1 treated samples.

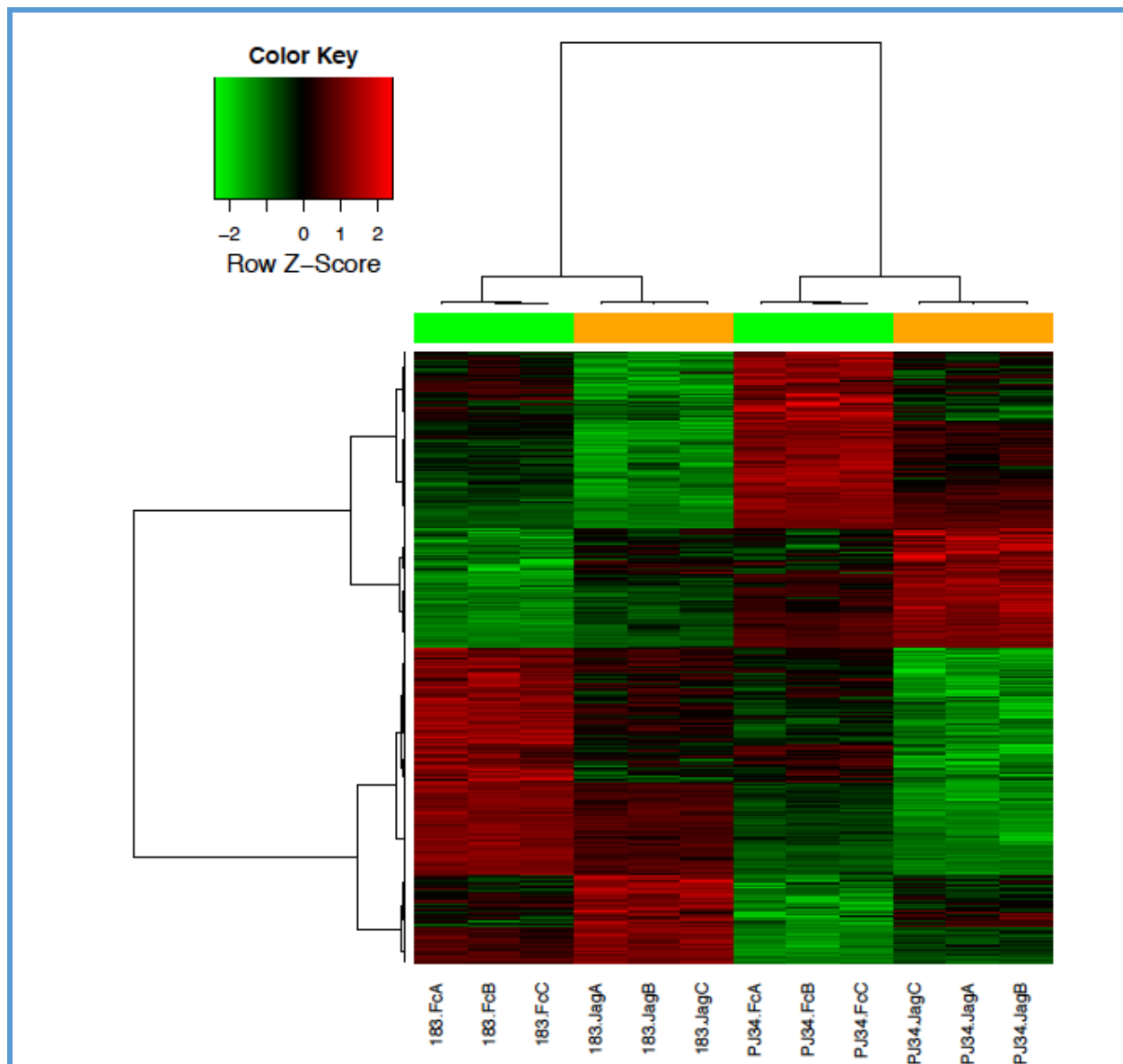


Figure 35: Heat map of 1571 differentially expressed genes that have both treatment and cell line effects. Top green bar: control samples. Top orange bar: Jagged1 treated samples

Chapter 6.2: NOTCH1 modulates AXL and CTNNAL1 (α -catulin) at the protein level

Rationale: We had previously observed induction of AXL and CTNNAL1 (α -catulin) at the gene expression level after activating NOTCH signaling in wild-type cell lines. AXL and α -catulin are overexpressed in many cancers (Dunne et al., 2014; Schultz et al., 1995). Elevated protein expression of AXL has been evaluated as a poor prognostic factor for overall survival in colon cancer, osteosarcoma, and pancreatic cancer (Dunne et al., 2014; J. Han et al., 2013; Song et al., 2011). Furthermore, AXL expression is also a prognostic for increased lymph node metastasis and clinical stage in lung adenocarcinoma, breast and ovarian cancer (D'Alfonso et al., 2014; Rankin et al., 2010; Shieh et al., 2005). Recently, Kreisde and colleagues have shown that α -catulin is highly expressed in melanoma cells and that α -catulin is a key driver of melanoma tumor formation, growth, invasion and metastasis (Kreiseder et al., 2013). In order to validate that the transcriptional modulation of AXL and α -catulin by NOTCH1, we performed a western blot to evaluate the expression of these two proto-oncogenes at the protein level.

Results: We first overexpressed the activated form of NOTCH1 (ICN1) in a NOTCH1 wild-type and mutant cell line (PJA34 and HN31 respectively) and evaluated protein expression of AXL and α -catulin 3 days and 5 days after infection. At both time points, there was significant suppression of both AXL and α -catulin in ICN1 infected cells compared to MigR1 (empty vector) infected cells suggesting that the activated form of NOTCH1 might be sufficient to modulate these two proto-oncogenes (Figure 36). Next, the full length NOTCH1 receptor (NFL1) was expressed in the mutant cell lines HN31, UM22A and UM47 and these cells were then cultured on Jagged1 for 3 days to evaluate AXL and α -catulin levels in a more physiological setting. Expression levels of

both the proto-oncogenes was diminished by at least 50% when NOTCH signaling was activated by Jagged1 compared to cells cultured on Fc and empty vector infected cells (Figure 37). To prove that the down modulation of AXL and α -catulin was indeed due to NOTCH signaling, the wild-type cells PJA34 were infected with dnMAML1 (to inhibit NOTCH signaling) before culturing these infected cells on Jagged1 or Fc for 3 days. Inhibiting the NOTCH signaling pathway using dnMAML1 reversed the Jagged1 mediated suppression of both these proto-oncogenes (Figure 38). In addition to using dnMAML1, we also knocked out NOTCH1 and NOTCH2 using the CRISPR-Cas9 system in the wild-type cell lines PJA34 and found that knocking out both NOTCH isoforms induces expression of AXL and α -catulin (Figure 39). The wild type cell line when cultured on Jagged1 suppresses AXL and α -catulin, however double knockout of NOTCH1 and NOTCH2 (dKO) reverses this suppression suggesting that NOTCH1 and NOTCH2 might be necessary to suppress these proto-oncogenes. Interestingly, restoration of NFL1 in the dKO PJA 34 cell line relieves the induction of these molecules when cultured on Jagged1. Furthermore, even restoration of NFL1 in the NOTCH1 KO PJA 34 inhibited AXL and α -catulin when cultured on Jagged1. This suggests that NOTCH signaling may be necessary and sufficient to inhibit AXL and α -catulin.

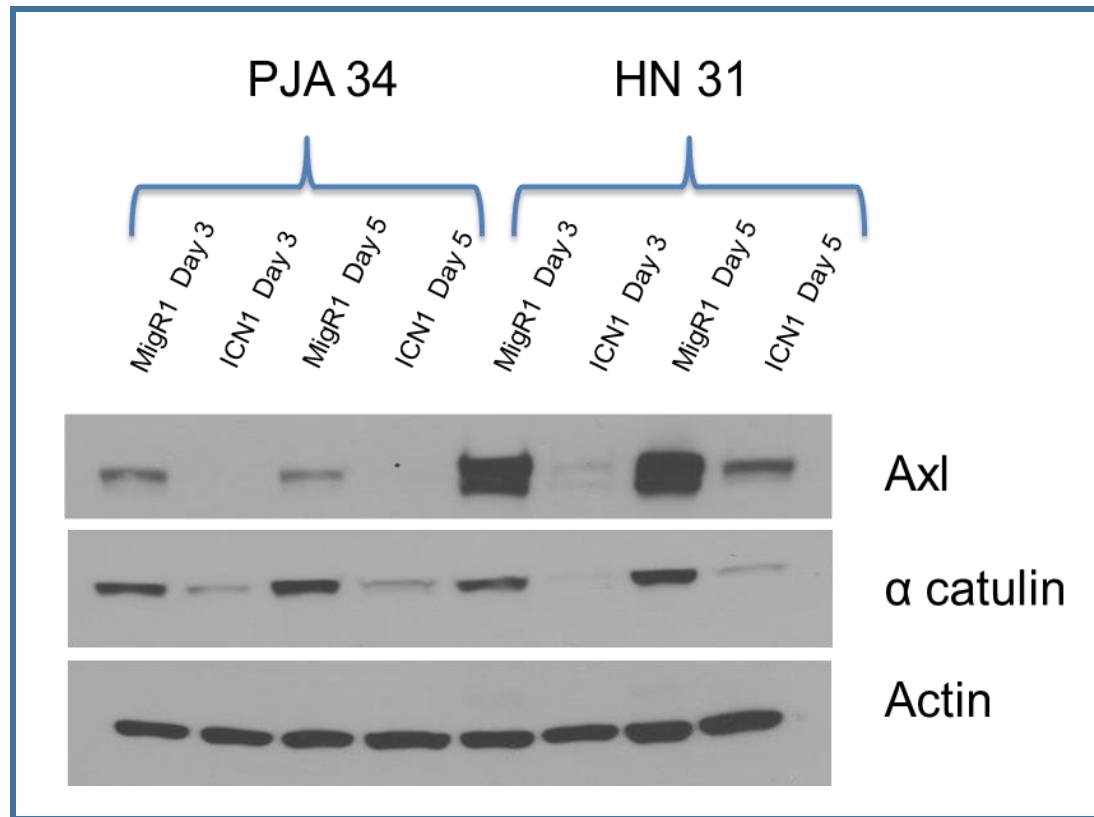


Figure 36: Activated NOTCH1 (ICN1) is sufficient to suppress AXL and α -catulin.

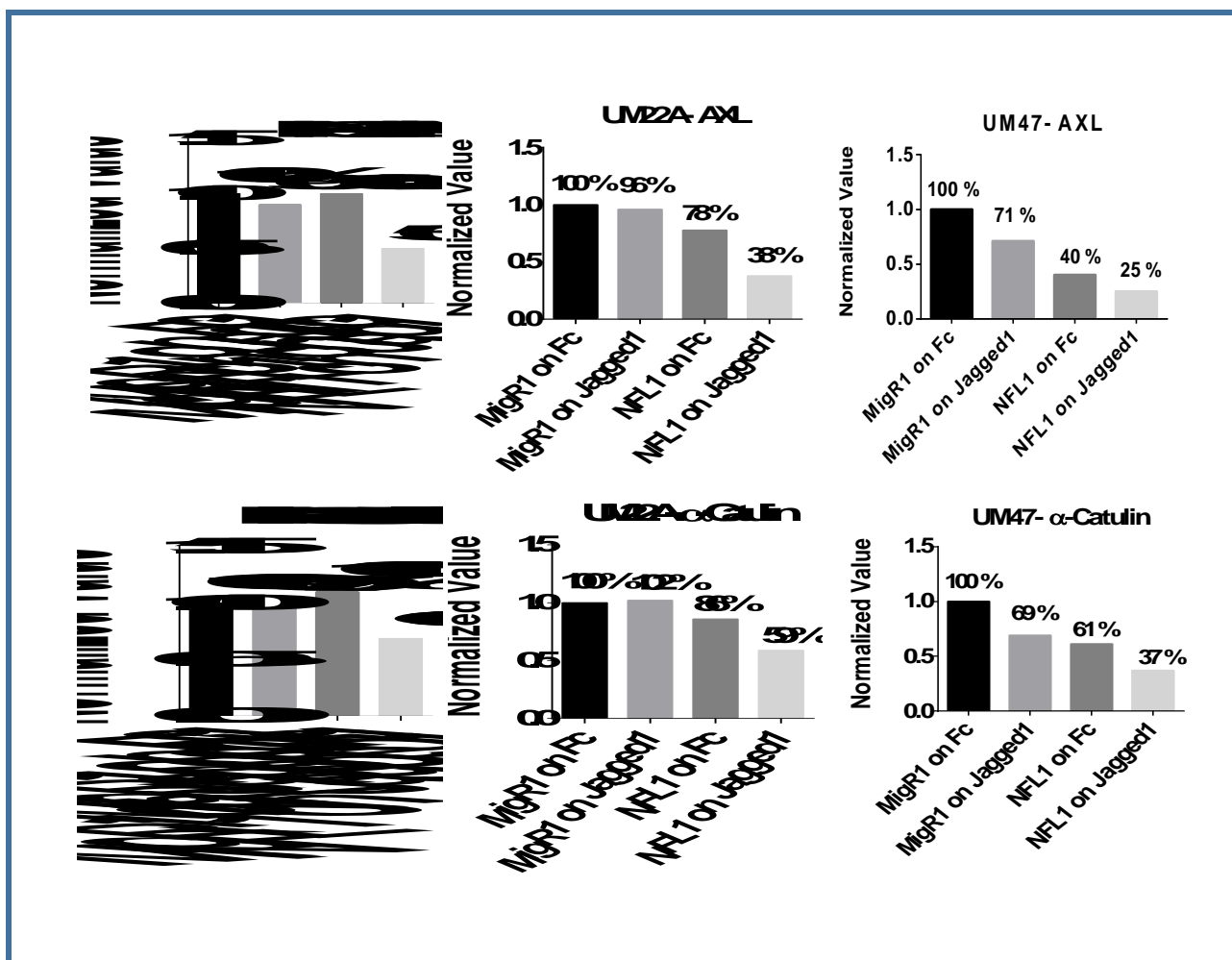
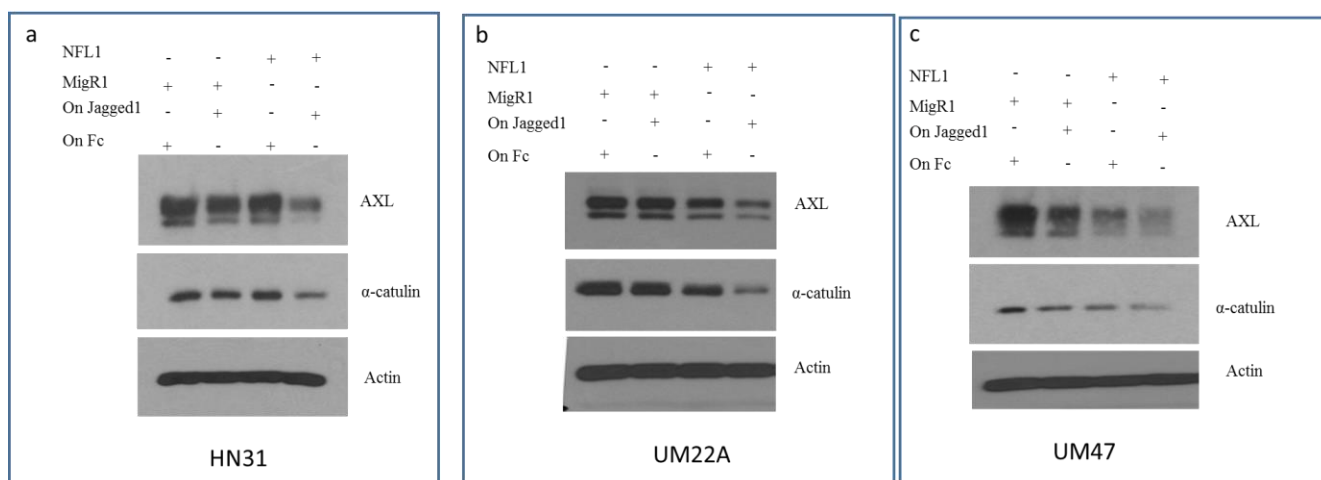


Figure 37: Restoration of full length NOTCH1 (NFL1) in the mutant cell lines: HN31, UM22A and UM47 after activation with Jagged1 suppress AXL and α-catulin

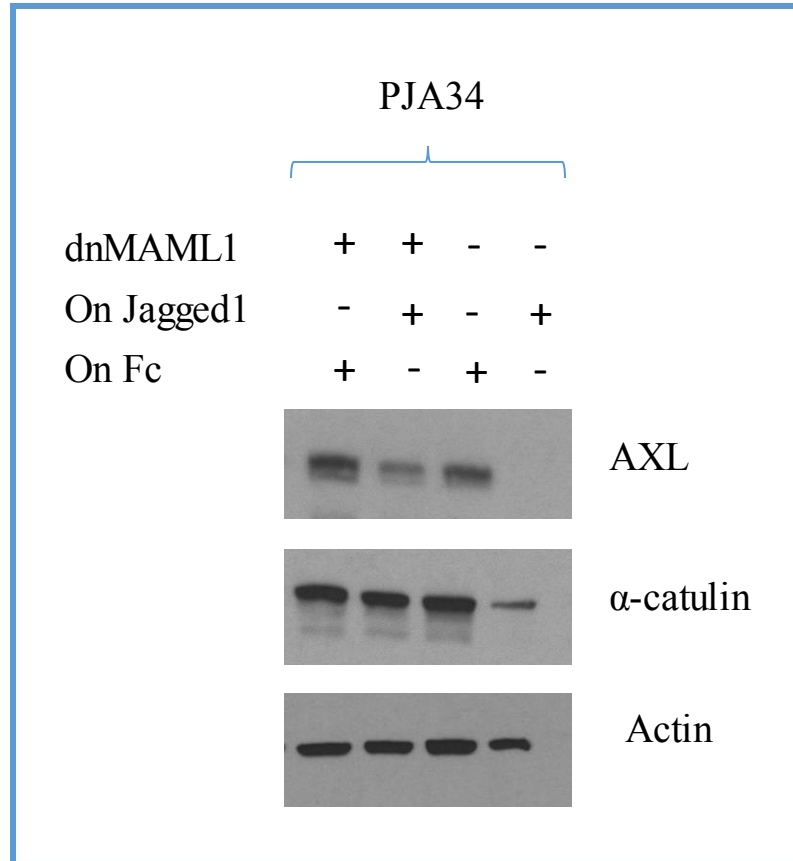


Figure 38: Inhibition of NOTCH signaling using dnMAML1 reverses Jagged1 induced suppression of AXL and α-catenin.

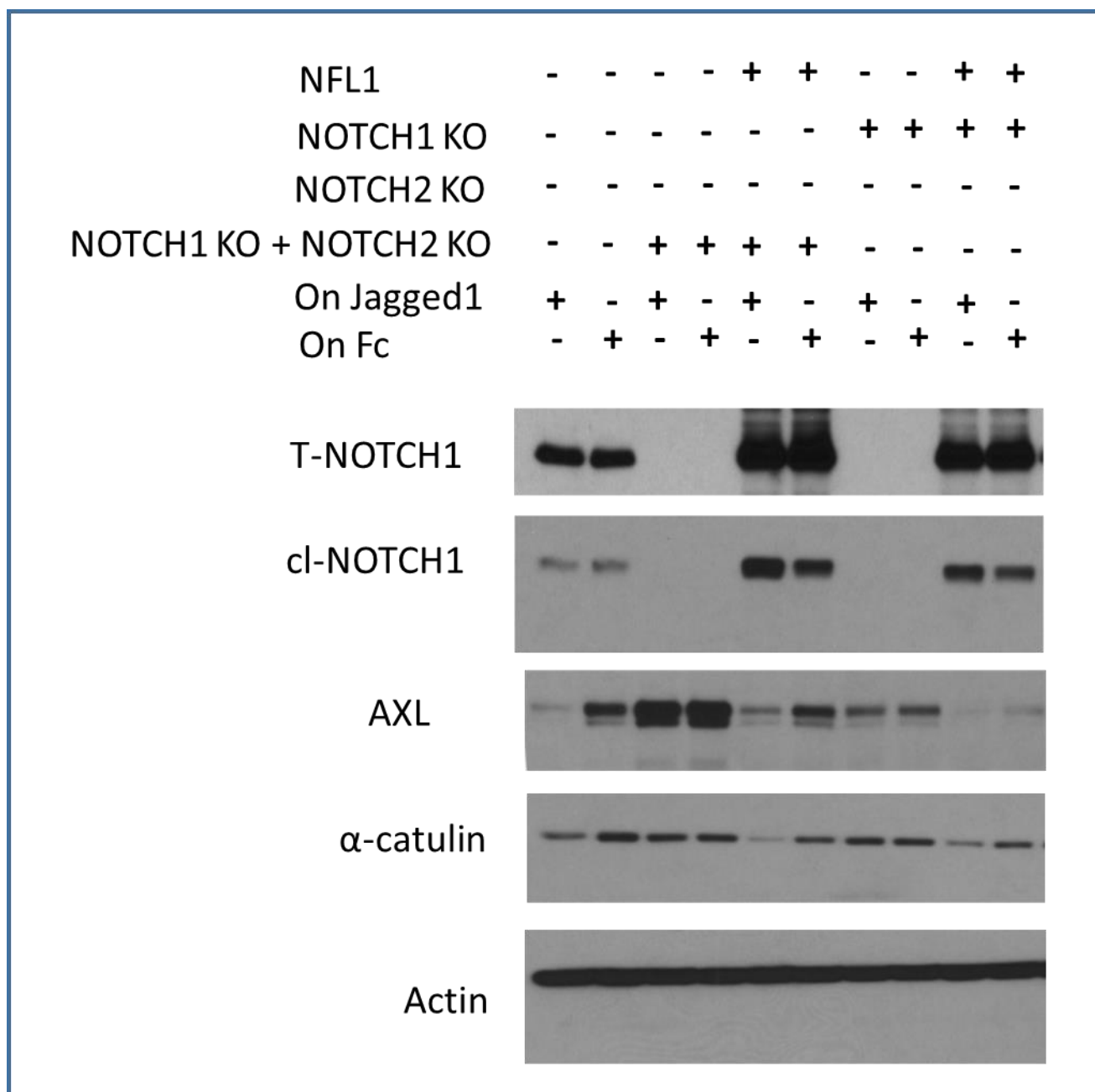


Figure 39: NOTCH signaling is necessary and sufficient to inhibit AXL and catulin: Knocking out NOTCH signaling using the CRISPR-Cas9 system induces AXL and α -catulin which is reversed when the same cell line is restored with NFL1.

Chapter 6.3: HES2 and HES5 may be sufficient to modulate AXL and α -catulin

Rationale: Canonically, the activation of the NOTCH pathway induces expression of the HES and HEY family of genes which are known transcriptional modulators (mostly repressors) of target genes involved with cell proliferation, differentiation, migration, and angiogenesis. We initially identified AXL and α -catulin suppression from gene expression arrays and since HES and HEY are direct downstream targets of the NOTCH signaling pathway, we hypothesized that HES or HEY members might be involved in regulating the expression of these proto-oncogenes.

Results: First, the mRNA expression levels of the HES and HEY family members after activating NOTCH signaling was evaluated in a NOTCH1-mutant cell line (HN31) expressing NFL1 and culturing cells on Jagged1 or Fc for 20h since hEs and HEY are early expression genes. Shown in Figure 40 is qRT-PCR analysis showing significantly altered members of HES and HEY after NOTCH activation. There was a 3-5 fold increase in HES2, HES5 and HEY2, but no significant change in HES1, HES3, HES4 and HEY1 (Figure 40). Among the selected candidate targets, HES2 and HES5 had the highest increase (3.5 and 5 fold respectively) compared to HEY2 (2.5 fold).

Following the identification of these downstream targets, we evaluated if these molecules are sufficient to inhibit AXL and α -catulin expression. For this, MigR1-flag tagged- GFP constructs of HES2 and HES5 were expressed in the NOTCH1 mutant cell line HN31. Forty-eight hours after infection, these cells were purified for GFP by flow cytometry, and were harvested for western blotting. Both HES2 and HES5 were sufficient to suppress protein levels of AXL by at least 55% and α -catulin by at least 33% compared to the parental and empty vector controls (Figure 42: Relative expression levels

of Flag-Tag, HES5, AXL, p-AXL, α -catulin and Gas6 from the western blot shown in Figure 41). Furthermore, there was also a decrease in phospho-AXL and Gas6 (a ligand for AXL) suggesting that AXL activity is also abrogated when HES2 and HES5 are overexpressed. Taken together, NOTCH1 can inhibit HES2 and HES5, which might be sufficient to modulate AXL and α -catulin protein expression.

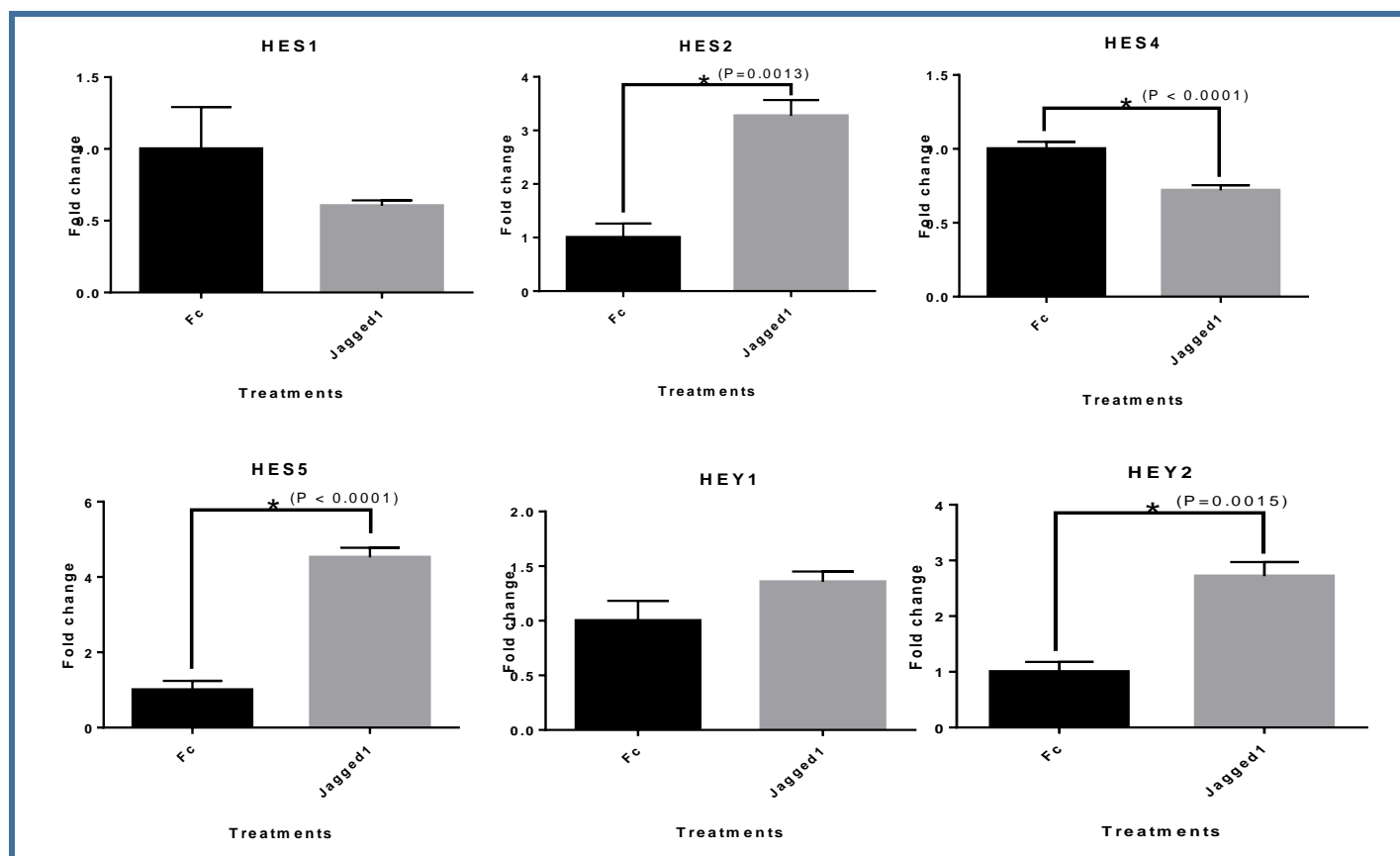


Figure 40: Modulation of HES and HEY members after restoration of NOTCH signaling in HN31 cells and culturing on Jagged1 for 20h

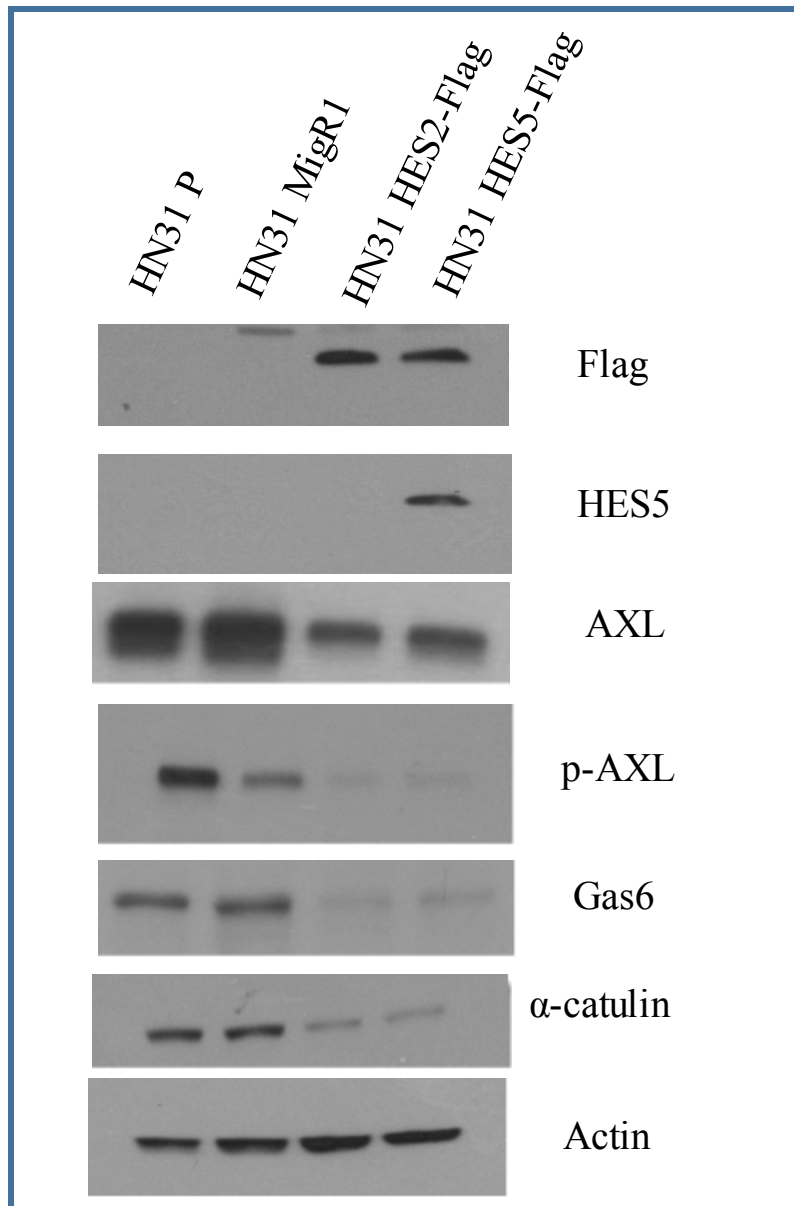


Figure 41: HES2 and HES5 might be sufficient to modular protein expression of AXL, p-AXL, Gad6 and α-catulin. Overexpressing HES2 and HES5 using Flag tagged constructs in the mutant cell line HN31 inhibits protein expression of proto-oncogenes AXL and α-catulin.

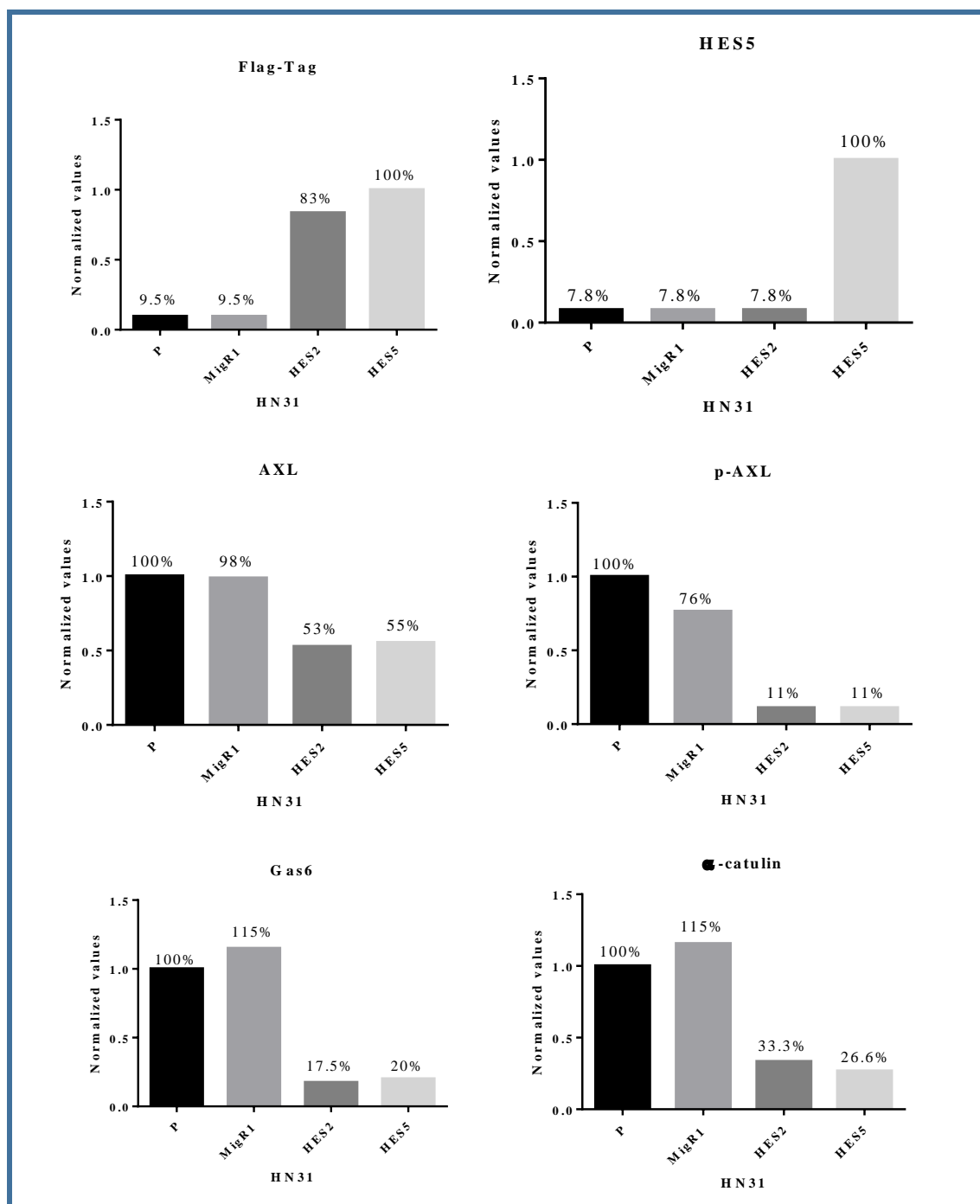


Figure 42: Relative expression levels of Flag-Tag, HES5, AXL, p-AXL, α-catulin and Gas6 from the western blot shown in Figure 41

Chapter 6.4: The 120 *in vitro* gene signature corresponds with NOTCH activation status in patients

Rationale: Previously, we identified 120 differentially regulated genes when the NOTCH signaling pathway was activated in wild-type cell lines PJA34 and 183. Some of these genes, such as AXL (Brand et al., 2015), CTNNAL1 (Cao et al., 2012), INTGA3 (Nakada et al., 2013), INTGA5 (Janes & Watt, 2006), VEGFC (Wang, Chen, Fang, & Yang, 2013), and keratins (Rangarajan et al., 2001) have shown to be overexpressed in different cancers. The correlation between NOTCH mutational status in HNSCC patients and expression of the identified genes is not known. Since the gene expression array was performed *in vitro* after activating NOTCH signaling, we evaluated the correlation between the 120 identified genes *in vitro* to NOTCH mutational status in HNSCC patients. We hypothesized that genes modulated by NOTCH signaling *in vitro* would correlate with HNSCC patients having an active NOTCH gene signature.

Results: We evaluated RNA-seq data from 498 TCGA HNSCC patient samples based on the *in vitro* gene signature. The 120 genes of interest originated from the significant gene list based on Affymetrix HuGene 2.0 ST array data. There are more than 20,000 genes for the expression data and the whole data set was divided into two parts according to tumor sites: Oral Cavity (OC) and Laryngeal/Hypopharyngeal (LH). The TCGA RNA-Seq data was downloaded from Broad GDAC Firehose and was processed and normalized by the Department of Bioinformatics (M.D. Anderson Cancer Center). We read the TCGA RNA-Seq data and subsetted the data into one with the expression of the interested genes. The NOTCH1 and NOTCH2 mutation status were overlaid and patients were assigned two or three groups based on clustering. We then produced heat

maps with pearson distance and ward linkage based on 498 patient samples, 120 genes and two anatomical sites. We found two distinct clusters; genes upregulated after NOTCH activation were grouped into cluster A (left red bar of Figure 43Figure 44) while all genes that were downregulated by NOTCH activation formed cluster B (left green bar of Figure 43 Figure 44). In cluster A of the Oral cavity subset, we found 49 genes upregulated by Jagged1 and 17 genes downregulated, while in cluster B, only 1 gene was upregulated by Jagged1 and 53 genes were downregulated (Table 9). Similarly, we observed 44 Jagged1 upregulated genes and 24 downregulated genes in cluster A of the Laryngeal/Hypopharyngeal subset, and 6 upregulated and 46 downregulated genes in cluster B of the same subset (Table 12). Since we performed an unsupervised clustering analysis, we observed similar clustering of the 120 genes to the cell lines *in vitro* and thus confirmed our previous *in vitro* microarray analysis. In the two anatomical sites, we observed at least two clusters; patients having an inactive NOTCH gene signature (cluster 1) or an active NOTCH gene signature (cluster 2). Since patients in cluster 1 had gene expression levels opposite of those in cell lines (i.e. genes upregulated in cell lines when NOTCH was active was downregulated in cluster 1 in patients and vice versa), those patients possibly have an inactive NOTCH pathway. Genes modulated in cluster 2 resemble cell lines with an activated NOTCH pathway. Thus, it is possible that these patients might have an active NOTCH pathway. Moreover, patients in cluster 2 lack any NOTCH1 or NOTCH2 mutations. In the Oral Cavity patient subset, 34 patients were mutant for NOTCH1 and 113 patients harbored a wild-type receptor in Cluster 1, while in cluster 2, only one patient had NOTCH1 mutations and 39 patients harbored the wild-type NOTCH1 (Table 10). In the Laryngeal/Hypopharyngeal cluster, cluster 1 had 15

NOTCH1 mutant patients and 28 wild-type, while cluster 2 had 1 NOTCH1 mutant patient and 29 wild-type NOTCH1 patients (Table 11). In cluster 3 of both sites, are patients that might have the NOTCH pathway inactivated in ways besides somatic mutation. Thus, these patients might be clustered under an active NOTCH gene signature but might have an inactive NOTCH downstream pathways. Correlation heat maps, and a histogram depicting the number of differentially expressed genes with various FDR cut-offs and p-values for the Oral Cavity group are shown in appendix 2 and 3 respectively. Shown in Table 13 are the associations of the 120 differentially expressed genes with the different clusters (in cell lines A versus B) in the TCGA patient samples in both anatomical sites. We observe that in patients, clustering is similar to cell lines and correlate with each other. In addition to subjecting the 120-gene signature to an unbiased clustering analysis in patients, we were also interested in the most significantly modulated genes among all the genes in patient tumors. We performed an unsupervised clustering and generated a heat map of the significantly differentially expressed genes from the t-test between group 1 and group 2 based on an FDR of 0.000001 at all anatomical sites (Figure 45 and Figure 46). When the differential expression of these genes were analyzed, we were surprised to find that in addition to high mRNA levels of keratins, integrins, AXL and modest increase in α -catulin, two of the top effectors were aldehyde dehydrogenase ALDH1A1 and ALDH1A3. Both these are stem cell markers whose mRNA levels was high in patients with an active NOTCH pathway. We observed a 32-fold increase in ALDH1A1 in Oral Cancer patients with active NOTCH pathway and 10 fold increase in ALDH1A3. Similarly, we found a 13 fold increase in ALD1A1 in Laryngeal/hypopharyngeal cancers and 19 fold increase in ALDH1A3. ALDH1A1 and

ALDH1A3 were two of the top stem cell makers that we didn't observe from the microarray in vitro. This finding is intriguing because it implies that activation of NOTCH signaling can potentially turn on a stem cell program and increase maintenance of stem cells. We had shown earlier that in mutant cells after restoring NOTCH1, and injecting these cells in mice, we observed the formation of keratin pearls indicating differentiation. While, we do observe differentiation markers from the TCGA data, we now also have evidence of a possible increase in stem cell markers. We speculate that NOTCH activation increases differentiation and thus inhibits cell growth, but the upregulation of ALDH1A3 and ALDH1A5 opens up new avenues on how NOTCH may regulate a stem cell phenotype that needs to be investigated in the future.

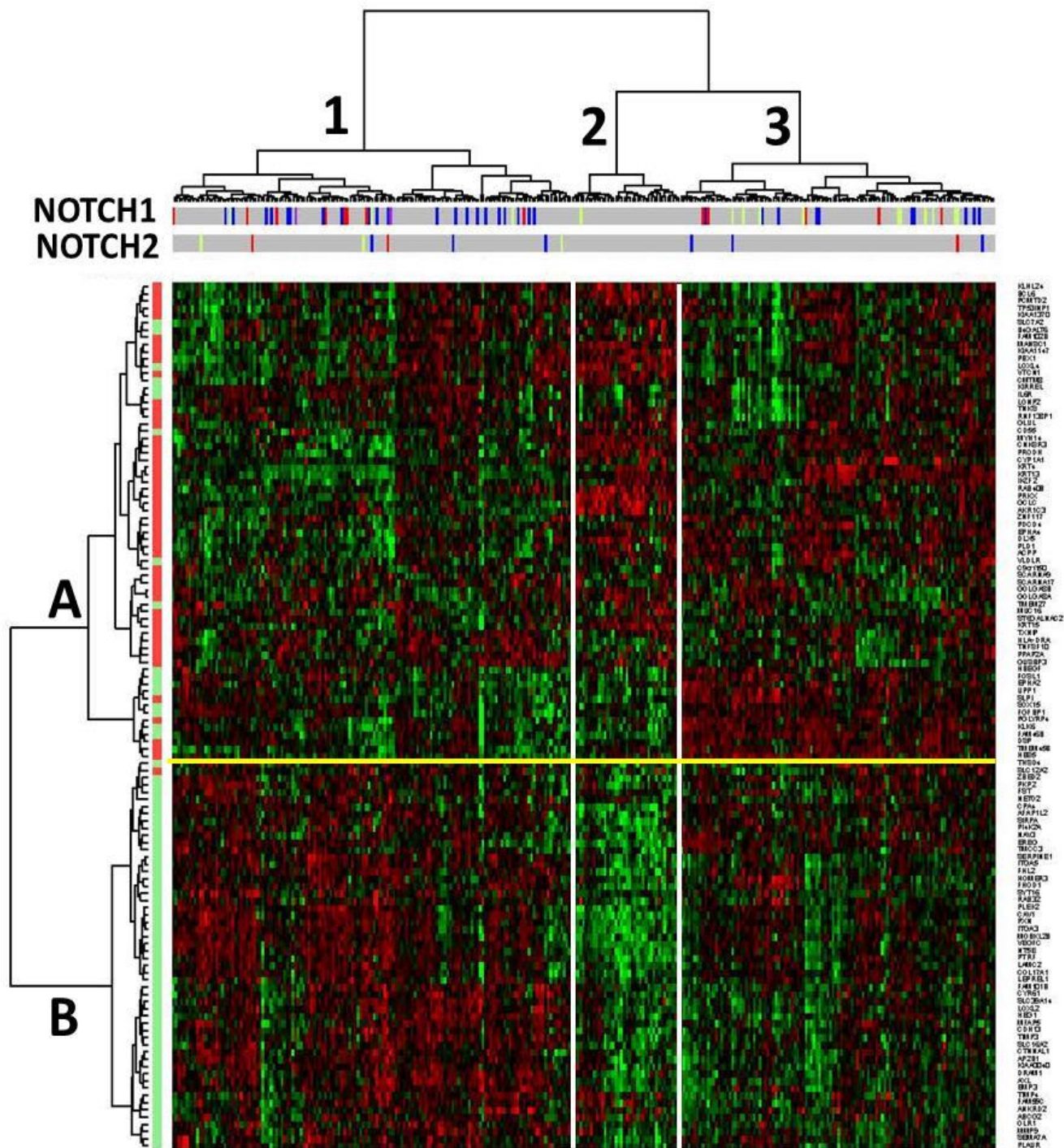


Figure 43: Heat-map of the 120 in vitro gene signature in Oral Cavity TCGA tumors

	Patient Cluster 1	Patient Cluster 2
NOTCH1 mutant	34 (27.5)	1 (7.5)
NOTCH1 wild type	113 (119.5)	39 (32.5)

Table 9: Total number of Oral Cavity (OC) patients in each cluster corresponding to NOTCH1 mutational status. Shown in parenthesis are expected numbers based on Chi-Squared test

	Gene Cluster A	Gene Cluster B
Up by Jag1	49 (27.5)	1 (22.5)
Down by Jag1	17 (38.5)	53 (31.5)

Table 10: Total number of genes in each cluster of Oral Cavity (OC) patients corresponding to modulation by Jagged1 in cell lines. Shown in parenthesis are expected numbers based on Chi-Squared test.

	Patient Cluster 1	Patient Cluster 2
NOTCH1 mutant	15 (9.4)	1 (6.6)
NOTCH1 wild type	28 (33.6)	29 (23.4)

Table 11: Total number of Laryngeal/Hypopharyngeal (LH) patients in each cluster corresponding to NOTCH1 mutational status. Shown in parenthesis are expected numbers based on Chi-Squared test

	Gene Cluster A	Gene Cluster B
Up by Jag1	44 (28.3)	6 (21.7)
Down by Jag1	24 (39.7)	46 (30.3)

Table 12: Total number of Laryngeal/Hypopharyngeal (LH) patients in each cluster corresponding to NOTCH1 mutational status. Shown in parenthesis are expected numbers based on Chi-Squared test

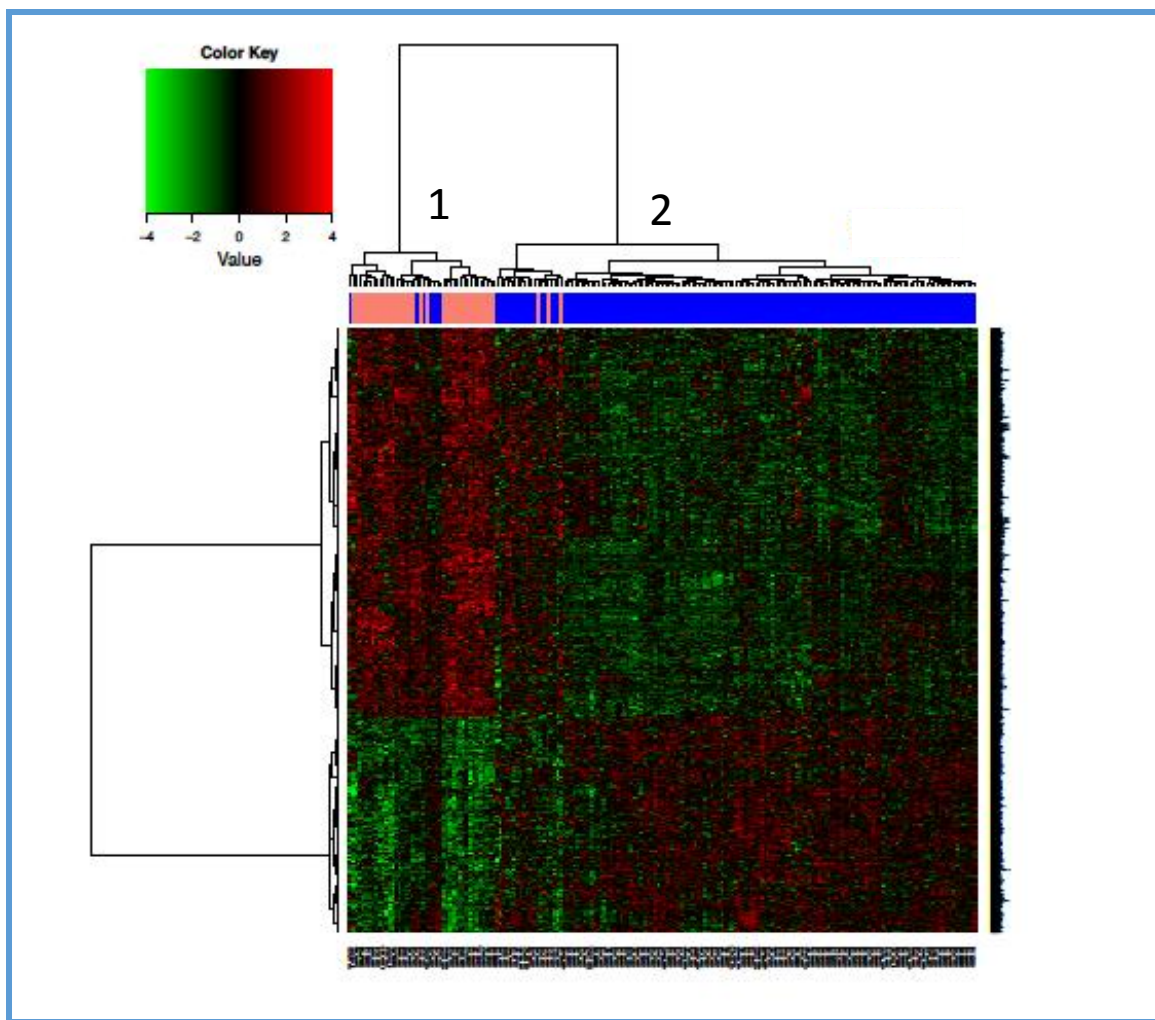


Figure 45: Unsupervised clustering of 498 TCGA Oral Cavity (OC) tumors based on 20,000 genes.

Official Gene Symbol	Gene Symbol used in TCGA	Regulated by NOTCH	Oral Cavity Gene Cluster (A or B)	Larynx Hypopharynx Gene Cluster (A or B)
CAV1	CAV1		B	B
AXL	AXL		B	B
FHL2	FHL2		B	B
CMTM8	CMTM8		B	B
SERPINE1	SERPINE1		B	B
PTRF	PTRF		B	B
NAV3	NAV3		B	B
LAMC2	LAMC2		B	B
DRAM1	DRAM1		B	A
AFAP1L2	AFAP1L2		B	B
NETO2	NETO2		B	A
TMCC3	TMCC3		B	A
SEMA7A	SEMA7A		B	B
ITGA5	ITGA5		B	B
HOMER3	HOMER3		B	B
ZBED2	ZBED2		B	B
SYT16	SYT16		B	A
SLC16A2	SLC16A2		B	B
FGFBP1	FGFBP1		A	B
FHOD1	FHOD1		B	B
ITGA3	ITGA3		B	B
PXN	PXN		B	B
PKP2	PKP2		B	A
THSD4	THSD4		A	A
KLK6	KLK6		A	B
SOX15	SOX15		A	B
PLEK2	PLEK2		B	B
MOB3B	MOBKL2B		B	B
LOXL2	LOXL2		B	B
PLAUR	PLAUR		B	B
MMP9	MMP9		B	B
UPP1	UPP1		A	B
LOXL4	LOXL4		A	A

SLC7A2	SLC7A2		A	A
TMEM27	TMEM27		A	A
ANKRD2	ANKRD2		B	A
AP2B1	AP2B1		B	A
LEPREL1	LEPREL1		B	B
SLC39A14	SLC39A14		B	A
CD55	CD55		A	B
HEG1	HEG1		B	A
PI4K2A	PI4K2A		B	B
FST	FST		B	B
NXPE3	FAM55C		B	A
VEGFC	VEGFC		B	B
SIRPA	SIRPA		B	B
KIRREL	KIRREL		A	A
OLR1	OLR1		B	B
KIAA0040	KIAA0040		B	A
CYR61	CYR61		B	B
VLDLR	VLDLR		A	A
RAB32	RAB32		B	B
TIMP4	TIMP4		B	A
ABCG2	ABCG2		B	A
FAM101B	FAM101B		B	B
MFAP5	MFAP5		B	A
NT5E	NT5E		B	B
COL17A1	COL17A1		B	B
CPA4	CPA4		B	B
EMP3	EMP3		B	B
CTNNAL1	CTNNAL1		B	A
TIMP3	TIMP3		B	B
CDH13	CDH13		B	B
FAM46B	FAM46B		A	A
IL6R	IL6R		A	A
HBEGF	HBEGF		A	B
EREG	EREG		B	B
EPHA2	EPHA2		A	B
FOSL1	FOSL1		B	B
B4GALT6	B4GALT6		A	B
BCL6	BCL6		A	A
TNKS	TNKS		A	A

HLA-DRA	HLA-DRA		A	A
SCARNA9	SCARNA9		A	A
LONP2	LONP2		A	A
SCARNA17	SCARNA17		A	A
GUSBP3	GUSBP3		A	A
AKR1C3	AKR1C3		A	A
ZNF117	ZNF117		A	A
MUC16	MUC16		A	A
PGLYRP4	PGLYRP4		A	B
IKZF2	IKZF2		A	A
DLX5	DLX5		A	A
KRT4	KRT4		A	A
PRODH	PRODH		A	A
MYH14	MYH14		A	A
TXNIP	TXNIP		A	A
KLHL24	KLHL24		A	A
KRT13	KRT13		A	A
GOLGA8A	GOLGA8A		A	A
GLUL	GLUL		A	A
TMEM45B	TMEM45B		A	B
GOLGA8B	GOLGA8B		A	A
MANSC1	MANSC1		A	A
FAM102B	FAM102B		A	A
DSP	DSP		A	B
PRKX	PRKX		A	A
PCMTD2	PCMTD2		A	A
CNKSR3	CNKSR3		A	A
GCLC	GCLC		A	A
RNF138P1	RNF138P1		A	A
FAM214A	KIAA1370		A	A
HES5	HES5		A	B
ST6GALNAC2	ST6GALNAC2		A	A
ACPP	ACPP		A	A
SLC12A2	SLC12A2		A	A
PBX1	PBX1		A	A
CYP1A1	CYP1A1		A	A
PPAP2A	PPAP2A		A	A
TNFSF10	TNFSF10		A	A
KIAA1147	KIAA1147		A	A

PDCD4	PDCD4		A	B
PLD1	PLD1		A	A
LURAP1L	C9orf150		A	A
SLPI	SLPI		A	B
TP53INP1	TP53INP1		A	A
EPHA4	EPHA4		A	A
VTCN1	VTCN1		A	A
KRT15	KRT15		A	A
RAB40B	RAB40B		A	A

Table 13: Clustering of genes modulated in both tumor sites corresponding to the genes clustered in cell lines

Discussion

In chapter 6, the identification of several downstream molecules of the NOTCH signaling pathway that may contribute to growth inhibition is elucidated. We have shown that activating NOTCH signaling in the wild-type cell lines PJA34 and 183 by culturing them on Jagged1 upregulates the expression of potential tumor suppressor genes and inhibits proto-oncogene expression. From this unbiased gene expression analysis, we were able to make associations of the NOTCH signaling pathway with effectors that were not known before. Among key genes down regulated by growth on JAG1 are CTNNAL1 (α -catulin), AXL kinase, integrins α 3 and α 5, LAMC2 (i.e., a component of Laminin-5), and several genes known to mediate invasion such as MMP9 and urokinase-type plasminogen activator receptor (PLAUR). Among genes upregulated by JAG1 exposure were keratins 4 and 13 (i.e., principal keratins produced by squamous epithelial cells during differentiation). Tumor suppressor genes upregulated by JAG1 included TRAIL (i.e., TNFSF10) as well as PDCD4, which is a negative regulator of the TRAIL inhibitor FLIP, and is also an established target of oncogenic microRNA 21 (miR-21). In both PJA34 and 183 cells, AXL, α -catulin, LAMC2, and keratin 4 (KRT4) were among the top 15 most significantly altered genes following growth on JAG1, based upon P-value. KRT4 and α -catulin had the largest changes in magnitude induced by JAG1 in 183 cells, whereas AXL and LAMC2 were among the top twelve genes with greatest fold-change in both cell lines.

We also confirmed the regulation of two downstream targets AXL and α -catulin at the protein level. Although the gene expression array suggests that these molecules may be regulated at the transcriptional level, we still need to explore the transcriptional

binding sites of these effectors. AXL has three AP1 binding motifs and five Sp1 binding sites in its promoter regions (Mudduluru & Allgayer, 2008). Chu et al. have demonstrated that the intracellular form of NOTCH1 (ICN1) can repress AP1 mediated transactivation (Chu, Jeffries, Norton, Capobianco, & Bresnick, 2002). Thus, it is possible that NOTCH1 may transcriptionally regulate AXL, however, since AP1 transcriptional factors regulate several other genes, it is difficult to attribute that the transcriptional modulation of AXL is due to NOTCH1 alone. CTNNA1 has five putative binding sites in the promoter region that can recruit LEF-1, AP-2 α and CREB (Xiang et al., 2012). Our future work will aim at how NOTCH1 or its canonical downstream targets (HES and HEY family members) modulate AXL and α -catulin.

Among the canonical downstream targets of the NOTCH pathway, we found that HES2 and HES5 were upregulated by more than 3-fold in comparison with HES1, 3, 4 and HEY1. In hematopoietic malignancies, the expression of HES1 and HES5 has been shown in several blood cell lineages including T-cells, B-cells and hematopoietic stem cells (Yu et al., 2006). The expression of HES and HEY family members is modulated in a cyclic fashion. We evaluated the expression of these genes 12h, 16h, 20h and 24h after activation of the NOTCH signaling pathway since these are early response genes, and observed maximum induction of HES2 and HES5 at the 20h time point, while other HES and HEY members had no difference at each time point between culturing them on Jagged1 versus Fc. It would be interesting to investigate the lack of induction of HES1, 2, 4 and HEY1 when NOTCH is activated. Epigenetic changes such as promoter methylations may contribute to this effect. In neuroblastoma cell lines, Zage et al. have shown moderate to heavy methylations in CpG islands of the promoter regions of HES2

and HES5 (Zage et al., 2012). In addition, frequent deletions in the regions of the 1p36 chromosome that harbors HES2, HES3, HES4 and HES5 is observed in neuroblastoma (Maris & Matthay, 1999). Thus, it might be possible that in HNSCC, methylations or deletions in such regions may modulate the expression levels of these genes.

TCGA analysis of NOTCH mutant head and neck cancer patient specimens revealed a surprising modulation of genes involved in the maintenance of stem cells. Alcolea and colleagues created an esophageal epithelial system in which they inhibited NOTCH signaling using dominant negative mastermind (dnMAML1) in just one cell of the basal cell population and monitored the expansion of these cells *in vivo* (Alcolea et al., 2014). They found that a year after inhibiting NOTCH signaling in basal cells, the population of differentiating cells drastically decreased selecting only for these undifferentiated basal cells. Although they don't claim these cells to be in a stem cell state, it is possible that this population was enriched and might contribute to tumor initiation. In our system, since we observe markers of stem cells from the TCGA patient tumors that have an active NOTCH1 gene signature, there might be a population of cells exhibiting stem cell characteristics after NOTCH activation. However, we did not observe significant modulation of these genes in cell lines. Differences between cell lines and tumors include intensity of NOTCH signaling, infiltrating muscle cells and tumor purity, microenvironment regulation, and other genetic alterations in tumors (NUMB, p63, etc.) may contribute to the discrepancies between genes regulated in cell lines versus tumors.

CHAPTER 7: INHIBITION OF AXL AND α - CATULIN MODULATES CELL GROWTH

Chapter 7: Inhibition of AXL and α -catulin modulates cell growth

Chapter 7.1: Knocking down AXL and α -catulin inhibits cell growth and tumor formation

Rationale: In chapter 5, we demonstrated that NOTCH inhibits cell growth and in chapter 6, we elucidated that NOTCH1 is sufficient and necessary to decrease the expression of AXL and α -catulin. AXL and α -catulin are proto-oncogenes that are overexpressed in several cancers. Both proto-oncogenes have shown to be involved with cell growth, proliferation, migration and metastasis (Cao et al., 2012; Graham, DeRyckere, Davies, & Earp, 2014). Moreover, targeting AXL in HNSCC cell lines increased their sensitivity to cetuximab and radiation (Brand et al., 2015). Fan et al. showed that α -catulin promoted the growth of oral squamous cell carcinoma by inhibiting senescence (Fan et al., 2011). Although there is evidence that AXL and α -catulin suppress growth, the functional relevance of these proto-oncogenes in a NOTCH mutant background hasn't been fully explored. We first demonstrated that restoration of NOTCH1 inhibits tumor growth, then we showed that NOTCH1 inhibits AXL and α -catulin. To evaluate AXL and α -catulin mediated modulation of cell and tumor growth, we knocked down the expression of these proto-oncogenes using shRNA's and hypothesized that AXL and α -catulin might be necessary for tumor growth.

Results: We obtained four different lentiviral sort hairpin RNA's that were GFP tagged for each target gene, AXL and α -catulin, and stably transfected the mutant cell lines HN31, and UMSCC22A and wild-type cell lines PJA34 and 183 with sh RNA's against AXL (shAXL) and α -catulin (shCAT) and purified them by flow cytometry. The percentage and intensity of GFP positive cells were matched for each lentiviral shRNA construct prior to transductions. After obtaining a pure population of cells expressing the

shRNA's, we cultured cells at low densities in a colony forming clonogenic assay for 10 days. Shown in Figure 47 and Figure 48 are western blots indicating that both AXL and catulin have been knocked down by more than 70%. Knocking down AXL and α -catulin significantly reduced cell growth in all cell lines (Figure 51). In all cell lines, we observed at least 50% decline in cell growth after inhibition of AXL and α -catulin. Based on our previous results, when NOTCH1 was activated in HN31 and PJA34, we observed greater than 50% decline in cell growth. Moreover, we have also shown that NOTCH1 is necessary and sufficient to inhibit AXL and α -catulin. Here we show that knocking down AXL and α -catulin recapitulates the NOTCH induced growth inhibition.

Since we found that decreasing AXL and α -catulin expression is associated with decreased cell growth *in vitro*, we then investigated the role of modulation of expression of these proto-oncogenes on tumor growth *in vivo*. After knocking down AXL and α -catulin using shRNA's in HN31 mutant cells, the cells were purified for GFP by flow cytometry and injected them into the tongue of mice in an orthotopic model of oral cancer. We injected 50,000 cells per mouse and had 11 mice in each condition. As seen in Figure 52, knocking down AXL and α -catulin led to significantly abrogated tumor growth by more than 75% compared to the shEMPTY and parental control cells injected mice at 17 days post injection ($P < 0.001$). Tumors in the control groups (parental and shEMPTY) were initiated 5 days post injection, while tumors in the AXL and CAT group began to develop only at day 10. In the parental and empty vector control groups, all 11 mice developed tumors 17 days after injection but in the shAXL and shCAT groups, only 6 and 8 mice respectively developed tumors. The overall survival in mice that had shAXL and shCAT cells injected was greater than the control groups ($P < 0.01$). The

median survival of mice in the parental and shEMPTY groups was 24 and 21 days respectively, while the shAXL and ShCAT mice groups survived for more than 35 days. The *in vivo* effect of AXL was slightly greater than α -catulin in that, tumor sizes in shAXL groups were smaller than in the shCAT group and the former had a slightly greater overall survival than the latter (although not significant). Comparing these results to restoration of NFL1 in vivo, we observe a similar trend in tumor growth inhibition. Restoration of NFL1 in HN31 cells lead to a 60-70% decline in tumor volumes at day 25 post injection, while knocking down AXL and α -catulin resulted in a similar decline slightly earlier (day 18). Taken together, our results imply that knockdown of AXL and α -catulin recapitulates the NOTCH induced phenotype in wild-type and mutant cells suggesting that AXL and α -catulin might be involved with NOTCH mediated suppression of tumor growth.

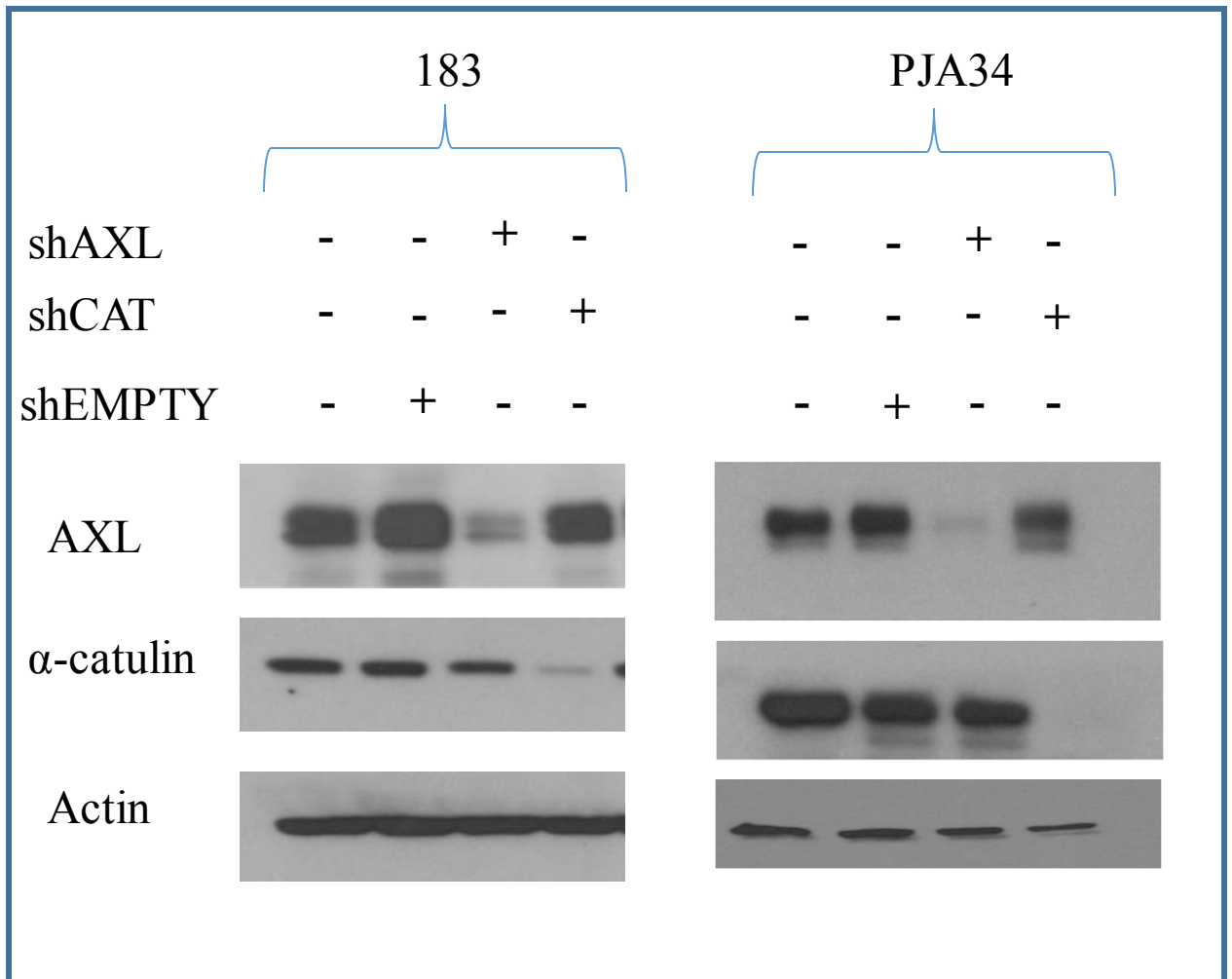


Figure 47: Knockdown of AXL and α -catulin in wild-type cell lines 183 and PJA34 using shRNA's

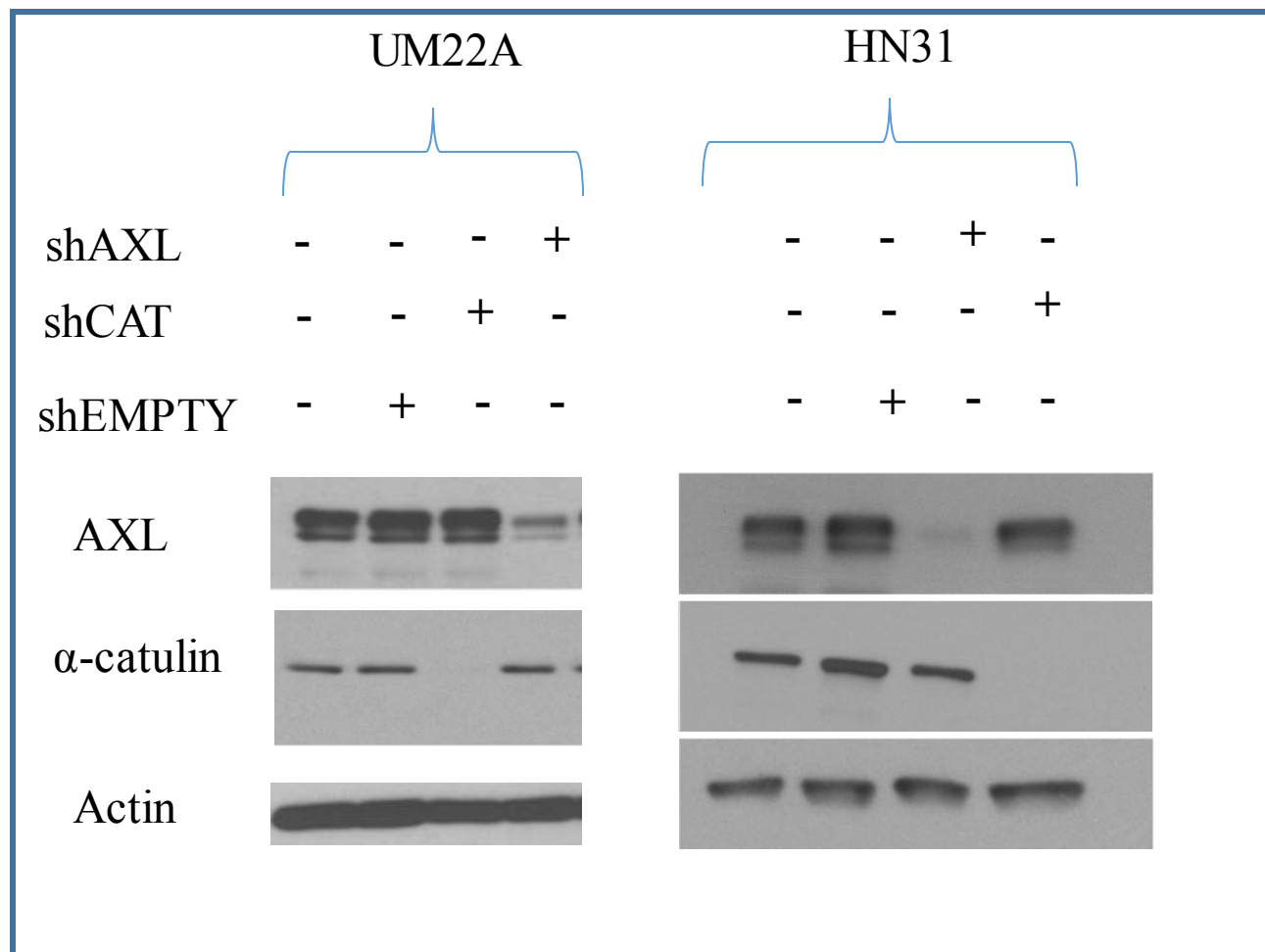


Figure 48: Knockdown of AXL and α -catulin in mutant cell lines UM22A and HN31 using shRNA's

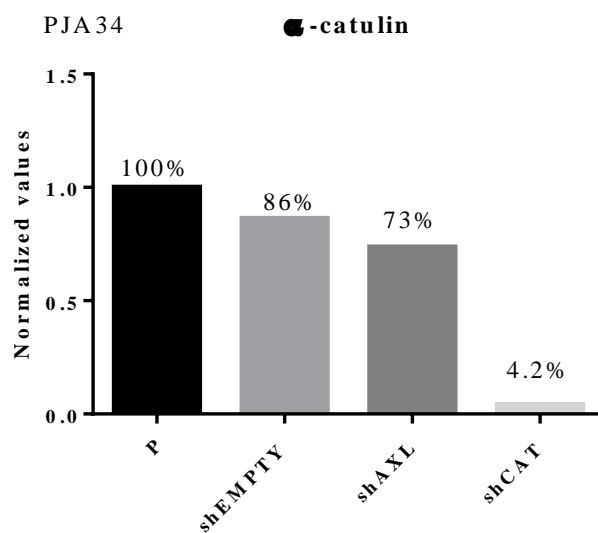
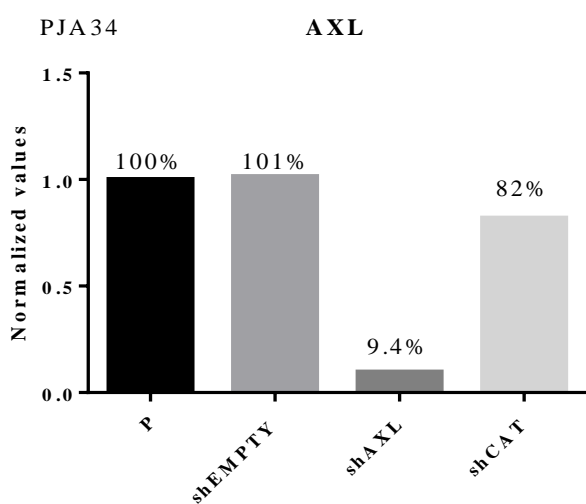
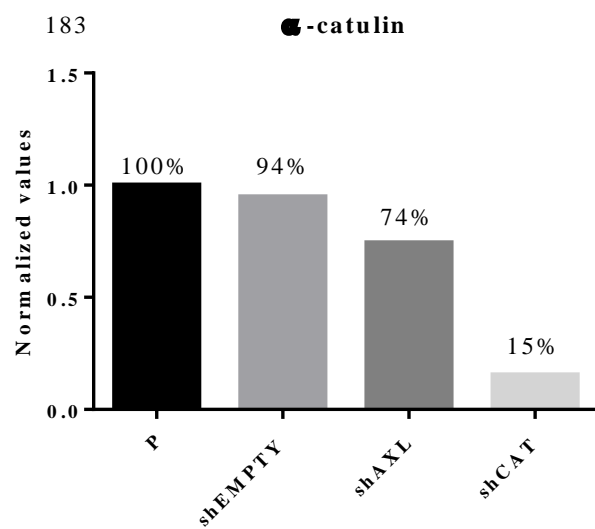
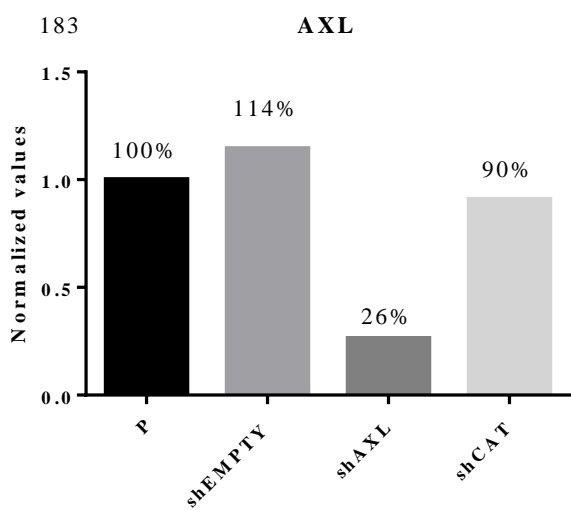


Figure 49: Quantitation of the western blots after knocking out AXL and catulin in wild-type cell lines 183 (above) and PJA 34 (below).

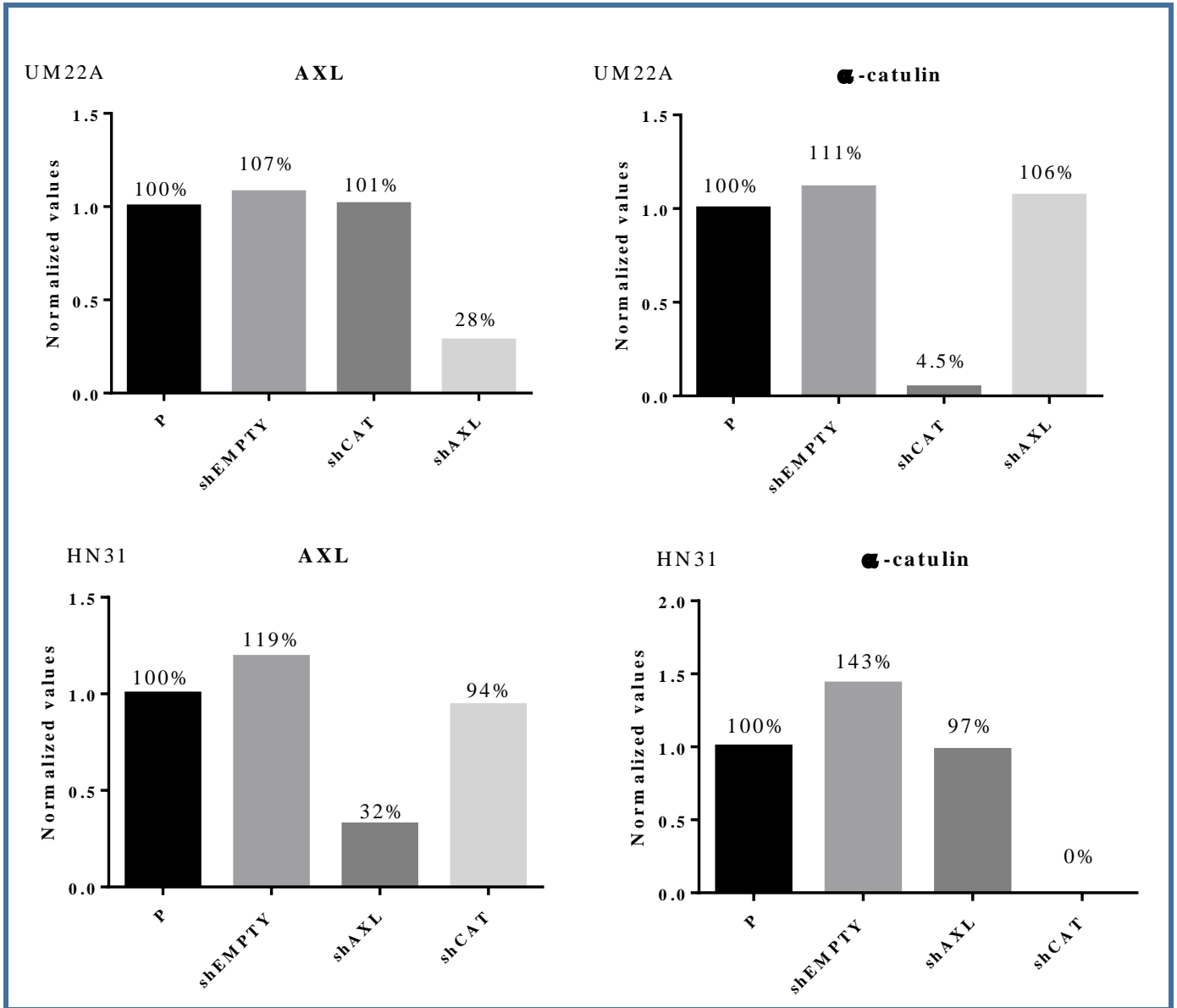


Figure 50: Quantitation of the western blots after knocking out AXL and catulin in mutant cell lines UM22A (above) and HN31 (below).

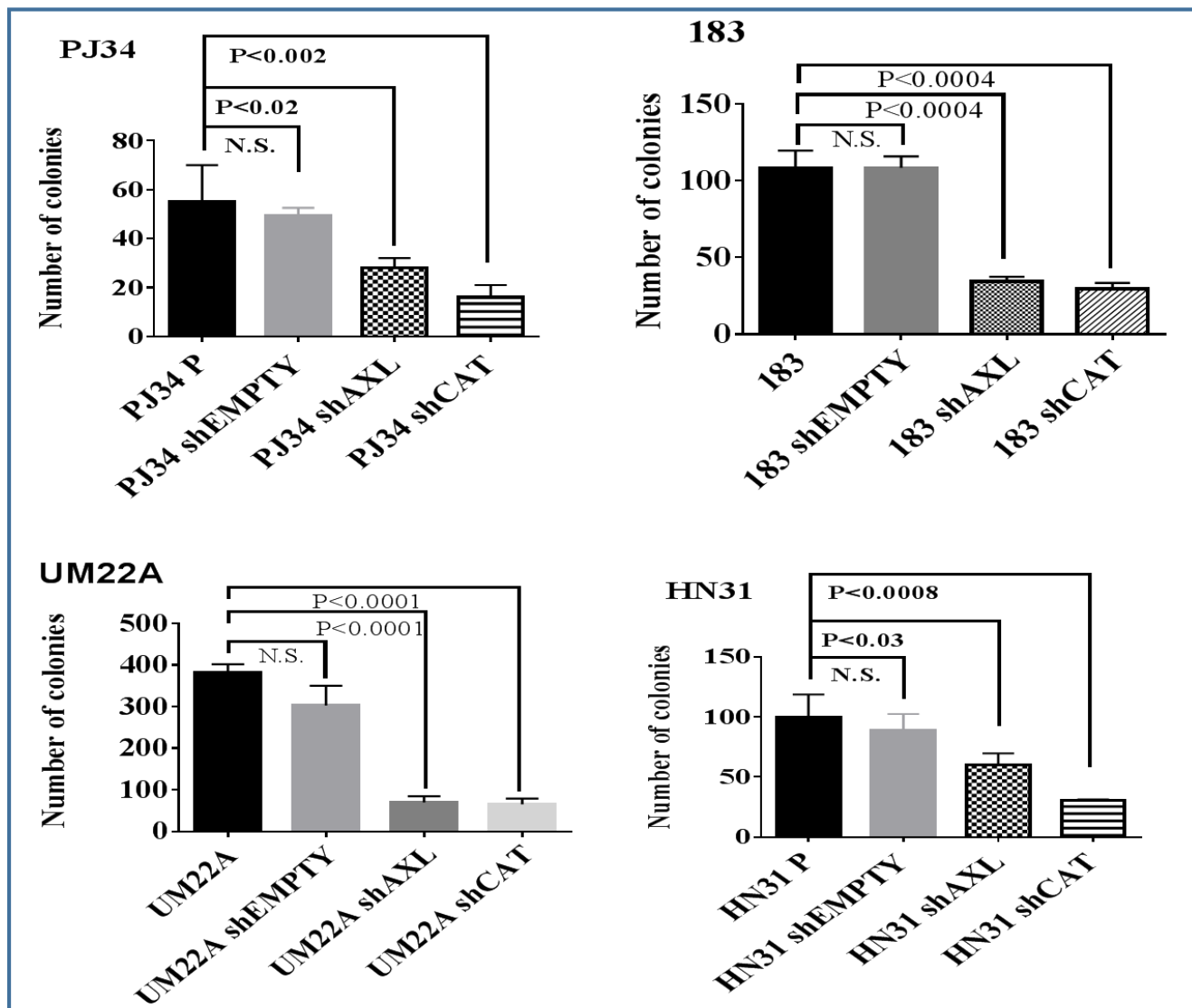


Figure 51: Clonogenic assay in wild-type (PJA34 and 183) and mutant cell lines (UM22A and HN31). Knocking down AXL (shAXL) and α -catulin (shCAT) inhibits cell growth in a colony forming clonogenic assay

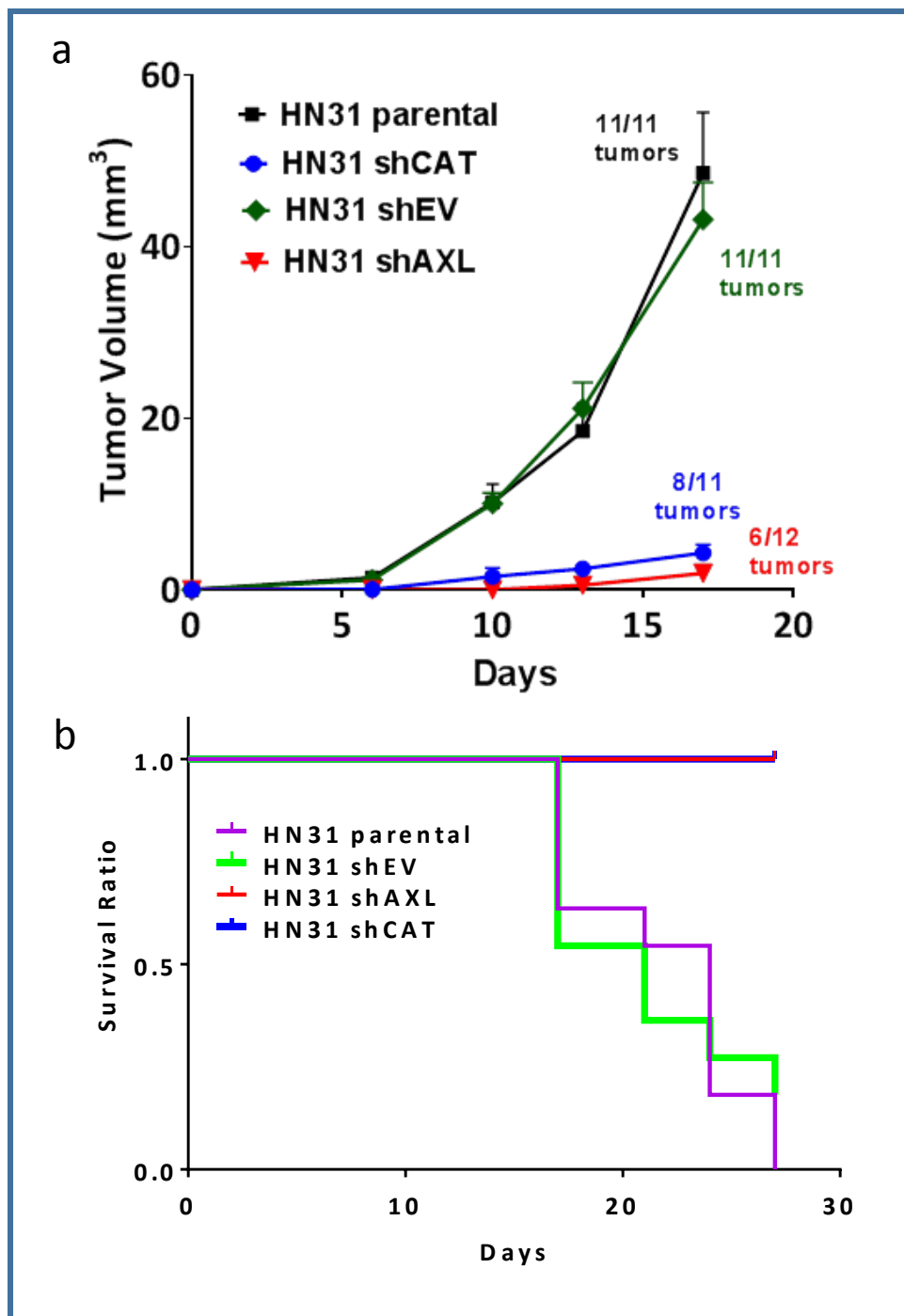


Figure 52: AXL and α -catulin modulates in vivo tumor formation and overall survival. Knocking down AXL and α -catulin using shRNA's in a mutant cell line significantly inhibits tumor growth and increases overall survival

Chapter 7.2: HES2 and HES5 might be sufficient to inhibit cell growth

Rationale: We have previously shown that HES2 and HES5 are canonical downstream targets of the NOTCH signaling pathway that is significantly up regulated in HNSCC cell lines compared to other HES and HEY family members (Figure 40). In addition, we have also shown that NOTCH1 is necessary and sufficient to inhibit cell growth and protein expression levels of AXL and α -catulin which might be downstream of NOTCH and are necessary for inducing the same phenotype. Furthermore, we have shown that HES2 and HES5 might be sufficient to inhibit protein expression of AXL and α -catulin. HES and HEY family are known canonical downstream transcriptional modulators (mostly repressors) of the NOTCH signaling pathway. Since AXL and α -catulin were suppressed after NOTCH activation resulting in growth inhibition, we wanted to investigate if these canonical targets are sufficient to modulate cell growth.

Results: Using HES2 and HES5 MigR1, GFP-tagged constructs, we overexpressed these genes in the NOTCH1 mutant cell line HN31. Prior to sorting these cells for pure population of GFP cells, viral titers were optimized such that each overexpression condition (HES2, HES5 and MigR1) express similar intensity and percentage of GFP positive cells. Since each virus may have varied efficacy after infection, it was imperative that the titers be matched to each other to avoid confounding variables that may be caused due to the infections process itself rather than the constructs. After sorting for a pure population of GFP positive cells and confirming the expression of these flag tagged constructs (Figure 41), we performed an *in vitro* colony forming clonogenic assay in which we plated 1000 cells from each sorted cell conditions into 6-well plates. HES2 and HES5 significantly inhibited growth compared to the parental and

empty vector conditions (Figure 53). The number of colonies in the parental and MigR1 were similar, but HES2 and HES5 were sufficient to induce more than 75% suppression in growth of HN31 cells ($P < 0.01$). This result suggested that NOTCH activated HES2 and HES5 appear to be sufficient in modulating cell growth. In future studies, we will examine the regulation of AXL and catulin by HES2 and HES5 in inhibiting cell growth.

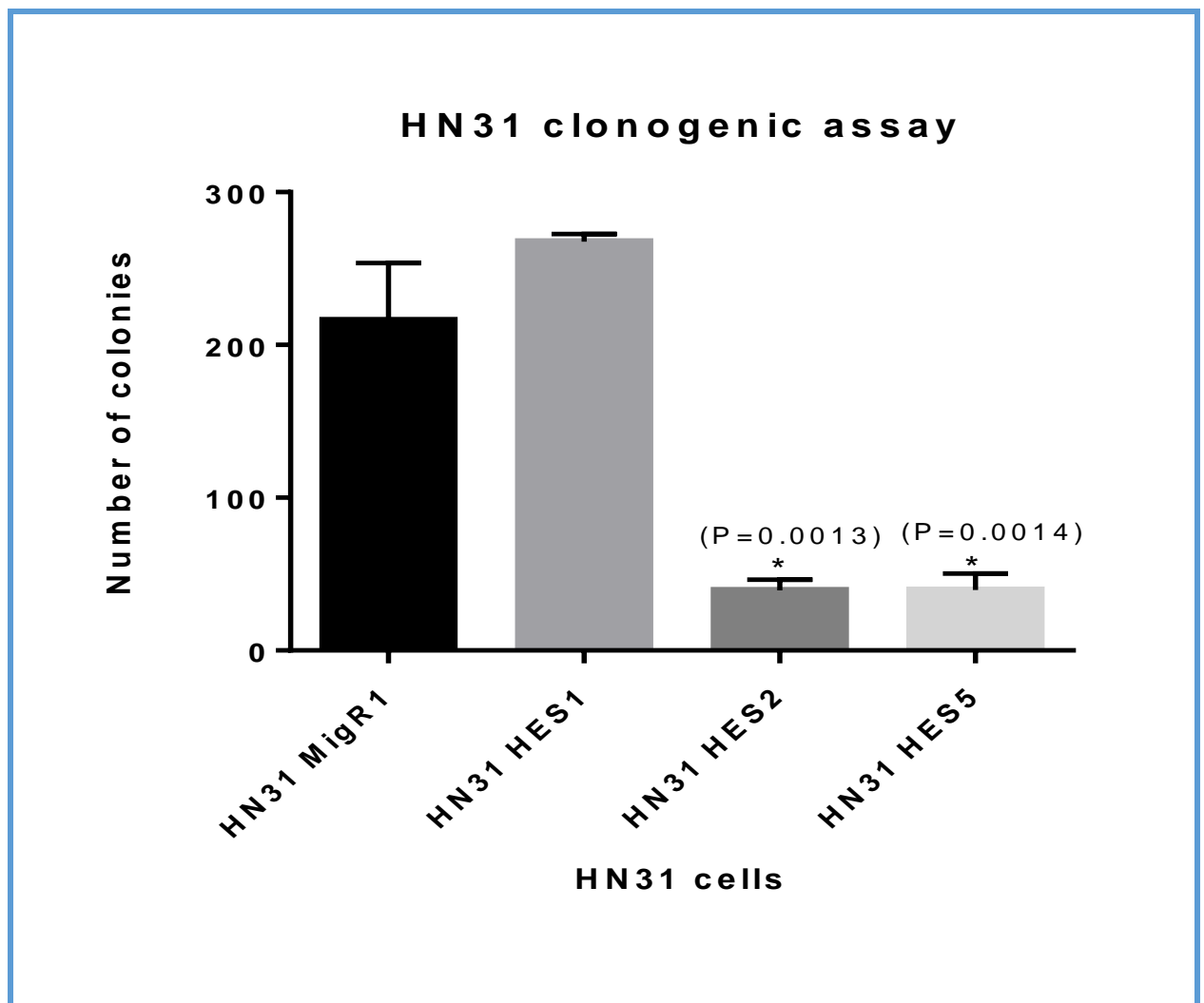


Figure 53: HES2 and HES5 are sufficient to inhibit cell growth

Discussion

In chapter 7, we demonstrate the roles of AXL and α -catulin in modulating cell growth *in vitro* and *in vivo*. We have shown that knocking down these proto-oncogenes using shRNA's significantly inhibits cell growth in a colony-forming assay. Previously, in chapter 5, after restoration of the NOTCH signaling pathway in wild-type and mutant cells, we show greater than a 50% decrease in cell growth. Then, in chapter 6, we demonstrated that NOTCH activation in mutant and wild-type cell lines inhibits AXL and α -catulin. Here, we observe that AXL and α -catulin might be necessary in modulating cell growth. Using siRNA's, Brand et al. demonstrated that cell lines expressing high levels of AXL are sensitive to siRNA-mediated inhibition of AXL (Brand et al., 2015). However, in their experiments, siRNA's against AXL induced less than a 50% inhibition in cell proliferation. Our results are more robust in that we performed stable transfections with shRNA's and assayed cell growth over a longer time period and observed more than a 60% inhibition in cell growth. A caveat to this experiment is that the role of AXL and α -catulin independent of NOTCH activation still remains unexplored. For this, we might have to overexpress these proto-oncogenes in a background in which NOTCH has been knocked out (for example in CRISPR-Cas9 knockout cells) before culturing these cells on Jagged1 to prove that AXL and α -catulin are sufficient to modulate growth. Finally, we show that HES2 and HES5 might be sufficient to modulate cell growth. We have previously shown that activation of NOTCH signaling induces HES2 and HES5 expression. Furthermore, HES2 and HES5 can possibly down regulate AXL and α -catulin. HES2 and HES5 may be sufficient to inhibit growth by more than 60% a mutant HNSCC cell line, HN31. In Acute Myelogenous Leukemia (AML), Zage et al. showed

that HES1 was sufficient to induce more than a five-fold decrease in growth of AML cells (Zage et al., 2012). At this point, we don't have evidence demonstrating that HES2 and HES5 are required for inhibiting cell growth. To prove that these targets are required, we are knocking down HES2 and HES5 in wild-type cell lines before culturing them on Jagged1 to show that loss of these molecules upregulates AXL and α -catulin and relieves NOTCH induced growth inhibition. The transcriptional targets of the HES and HEY family have not been well studied. Genes like Achaete-scute-like 1 (ASCL/HASH1), atonal homolog-1 (ATOH1) and neurogenin-1 have been reported before (Kageyama, Ohtsuka, Hatakeyama, & Ohsawa, 2005). In the future, we aim to understand NOTCH signaling at the transcriptional level and elucidate how NOTCH modulates AXL and α -catulin in regulating cell growth.

CHAPTER 8: DISCUSSION AND FUTURE DIRECTIONS

Discussion and future directions

The main goal of my thesis is to understand the tumor suppressive role of NOTCH1 in HNSCC. In 2011, our lab had published results from whole exome sequencing of 32 primary patient tumors in which frequent somatic mutations in NOTCH1 was identified (Agrawal et al., 2011). Until then, TP53 was known to be mutated frequently, followed by p16, PIK3CA, Hras and overexpression/amplifications in Cyclin D1 and EGFR. The sequencing studies performed by Agarwal et al. (Agrawal et al., 2011) and Stransky et al. (Stransky et al., 2011) identified for the first time frequent somatic mutations in NOTCH1. More recently, the TCGA utilized a broader sequencing platform and observed NOTCH1 mutations at a similar frequency as the other two studies ("TCGA Releases Head and Neck Cancer Data," 2015). The role of NOTCH1 in cancers surfaced from studies in T-ALL in which this receptor has activating mutations in the transmembrane and PEST domains that results in constitutive activation of the pathway rendering it an oncogene in this tumor type (Weng et al., 2004). In HNSCC, inactivating mutations were primarily located at the extracellular domain of NOTCH1 and were mostly missense and nonsense mutations. These mutations prevented the binding of the NOTCH receptor with the ligand inactivating this pathway in a subset of HNSCC. Based on sequencing studies, only a small fraction of HNSCC (15-19%) harbor inactivating NOTCH1 mutations while the majority seems to express the wild-type NOTCH1 receptor. Although wild-type NOTCH1 is expressed in many tumors, these tumors resemble the mutant subset. In such tumors, there might be other aberrations such as overexpression of NUMB; a negative regulator of NOTCH activation, overexpression of Jagged1; resulting in cis-inhibition or modulations in fringe glycosylation; that results in

improper receptor-ligand binding. Indeed, we have seen the overexpression in NUMB in some of our cell lines that are both wild-type and mutant for NOTCH1 (

Figure 54). In addition, cell lines that are both wild-type and mutant for NOTCH1 express Jagged1 (Figure 55) that can potentially lead to cis-inhibition (Figure 33). In this dissertation, I hypothesized that the inactivating mutations observed in NOTCH1 in HNSCC render it a tumor suppressor in this tumor type and the activation of a functional NOTCH pathway would inhibit growth of these tumors.

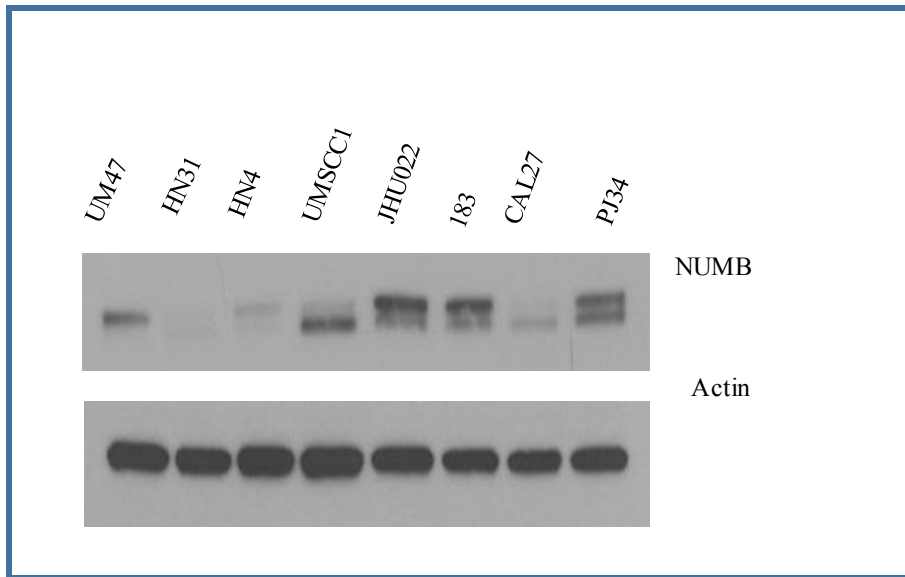


Figure 54: Basal NUMB expression in wild-type and mutant HNSCC cell line

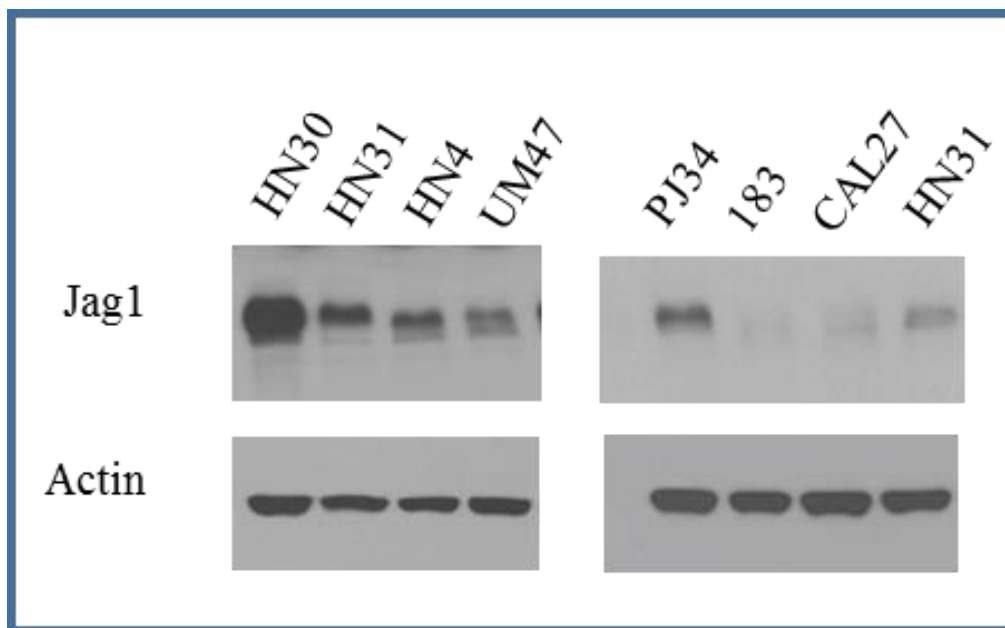


Figure 55: Jagged1 expression in wild-type and mutant HNSCC cell lines

Activation of NOTCH signaling inhibits growth

Based on sequencing data that showed frequent inactivating mutations in NOTCH1 in this cancer type (Agrawal et al., 2011), for the first time, we demonstrate the functional relevance of these inactivating mutations. Using the intracellular and full-length NOTCH1 constructs (ICN1 and NFL1) in mutant cell lines, we observed a decrease in the population of cells expressing NOTCH1. Cells expressing NOTCH1 were selected against cells expressing the empty vector in a competitive cell proliferation assay. In a similar assay, Kannan et al. have shown that ICN was sufficient to inhibit AML cell growth (Kannan et al., 2013). Although, we do not completely understand what causes growth inhibition, we did observe morphological changes after transducing cells with ICN1 or NFL1 that might explain this observance.

NOTCH and senescence

Cellular senescence was a phenotype that accompanied growth inhibition in mutant cell lines after transduction with ICN1 and NFL1 when cultured on Jagged1. Senescence partially explains the flat, enlarged and pancake-like morphology that we observe after NOTCH activation. Senescence serves as a fail-state mechanism to prevent oncogene-induced aberrant proliferation. It has been shown that in esophageal keratinocytes, ICN1 inhibited cell proliferation, induced expression of p21 and arrested cells in the G1 phase of the cell cycle (Kagawa et al., 2015). We observed a similar phenotype in that ICN1 did inhibit p21, and arrest cell in the G1 phase of the cell cycle. Senescence, however, was observed only in a small fraction of cells and it is unclear what inhibits growth in cells that do not undergo senescence. Mechanisms other than

senescence governing growth inhibition such as cell death, or mitotic catastrophe still need to be explored.

NOTCH and differentiation

The NOTCH pathway is known to regulate differentiation and it is possible that NOTCH induced differentiation might inhibit cell growth. Studies performed in mice keratinocytes with specific deletion of NOTCH1 in the epidermis abolished cell growth and disrupted well-defined borders between the basal and upper differentiating layers (Rangarajan et al., 2001). Induction of p21 is one of the earliest events underlying differentiation induced growth arrest (Missero, Di Cunto, Kiyokawa, Koff, & Dotto, 1996) and we show here that ICN1 is sufficient to induce p21 in a NOTCH1 mutant cell line. Furthermore, mice injected with the mutant cell line UM47 expressing NFL1 showed the formation of keratin pearls indicative of differentiation. Signaling between NOTCH ligands, Jagged1 and Jagged2 and NOTCH receptors 1 and 2 increases in differentiating keratinocytes in the suprabasal layers of the epidermis (Luo, Aster, Hassserjian, Kuo, & Sklar, 1997). This suggests that they are part of a positive feedback mechanism required for differentiation and epidermal border formation (Rangarajan et al., 2001). Another line of evidence that NOTCH1 might induce differentiation is modulation of p63, a p53 family member that is involved with cell fate determination and stem cell maintenance (Mills et al., 1999; Yang et al., 1999). We observed a marked suppression in protein levels of Δ Np63 after infecting a mutant cell line with ICN1 (Figure 56). In the murine system, p63 is likely to play a significant function in preventing differentiation and maintenance of premature senescence (Keyes et al., 2005; King et al., 2003). Elevated levels of Δ Np63 has been shown to be associated with a

variety of epithelial tumors, including squamous cell carcinomas in which NOTCH expression is suppressed (Lefort et al., 2007; Parsa, Yang, McKeon, & Green, 1999; Pellegrini et al., 2001). This suggests that NOTCH and Δ Np63 might be linked. Here, we show that ICN1 might induce Δ Np63, thus promoting differentiation and contributing to growth inhibition. NOTCH and Δ Np63 can have opposing effects. While NOTCH1 suppresses expression of Δ Np63, overexpression of Δ Np63 has been shown to inhibit NOTCH activity and maintenance of immature keratinocytes (Okuyama et al., 2008). We have not shown the expression levels of Δ Np63 in NOTCH1 wild-type cells, but it may be possible that the activity of Δ Np63 might inhibit NOTCH activation although these cells express a functional receptor. Taken together, we have independent evidences of NOTCH inducing p21 and NOTCH inducing differentiation. Whether there is a link between NOTCH, p21 and differentiation in HNSCC needs to be explored in the future. Interestingly, although ICN1 causes cells to round up and appears to come off the substrate, we did not observe the induction of apoptosis. Infection of mutant cells with ICN1 arrested 15% of the cells in the sub G0 phase of the cell cycle indicative of cell death. In B-ALL, one of the mechanisms of NOTCH induced apoptosis involves HES1 activating PARP1 leading to self and global PAR-ylation, reduction in NAD and ATP levels, nuclear translocation of AIF and subsequent B-ALL apoptosis (Kannan et al., 2011). However, when we performed a western blot for cleaved PARP and total PARP, we did not observe induction of apoptosis after NOTCH activation. This rules out the possibility of apoptotic cell death.

Roles of NOTCH1 and NOTCH2

The majority of the data in my dissertation focuses on the role of NOTCH1 in HNSCC. However, mutations in NOTCH2 are also observed in this tumor type. More recently, a publication by Li et al. found deletions in NOTCH2 in primary tumors and HNSCC cell lines (H. Li et al., 2014). Since NOTCH1 and NOTCH2 mutations are not mutually exclusive, it is hard to predict if the mutations in one of the NOTCH members can be overcome by another functional receptor. We observed that ICN1 and ICN2 are sufficient to inhibit growth in a wild-type and mutant cell line. Furthermore, we have also shown that both NOTCH1 and NOTCH2 are necessary to inhibit cell growth. The functional difference between NOTCH1 and NOTCH2 lies in the intracellular region of the receptor. Kraman and McCright performed a study in which they replaced the non-conserved region of ICN2 with the homologous region of ICN1 and created mice with NOTCH1-NOTCH2 fusion protein (Kraman & McCright, 2005). Mice homozygous for this fusion were phenotypically normal and organs that required NOTCH2 functionality had developed normally with the fusion protein. They suggested that ICN1 can functionally replace the corresponding region of ICN2. Since we used the intracellular form of NOTCH1 and NOTCH2, our results are consistent with findings from Kraman and McCright and also corroborates the study that demonstrates that ICN1 and ICN2 could activate transcription *in vitro* (Kurooka, Kuroda, & Honjo, 1998). Our results are also consistent with another finding that elucidates that ICN1 and ICN2 could both induce growth arrest and senescence in small cell lung cancer cells (Sriuranpong et al., 2001). In our evaluation of NOTCH2 induced growth inhibition, we only overexpressed the activated form of this protein. To gain a complete understanding of the role of

NOTCH2 in HNSCC, we will clone the full length NOTCH2 receptor similar to NFL1 and perform similar functional studies.

Although we have shown that either ICN1 or ICN2 can inhibit cell growth, it appears that knocking out both together is necessary to relieve growth inhibition. Using the CRISPR-Cas9 technique to knock out NOTCH1 (NOTCH1 KO), NOTCH2 (NOTCH2 KO) or both (double KO) and then culturing the cells on Jagged1, we observed that the dKO is required to relieve Jagged1 induced growth inhibition. It appears that both NOTCH1 and NOTCH2 are able to signal through Jagged1. The other compensates the loss of one of the NOTCH receptors. To circumvent the issue of which particular NOTCH receptor contributes to tumorigenesis, we used a pan NOTCH inhibitor, dnMAML1 to evaluate tumor formation. The dnMAML1 significantly increased tumor growth in a weakly tumorigenic cell line but only 50% of the mice injected formed tumors. This can possibly be attributed to the lack of nuclear localization of dnMAML1 because of which its inhibitory effects on NOTCH signaling wasn't exerted. Mastermind-like 1 functions as a transcriptional co-activator in the nucleus where it binds to ICN. To determine if NOTCH signaling was indeed inhibited in 50% of mice from the dnMAML1 group, we have to immunostain these tumors with HES or HEY. Alternatively, in the other 50% dnMAML1 mice without tumors, nuclear localization of dnMAML1 can be determined. It is possible that the lack of nuclear localization of dnMAML1 after transduction in these wild-type cells might have caused decreased inhibition of NOTCH activity. Another shortcoming to inhibiting the NOTCH pathway using dnMAML1 is the difficulty in incorporating both copies of the construct in mammalian cells after infection. We sorted cells after infection based on optimal GFP

intensity and number of GFP infected cells. There is a possibility that some cells incorporate only one copy of the gene that may not have an immediate effect *in vitro*, but may decline in efficacy *in vivo*. Lastly, technical limitations while injecting these cells in the tongue of mice might have also contributed to such aberrations.

Since our results from inhibiting NOTCH activity had these discrepancies, we exploited the CRISPR-Cas9 technology to knockout NOTCH1 and NOTCH2 in the same wild-type cell line; PJA34. Until now, loss-of-function studies using the CRISPR-Cas9 technology in HNSCC have not been performed. In other cancer types such as AML, melanoma, colon, PDAC, NSCLC and liver cancer, this system has been used to knock out genes such as p53, KRas, PIK3CA, APC and Smad4 (Castro et al., 2015; C. Chen et al., 2014; S. Chen et al., 2015; Heckl et al., 2014; Shalem et al., 2014). Here, we show for the first time that knocking out NOTCH1 and NOTCH2 relieves Jagged1 induced growth inhibition *in vitro*. When NOTCH1 is knocked out in PJA34 cells and cultured on Jagged1, there is some signaling through NOTCH2 which partially relieves growth inhibition when compared to the parental cells cultured on Jagged1 (grey bar of parental versus grey bar of NOTCH1 KO in Figure 27). Similarly, when NOTCH2 is knocked out, signaling through NOTCH1 partially relieves growth suppression compared to parental controls (grey bar of parental versus grey bar of NOTCH2 KO in Figure 27). This shows that NOTCH1 or NOTCH2 is not sufficient to completely prevent the growth inhibitory phenotype. Interestingly, knocking out NOTCH1 and NOTCH2 completely relieves growth inhibition suggesting that both NOTCH1 and NOTCH2 are required for cell growth suppression. It is intriguing that knocking out either NOTCH1 or NOTCH2 individually inhibits growth in the Fc controls compared to the parent cells cultured on

Fc (black bar of parental cells versus black bars of NOTCH1 KO or NOTCH2 KO cells in Figure 27). PJA34 cells express the ligand Jagged1. It might be possible that knocking out one of the NOTCH receptors increases ligand sensitivity to the other NOTCH receptor enhancing signaling activity. For example, NOTCH1 KO cells may have enhanced sensitivity of the NOTCH2 receptor to the ligand and vice versa. In skin keratinocytes, Demehri et al. have shown that conditional deletion of NOTCH2 in the epidermis does not exacerbate carcinogen induced tumor initiation in the presence of NOTCH1 as much as conditional deletion of NOTCH1 that generated spontaneous tumors (Demehri et al., 2009), but progressive deletion of NOTCH1 and NOTCH2 enhanced epidermal hyperplasia. Our results are similar to this previously reported study in that knocking out NOTCH1 or NOTCH2 separately could not relieve growth suppression but knocking out both enhanced cell growth. In the previous study, conditional deletion of NOTCH1 or NOTCH2 resulted in late tumor onset but conditional deletion of both initiated early onset of tumors (Demehri et al., 2008). It might be possible that NOTCH1 and NOTCH2 play roles in different stages of tumor development. In cervical keratinocytes, loss of NOTCH1 with retention of NOTCH2 occurs in cells that are more aggressive and invasive implying that different NOTCH receptors may participate in early and late stages of tumor progression (Talora, Sgroi, Crum, & Dotto, 2002). Restoration of NFL1 in the dKO PJA34 cells rescues abrogation of growth inhibition. This shows that NOTCH1 alone might be sufficient to mirror the parental phenotype in the double knockout cell line. NOTCH2 might also result in a similar phenotype, but at this point, we are unaware if NOTCH2 alone is sufficient to rescue the dKO mediated growth.

Identification of downstream effectors of the NOTCH signaling pathway

After we established a growth inhibitory phenotype after NOTCH activation in wild type and mutant HNSCC cell lines, we evaluated the mechanism behind such an effect. In our study, 1808 genes were differentially modulated after NOTCH activation. We set a threshold of 1.4 fold, which filtered the 1808 genes to 120. Among these 120 genes, 50 were up regulated and 70 were down regulated. We report here that NOTCH activation significantly alters cell growth and proliferation pathways based on “Ingenuity Pathway Analysis” of the differentially expressed genes. This finding corroborates our earlier report of NOTCH activation inhibiting cell growth (Chapter 5). In a study performed in laryngeal squamous cell carcinoma, in which NOTCH is overexpressed, Dai et al. show that inhibiting NOTCH activity down regulates genes associated with cell growth, proliferation, apoptosis, invasion and migration (Dai et al., 2015). In our system, since NOTCH1 acts as a tumor suppressor, we found that NOTCH activation down regulates genes associated with cell growth, proliferation and migration.

The oncogenic protein α -catulin found to be down regulated by NOTCH in our experiments is overexpressed at the invasive front of human HNSCC tumors (Cao et al., 2012). It is associated with poor clinical outcome in non-small cell lung cancer (NSCLC) (Liang et al., 2013). Silencing α -catulin induces senescence in HNSCC (Fan et al., 2011), and inhibits proliferation, migration, and invasion in both HNSCC and NSCLC cell lines. Alpha-catulin interacts with molecules regulating cell adhesion and the cytoskeleton, functions as an activator of Rho GTPase and NF- κ B signaling, and is a downstream target of integrin-linked kinase (Fan et al., 2011). AXL, also downregulated by JAG1 in our experiments, encodes a receptor tyrosine kinase frequently overexpressed in cancers,

where it has been associated with poorer survival and increased metastasis (Paccez, Vogelsang, Parker, & Zerbini, 2014), including in HNSCC (C. H. Lee et al., 2012). Oncogenic properties of AXL have been attributed to proliferative and pro-survival signaling, and inhibiting AXL reportedly blocks migration, invasion, and growth of certain HNSCC cell lines (C. H. Lee et al., 2012). Integrins mediate attachment to extracellular matrix proteins and are involved in proliferation, survival, migration and invasion of tumor cells. Integrin $\alpha 3$, also downregulated by NOTCH signaling in our experiments, is a major receptor for lamin-5; the principal component of the basement membrane extracellular matrix (ECM) found in squamous epithelial of the skin and upper aerodigestive tract. Loss of adhesion to ECM leads to apoptotic death known as anoikis, and integrin $\alpha 3$ is necessary for survival of keratinocytes in culture (Manohar et al., 2004). Overexpression of integrin $\alpha 3$ has been associated with lymph node metastasis in HNSCC (Kurokawa et al., 2008; Nagata et al., 2013) while expression of integrin $\alpha 5$ has been linked to increased metastasis and proliferation in laryngeal cancers (Lu, Sun, Wang, Jin de, & Liu, 2009). We don't know if NOTCH activation directly inhibits integrins or there is a mediator downstream of NOTCH signaling that facilitates this modulation. P63 has previously been shown to inhibit integrins in the basal layer of keratinocytes (Okuyama et al., 2008). We show that in one of the mutant cell lines ICN1 could significantly downregulate protein expression of Δ NP63 (Figure 56). However, in wild-type cell lines, activation of NOTCH signaling using Jagged1 only modestly suppressed Δ Np63 (Figure 57). Moreover, Δ NP63 was not significantly modulated after NOTCH activation in the gene expression analysis. Mutations in NOTCH1 and TP63

tend to be mutually exclusive (Figure 58). Thus, it is possible that in HNSCC, modulation of integrins may be p63 independent.

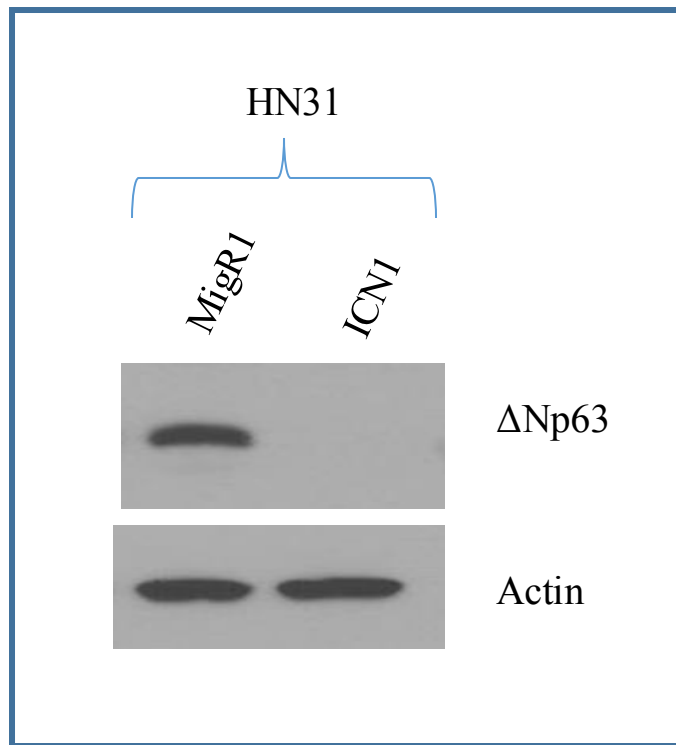


Figure 56: *ICN1 inhibits p63 expression*

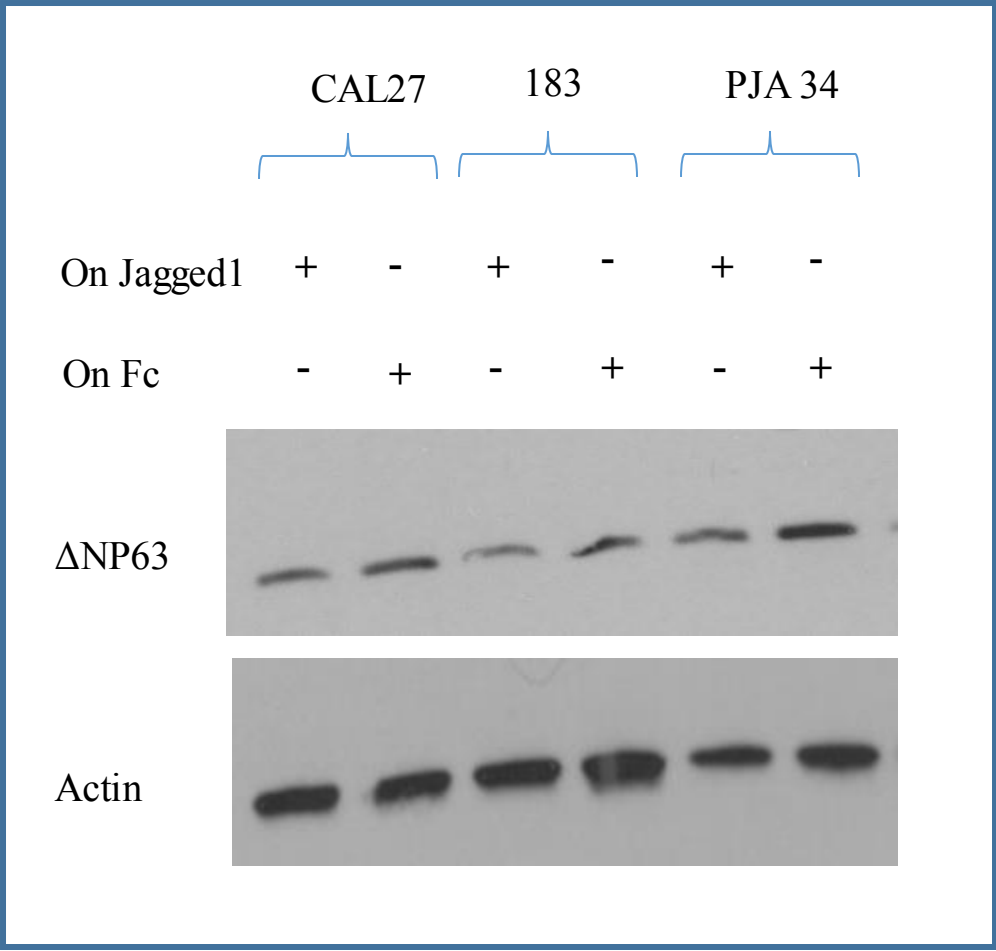


Figure 57: Activation of NOTCH signaling by Jagged1 slightly inhibits protein expression of Δ NP63

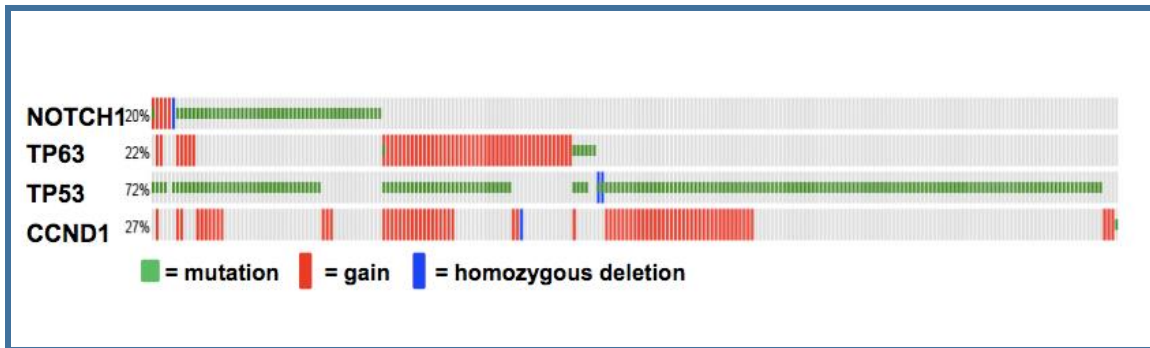


Figure 58: NOTCH1 and TP63 mutations tend to be mutually exclusive

The gene expression analysis is based on mRNA levels of effectors altered after NOTCH activation. We observed increased gene expression of potential tumor suppressor genes and decreased levels of proto-oncogenes. Since we are interested in the subset of patients that have inactive NOTCH signaling, we focused on proto-oncogenes that had increased expression in the absence of NOTCH activation. We confirmed that NOTCH indeed inhibited protein expression levels of AXL and α -catulin by inhibiting NOTCH activity using the pan-NOTCH inhibitor dnMAML1. Blocking NOTCH activity completely relieved NOTCH mediated inhibition of α -catulin and partially relieved AXL inhibition. The dnMAML1 functions in the nucleus, suggesting that blocking of NOTCH activity in the nucleus prevents inhibition of these proto-oncogenes. There are two possible ways in which NOTCH activation could downregulate proto-oncogenes; by directly binding to the promoter of these genes and impinging transcription (non-canonical NOTCH signaling) or by activating its canonical downstream targets (HES and HEY), which then repress proto-oncogenes (canonical NOTCH signaling).

Non-canonical NOTCH signaling

Activated NOTCH by itself can regulate targets independent of HES and HEY. For example, Rangarajan et al. have shown that expression of the activated form of NOTCH1 caused a significant increase in p21 (Rangarajan et al., 2001) in keratinocytes. Furthermore, they also showed that at the transcriptional level, p21 has an RBP-J κ binding site within close proximity to the TATA box to which ICN binds. In addition, involucrin, a differentiation marker was found to be under transcriptional control of NOTCH when keratinocytes differentiate at the basal layer. The promoter of involucrin has two critical regions that contribute to its activation; sp1 and AP1 binding sites at the

distal promoter region and a TATA box at the proximal region with a critical AP-1 binding site that overlaps with a motif for ets transcription factor binding sites (Efimova, LaCelle, Welter, & Eckert, 1998). Rangarajan et al. have shown that intracellular NOTCH binds to this promoter region independent of RBP-J κ and upregulates expression levels of involucrin. NF- κ B is another target that is transcriptionally activated when ICN binds to its promoter (Vilimas et al., 2007). NOTCH1 also directly interacts with the transcription factor YY1 to drive c-myc transcription in human myelogenous leukemia (Liao et al., 2007). In breast cancer, Lin et al. have shown that NOTCH activity transcriptionally upregulates IL-6 that results in the activation of the JAK-STAT pathway (Jin et al., 2013). We haven't investigated if NOTCH activation transcriptionally regulates AXL and α -catulin. Both these proto-oncogenes have AP1 and sp1 binding sites. Chu et al. had demonstrated that ICN could inhibit the expression of AP-1 dependent genes. Overexpression of ICN in cells transfected with AP-1 component gene strongly decreased AP1-mediate gene expression such as IL-8, MMP1 and I κ B α (Chu et al., 2002). It might be possible that in our system, activation of NOTCH signaling by culturing cells on Jagged1 inhibits AP1 mediated transcriptional activation of AXL and CTNNAL1. Transcriptional regulation of α -catulin is not completely explored. Xiang et al. suggested that AP-2 α and LEF-1 transcription factors regulate expression of CTNNAL1 (Xiang et al., 2012). However, their evidence was limited to ozone-induced stress activation of CTNNAL1.

Canonical transcriptional modulation of NOTCH targets

The canonical downstream targets of the NOTCH signaling pathway include members of the HES and HEY family genes. We show here that restoration of NFL1 in a

mutant cell line HN31 increased expression levels of HES2, HES5 and HEY2 by a least two fold. Previously, we found at least 500-fold increase in HES5 after activating wild-type and mutant cell lines with ICN1. These levels however, are not physiological since cells were transduced with high amounts of ICN1. Zage et al. have shown that in neuroblastoma cell lines, ICN1 could induce more than 1000-fold increase in HES4 and more than a 100,000-fold increase in HES5. When these cells were cultured on Jagged1, they observed a 100-fold and 20-fold increase in HES4 and HES5 respectively (Zage et al., 2012). Since HES and HEY family are known canonical repressors, we hypothesized that HES2 and HES5 might transcriptionally suppress expression levels of AXL and CTNNAL1. Thus, we overexpressed HES2 and HES5 in the mutant cell lines HN31 and evaluated expression levels of AXL and CTNNAL1 by qRT-PCR. HES2 and HES5 didn't seem to modulate mRNA expression levels of either proto-oncogenes (Figure 60). HES and HEY transcriptionally modulate genes such as Achaete-scute-like 1 (ASCL1/HASH1), atonal homolog-1 (ATOH) and neurogenin (NGN1) have been reported as targets of HES in neural tissues (Kageyama et al., 2005). Among the HES and HEY1 family, the downstream effectors of HES1 and HEY1 have been well characterized. Genes downregulated by HES1 included NEUROG3 (J. C. Lee et al., 2001), GAA (Yan, Raben, & Plotz, 2002), CDKN1B (Murata et al., 2005), RCOR1, and CFD and genes downregulated by HEY1 include GATA4 and GATA6 (Fischer et al., 2005). Hes factors play critical roles in the development of many organs and expand progenitor cell pools regulating cell fate decisions. HES1 and HES5 are regulated by auto-negative feedback loops and function as effectors of NOTCH signaling coordinating cell proliferation and differentiation via cell-cell interaction (Kobayashi & Kageyama,

2014). Hey proteins are also basic helix-loop-helix (bHLH) transcription factors related to the HES family. HEY proteins play critical roles in embryonic development, differentiation and tissue homeostasis (Weber, Wiese, & Gessler, 2014).

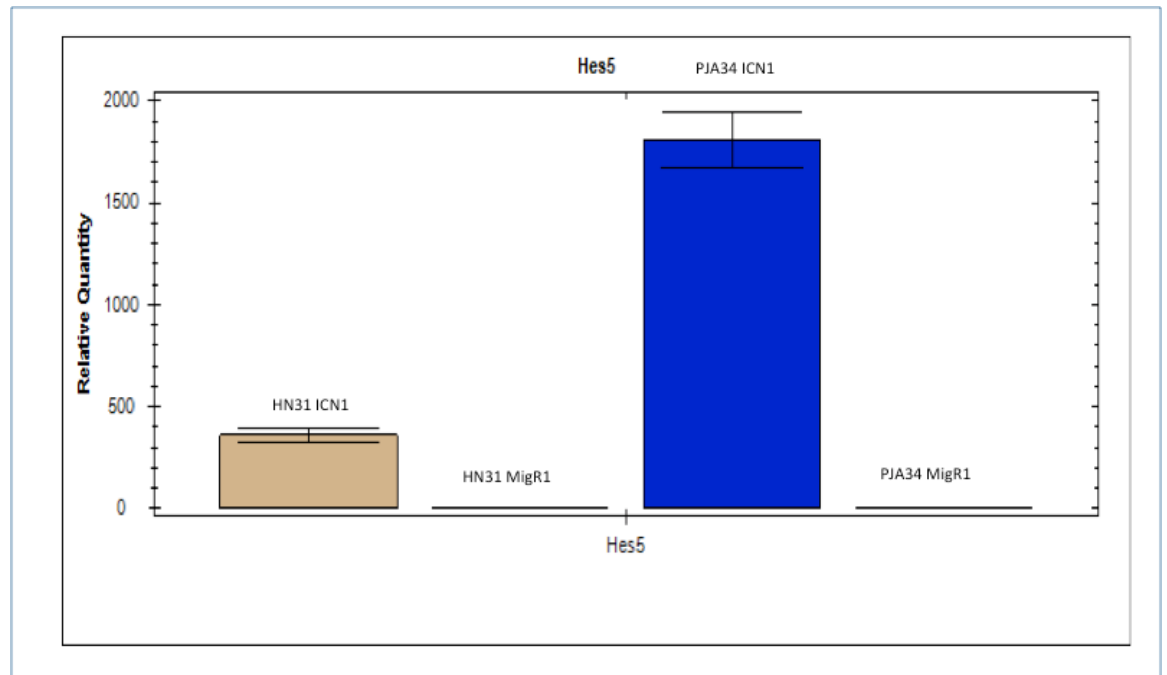


Figure 59: Activated *NOTCH1* increases gene expression of *HES5*

Both HES and HEY proteins have a conserved bHLH domain that is essential for DNA binding and homo and heterodimer formation. The N-terminal region defines the specificity of binding to target DNA sequences which are N-box (CACNAG), E-box (CANNTG) and class C site (CACG(C/A)G) (Sasai, Kageyama, Tagawa, Shigemoto, & Nakanishi, 1992). It has been suggested that certain proline residues, which is conserved in all HES factors, may be involved in target specificity, providing higher affinity for N-box sites rather than E-box sites. On the contrary, the bHLH domain of HEY proteins preferentially to E-box sites (Heisig et al., 2012). HES itself is regulated canonically after ICN binds with RBP-J κ upstream of the HES promoter (Katoh & Katoh, 2007). The promoter sequences of AXL and CTNNAL1 did not harbor the N-box or E-box binding motifs (Figure 61Figure 62) (Mudduluru & Allgayer, 2008; Xiang et al., 2012). At the same time, non-canonical NOTCH signaling also upregulates HES proteins. These pathways include bone morphogenetic protein (BMP), fibroblast growth factor (FGF), leukemia inhibitory factor (LIF), NF- κ B, sonic hedgehog (Shh) and Wnt signaling pathways (Nakayama, Satoh, Igari, Kageyama, & Nishida, 2008).

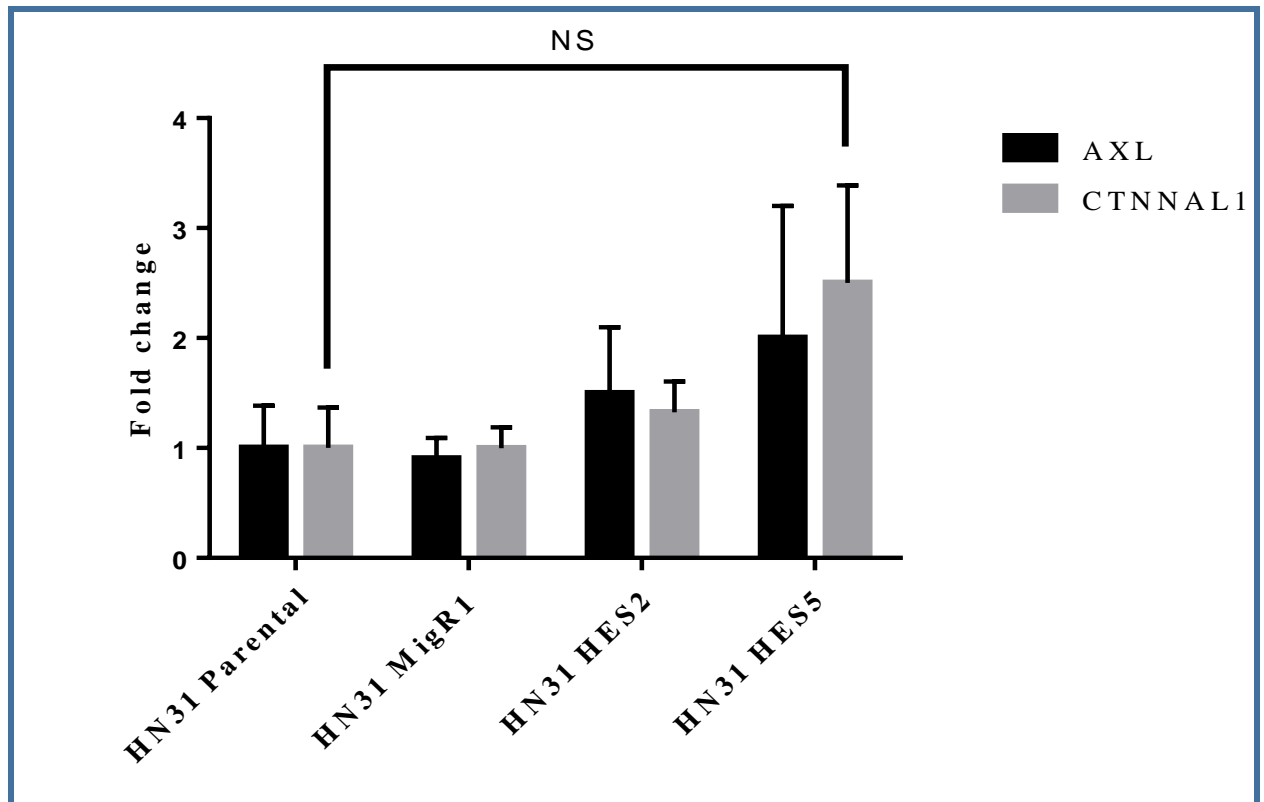


Figure 60: HES2 and HES5 don't seem to transcriptionally modulate levels of AXL or CTNNAL1.

a) Axl sequence of the 5' upstream region

```

-627 CGTGC GTGCGTGC GTGCGTGTGTGTGTGTGTGTGTCTTGTCCGAG
           MZF1                               Sp e
-577 GAGCCGAGAGAGTGAGGGGAATGAAGGGCCAAGGAGGCCTGGCTGGGGC
           Sp d           Sp c
-527 TGGGCTGGGGGTGGAGGCGGGGAGAGGGGCGTCACGGCCTGAGCTGAGAG
           ST
           └─┬─┘
-477 GGGAGTGGAGTTC TGAGGAATGTTTACCAGACACAGAGCCCAGAGGGAC
-427 AGCGCCAGAGCCCGGATAGAGAGACACGGCCTCACTGGCTCAGGACAGG
-377 GGGCACAGCCACCAGGGTCCCCTTCCCCCTCCTCAGCTCCCTCCCTGGCC
           AP1
-327 CCTTTAAGAAAGAGCTATCCTCTCCTCTCTTGAGTTAACCCCTGATTGTC
           Sp b
-277 CAGGTGGCCCCCTGGGCTCTGGCCCTGGTGGGCGGAGGCAAAGGGGGAGCC
           Sp a
-227 AGGGGCGGAGAAAGGGTTTGCCCAAGTCTGGGAGTGAGGGAAAGGAGGCAG
           MT
           └─┬─┘
-177 GGGTGCTGAGAAGGCGGCTGCTGGGCAGAGCCGGTGGCAAGGGCCTCCCC
-127 TGCCGCTGTGCCAGGCAGGCAGTGCCAAATCCGGGGAGCCTGGAGCTGGG
-77  GGGAGGGCCGGGGACAGCCCGGCCCTGCCCCCTCCCCGCTGGGAGCCCA
           TSS
-27  ACAACTTCTGAGGAAAGTTTGGCACCCATGGCGT +7

```

Figure 61: Promoter sequence of AXL lacks N-box or E-box motifs suggesting that HES and HEY might not directly transcriptionally regulate AXL gene expression.



Figure 62: Promoter sequence of *CTNNAL1* lacking N-box and E-box binding sites.

Gene expression in TCGA HNSCC patient tumors

TCGA analysis of patient tumors using the 120-gene signature confirmed our previous microarray analysis performed in cell lines. In addition, we also analyzed more than 20,000 genes from the TCGA RNA-Seq data for differentially expressed genes at two anatomical sites: Oral Cavity and Larynx/Hypopharynx. We found a few stem cell markers among the top upregulated genes in patients harboring an active NOTCH signature. These markers included Aldehyde Dehydrogenase ALDH1A1 and ALDH1A3, which were not among the top modulated genes in cell lines. This finding is interesting because it suggests that NOTCH activation might promote maintenance of stem cells, which is contradictory to our hypothesis that NOTCH activation inhibits tumor growth. Biologically, this is not surprising, since NOTCH signaling can promote stem cell maintenance and suppress differentiation in certain lineages while promoting differentiation in other lineages (Artavanis-Tsakonas, Rand, & Lake, 1999). NOTCH activation is known to suppress growth of AML, however, there are reports that activating mutations in β -catenin in osteoblasts stimulated Jagged1, which subsequently activates NOTCH signaling in hematopoietic stem cells causing AML (Kode et al., 2014). The hallmarks distinguishing normal stem cells from cancer stem cells is self-sufficiency in growth signals and insensitivity to anti-growth signals (L. Li & Neaves, 2006). The molecular pathways used by normal stem cells for homing to their niche may be hijacked by cancer stem cells that promote invasion and metastasis. These results suggest that activation of NOTCH signaling by ligands expressed by the supporting ECM may contribute to a stem cell phenotype. We haven't confirmed a cancer stem cell phenotype in our panel of cell lines after NOTCH activation since we observed only two

of the stem cell markers in patient samples. The most commonly used cancer stem cell markers to date have been CD34, CD133, CD24, CD44, CD29 and CD31. Aldehyde Dehydrogenase has only recently been propounded as a marker for HNSCC (Hoffmann, Matthes, Stucker, Segerling, & Altmeyer, 1990). ALDH positive cells exhibit high self-renewal capacity and radioresistance (Fabian, Barok, Vereb, & Szollosi, 2009). In HNSCC cancer cell lines that have been evaluated previously, specifically- oral cavity, pharynx, larynx, nasopharynx and hypopharynx, the most common cancer stem cell markers include CD34 (Barth, Schenck zu Schweinsberg, Ramaswamy, & Moll, 2004), CD117 (Tan, Selvaratnam, Kananathan, & Sam, 2006), CD44 (Kojc, Zidar, Vodopivec, & Gale, 2005) and SCF (Pries, Witkopf, Trenkle, Nitsch, & Wollenberg, 2008). We did not observe these markers in our cell lines and patient tumors. Stem cell proliferation is regulated by nice signaling. Maintaining the balance between proliferation and anti-proliferation is an important contributor to stem cell regulation. Any genetic mutation that leads normal stem cells to become independent of growth control will cause them to become cancer stem cells. Although the molecular markers of CSC's may provide useful information about the tumor pathogenicity, it is unclear whether every stem cell possess some or all of these markers that enable a cancer cell to be stem cell like. Thus, the stability of these CSC's need to evaluate by sphere forming assays. It might be worth considering an activated NOTCH1 inducible system in mutant cell lines and evaluating sphere formations in 3-D cultures. Physiological and artefactual differences between cell lines and patient tumors may also contribute to the differences in gene signatures we observe in the two systems. The intensity of NOTCH activation varies from cell lines to tumors. We are unaware of the physiological levels of NOTCH signaling needed to

modulate these stem cell markers and this might confound our understanding of stem cell regulation by NOTCH activation. Also, other genetic alterations in patient tumors such as NUMB overexpression of p63 activation may also contribute to such a difference. The microenvironment also plays an important role in stem cell regulation which we cannot elucidate in a 2-D in vitro culture system. Alternatively, the modulation of stem cell markers may not be specific to the tumor site due to infiltration of muscle or immune cells in the tumor creating an artifact in our data. Lastly, two different techniques were used to analyze differentially expressed genes in cell lines and TCGA patient tumors. While we used the Affymetrix 2.0 microarray technique, TCGA analysis was performed by RNA-Seq. Such differences in analysis may have confounded our results.

Inhibition of AXL and α -catulin modulates cell growth

In the last chapter, we show evidence that inhibition of AXL and α -catulin modulates cell and tumor growth in mutant HNSCC cell lines. AXL is an attractive target since it is overexpressed in several cancers including HNSCC where it is activated and tightly correlated with cetuximab resistance (Brand et al., 2015). Here we show that inhibition of AXL significantly inhibits cell and tumor growth. Brand et al. have recently demonstrated that knocking down AXL using siRNA's and a pharmacological inhibitor R428 significantly inhibits growth. Our results corroborate with published data and suggest that the AXL inhibitor can be effective in patients with inactivated NOTCH signaling. We also observed that knocking down AXL *in vivo* is more effective than α -catulin. Clonogenic assays showed that knocking down α -catulin had the most significant reduction in cell growth. It will be interesting to investigate the combined effect of inhibiting both AXL and α -catulin *in vivo*. Since we observed significant suppression of

growth when individually knocking down AXL or α -catulin, we assumed that combined inhibition would produce a more aggressive suppressive effect. A limitation to our study is that we haven't proved NOTCH dependent modulation of AXL and α -catulin *in vivo*. To show an *in vivo* effect, we will use the wild-type cell line PJA34 in which NOTCH1 and NOTCH2 have been knocked out using CRISPR-Cas9 and examine if they accelerate tumor growth. Further, we will stain these tumors for AXL and α -catulin. It is possible that the absence of NOTCH activation increases expression levels of these proto-oncogenes. This would give us a definitive correlation between NOTCH, AXL and α -catulin in a more physiological system. We will also evaluate the AXL inhibitor R428 on tumorigenesis in comparison with mutant cells after NFL1 is restored. The restoration of the NOTCH pathway could possibly provide a similar protective effect to the tumors as those treated with R428. Although there is an inhibitor of AXL, currently there is no pharmacological inhibitor of α -catulin. Recently Zheng et al. showed that overexpression of α -catulin possibly plays an important role in malignant transformation of HNSCC by inducing apoptotic resistance, promoting proliferation, cell cycle progression, migration, and invasion. They also suggested that knockdown or silencing α -catulin might reverse the aggressive phenotypes and EMT process (Z. Zhang et al., 2015). They demonstrate that overexpression of α -catulin in a cell line that had low α -catulin mRNA expression accelerated cell growth. Here, we show that knocking down α -catulin in a NOTCH1 mutant HNSCC cell line reverses cell growth and aggressive tumor formation and prolongs overall survival. Besides cell growth, AXL and α -catulin are also involved with cell migration and invasion. We haven't demonstrated the effects of modulating AXL and α -catulin on invasion since our primary focus was on NOTCH mediated growth

suppression. Cell migration and invasion was the second most modulated pathway based on IPA of our unbiased microarray. Thus, the role of NOTCH signaling in regulation cell migration/invasion mediated by AXL and α -catulin can potentially be explored in the future.

HES2 and HES5 inhibit cell growth

After restoring NOTCH signaling in a mutant cell line HN31, we observed elevated levels of HES2, HES5 and HEY2 about 20h after culturing these cells on Jagged1. We did not observe a significant change in HES1, HES3, HES4 and HEY1. The experiments were performed at 4 different time points after culturing cells on Jagged1. While we did observe maximal upregulation of HES2, HES5 and HEY2 at 20h, other time points (12h, 16h and 24h) also had higher expression, which was not seen in HES1, HES3, HES4 and HEY1.

A critical aspect of HES regulation is its oscillatory nature on cell proliferation in cultured cells. HES1 expression oscillates in many cell types including fibroblasts, myoblasts and neuroblasts. The period of HES1 oscillation is about 2h in many murine cell lines. After HES1 activation, the translated HES1 protein represses its own activity by directly binding to the N-box sequence of its own promoter. HES1 gene products: mRNA and protein are very unstable and have a half-life of about 20 min. Thus, they disappear rapidly, indicating that auto repression is short and transient. HES1 autonomously initiates oscillatory expression with short periodicity. Several studies have indicated HES1 oscillation and cell proliferation correlate with each other (Yoshiura et al., 2007). While we do not observe modulations in HES1 levels, it might be possible that in our system oscillations in HES2 and HES5 modulate cell growth and proliferation.

HES1 can also repress cell cycle related genes such as E2F1, p27 and p57 (Castella, Sawai, Nakao, Wagner, & Caudy, 2000; Georgia, Soliz, Li, Zhang, & Bhushan, 2006; Hartman et al., 2004). We show that overexpression of HES2 and HES5 can suppress AXL and α -catulin at the protein level. Whether HES2 and HES5 transcriptionally modulates AXL and α -catulin is yet to be explored. AXL and α -catulin both lack N-box or E-box motifs at their promoter sites. Thus, it might be possible that HES 2 or HES5 may not transcriptionally regulate AXL and α -catulin. Takata and Ishikawa have shown that HES1 can repress target genes in a transcription-independent manner by recruiting Sirt1, a homologue of silent information regulator 1 and class 3 histone deacetylase through its bHLH domain, thereby suppressing target gene expression (Takata & Ishikawa, 2003). HEY1 has been shown to directly interact with NcoR and Sin3a via its bHLH domain. This forms part of the Sin3 corepressor complex which recruits histone deacetylase-1 (HDAC1) (Gould, Harrison, Hewitt, & Whitehouse, 2009). Hey proteins were also shown to bind to the androgen receptors and its co-activator Src1 to repress transcription from promoters that depend on androgen (Belandia et al., 2005). In order to address such non-transcriptional inhibition of AXL and α -catulin by HES2 and HES5, we would have to perform a high-throughput screen to identify potential binding partners. Techniques such as yeast 2-hybrid screens could be employed that would screen for a library of potential interacting proteins.

Lastly, we show that overexpression of HES2 and HES5 inhibits growth that is possibly mediated by AXL and α -catulin. First, we demonstrated that overexpression of NOTCH1 inhibits cell and tumor growth. Next, we showed that NOTCH1 inhibits AXL and α -catulin, which produces a similar growth inhibitory effect. Lastly, we prove that

HES2 and HES5 may be sufficient to inhibit AXL and α -catulin. Taken together, these results suggest that NOTCH mediated inhibition of cell growth might involve HES2, HES5, AXL and α -catulin (Figure 54). Following NOTCH activation, the NOTCH-CBF1 complex binds to the HES promoter and activates transcription. In neural development, Ohtsuka et al. have shown that HES1 and HES5 are required for mammalian neuronal differentiation (Ohtsuka et al., 1999). In their model, overexpression of NOTCH1 in HES1 or HES5 null mice inhibited cell differentiation and increased cell proliferation suggesting that HES1 and HES5 may be required for NOTCH mediated inhibition of cell proliferation and induction of differentiation. We haven't completely evaluated the roles of HES2 and HES5 in modulating AXL, α -catulin and cell growth. We have shown that HES2 and HES5 may be sufficient to inhibit AXL and α -catulin in a cell line that has inactivated NOTCH signaling. To prove that these canonical downstream targets are necessary, we might have to overexpress NFL1 in cell lines that have HES2 and HES5 knocked out (by CRISPR-Cas9 system) and evaluate tumor formation, further staining the tumors for AXL and α -catulin. This would indicate if HES2 and HES5 are necessary for tumor growth and inhibition of AXL and α -catulin.

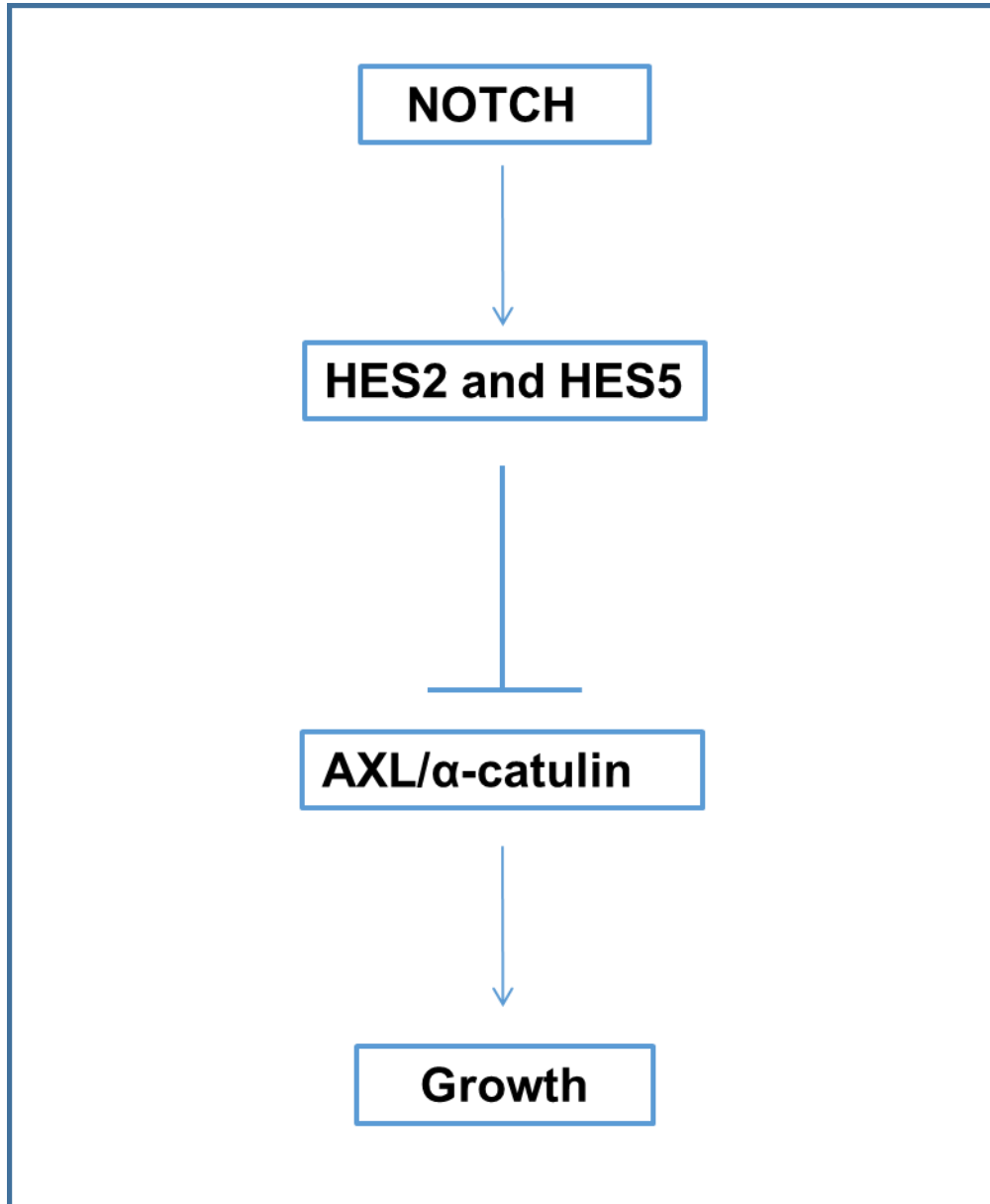


Figure 63: Mechanistic model of NOTCH mediated growth suppression

CHAPTER 9: CONCLUSIONS

Conclusions

We were among the first group to identify frequent inactivating somatic mutations in HNSCC (Agrawal et al., 2011). Recent TCGA data has shown that NOTCH is mutated at a frequency of 15-19% in primary tumors ("TCGA Releases Head and Neck Cancer Data," 2015), however the functionality of NOTCH in this cancer type was unknown. In this thesis, we have shown evidence that NOTCH1 acts as a tumor suppressor in HNSCC. For the first time, we cloned the full length NOTCH1 receptor and restored NOTCH signaling in mutant cell lines and showed a growth inhibitor effect *in vitro* and *in vivo*. Furthermore, we also evaluated the downstream effectors of the NOTCH signaling pathway that mediate growth inhibition. We identified a novel link of two proto-oncogenes AXL and α -catulin in relation to the NOTCH signaling pathway. We propose that NOTCH regulates these molecules at the protein expression level that might be mediated by HES2 and HES; canonical downstream effectors of NOTCH signaling.

There are limitations to this study that need to be addressed. Firstly, how NOTCH inhibits growth is not completely elucidated. We have shown partial evidence of senescence and G1 growth arrest. However, the appearance of spherical ball like structures after NOTCH is activated in a few cell lines like UM22A and HN31 are reminiscent of stem cell morphology. In addition, stem cell markers ALDH3A1 and ALDH1A1 were significantly upregulated in patients with an active NOTCH gene signature. This necessitates the need to understand the balance between stem cell maintenance and differentiation after NOTCH activation in our system. Secondly, we

selected two proto-oncogenes AXL and α -catulin based on significance of modulation, intensity of change and novelty to literature. There are several other molecules like KRT13, KRT15, INTGA5 and INTGA3 that are involved with differentiation and adhesion that were also upregulated after NOTCH activation. We couldn't address adhesion and cell migration/invasion in this study. Since cell migration/invasion was the also one of significantly modulated pathways, it will be worth understand this aspect of NOTCH signaling. Lastly, how NOTCH activation regulates AXL and α -catulin is unknown. From our data, NOTCH might transcriptionally regulate AXL and α -catulin but this might happened independent of HES2 and HES5. ChIP assays to evaluate binding sites along the promoter regions of AXL and α -catulin will help address transactional regulation of AXL and α -catulin by NOTCH signaling.

Besides these limitations, the identification of AXL being downstream of NOTCH signaling has clinical relevance. Patients that are mutant for NOTCH1 have high expression levels of AXL. Using the AXL inhibitor, it might be plausible to identify this subset of patients for treatment with this inhibitor. Taken together, NOTCH1 acts as a tumor suppressor in HNSCC, activates HES2 and HES5 and suppresses proto oncogenes AXL and α -catulin which can potentially be exploited to treat patients harboring inactivating NOTCH1 mutations.

Appendix

Appendix 1: Differentially expressed genes after activation of NOTCH signaling in PJA34 and 183 cells. Green highlighted “Significance” cells show genes modulated based on treatment, independent of cell lines. Orange highlighted “Significance” cells show genes modulated based on treatment and cell lines

	Test statistics	Significance	Fold changes	
GENE	P-VALUE	SIGNIFICANCE	PJA34 on Fc	183 on Fc
NETO2	1.31E-06	TRUE	-1.786766469	-1.591373679
ORC1	2.03E-06	TRUE	-1.293608993	-1.259996923
SVIL	2.19E-06	TRUE	1.223653112	1.250670199
HYOU1	9.68E-06	TRUE	-1.495332483	-1.292542472
SNX9	1.06E-05	TRUE	-1.262373825	-1.334064475
SDC4	1.09E-05	TRUE	-1.368789079	-1.283115657
LOC100131564	1.48E-05	TRUE	1.875013231	1.623158874
BUB1	1.58E-05	TRUE	-1.226914977	-1.200692744
PLEK2	1.86E-05	TRUE	-1.786902142	-1.605018829
LOXL2	2.16E-05	TRUE	-2.494472424	-1.62763903
TMEM55A	2.32E-05	TRUE	-1.478416916	-1.322108616
GLTP	2.64E-05	TRUE	1.376199925	1.313716811
EPHX1	3.02E-05	TRUE	1.35263688	1.449610284
TRAF6	3.86E-05	TRUE	-1.152709899	-1.267995575
MTA2	4.28E-05	TRUE	-1.12559422	-1.152395292
RBBP8	5.12E-05	TRUE	-1.258116005	-1.308456843
PFDN1	5.39E-05	TRUE	-1.219056404	-1.345029118
CCNE1	5.45E-05	TRUE	-1.474795156	-1.335716497
CHKA	5.90E-05	TRUE	-1.234297491	-1.456601315
EHD4	5.99E-05	TRUE	-1.487946593	-1.295572884
TMEM45B	6.02E-05	TRUE	1.429789064	2.055369763
PIGK	6.27E-05	TRUE	-1.175155846	-1.172503044
ACD	7.57E-05	TRUE	-1.157926571	-1.213096054
VPS13D	7.72E-05	TRUE	1.268872579	1.132285777
CAP1	8.26E-05	TRUE	-1.229542907	-1.138716253
KRT13	9.57E-05	TRUE	1.77026689	3.60191253
TRIM21	9.63E-05	TRUE	-1.179553244	-1.193941252
LAMC1	9.95E-05	TRUE	-1.319869362	-2.021028169
LOC100505648	0.000103862	TRUE	1.813266152	1.463558142
NEK4	0.000104204	TRUE	-1.130451774	-1.209764606
FKSG49	0.000114433	TRUE	1.574041091	1.549512174
CDCA2	0.000115175	TRUE	-1.219181131	-1.265979904
SPATA5	0.000115519	TRUE	-1.19604649	-1.252998702
E2F7	0.000158426	TRUE	-1.289616457	-1.302467882
LINC00305	0.000163931	TRUE	1.120782192	1.117798109
PRODH	0.00016933	TRUE	1.82869686	1.593180575
ALDH1B1	0.000194034	TRUE	-1.414398822	-1.209027432

C22orf32	0.000197178	TRUE	1.160389924	1.199436895
VPRBP	0.000201273	TRUE	-1.293232462	-1.169661492
BIN1	0.000202017	TRUE	-1.322500096	-1.514343369
GRWD1	0.000207466	TRUE	-1.36700702	-1.141186622
TOE1	0.000214969	TRUE	-1.336199744	-1.326452408
GALT	0.00021556	TRUE	1.297673436	1.185341207
FADS3	0.000216641	TRUE	-1.223837056	-1.341600513
C16orf57	0.000223521	TRUE	-1.346730387	-1.32449736
SQRDL	0.000224705	TRUE	-1.516282869	-1.33368959
TWF2	0.000225339	TRUE	-1.37447999	-1.176127818
SLAMF7	0.000234851	TRUE	-1.283074106	-1.167099379
TP53BP2	0.000241564	TRUE	-1.179167952	-1.316301924
CDCA8	0.000249332	TRUE	-1.273954509	-1.171928341
H3F3B	0.00026069	TRUE	1.329345141	1.364899342
MALAT1	0.000264194	TRUE	2.066669804	1.355450487
HSPH1	0.000270567	TRUE	-1.160921812	-1.224394234
CBL	0.000314101	TRUE	-1.194529075	-1.273433504
CTNNBIP1	0.000315766	TRUE	-1.393831987	-1.347872954
ABHD3	0.000343651	TRUE	-1.346209522	-1.202183782
ZBTB25	0.000355473	TRUE	1.228214388	1.240702106
ADAM15	0.000358385	TRUE	-1.224466846	-1.235001168
FAM219A	0.000379691	TRUE	-1.290578907	-1.348998551
TOMM40	0.000383483	TRUE	-1.29218039	-1.135574829
NBR1	0.000386537	TRUE	1.260411621	1.175231438
PCMTD1	0.000392268	TRUE	1.231978882	1.345370524
NOL11	0.000392324	TRUE	-1.199564185	-1.165537578
LSM2	0.000397076	TRUE	-1.11575537	-1.257140018
WDR44	0.000400631	TRUE	-1.167975473	-1.15586707
IGHG3	0.000405287	TRUE	1.450297705	1.52644626
DPP7	0.000407105	TRUE	1.267265071	1.145468908
CPD	0.000414971	TRUE	1.203387714	1.557163358
SMURF2	0.000431243	TRUE	-1.239318784	-2.068924561
LINC00511	0.000455291	TRUE	1.202667989	1.443979779
LOC647012	0.000458961	TRUE	-1.202200671	-1.09464217
SOX13	0.000468285	TRUE	-1.166520205	-1.364274341
IL1R1	0.0004875	TRUE	1.289275026	1.938324922
EIF2S2	0.00050376	TRUE	-1.073577415	-1.128741207
UHRF1	0.000507888	TRUE	-1.30266581	-1.202528743
FEN1	0.000510527	TRUE	-1.380328609	-1.141452263
SPRED1	0.00052766	TRUE	-1.339721849	-1.392720777
ZNF594	0.000556438	TRUE	1.410535469	1.276505876
VKORC1L1	0.000564705	TRUE	-1.170939583	-1.094360572
HSPA5	0.000572539	TRUE	-1.147947658	-1.203772664
LOC100272216	0.000585628	TRUE	1.738720093	1.514815069

HSPA13	0.000590424	TRUE	-1.054196479	-1.150919628
FAM157B	0.000594079	TRUE	1.909602286	1.387007581
GPD2	0.000635699	TRUE	-1.12685908	-1.428244225
FAM57A	0.000648745	TRUE	-1.328236535	-1.251381626
OR8B3	0.000678339	TRUE	-1.206940332	-1.165626136
FRK	0.000694778	TRUE	1.388054496	1.167870118
PRORS1P	0.000703802	TRUE	1.394405033	1.244419143
MAP2K1	0.000716848	TRUE	-1.394362066	-1.110948043
SLC9A1	0.000718803	TRUE	-1.273198995	-1.304208168
VARS	0.000806383	TRUE	-1.314578851	-1.141278214
ZBTB8A	0.000812592	TRUE	-1.480987827	-1.352056694
GJC1	0.000821452	TRUE	-1.156469072	-1.447435154
LOC100131434	0.000822597	TRUE	1.683313028	1.482152043
MCM6	0.000825588	TRUE	-1.208127076	-1.115939086
CD97	0.000832563	TRUE	-1.287670548	-1.363728948
TTI1	0.000854126	TRUE	-1.279442153	-1.176280036
CRYZL1	0.000883016	TRUE	1.207725873	1.204011237
ESYT1	0.00088412	TRUE	-1.595067548	-1.149591818
UAP1	0.000892989	TRUE	-1.466897988	-1.144797967
PCYT2	0.000919649	TRUE	-1.207264975	-1.363135773
EIF3F	0.00097262	TRUE	1.159942667	1.086747285
THRAP3	0.000974314	TRUE	-1.098936044	-1.088246955
FLJ45340	0.000987726	TRUE	1.782429293	1.304067101
UFD1L	0.000989381	TRUE	-1.166051339	-1.097111777
SMCR9	0.001008265	TRUE	-1.298573703	-1.26293699
SLC16A1	0.00101877	TRUE	-1.154026654	-1.451774579
NT5C2	0.001030223	TRUE	1.119115853	1.337324108
RABGEF1	0.001037365	TRUE	-1.178031674	-1.102004091
AMPD3	0.001042321	TRUE	-1.265653826	-1.422929114
RAB26	0.001050574	TRUE	1.222881856	1.216314483
IL20RA	0.001086824	TRUE	1.318803561	2.148012943
PSMC3	0.001092144	TRUE	-1.322784003	-1.129624084
TRBV5-1	0.00110443	TRUE	-1.327061294	-1.21561504
TUBGCP4	0.001113621	TRUE	-1.145609803	-1.1032789
MYSM1	0.001129062	TRUE	1.269770512	1.129472381
CSE1L	0.001141472	TRUE	-1.152464387	-1.083511616
LOC100288069	0.001141889	TRUE	1.765061556	1.328881943
GSG2	0.001163901	TRUE	-1.262337699	-1.334676676
PSMD12	0.001170838	TRUE	-1.285504432	-1.122910038
NDST1	0.001181211	TRUE	-1.380693357	-1.169410689
OCIAD2	0.001182903	TRUE	-1.556949385	-1.122781668
KCTD9	0.001210061	TRUE	-1.20445099	-1.128654543
CLK4	0.001212289	TRUE	1.398852928	1.263704401
HNRNPU-AS1	0.00122636	TRUE	2.157469333	1.453534529

PSMA1	0.001259243	TRUE	-1.196766829	-1.095626295
SLC35E2	0.001264955	TRUE	1.200316252	1.126374789
CLEC17A	0.001276609	TRUE	-1.283001599	-1.340105009
TCTN1	0.0012788	TRUE	1.177566714	1.250927959
EPHB4	0.001313916	TRUE	-1.117776332	-1.296898448
TTK	0.001350236	TRUE	-1.172201035	-1.088664024
CLK1	0.001398848	TRUE	1.3904032	1.194132732
COX10	0.001410188	TRUE	-1.104828409	-1.173120573
LOC100506479	0.001452983	TRUE	1.918322565	1.306739336
LOC100132062	0.001482583	TRUE	1.810779445	1.300552223
LOC100653348	0.001493134	TRUE	1.871788981	1.32519271
CDH3	0.001518356	TRUE	-1.205714629	-2.323396352
SNORD84	0.001529692	TRUE	-1.108867356	-1.133102691
STK4	0.001544275	TRUE	-1.098528954	-1.133062626
SFR1	0.001550509	TRUE	-1.326122306	-1.274766477
FOXN2	0.001585853	TRUE	-1.123577645	-1.273755938
CDC27	0.001614763	TRUE	-1.182725124	-1.085424244
SNORD91B	0.001617171	TRUE	1.130501138	1.257632747
ZNF35	0.001691019	TRUE	-1.394711983	-1.221597473
FAM118B	0.001699061	TRUE	-1.21144686	-1.143650655
LAMA3	0.001738458	TRUE	-1.205982894	-2.62113096
ATL2	0.001763792	TRUE	1.189065324	1.451325041
ODF3B	0.001778024	TRUE	1.246758179	1.290313533
TPD52	0.001778274	TRUE	1.124090552	1.105773284
CCNF	0.001821216	TRUE	-1.266024078	-1.182778925
EIF3I	0.001836842	TRUE	-1.204890771	-1.122326063
NCAPH	0.001849109	TRUE	-1.183510252	-1.105393594
C1orf146	0.001852168	TRUE	-1.105574468	-1.141910078
OCA2	0.001862792	TRUE	1.372399845	1.21903518
IGFL4	0.001863598	TRUE	1.248627502	1.354082104
DCAF8	0.001887869	TRUE	1.290723733	1.119782767
PAN2	0.001906978	TRUE	1.250390504	1.202139158
MRPS11	0.001919266	TRUE	-1.310008296	-1.10850888
SH3BGRL3	0.001926675	TRUE	-1.351744876	-1.168113905
TAF5	0.001948789	TRUE	-1.141204504	-1.243739076
FAM122C	0.001985931	TRUE	1.151456395	1.282829205
OR6B3	0.002004681	TRUE	-1.679502672	-1.257620124
FAM46A	0.002008932	TRUE	-1.479562317	-1.216231584
PSMA7	0.002063621	TRUE	-1.304162877	-1.115425852
CTSA	0.002072446	TRUE	1.181721107	1.104804888
GOLGA8C	0.002143645	TRUE	1.258968127	1.247813024
POGK	0.002145979	TRUE	-1.195107669	-1.210291568
GLT25D1	0.002159086	TRUE	-1.374305197	-1.162192046
RASA4	0.002168785	TRUE	1.130235813	1.174806859

LOC100506636	0.002182729	TRUE	1.965580857	1.298851484
AP3B2	0.002185912	TRUE	-1.139617117	-1.209679085
TOMM34	0.00222442	TRUE	-1.155041684	-1.413960853
RAD54B	0.002234403	TRUE	-1.198440837	-1.234573886
ELOF1	0.002236058	TRUE	-1.190819571	-1.071162823
TAF13	0.002248343	TRUE	-1.301445786	-1.09392258
ARMC9	0.002268096	TRUE	-1.348939983	-1.220935505
ZNF593	0.002272196	TRUE	-1.221642777	-1.252188572
ABCA5	0.002275699	TRUE	1.446113105	1.199999554
ADAT1	0.002293045	TRUE	-1.159905253	-1.266511687
ABCA2	0.002317235	TRUE	1.277503114	1.143709909
PCDHB18	0.002327844	TRUE	1.376796784	1.114361557
SLC4A1AP	0.002372555	TRUE	-1.15309246	-1.164520462
HSPA14	0.002380471	TRUE	-1.259227341	-1.245634752
C9orf78	0.002406737	TRUE	-1.151618977	-1.168343497
ASNA1	0.002442203	TRUE	-1.279293663	-1.101563842
WDR36	0.002462321	TRUE	-1.140522857	-1.046372381
OXNAD1	0.002467984	TRUE	-1.224988221	-1.156874243
SPATA5L1	0.002489387	TRUE	-1.40801875	-1.181282725
ROR1	0.002546865	TRUE	-2.771381193	-1.334780243
MLLT11	0.002551575	TRUE	-1.551308408	-1.118740801
LOC100653350	0.002557473	TRUE	-1.604746916	-1.380776818
C3orf38	0.002584638	TRUE	-1.180209063	-1.16586902
RDH11	0.002611957	TRUE	-1.240587233	-1.082844886
DUX4L9	0.002635471	TRUE	1.088351303	1.426573737
MCM3	0.002635823	TRUE	-1.123201497	-1.105011312
LOC100133032	0.00263938	TRUE	1.133191665	1.254169884
LYST-IT2	0.002648508	TRUE	1.409364984	1.167814212
SNORA16B	0.002660148	TRUE	1.432638092	1.714984897
PDCD1LG2	0.002668483	TRUE	-1.251598029	-3.302925645
PBXIP1	0.00269523	TRUE	1.248909473	1.191319012
ARHGDI	0.002736477	TRUE	-1.388162796	-1.173613809
CTCF	0.002762059	TRUE	-1.062049945	-1.114575891
RNF207	0.002783972	TRUE	1.332365881	1.278784301
PTPLAD1	0.002844242	TRUE	-1.175048628	-1.090491122
DOLK	0.002894157	TRUE	-1.134445711	-1.243752331
MLKL	0.002901199	TRUE	-1.204360821	-1.212046639
BORA	0.002920487	TRUE	-1.237885463	-1.177660205
MIR3689D1	0.002946025	TRUE	1.131992593	1.476894034
SLC25A34	0.002980464	TRUE	1.369878113	1.141297974
HHAT	0.003022559	TRUE	1.229899811	1.208087909
USP48	0.003022715	TRUE	1.170695227	1.094216952
LOC100506926	0.003039253	TRUE	-1.157971455	-1.129393974
LDLRAD1	0.003041538	TRUE	1.211917067	1.531508357

ZCCHC17	0.003051979	TRUE	-1.302214406	-1.118168788
NOLC1	0.003058899	TRUE	-1.150051442	-1.087622331
ANO1	0.003072006	TRUE	1.139045653	2.076667977
APCDD1L	0.00311888	TRUE	-2.026960024	-1.143485905
GPM6A	0.003191475	TRUE	-1.219558763	-1.199435033
C17orf96	0.003209697	TRUE	-1.099247753	-1.41801
BOLA3	0.003217741	TRUE	-1.232781555	-1.159255018
LOC654342	0.003246446	TRUE	-1.523898262	-1.309840007
VASP	0.003281192	TRUE	-1.234048503	-1.334912987
PLAC8L1	0.003283025	TRUE	1.206297563	1.236947949
MIR4668	0.003283186	TRUE	1.398813602	1.572780922
GOLGA8F	0.003304404	TRUE	1.181782911	1.126158306
ANXA2P3	0.003324505	TRUE	-1.523805742	-1.334015604
LRWD1	0.003335295	TRUE	-1.355611739	-1.190733455
SCARNA21	0.003342125	TRUE	1.410408644	1.137917443
LINC00514	0.003363033	TRUE	1.156422128	1.168801951
THOP1	0.003389264	TRUE	-1.304545151	-1.151971597
GRIK1-AS1	0.003407719	TRUE	1.301317831	1.161168282
LOC729737	0.003409182	TRUE	2.103759441	1.294475749
AMMECR1-IT1	0.003442353	TRUE	1.139656571	1.139566251
ADPGK	0.003465772	TRUE	-1.203901795	-1.156404935
TBC1D8	0.003468426	TRUE	1.185818317	2.313449352
ADIPOR2	0.003482462	TRUE	1.144721272	1.081682242
EPHA2	0.003589923	TRUE	-1.485376135	-1.616781185
DBP	0.003608038	TRUE	1.175918938	1.339803253
DNER	0.003626329	TRUE	-1.614963336	-1.235236778
LOC554249	0.003690705	TRUE	1.311408353	1.31568982
GPR65	0.003692228	TRUE	-1.256768361	-1.122144414
IRF6	0.00372726	TRUE	1.063972323	1.264426131
C9orf118	0.003737204	TRUE	-1.043415261	-1.181264887
DNLZ	0.003740105	TRUE	-1.388288522	-1.255445771
FAF1	0.003743002	TRUE	1.094334874	1.149666445
LOC100287314	0.003817511	TRUE	-2.081614963	-1.211822115
GBA	0.003826381	TRUE	1.327467973	1.281804471
TRDJ2	0.003858077	TRUE	1.278546253	1.168678249
NFYA	0.003865274	TRUE	-1.148997031	-1.143601777
ZFAND2A	0.003878197	TRUE	-1.107301118	-1.249088208
BMS1P5	0.003882601	TRUE	1.15825541	1.154195964
ATP5S	0.003915878	TRUE	1.288044456	1.11439769
MIR146B	0.003934832	TRUE	-1.712102686	-1.141662684
SRD5A1P1	0.003985077	TRUE	1.216775526	1.359809448
SNORD41	0.003990502	TRUE	1.314774035	1.238238355
SELK	0.00400774	TRUE	-1.209650652	-1.258921629
ITPA	0.004018787	TRUE	1.07017234	1.114499093

PRMT7	0.00404008	TRUE	-1.272695461	-1.077379596
BLM	0.004068344	TRUE	-1.136694174	-1.199473082
CRISP1	0.004206731	TRUE	-1.221353692	-1.105957874
PAFAH1B2	0.004213345	TRUE	-1.231352047	-1.083086604
PIWIL4	0.004224568	TRUE	-1.336913491	-1.311766301
UBE3A	0.004312855	TRUE	-1.089941778	-1.087460488
RNU105C	0.004339569	TRUE	-1.158404128	-1.120062761
FOSL1	0.004399443	TRUE	-2.537182189	-1.816340812
MIR4742	0.004420224	TRUE	1.448336912	1.886408558
AHNAK	0.004497224	TRUE	1.188870686	1.266188378
TBC1D22A	0.004514445	TRUE	1.056050372	1.298516422
SRA1	0.004609955	TRUE	-1.231012615	-1.117901999
IARS	0.004613694	TRUE	-1.067750282	-1.071573565
SNRPB	0.004633707	TRUE	-1.181061134	-1.103884557
FUBP3	0.004675741	TRUE	-1.100113723	-1.042948477
ND3	0.00478452	TRUE	1.149465184	1.077011755
ARHGEF10	0.004812048	TRUE	-1.283419759	-1.244259404
PSMD8	0.00484086	TRUE	-1.198190776	-1.063805748
TMPRSS11BNL	0.004849467	TRUE	-1.075984204	-1.159451655
GCFC1	0.004863511	TRUE	1.248138338	1.114546701
CAV1	3.59E-09	TRUE	-1.879864475	-2.213279734
AXL	6.41E-09	TRUE	-2.740535194	-3.550417429
RAB40B	1.78E-08	TRUE	1.700767531	1.981179136
KRT15	2.22E-08	TRUE	1.901707382	1.686342124
VTCN1	2.24E-08	TRUE	3.084901816	2.960660781
C11orf54	3.57E-08	TRUE	1.430378176	1.436548543
EPHA4	8.73E-08	TRUE	1.651338226	1.937497399
FHL2	1.15E-07	TRUE	-1.793647944	-2.050525456
TP53INP1	1.21E-07	TRUE	2.990640742	2.270578316
SLPI	1.58E-07	TRUE	1.435747632	1.556415025
CMTM8	1.64E-07	TRUE	-1.467111422	-1.621031591
LOC645553	1.78E-07	TRUE	1.953409711	1.785603835
SERPINE1	2.07E-07	TRUE	-2.737937127	-2.216887593
ACSS1	2.27E-07	TRUE	1.330140299	1.292522869
PTRF	3.53E-07	TRUE	-2.018511855	-2.160152521
NAV3	4.33E-07	TRUE	-2.015300831	-1.840096007
LAMC2	5.09E-07	TRUE	-2.601950467	-4.660258605
MIR622	5.60E-07	TRUE	-1.713406578	-1.927822216
DRAM1	5.62E-07	TRUE	-1.88475279	-2.08255253
AFAP1L2	6.00E-07	TRUE	-1.48813128	-1.599475888
ANK3	6.37E-07	TRUE	1.38241757	1.536904057
LURAP1L	7.13E-07	TRUE	1.743066142	2.034945317
SUV39H1	8.88E-07	TRUE	-1.236273258	-1.256763713
PLD1	8.95E-07	TRUE	1.65776883	2.024055226

SKA1	1.29E-06	TRUE	-1.430599512	-1.283475658
TJP1	1.32E-06	TRUE	-1.403405606	-1.258711109
ELK3	1.50E-06	TRUE	-1.25967842	-1.326464126
CXorf49	1.70E-06	TRUE	-2.373220082	-1.770249814
MICB	1.78E-06	TRUE	-1.386492784	-1.609662747
PDCD4	2.01E-06	TRUE	1.722340546	2.077520061
FUCA2	2.13E-06	TRUE	-1.460606691	-1.34140004
ME2	2.21E-06	TRUE	-1.21872262	-1.256448596
TMCC3	2.29E-06	TRUE	-1.718795461	-1.879758243
SEMA7A	2.29E-06	TRUE	-1.57210976	-1.593661908
ITGA5	2.34E-06	TRUE	-1.548089254	-1.66591199
HOMER3	2.38E-06	TRUE	-1.605475502	-1.464097707
ZBED2	2.55E-06	TRUE	-1.892263387	-1.69646004
TUBB	2.59E-06	TRUE	-1.130891546	-1.119801012
SYT16	2.68E-06	TRUE	-1.762607899	-1.621434495
SLC44A2	2.69E-06	TRUE	-1.285656293	-1.210443909
TINAGL1	2.94E-06	TRUE	-1.409760798	-1.386166566
MCM5	3.03E-06	TRUE	-1.26952641	-1.204929668
KIAA1147	3.24E-06	TRUE	1.467491511	1.705353015
PANX1	3.28E-06	TRUE	-1.363988338	-1.260007079
USP10	3.30E-06	TRUE	-1.115595875	-1.180940474
SLC16A2	3.34E-06	TRUE	-1.802144115	-2.572954157
TNFSF10	3.47E-06	TRUE	1.409020665	1.626315216
FGFBP1	3.66E-06	TRUE	-1.843775565	-2.194481884
FHOD1	3.75E-06	TRUE	-1.44140405	-1.467252458
GALNT2	3.92E-06	TRUE	-1.352325102	-1.585801864
TC2N	4.16E-06	TRUE	1.424823062	1.265983844
UTP20	4.29E-06	TRUE	-1.386989262	-1.250498328
PPAP2A	4.43E-06	TRUE	1.832492561	3.047363185
SKP2	4.46E-06	TRUE	-1.26281721	-1.455441508
ITCH	4.79E-06	TRUE	-1.175851935	-1.137027189
CTSC	4.94E-06	TRUE	1.587310285	1.366280459
P4HA1	4.95E-06	TRUE	-1.419798997	-1.303381516
ITGA3	5.03E-06	TRUE	-1.561938907	-1.882561378
PYGL	5.22E-06	TRUE	-1.275687899	-1.22819576
PXN	5.48E-06	TRUE	-1.509970786	-1.831901732
KRT18P10	5.51E-06	TRUE	-1.655976362	-1.665664242
MAP4K4	5.53E-06	TRUE	-1.383645241	-1.265791535
MBTD1	5.65E-06	TRUE	1.247070835	1.220390928
PKP2	5.73E-06	TRUE	-1.509984202	-1.542301169
GLTSCR2	6.21E-06	TRUE	1.334066127	1.226318855
CYP1A1	6.40E-06	TRUE	1.652873806	2.249775191
THSD4	6.42E-06	TRUE	-1.49717886	-1.54261147
NEDD4	6.86E-06	TRUE	-1.139600153	-1.183365917

PBX1	7.54E-06	TRUE	1.636231577	1.820221527
NOP2	7.91E-06	TRUE	-1.272774869	-1.198788856
PNRC1	8.05E-06	TRUE	1.337523493	1.422605915
DFNA5	8.18E-06	TRUE	-1.337065625	-1.760828617
SLC12A2	8.22E-06	TRUE	1.574053144	2.286239693
WDHD1	8.32E-06	TRUE	-1.205294668	-1.217696276
ANLN	8.40E-06	TRUE	-1.161794953	-1.173841188
GCNT1	8.44E-06	TRUE	-1.317217456	-1.333733481
RCN3	8.87E-06	TRUE	1.165354094	1.272609596
SHMT1	9.17E-06	TRUE	-1.24460801	-1.182589194
RIPK4	9.50E-06	TRUE	1.32600794	1.375810181
E2F4	9.52E-06	TRUE	-1.318311614	-1.361232757
KIF14	9.64E-06	TRUE	-1.185854918	-1.194170515
ACPP	9.76E-06	TRUE	1.618462626	1.441360018
PLXDC2	1.03E-05	TRUE	1.589624055	1.339970703
HBP1	1.07E-05	TRUE	1.352290858	1.228506724
SPAG5	1.08E-05	TRUE	-1.207325799	-1.193867684
KLK6	1.11E-05	TRUE	-1.833552194	-1.761434628
FAM83D	1.11E-05	TRUE	-1.221983101	-1.136892115
HES5	1.15E-05	TRUE	1.455861404	1.640565012
ST6GALNAC2	1.15E-05	TRUE	1.456881687	1.566976092
LCN2	1.19E-05	TRUE	1.507570226	1.373787535
MCM8	1.22E-05	TRUE	-1.277139977	-1.26620438
SF3A3	1.26E-05	TRUE	-1.152827264	-1.179602843
FAM214A	1.28E-05	TRUE	1.40523228	1.46286467
SGSM2	1.28E-05	TRUE	1.376786204	1.333257908
CDCP1	1.30E-05	TRUE	-1.360600651	-1.463711133
DNAJC10	1.33E-05	TRUE	-1.215384665	-1.279713107
SOX15	1.34E-05	TRUE	-1.761679288	-1.402531829
ZWILCH	1.36E-05	TRUE	-1.198039909	-1.267075109
TUBB6	1.42E-05	TRUE	-1.469844481	-1.250822924
RNF138P1	1.42E-05	TRUE	2.983802218	2.426622264
INADL	1.45E-05	TRUE	1.327631165	1.242823532
ABCC3	1.46E-05	TRUE	-1.397553493	-1.761489599
LRFN4	1.47E-05	TRUE	-1.405695071	-1.357507549
RN5S496	1.52E-05	TRUE	-3.410915511	-1.917774556
GCLC	1.57E-05	TRUE	1.774180387	1.412309223
NMT1	1.59E-05	TRUE	-1.106073586	-1.123937492
CNKSR3	1.67E-05	TRUE	1.405179404	1.917444165
NF2	1.91E-05	TRUE	-1.247962622	-1.216113273
GATA6	1.93E-05	TRUE	-1.478216462	-1.31407147
YIPF1	1.94E-05	TRUE	-1.272397024	-1.329164765
CALB1	1.94E-05	TRUE	1.427729205	1.339999325
MOB3B	1.94E-05	TRUE	-1.584894299	-1.51973541

WNT7A	1.97E-05	TRUE	-1.332383813	-1.683790922
PCMTD2	2.07E-05	TRUE	1.409059196	1.481326956
CAP2	2.08E-05	TRUE	-1.50968777	-1.313624236
DNAJC2	2.17E-05	TRUE	-1.29249164	-1.24023538
CLSPN	2.22E-05	TRUE	-1.306358909	-1.286925784
KPNA2	2.31E-05	TRUE	-1.136255138	-1.080337381
PLAUR	2.35E-05	TRUE	-1.910431499	-1.743558843
MMP9	2.35E-05	TRUE	-1.598714895	-2.528770321
PRKX	2.37E-05	TRUE	1.562484797	1.660797133
MPV17L2	2.42E-05	TRUE	-1.400850335	-1.300737366
NPLOC4	2.46E-05	TRUE	-1.18580229	-1.157307387
DSP	2.46E-05	TRUE	1.467566441	1.651192413
FLII	2.47E-05	TRUE	-1.340949221	-1.278247522
RHOD	2.57E-05	TRUE	-1.412526842	-1.297628171
C20orf20	2.57E-05	TRUE	-1.339681283	-1.31992651
GPX8	2.75E-05	TRUE	-1.204988833	-1.370357629
TCF19	2.78E-05	TRUE	-1.215235775	-1.155721191
MFN2	2.80E-05	TRUE	-1.181066435	-1.12823715
NFE2L3	2.80E-05	TRUE	-1.389423572	-1.46206054
UPP1	2.80E-05	TRUE	-1.432519049	-1.548333718
FAM102B	2.85E-05	TRUE	1.660198946	1.408780083
CFLAR	2.86E-05	TRUE	1.220136259	1.283926877
UBE2T	2.91E-05	TRUE	-1.224744388	-1.20240708
LOXL4	2.94E-05	TRUE	-3.122215928	-1.797933225
SLC7A2	3.00E-05	TRUE	-1.504287819	-2.240838573
CYB5A	3.02E-05	TRUE	1.329640469	1.394810557
BRCA1	3.03E-05	TRUE	-1.135070532	-1.116543091
MCM7	3.09E-05	TRUE	-1.191800102	-1.208786606
TMEM27	3.16E-05	TRUE	-1.63390962	-1.484812487
GTF2IP1	3.23E-05	TRUE	1.260071836	1.195103599
DOCK5	3.38E-05	TRUE	-1.146817587	-1.109710407
CDS1	3.47E-05	TRUE	-1.471580804	-1.365683477
RAP2B	3.50E-05	TRUE	-1.261172536	-1.246133097
ANKRD2	3.72E-05	TRUE	-1.665783348	-1.563020181
BAG2	3.76E-05	TRUE	-1.474943714	-1.29861083
ISYNA1	3.88E-05	TRUE	1.349583497	1.344983351
MPPE1	3.90E-05	TRUE	1.252157724	1.146987714
P4HTM	3.91E-05	TRUE	1.225615466	1.169545978
WNK2	3.92E-05	TRUE	1.485789317	1.350053332
FANCD2	3.95E-05	TRUE	-1.116855619	-1.120172785
1-Mar	4.02E-05	TRUE	-1.379733209	-1.209994276
CCDC85C	4.03E-05	TRUE	-1.333526241	-1.213183336
ADD3	4.08E-05	TRUE	1.358820282	1.410445919
KRT18P54	4.08E-05	TRUE	-1.371958391	-1.604895302

FAM116A	4.14E-05	TRUE	1.205069728	1.195905164
CIRH1A	4.17E-05	TRUE	-1.397767207	-1.232822721
ARHGDIB	4.24E-05	TRUE	-1.96602048	-1.391176075
DARS2	4.26E-05	TRUE	-1.199047349	-1.131005693
AP2B1	4.28E-05	TRUE	-1.431655239	-2.222986212
PEA15	4.30E-05	TRUE	-1.509446711	-1.253661547
TPMT	4.37E-05	TRUE	-1.601193275	-1.303637071
PLOD3	4.40E-05	TRUE	-1.36954968	-1.976501665
FAM21A	4.44E-05	TRUE	1.163310643	1.141073698
LOC439990	4.50E-05	TRUE	-1.97086006	-1.581887867
SH3TC2	4.54E-05	TRUE	1.288006009	1.280236117
MANSC1	4.58E-05	TRUE	1.562403784	1.730101187
H3F3A	4.58E-05	TRUE	1.185208302	1.149451876
SMS	4.58E-05	TRUE	-1.215885914	-1.182905969
INTS7	4.62E-05	TRUE	-1.182604393	-1.26712887
SOX2	4.62E-05	TRUE	1.439008166	1.375236492
SLC25A13	4.62E-05	TRUE	-1.168402185	-1.210186803
LY6K	4.62E-05	TRUE	-1.510338848	-1.267068197
CD3EAP	4.64E-05	TRUE	-1.533856284	-1.314359608
CDC25A	4.70E-05	TRUE	-1.453085166	-1.316096195
GOLGA8B	4.87E-05	TRUE	1.755164941	1.430585282
FERMT2	4.92E-05	TRUE	-1.525847841	-1.310791219
SDF2L1	4.92E-05	TRUE	-1.377527908	-1.269674802
SFSWAP	5.00E-05	TRUE	-1.126488176	-1.116264512
ANKRA2	5.03E-05	TRUE	1.342585244	1.275819028
ZC3H14	5.04E-05	TRUE	-1.100060431	-1.071990957
MCM10	5.06E-05	TRUE	-1.335189746	-1.163231602
PRIM2	5.45E-05	TRUE	-1.231896516	-1.221243314
JAG2	5.48E-05	TRUE	-1.213845854	-1.392949812
GEMIN5	5.48E-05	TRUE	-1.271575948	-1.188542557
PSMB1	5.52E-05	TRUE	-1.283745597	-1.121026262
CASD1	5.69E-05	TRUE	1.198303744	1.138690168
LSR	5.82E-05	TRUE	-1.160269975	-1.216788602
SRP68	5.86E-05	TRUE	-1.125162221	-1.112908479
CACNG4	5.87E-05	TRUE	-1.267468044	-1.32472122
ORC6	5.91E-05	TRUE	-1.467914621	-1.222637654
DLL1	5.92E-05	TRUE	-1.338208803	-1.646450978
FXYD5	5.93E-05	TRUE	-1.175943928	-1.384971547
BFAR	6.02E-05	TRUE	-1.207693857	-1.132621484
TBC1D3G	6.07E-05	TRUE	1.196220852	1.274581238
CRIM1	6.27E-05	TRUE	-1.198495189	-1.397970117
LEPREL1	6.37E-05	TRUE	-1.629279347	-1.505439876
SERINC2	6.53E-05	TRUE	-1.618478241	-1.376283612
DDX56	6.53E-05	TRUE	-1.239628019	-1.140127332

SLC39A14	6.56E-05	TRUE	-1.460453143	-2.261275184
GOLGB1	6.57E-05	TRUE	1.324327257	1.267323124
GLUL	6.63E-05	TRUE	1.671557955	1.434873429
PPAP2C	6.79E-05	TRUE	1.16900111	1.385468694
WDR19	6.82E-05	TRUE	1.308874626	1.250091094
PDIA4	6.94E-05	TRUE	-1.249534891	-1.217454913
MELK	7.00E-05	TRUE	-1.296728801	-1.19070894
LETMD1	7.01E-05	TRUE	1.289321084	1.296732181
FAF2	7.04E-05	TRUE	-1.167500406	-1.195980278
DNMT1	7.09E-05	TRUE	-1.15081456	-1.211846273
SLC3A2	7.27E-05	TRUE	-1.229056493	-1.193028566
CANT1	7.28E-05	TRUE	-1.263101153	-1.325381965
TPR	7.30E-05	TRUE	1.155543982	1.165324222
PKD1P1	7.33E-05	TRUE	1.381327638	1.22173835
YARS2	7.38E-05	TRUE	-1.335294464	-1.21395653
STAC	7.54E-05	TRUE	-1.724328789	-1.368932259
RHOV	7.68E-05	TRUE	1.309605705	1.615115896
EIF2C4	7.76E-05	TRUE	1.316108752	1.282118598
GOLGA8A	7.85E-05	TRUE	1.696759181	1.403030571
B4GALNT1	7.86E-05	TRUE	-1.313654459	-1.657225633
CUL1	7.92E-05	TRUE	-1.22546041	-1.15876126
TMEM59	8.35E-05	TRUE	1.37694188	1.228639864
CD55	8.36E-05	TRUE	-1.42095849	-1.72847595
THSD1	8.37E-05	TRUE	-1.701477442	-1.310144595
KHNYN	8.44E-05	TRUE	1.194914334	1.148038266
NUP88	8.56E-05	TRUE	-1.132512485	-1.137218206
C1QBP	8.56E-05	TRUE	-1.169364152	-1.135026527
GCH1	8.60E-05	TRUE	-1.364705711	-1.666349608
KPNA3	8.62E-05	TRUE	-1.157837018	-1.139180939
CHRNA5	8.64E-05	TRUE	-1.253404087	-1.222216732
MTM1	8.69E-05	TRUE	-1.11230361	-1.228309266
HEG1	8.76E-05	TRUE	-1.489284699	-1.867101731
SCRN1	8.84E-05	TRUE	-1.156697525	-1.313001516
SERPINE2	8.89E-05	TRUE	-1.369715324	-1.598968503
ZAK	9.32E-05	TRUE	-1.240993049	-1.397499274
OLFML3	9.39E-05	TRUE	-1.376356582	-1.285810891
HLTF	9.39E-05	TRUE	1.222382931	1.487774907
WDR60	9.44E-05	TRUE	1.243347578	1.262711226
SLC11A2	9.48E-05	TRUE	1.168255724	1.282132254
CENPN	9.55E-05	TRUE	-1.274710571	-1.240757009
SLC25A6	9.55E-05	TRUE	1.126789546	1.119678886
TIMP1	9.57E-05	TRUE	-1.18153691	-1.356171271
TYMS	9.60E-05	TRUE	-1.241345088	-1.153860772
PI4K2A	9.68E-05	TRUE	-1.4942046	-1.400038662

STAM	9.74E-05	TRUE	-1.387963716	-1.312774585
EXO1	9.78E-05	TRUE	-1.23873618	-1.247638667
NOMO3	9.80E-05	TRUE	-1.195281414	-1.101620962
PKP1	9.86E-05	TRUE	1.232903721	1.360957134
IPO9	0.000100404	TRUE	-1.188523973	-1.172573525
FST	0.00010061	TRUE	-1.985150282	-5.3153921
CLOCK	0.0001013	TRUE	-1.24239604	-1.147297409
NP1P	0.000103775	TRUE	1.351216977	1.23180045
KLHL24	0.00010392	TRUE	1.741500364	1.545723369
DLAT	0.000104889	TRUE	-1.180222797	-1.150167221
DIAPH3	0.000105834	TRUE	-1.304281888	-1.252877818
PELI2	0.000106871	TRUE	1.486457442	1.258656044
LPAR1	0.000107489	TRUE	-1.336840129	-1.407432313
ACO1	0.000107568	TRUE	-1.77471041	-1.293598741
MAL2	0.000107997	TRUE	-1.219185367	-1.175573379
CDC6	0.000109142	TRUE	-1.239669677	-1.287635628
ZNF658B	0.000109385	TRUE	1.390951125	1.209824992
NXPE3	0.000109425	TRUE	-1.520349076	-1.690504953
VEGFC	0.000109475	TRUE	-2.014026443	-1.497205405
CXCL16	0.000110021	TRUE	-1.422118031	-1.395273239
ETV4	0.000110256	TRUE	-1.260040685	-1.33407348
NEK3	0.000110287	TRUE	-1.393380197	-1.536496255
ETHE1	0.000110842	TRUE	-1.454724904	-1.25989776
CPPED1	0.000113126	TRUE	-1.307208579	-1.397153705
MICAL3	0.00011452	TRUE	-1.324226219	-1.243332578
CLIC1	0.000115447	TRUE	-1.225052491	-1.15332439
PLXNA2	0.000116539	TRUE	-1.298680192	-1.372448664
HSP90B1	0.000117002	TRUE	-1.131376806	-1.178549854
RAB3D	0.000118126	TRUE	1.311233188	1.294328322
GBP2	0.000119409	TRUE	1.360413598	1.640683921
TJP2	0.000119862	TRUE	-1.194202233	-1.14433086
EMC1	0.000120037	TRUE	-1.174426978	-1.167427417
ZDHHC16	0.000120428	TRUE	-1.264630158	-1.104047711
PVR	0.000120639	TRUE	-1.468257426	-1.186739576
SIRPA	0.000121239	TRUE	-1.798870851	-1.416787658
TXNIP	0.000124053	TRUE	2.626598723	1.665566548
STXBP1	0.000124291	TRUE	-1.316633091	-1.298607274
TTC13	0.000125826	TRUE	-1.283584096	-1.197292853
RFWD3	0.000125975	TRUE	-1.161337313	-1.237966391
KIRREL	0.000126131	TRUE	-1.770394052	-1.455777418
MAML2	0.000126779	TRUE	1.200555625	1.26831129
CERS6	0.000126906	TRUE	1.253810849	1.273062251
NOMO2	0.000127704	TRUE	-1.197527939	-1.095538934
VGLL3	0.000128607	TRUE	-1.151060371	-1.295448274

RBL2	0.000128657	TRUE	1.148332559	1.18979772
PIM1	0.000130393	TRUE	-1.338092789	-1.287994761
OLR1	0.00013061	TRUE	-6.593014033	-2.079015688
PSMD2	0.000131133	TRUE	-1.241205525	-1.162526183
VPS36	0.00013134	TRUE	1.291499687	1.129650201
TXNDC12	0.000131498	TRUE	-1.085144955	-1.083696684
MPHOSPH6	0.00013259	TRUE	-1.292402445	-1.214202508
NEBL	0.000134046	TRUE	1.286885398	1.643426513
SEH1L	0.000135952	TRUE	-1.125631789	-1.130986249
CYB5B	0.000136916	TRUE	-1.129290092	-1.228622902
ZCCHC2	0.000136977	TRUE	-1.173435814	-1.298030922
ACOT9	0.000137038	TRUE	-1.351231814	-1.2684911
HSF4	0.000137223	TRUE	1.148093441	1.175934745
FKBP14	0.000137232	TRUE	-1.436561452	-1.173360801
STAMBPL1	0.000138956	TRUE	-1.306682129	-1.43335589
ANXA3	0.000139997	TRUE	-1.583029242	-1.349604018
DBNL	0.000140159	TRUE	1.146970395	1.191510937
MYH14	0.000141238	TRUE	1.572475683	1.730454879
RPS27	0.00014398	TRUE	1.055957332	1.086223937
CTSB	0.000145272	TRUE	1.185355928	1.231324654
BMP2K	0.000145427	TRUE	-1.330493071	-1.552107745
TCOF1	0.000145856	TRUE	-1.41542631	-1.266377001
FAM21C	0.000146041	TRUE	1.270631874	1.199604992
LOC401561	0.000148086	TRUE	1.649211391	1.470136681
TK1	0.000149338	TRUE	-1.331678598	-1.321397108
NLRP2	0.000149947	TRUE	-1.232331092	-1.32647322
KIAA0040	0.000150652	TRUE	-1.55138277	-1.461947231
DPP4	0.000152024	TRUE	-1.303076488	-1.183726898
AKAP9	0.000153399	TRUE	1.209742836	1.24546084
GABARAP	0.000154087	TRUE	1.160762625	1.162612807
CYR61	0.000154488	TRUE	-1.917068636	-1.697498787
MGEA5	0.000154813	TRUE	1.260700811	1.229362711
MIR4640	0.000155638	TRUE	1.177069801	1.215226637
MRPL39	0.000156396	TRUE	-1.21625183	-1.126594416
C8orf46	0.000157188	TRUE	-1.248317153	-1.251454368
RRAS	0.00015826	TRUE	-1.28076513	-1.183682416
PTAFR	0.000158438	TRUE	-1.353423693	-1.804724925
MCMBP	0.000158533	TRUE	-1.170769472	-1.159160244
OAT	0.000160086	TRUE	-1.285508001	-1.607076323
JMJD6	0.000162102	TRUE	-1.324361315	-1.151635456
DIAPH1	0.000163211	TRUE	-1.215219668	-1.250376819
DCLRE1B	0.000166884	TRUE	-1.36373508	-1.192861699
CHML	0.000167976	TRUE	-1.597081385	-1.279224973
FAM21B	0.000168372	TRUE	1.146016411	1.155356286

CCNA2	0.000174051	TRUE	-1.174797098	-1.091181929
NKX1-2	0.000177005	TRUE	-1.492677011	-1.335451615
ZC3HAV1	0.000177802	TRUE	-1.192226982	-1.286243346
PRKCDBP	0.000179403	TRUE	-1.664242664	-1.218909765
LASP1	0.000181513	TRUE	-1.252079602	-1.29549853
KARS	0.00018201	TRUE	-1.179188418	-1.088139507
VLDLR	0.00018433	TRUE	-1.582824968	-2.03474913
SORL1	0.000184793	TRUE	1.229216004	1.45642516
HEATR1	0.000185163	TRUE	-1.17483543	-1.098202489
TEAD4	0.000185529	TRUE	-1.205489319	-1.200823774
RALGAPA2	0.000186118	TRUE	1.244111383	1.37276222
ABCC5	0.000186165	TRUE	1.633557517	1.347721622
PRPF4	0.000186629	TRUE	-1.260510032	-1.177526575
ADAM9	0.000187849	TRUE	-1.183954662	-1.092258817
ATP11C	0.000188532	TRUE	-1.343794796	-1.299415373
FAM53A	0.000188586	TRUE	-1.211837916	-1.331239224
SLC30A6	0.000189679	TRUE	-1.222344786	-1.119678722
FOXN3	0.000189923	TRUE	1.281457321	1.303567232
FZD6	0.000190746	TRUE	1.229515086	1.148164809
ITGB6	0.000193008	TRUE	-1.334627181	-1.340142473
ARID3B	0.000194849	TRUE	-1.376856696	-1.823429638
ATP2C1	0.000197257	TRUE	1.272914338	1.193186263
SYF2	0.000198774	TRUE	1.186657176	1.159074472
LAMB1	0.000201107	TRUE	-1.208656242	-1.520539289
SKA3	0.000201989	TRUE	-1.256462495	-1.269966115
FAM84A	0.000207119	TRUE	1.320521161	1.22475819
KLF5	0.000208562	TRUE	1.1617269	1.213677895
RAB32	0.000209603	TRUE	-1.479021293	-1.801964392
TMEM30A	0.000210213	TRUE	1.263619983	1.113659747
SAMD4A	0.000217179	TRUE	-1.377379174	-1.128595584
SPR	0.000217473	TRUE	-1.184735714	-1.246897802
PTBP1	0.000218831	TRUE	-1.173585682	-1.137846803
ERV3-1	0.000219413	TRUE	1.375311101	2.052480665
C6orf165	0.000223184	TRUE	1.381043681	1.170540974
MOCOS	0.000226977	TRUE	-1.423209418	-1.21834116
PALLD	0.000228332	TRUE	-1.414526972	-1.222083655
FAM63B	0.000230183	TRUE	-1.284453124	-1.190846517
SLC7A5	0.000230817	TRUE	-1.248829373	-1.149629545
TMEM179B	0.0002314	TRUE	1.260924525	1.172412358
HAS3	0.000231477	TRUE	-1.578672124	-1.302197181
TCHH	0.00023262	TRUE	1.579845583	1.348696719
RUSC2	0.000233435	TRUE	-1.306457967	-1.437612054
LHFP	0.00023378	TRUE	-1.723069618	-1.220986856
DOCK10	0.000234026	TRUE	-1.296767806	-1.929596045

NAT10	0.000234149	TRUE	-1.168857975	-1.103733029
IMPDH1	0.000234618	TRUE	-1.235753742	-1.368780499
TBC1D3B	0.000237602	TRUE	1.264148035	1.212473727
ATIC	0.00023766	TRUE	-1.20604795	-1.13518368
ACTN1	0.000238037	TRUE	-1.210219655	-1.2533989
UBLCP1	0.000239024	TRUE	-1.253229939	-1.231617332
NUDC	0.000239859	TRUE	-1.276227195	-1.130574209
EHD1	0.000241775	TRUE	-1.236428606	-1.130977491
UGGT1	0.000242424	TRUE	-1.156504447	-1.122268492
LOC100506642	0.000242446	TRUE	1.283913602	1.283086491
GALNT5	0.000246347	TRUE	-1.217249433	-1.163914074
CENPO	0.000247984	TRUE	-1.211149201	-1.186898785
CUL7	0.000248577	TRUE	1.400573398	1.215672681
RAD51	0.000251478	TRUE	-1.43068189	-1.243320085
MIR525	0.000252032	TRUE	-1.266632404	-1.264326579
FOXD1	0.000252063	TRUE	-1.222640877	-1.332116549
ESCO2	0.000253454	TRUE	-1.269443153	-1.216026834
TIPARP	0.000254503	TRUE	-1.449674808	-1.27682851
TCF25	0.000254555	TRUE	1.15803223	1.131243501
WDR27	0.000254571	TRUE	1.250768761	1.283727916
LRBA	0.000255492	TRUE	1.228653437	1.090909674
TMEM205	0.000258499	TRUE	1.252828633	1.359534642
QSOX1	0.000260581	TRUE	-1.805719258	-1.307023989
TIMP4	0.000261133	TRUE	-1.404216098	-1.460939361
PLAU	0.000263114	TRUE	-1.647117974	-1.319414987
KRT4	0.000263173	TRUE	2.00019907	7.953067935
LIMK1	0.000264328	TRUE	-1.428165077	-1.210252291
SNORD59B	0.000265121	TRUE	1.510727321	1.232666676
PPP1R3E	0.000265159	TRUE	1.152240112	1.134403823
CDV3	0.00026529	TRUE	-1.122606238	-1.115015548
PTPN1	0.000265926	TRUE	-1.158598226	-1.144637111
PLEKHG1	0.000269287	TRUE	1.315911808	1.363640669
TARS	0.000273428	TRUE	-1.11458299	-1.098573674
GALNTL4	0.000275503	TRUE	-1.525054857	-1.207628203
BCAT1	0.000276784	TRUE	-1.283464515	-1.871113366
TGFBRAP1	0.000277133	TRUE	-1.237017388	-1.315893799
RRP12	0.000277682	TRUE	-1.438354478	-1.230514184
FAM49B	0.000279676	TRUE	-1.187853366	-1.397427958
METTL7A	0.00027996	TRUE	2.169741035	1.335303208
ZNF84	0.000280049	TRUE	1.344416222	1.364854842
UBE2Q2P3	0.000281714	TRUE	1.315607567	1.185772599
STIL	0.000283325	TRUE	-1.209125943	-1.174571755
OGT	0.000283938	TRUE	1.239065213	1.180666549
PCDH1	0.000286697	TRUE	-1.960020009	-1.355610088

FAM98A	0.000287065	TRUE	-1.442439238	-1.156892608
RNASEH2A	0.000290059	TRUE	-1.207746271	-1.117177962
ORC3	0.000291348	TRUE	-1.194760527	-1.140101193
RPL31	0.000293117	TRUE	1.25640145	1.145365005
FOXO4	0.000293421	TRUE	1.557674534	1.250727071
CTSS	0.000295009	TRUE	1.129789489	1.217655031
PLXDC1	0.000298272	TRUE	1.141517911	1.139270165
FLOT1	0.000300376	TRUE	1.100666417	1.088624747
LOC100506935	0.000302553	TRUE	1.430678231	1.424488892
ABCG2	0.000307053	TRUE	-1.840993127	-6.595932251
PLEKHM3	0.000310256	TRUE	1.283268195	1.227954822
TRIP13	0.000310665	TRUE	-1.353190978	-1.145040559
CDC7	0.000310739	TRUE	-1.10572237	-1.241761546
SRI	0.000312296	TRUE	1.175916012	1.217541175
ASNS	0.000312816	TRUE	-1.149648453	-1.226739845
ALS2CR8	0.00031319	TRUE	1.631122823	1.319786257
JMY	0.000315048	TRUE	1.456572275	1.272182613
ACER3	0.000316994	TRUE	-1.551363012	-1.243252732
DONSON	0.00031732	TRUE	-1.22742729	-1.128293933
PLCE1	0.000318331	TRUE	1.540953497	1.199927888
MRP63	0.000320155	TRUE	-1.174698757	-1.100974838
HSPA4	0.00032145	TRUE	-1.130127173	-1.146876655
RAB7L1	0.0003233	TRUE	-1.329652548	-1.192857565
RPN1	0.000324194	TRUE	-1.117483298	-1.085571681
GLA	0.000324335	TRUE	-1.549920116	-1.221684458
ADAM8	0.000325857	TRUE	-1.24321647	-1.227970694
TXNL1	0.000325906	TRUE	-1.14475063	-1.110377152
DPYD	0.000328209	TRUE	1.975114736	1.29580529
OAZ1	0.000328364	TRUE	-1.121996324	-1.12764447
SERPINH1	0.000329939	TRUE	-1.2716395	-1.964693633
ECH1	0.00033046	TRUE	1.199772041	1.140797118
MRM1	0.000331348	TRUE	-1.368464778	-1.160283049
ZNF250	0.000331756	TRUE	1.165688967	1.094164499
DLX5	0.000332635	TRUE	1.773681707	1.643323949
IKZF2	0.00033363	TRUE	1.409508975	1.446120059
ZNF22	0.000335975	TRUE	-1.326502968	-1.298118361
VPS13C	0.000339616	TRUE	1.335101102	1.187367721
TMEM184C	0.000342295	TRUE	-1.168528379	-1.137299011
C2orf18	0.000345685	TRUE	-1.279155646	-1.222216226
RN5S402	0.00034665	TRUE	-2.094243389	-1.82277049
LOC100130476	0.00034892	TRUE	-1.502695813	-1.503344309
ARHGEF12	0.000349716	TRUE	1.147202384	1.076751774
U2AF2	0.000350018	TRUE	-1.184107597	-1.125368369
DNM1P41	0.000352588	TRUE	1.483164879	1.275378048

DGKE	0.000353441	TRUE	-1.260957911	-1.337517938
GPRC5A	0.00035589	TRUE	-1.311761982	-1.327476756
NUP93	0.000356243	TRUE	-1.271206327	-1.107937094
PRMT5	0.00035667	TRUE	-1.165549375	-1.168698641
KRT18P49	0.000357895	TRUE	-1.292834105	-1.605403809
TES	0.000357904	TRUE	-1.160941069	-1.110593195
PMS2L2	0.000359986	TRUE	1.439119651	1.212335364
PMS2P5	0.000359986	TRUE	1.439119651	1.212335364
GSTA4	0.000361327	TRUE	1.590912499	1.274311438
C6orf211	0.000364231	TRUE	-1.17348653	-1.225366797
AKT1S1	0.000364962	TRUE	-1.1100692	-1.13104742
CDK8	0.000365801	TRUE	-1.228256127	-1.276149129
DBT	0.000367342	TRUE	1.086812505	1.180747621
CASK	0.000370181	TRUE	1.138163985	1.46202143
NLN	0.000370875	TRUE	-1.177901578	-1.146674214
STK10	0.000371016	TRUE	-1.189543578	-1.618581834
PGLYRP4	0.000373443	TRUE	1.435101296	2.226299786
FAM101B	0.000374899	TRUE	-2.277261896	-1.450537858
RNF219	0.000378321	TRUE	-1.147913364	-1.192659235
MYBL2	0.000379107	TRUE	-1.314265138	-1.173781215
USP39	0.000379132	TRUE	-1.080629468	-1.182676322
SLC41A1	0.000380477	TRUE	-1.199676563	-1.452884206
PPT1	0.000380835	TRUE	-1.093386609	-1.097100531
GUSBP9	0.000383478	TRUE	1.521824158	1.326504944
RNF19B	0.000384782	TRUE	-1.371650258	-1.183815139
MYO1B	0.000385759	TRUE	-1.248379215	-1.648823193
MIR3118-4	0.000386184	TRUE	1.498860631	1.256512862
ARNTL2	0.00038825	TRUE	-1.193232673	-1.522893129
EBP	0.000391217	TRUE	-1.263148341	-1.132080357
NDST2	0.000392231	TRUE	1.254525871	1.201595683
RPN2	0.000392231	TRUE	-1.13038129	-1.05901345
ERLIN1	0.000394002	TRUE	-1.148578165	-1.164722288
XPO5	0.000394361	TRUE	-1.210434815	-1.117951235
ISG15	0.000394798	TRUE	-1.182644619	-1.264439744
GIN52	0.000396571	TRUE	-1.376554814	-1.141047609
SH3BP4	0.000397478	TRUE	-1.193214817	-1.579219229
ABLIM1	0.000398989	TRUE	1.298356204	1.238585109
RAD51C	0.000399977	TRUE	-1.252490529	-1.288075293
GLIPR1	0.000400231	TRUE	-1.905034225	-1.248103139
ARFGEF1	0.000400335	TRUE	1.252426728	1.106949583
PERP	0.000410611	TRUE	1.214338733	1.167502082
SLC25A44	0.000410707	TRUE	-1.362905828	-1.25459698
PIR-FIGF	0.000411148	TRUE	1.239320758	1.25333293
SH2B2	0.000412761	TRUE	1.267326869	1.371170765

TMEM222	0.000418161	TRUE	-1.132163406	-1.181137478
MEA1	0.000420433	TRUE	-1.19018474	-1.187661609
QARS	0.000426096	TRUE	1.129330411	1.144844025
RFC2	0.000426119	TRUE	-1.21783339	-1.10985627
HAUS2	0.000426211	TRUE	-1.318649401	-1.170033909
LOC647979	0.000427466	TRUE	1.240307358	1.247846774
TIPIN	0.00042835	TRUE	-1.219811799	-1.302642991
HPRT1	0.000428437	TRUE	-1.17903191	-1.196121536
UTP15	0.000430994	TRUE	-1.37843241	-1.245847317
MUC16	0.000431455	TRUE	2.026128216	1.468663634
LOC100506290	0.000432292	TRUE	1.670214782	1.554751672
PSMD1	0.000434354	TRUE	-1.394527668	-1.126170689
TRIM2	0.000436444	TRUE	1.375156749	1.394340441
SBF1P1	0.000437353	TRUE	-1.214372994	-1.159817018
ALOX12	0.000442432	TRUE	-1.162794445	-1.240116603
HK2	0.000450298	TRUE	-1.550770824	-1.241913665
MPP5	0.000451158	TRUE	-1.116850495	-1.162400946
RPAP3	0.000451444	TRUE	-1.146979965	-1.216548346
ZDHHC7	0.000453953	TRUE	-1.106400032	-1.092583846
ABCD3	0.000454202	TRUE	-1.219134	-1.174268814
PDLIM1	0.000454591	TRUE	-1.095258272	-1.337934288
MFAP5	0.000455964	TRUE	-1.478819118	-3.139033811
STS	0.000460998	TRUE	-1.340771707	-1.265197302
RARRES1	0.000461643	TRUE	1.226912609	1.465701522
NOL10	0.000461765	TRUE	-1.251842777	-1.101358409
CDK4	0.000463178	TRUE	-1.194554413	-1.087780014
NT5E	0.000464717	TRUE	-1.480174664	-2.337974947
TGFA	0.000468305	TRUE	-1.418222296	-1.313560883
TMC7	0.00047177	TRUE	-1.284458373	-1.907917739
NCS1	0.000478377	TRUE	-1.533531795	-1.251854445
COL17A1	0.000479488	TRUE	-1.430252434	-3.369209972
SAT1	0.000480785	TRUE	1.398732593	1.21063313
RANBP3	0.000482191	TRUE	-1.198483587	-1.23327753
MICA	0.000483363	TRUE	-1.198544144	-1.651612814
LENG8	0.000483747	TRUE	1.368191747	1.263895588
MIR3676	0.000487013	TRUE	-1.843221848	-1.323379118
GOLGA8G	0.000490984	TRUE	1.202486305	1.178326662
FAM129A	0.000492087	TRUE	-1.303456156	-2.062373963
STARD13	0.000492427	TRUE	-1.221427498	-1.265248543
GOT2	0.000493577	TRUE	-1.187586043	-1.094510737
SNAI2	0.000495325	TRUE	-1.232970827	-1.452932665
RHOF	0.000504387	TRUE	-1.132011235	-1.406164656
LMBRD1	0.000505787	TRUE	1.272861006	1.143712271
ZNF117	0.000509494	TRUE	1.626818393	2.632758366

MIR604	0.00051253	TRUE	1.373334152	1.548266438
ATP6V1B1	0.000513896	TRUE	1.345765004	1.678777376
DSG3	0.000515293	TRUE	1.152599008	1.563168816
DUSP11	0.00051542	TRUE	-1.142985362	-1.161218734
COTL1	0.000518556	TRUE	-2.038697352	-1.250166583
GLT8D2	0.000519097	TRUE	-1.637172733	-1.333282501
PXDC1	0.000521503	TRUE	-1.544102236	-1.215308425
R3HDM2	0.000522297	TRUE	1.448574992	1.20282285
RNF115	0.000523985	TRUE	-1.130255846	-1.201886197
COL16A1	0.000526458	TRUE	-1.13954184	-1.149237932
C11orf92	0.000526987	TRUE	1.766385454	1.255404344
LOC100507246	0.000527199	TRUE	1.081239626	1.114368834
TPBG	0.000529801	TRUE	-1.134853603	-1.128199138
GJB3	0.000531072	TRUE	-1.645448784	-1.300553429
WDR54	0.000531552	TRUE	-1.155332006	-1.173694769
PDLIM7	0.000538951	TRUE	-1.324166234	-1.327565362
PSMB4	0.000541015	TRUE	-1.20102979	-1.199348861
AKR1C3	0.00054151	TRUE	1.52382786	1.760795703
C3	0.00054209	TRUE	1.403875859	1.171946658
CAV2	0.000544092	TRUE	-1.196683459	-1.168171517
RAPGEF1	0.000544619	TRUE	-1.203831512	-1.383980847
ECI2	0.000546006	TRUE	-1.243921845	-1.197036583
APEX2	0.000546729	TRUE	-1.402186037	-1.203790916
DDX27	0.000547319	TRUE	-1.157790264	-1.133284579
HAUS8	0.00054765	TRUE	-1.32905615	-1.277787951
POP1	0.000553031	TRUE	-1.312847662	-1.132281077
MRPL3	0.000556298	TRUE	-1.204463552	-1.157523394
GUSBP3	0.000559537	TRUE	1.499782294	1.459929138
POC5	0.000564986	TRUE	-1.358779735	-1.205240311
GTF2I	0.000567686	TRUE	1.191963145	1.276633066
MLL3	0.000570346	TRUE	1.276481595	1.224283141
ADHFE1	0.000570583	TRUE	1.18943858	1.30070258
CX3CL1	0.000573927	TRUE	1.392881848	2.146916292
SRPK2	0.000574199	TRUE	-1.104144483	-1.152969708
GRAMD2	0.000574281	TRUE	-1.298022503	-1.487095197
ELF4	0.00058007	TRUE	-1.417224458	-1.332432954
CPA4	0.000582963	TRUE	-1.452735428	-1.555289209
SLFN11	0.000584503	TRUE	-1.208243553	-1.675638131
USP9X	0.000585833	TRUE	1.290694487	1.172403498
TMOD3	0.000589855	TRUE	-1.133693413	-1.210097482
FHL3	0.000590076	TRUE	-1.497665466	-1.291103098
PFN1	0.000596219	TRUE	-1.188416809	-1.178498982
SEMA3C	0.00059906	TRUE	-1.217572308	-1.841082541
OXSRI	0.000599963	TRUE	-1.081237746	-1.1748069

KIAA1524	0.000600491	TRUE	-1.161790468	-1.211277624
PMS1	0.000601916	TRUE	-1.196767418	-1.161239175
MATN2	0.000607162	TRUE	-1.131501159	-1.314854132
MFSD6	0.000612958	TRUE	1.154980046	1.123077081
CENPI	0.000614203	TRUE	-1.19362436	-1.341475072
EPPK1	0.000614982	TRUE	1.357365752	1.550650431
TACO1	0.000619082	TRUE	-1.235714167	-1.126352335
EFEMP1	0.000625158	TRUE	-1.068481485	-1.242841909
RBM28	0.000627341	TRUE	-1.245365292	-1.176991541
NUP205	0.000630118	TRUE	-1.159102832	-1.085691289
ADRM1	0.000631168	TRUE	-1.254267956	-1.212769425
VAV2	0.000635237	TRUE	-1.247269079	-2.150572863
NEIL3	0.000638708	TRUE	-1.190166654	-1.132852287
KIF3C	0.000641728	TRUE	-1.270073417	-1.501714934
GPR126	0.00064457	TRUE	1.172385976	1.538376925
SMCR8	0.000646064	TRUE	-1.194083482	-1.155493075
DDAH1	0.00064659	TRUE	-1.612827728	-1.290432962
IFNAR2	0.000646843	TRUE	-1.176321531	-1.176280562
TTL	0.000647001	TRUE	-1.390035739	-1.292778826
FAM96B	0.000647143	TRUE	-1.315690673	-1.164691432
HIST1H1B	0.000649139	TRUE	-1.238476216	-1.101216363
TMPRSS11E	0.000652038	TRUE	-1.575440077	-1.150112353
PSMC4	0.000654542	TRUE	-1.245044655	-1.13838766
GSN	0.000662043	TRUE	1.43268062	1.300659931
TRIM6-TRIM34	0.000667451	TRUE	-1.302742315	-1.295112938
TMEM168	0.00066816	TRUE	1.203686861	1.115470967
SGCB	0.00066888	TRUE	-1.299292514	-1.236033406
GNPTAB	0.000670713	TRUE	-1.262080244	-1.118202952
CRIPAK	0.000674297	TRUE	1.147877381	1.419845249
PTP4A1	0.000674702	TRUE	-1.172085151	-1.271938886
TSPAN6	0.000675882	TRUE	1.267655651	1.113359649
PRIM1	0.000676564	TRUE	-1.169707264	-1.185184813
PZP	0.00067711	TRUE	1.135515437	1.144630519
DEPDC1B	0.000677189	TRUE	-1.220824114	-1.205779355
PON2	0.000677898	TRUE	1.140415914	1.460477642
SERPINB8	0.000683735	TRUE	-1.572617062	-1.169322031
SIDT1	0.00068595	TRUE	1.249483044	1.326082932
FOXMI	0.000687367	TRUE	-1.143699705	-1.186810517
EMP3	0.000688038	TRUE	-2.13164752	-1.533763012
ACTN4	0.000690755	TRUE	-1.108242299	-1.083746207
RAMP1	0.000696378	TRUE	-1.232846735	-1.636862421
PARS2	0.000699299	TRUE	-1.187451354	-1.281943012
RPP30	0.000699974	TRUE	-1.198628194	-1.13928284
HDAC5	0.000703172	TRUE	1.265584926	1.686525798

SYMPK	0.000705142	TRUE	-1.194820892	-1.105386936
IPMK	0.000706133	TRUE	1.139967642	1.372578269
IL27RA	0.000707473	TRUE	-1.762852686	-1.364678351
CYP2E1	0.000710732	TRUE	-1.184018094	-1.254291737
PCMI	0.000710742	TRUE	1.129808309	1.071666752
IGFBP7	0.00071841	TRUE	-1.201820747	-1.889165242
RAD18	0.000718892	TRUE	-1.202941018	-1.264784061
OGFOD1	0.0007229	TRUE	-1.399891803	-1.167897024
ING4	0.00072356	TRUE	1.373876609	1.256140318
BRCA2	0.00072591	TRUE	-1.206593226	-1.288603607
SDR42E1	0.000727985	TRUE	-1.266016649	-1.276865668
BNC1	0.000730132	TRUE	-1.391265953	-1.804120297
MRPS12	0.000734108	TRUE	-1.282189999	-1.164266633
TNFRSF4	0.000742016	TRUE	1.272879369	1.147809916
UTP11L	0.000745753	TRUE	-1.244012792	-1.158951889
SBF2	0.000748578	TRUE	1.239079636	1.125902342
DDX21	0.000754224	TRUE	-1.187994768	-1.099063769
LY6G6C	0.000757731	TRUE	-1.14179877	-1.50388925
CKS2	0.000758207	TRUE	-1.206545999	-1.167190834
SDAD1	0.000760505	TRUE	-1.181120772	-1.120854822
AGR2	0.000760828	TRUE	1.570548479	1.184839389
SMYD2	0.000760963	TRUE	-1.233490616	-1.322790227
KCTD12	0.00076218	TRUE	-1.305265428	-1.543834715
ZNF12	0.000775308	TRUE	1.164404702	1.121825476
MFAP2	0.000779268	TRUE	1.308821679	1.377890923
NUAK2	0.000780394	TRUE	-1.279698412	-2.015706524
NUP107	0.000782383	TRUE	-1.230140632	-1.14539431
CMTM4	0.000784435	TRUE	1.190056553	1.124137908
ABCG1	0.00078468	TRUE	1.319185818	1.319885066
GPR39	0.000790115	TRUE	-1.299924627	-1.776531126
RALGPS1	0.000790922	TRUE	1.431086128	1.213487846
INF2	0.00080018	TRUE	-1.205505186	-1.294277323
XPO6	0.000803822	TRUE	-1.27585122	-1.204310554
DDX47	0.000808368	TRUE	-1.100556232	-1.16212792
CDK19	0.000809867	TRUE	1.337778649	1.103699299
PTGS2	0.000810904	TRUE	1.313527574	1.664072431
SLC5A6	0.000823949	TRUE	-1.350732224	-1.198367857
CENPP	0.000825169	TRUE	-1.16026611	-1.113769723
WDR75	0.000829648	TRUE	-1.138632674	-1.211119358
COL4A2	0.000830712	TRUE	-1.335384404	-1.134269488
DTL	0.000831615	TRUE	-1.175425313	-1.241206589
OSBPL11	0.000834721	TRUE	-1.091437979	-1.194842683
MRPL11	0.000836706	TRUE	-1.15753979	-1.17193492
IL4R	0.000844586	TRUE	-1.265541503	-1.358132448

ILF3	0.000844973	TRUE	-1.121739257	-1.09659805
TUBG1	0.000850654	TRUE	-1.233498731	-1.176974014
ABCC2	0.000851326	TRUE	-1.190850677	-1.48445276
HAT1	0.000853277	TRUE	-1.116941957	-1.14741
CKAP2L	0.000859114	TRUE	-1.386751006	-1.110742856
C10orf57	0.000874993	TRUE	1.183573898	1.321097418
BDNF-AS	0.000879984	TRUE	1.243420102	1.121108378
ARG2	0.000880077	TRUE	-1.222868307	-1.258138711
TTC27	0.000880758	TRUE	-1.145647674	-1.231327079
KLHL5	0.000881204	TRUE	1.106142661	1.38037741
IL13RA1	0.000881814	TRUE	-1.103225969	-1.152708679
NSFL1C	0.000882103	TRUE	-1.23124561	-1.126874773
RQCD1	0.000884378	TRUE	-1.153499595	-1.142083281
RRM2	0.000888959	TRUE	-1.200327209	-1.066997389
EEF2	0.000891413	TRUE	1.056604702	1.061013909
DUSP14	0.000895603	TRUE	-1.210354566	-1.287170303
ASAP2	0.000896129	TRUE	-1.132627535	-1.397973834
CD24	0.000904049	TRUE	-1.218456986	-1.171777607
GMPS	0.000904791	TRUE	-1.120059474	-1.171919008
SCARNA17	0.00090611	TRUE	1.469796093	1.67313633
CXorf26	0.000910121	TRUE	-1.364148411	-1.24963176
EMC8	0.000910899	TRUE	-1.275316153	-1.126519202
PPP1R18	0.00091436	TRUE	-1.211788233	-1.151363923
NTN4	0.000914917	TRUE	1.473587882	1.122463003
RN5S141	0.000915637	TRUE	-1.621217205	-2.128259883
FLJ38717	0.00091743	TRUE	1.575567637	1.298999224
VPS13B	0.000921359	TRUE	1.24827577	1.144901959
ARGLU1	0.000923889	TRUE	1.23818442	1.176963458
CDH1	0.00092567	TRUE	-1.091796841	-1.178500458
PHTF1	0.000929853	TRUE	-1.293587747	-1.191933219
PTGS1	0.000932815	TRUE	-2.352679179	-1.292299307
C1orf116	0.000932931	TRUE	-1.445451554	-1.167236979
PARP4	0.000933158	TRUE	1.091828536	1.153117476
CYLD	0.000935093	TRUE	1.130257723	1.384883899
AAED1	0.00093778	TRUE	-1.48094638	-1.255276215
PLEKHA7	0.000938517	TRUE	1.096132261	1.255650101
ZCCHC10	0.000938548	TRUE	-1.205033556	-1.244907763
ZNF608	0.000939121	TRUE	1.234019542	1.770837086
SFN	0.000939983	TRUE	-1.609135183	-1.163326399
GUSBP2	0.000941458	TRUE	1.398116632	1.681486061
POLA1	0.000947849	TRUE	-1.13507446	-1.228171987
CACYBP	0.000948221	TRUE	-1.18556201	-1.157731116
EPHA1	0.000950274	TRUE	-1.19533359	-1.166914062
ACAD10	0.000950563	TRUE	1.386545331	1.225719954

ICMT	0.000952607	TRUE	-1.162943999	-1.077875997
ABLM3	0.00095293	TRUE	-1.234230909	-1.956271505
RMND5A	0.000957436	TRUE	1.110575416	1.244916254
FLJ42969	0.000959406	TRUE	-1.260569561	-1.137984484
SYNE2	0.000959855	TRUE	1.78113032	1.210340979
SYK	0.000964668	TRUE	-1.177421271	-1.471814497
RRM1	0.000972796	TRUE	-1.076512083	-1.112546198
POMGNT1	0.000973227	TRUE	-1.140911679	-1.42278981
SLC25A30	0.000974159	TRUE	-1.447048358	-1.250804223
SEMA3A	0.000975056	TRUE	-1.882510187	-1.199523659
POLR2J4	0.000980301	TRUE	1.479629678	1.358347929
SNORD89	0.00098063	TRUE	1.318861215	1.140530145
PHF10	0.000981202	TRUE	1.167819638	1.37985371
EMP1	0.00098153	TRUE	-1.171674389	-1.113216819
GPNMB	0.000981954	TRUE	1.48014167	1.309320424
CTNNAL1	0.0009852	TRUE	-2.1214858	-24.8561035
MTHFD1	0.000987164	TRUE	-1.076583605	-1.138626508
NYNRIN	0.000994242	TRUE	1.536353114	1.236500873
LOC100506394	0.000994914	TRUE	-1.329984927	-1.288546039
UBE2I	0.000994964	TRUE	-1.130555975	-1.097049356
ZNF142	0.000996292	TRUE	-1.113324395	-1.15118056
TNFAIP1	0.00100187	TRUE	-1.248208544	-1.201887735
PLEKHJ1	0.001002547	TRUE	-1.283739269	-1.092581987
OGFRL1	0.001008465	TRUE	1.199222376	1.105500785
MEIS1	0.001020179	TRUE	1.368418649	1.179074824
APBB2	0.001027845	TRUE	-1.293902126	-1.578561538
ALDH3B2	0.001033554	TRUE	1.704218782	1.271750792
CALCOCO1	0.001034386	TRUE	1.260380629	1.437899244
SERINC5	0.001035734	TRUE	1.178625735	1.468007583
XRN1	0.001038287	TRUE	1.116664415	1.08812908
MCOLN2	0.001040274	TRUE	-1.173969397	-1.146565398
ZNHIT6	0.001040426	TRUE	-1.198937576	-1.285648331
KIF20B	0.001042811	TRUE	-1.133560114	-1.109959442
10-Sep	0.001047817	TRUE	1.196196205	1.11100309
PDPN	0.001053677	TRUE	-1.265802281	-1.494904294
DEGS1	0.001065155	TRUE	-1.286993708	-1.205410308
NOTCH3	0.001065657	TRUE	1.370106227	1.710864492
KRT80	0.001067682	TRUE	-2.492491213	-1.287124069
COBL	0.001070467	TRUE	-1.264742265	-1.156731987
PSME3	0.001071623	TRUE	-1.152352813	-1.180757177
C12orf52	0.0010766	TRUE	-1.216881728	-1.207517135
NBPF9	0.001079741	TRUE	1.403796627	1.202039762
MIR554	0.001080725	TRUE	1.362702231	1.597081576
CLMP	0.001080808	TRUE	-2.253807061	-1.321050289

GRB2	0.001103725	TRUE	-1.146271929	-1.167525031
LONP2	0.001107504	TRUE	1.450078588	1.41392497
LRP12	0.001111252	TRUE	-1.477680992	-1.228810374
UBE2Q2	0.001114725	TRUE	-1.180200009	-1.185070249
NUP153	0.001114848	TRUE	-1.277902877	-1.18501199
HCCS	0.001115016	TRUE	-1.205638121	-1.172626097
RRP36	0.001118257	TRUE	-1.224368754	-1.101229487
TCP11L2	0.001120543	TRUE	1.276431961	2.70759893
RMI1	0.001121308	TRUE	-1.138795518	-1.245052125
PRNP	0.001123621	TRUE	-1.169093629	-1.247101301
ESRP1	0.001128	TRUE	1.087027442	1.10706682
EIF3L	0.001129478	TRUE	1.167946855	1.068528314
NUDCD1	0.00113594	TRUE	-1.337414797	-1.194440988
HNRNPF	0.001137028	TRUE	-1.109532511	-1.127922669
CCDC41	0.001145757	TRUE	-1.19969162	-1.160625013
LYAR	0.001148631	TRUE	-1.655435064	-1.222563388
ANXA7	0.001151527	TRUE	-1.101708845	-1.101959531
ISG20L2	0.00115211	TRUE	-1.371536389	-1.123069287
HIF1A	0.001153776	TRUE	1.155249778	1.086477386
FSCN1	0.001162646	TRUE	-1.453754223	-1.191782033
TBC1D3H	0.001163475	TRUE	1.14149564	1.316820649
DUOX1	0.001166187	TRUE	1.230226047	1.271301736
CXorf1	0.001166442	TRUE	-1.222916324	-1.222808101
DCTPP1	0.001169036	TRUE	-1.314334006	-1.122237651
TMEM123	0.001169914	TRUE	1.198501196	1.218780078
RNF41	0.00117257	TRUE	-1.189564188	-1.12559562
TOR1A	0.001178727	TRUE	-1.173399842	-1.125277622
ITPRIPL2	0.001181298	TRUE	1.160803361	1.196214415
EDEM2	0.001184432	TRUE	1.305955459	1.27038979
MYO5A	0.001185833	TRUE	-1.1382975	-1.390018502
XGPY2	0.001186003	TRUE	-1.253044767	-1.444222901
SLC39A11	0.001187415	TRUE	1.326893172	1.178954266
GSTA1	0.001190598	TRUE	2.046465982	1.328055528
MIR21	0.001191982	TRUE	1.402867727	1.71199778
CCT4	0.001201646	TRUE	-1.223712629	-1.078968048
AUP1	0.001204002	TRUE	-1.159905891	-1.05730467
TIMP3	0.001204042	TRUE	-1.535393281	-1.407362715
SPDYE1	0.001205404	TRUE	1.37727744	1.151626391
CD276	0.001209768	TRUE	-1.133457612	-1.389832655
PXMP4	0.001211502	TRUE	1.184284753	1.502300451
ZW10	0.001213644	TRUE	-1.330751406	-1.118262471
GTF2F1	0.001215589	TRUE	-1.128889767	-1.085278368
F2RL1	0.001218105	TRUE	1.14258099	1.232083625
PCGF3	0.001222003	TRUE	-1.07418608	-1.144362927

PLCD3	0.00122295	TRUE	-1.223228996	-1.542141136
SPATS2	0.00122521	TRUE	-1.269512824	-1.210292566
IL36RN	0.001227352	TRUE	-1.519358394	-1.32328596
FAM65A	0.001227516	TRUE	-1.180200472	-1.48176942
RAPGEF5	0.001229062	TRUE	1.593934756	1.187385291
LOC100130171	0.001245601	TRUE	-1.579934549	-1.276187074
GAD1	0.001246999	TRUE	1.226049648	1.219059775
NFKBIZ	0.001254104	TRUE	1.340959627	1.124132784
PSMB2	0.001257414	TRUE	-1.235256785	-1.069332385
IKBKAP	0.001262905	TRUE	-1.111470244	-1.148359671
RNU12	0.001269223	TRUE	-1.255494977	-1.375663431
VANGL1	0.001269286	TRUE	-1.204117527	-1.073931496
ITGA1	0.001269749	TRUE	-1.251228127	-1.333835705
PDSS1	0.001270522	TRUE	-1.261479372	-1.303877898
ST6GALNAC1	0.00127404	TRUE	1.293984271	2.574589481
CDH13	0.001276195	TRUE	-1.614135001	-1.446680393
NOC4L	0.001277621	TRUE	-1.306206527	-1.1995611
NSDHL	0.001281565	TRUE	-1.187281305	-1.234055201
SH3D19	0.001286112	TRUE	-1.117426667	-1.295806422
BCL11A	0.00129014	TRUE	1.477987883	1.174073775
CCL22	0.001290235	TRUE	1.133301254	1.339513612
CWC22	0.001296268	TRUE	-1.169882832	-1.108304725
NUP188	0.001302387	TRUE	-1.174814169	-1.097677622
CNTNAP3B	0.001303376	TRUE	1.314725495	1.327010122
CDK2	0.001308565	TRUE	-1.178840228	-1.093650308
FJX1	0.001309318	TRUE	-1.699628722	-1.240860842
TP53	0.001329223	TRUE	1.161568959	1.38633366
ERBB3	0.001333768	TRUE	1.203510441	1.109930721
PTPLA	0.00133508	TRUE	-1.183297545	-1.506405162
CHAF1B	0.001335356	TRUE	-1.434941192	-1.151303398
DHRS3	0.001337919	TRUE	1.190412238	1.98806535
SLC46A3	0.0013397	TRUE	1.319384912	1.710798254
NAA15	0.001340886	TRUE	-1.228657283	-1.094936649
SSBP2	0.001345234	TRUE	1.789325193	1.186165227
PHF19	0.001347785	TRUE	-1.254595002	-1.185347131
AVPI1	0.00134918	TRUE	-1.266114165	-1.064712166
TM7SF2	0.001350825	TRUE	1.365953495	1.141461865
ABCF2	0.001351503	TRUE	-1.206556532	-1.08445368
RERE	0.001354473	TRUE	1.156347965	1.130032467
BUB1B	0.001355748	TRUE	-1.093631037	-1.089008767
GRB14	0.001359199	TRUE	-1.232016477	-1.317410636
FADS2	0.00135952	TRUE	-1.197218216	-1.286840355
ABCB7	0.001361836	TRUE	1.137172633	1.171729623
ITGB8	0.001381044	TRUE	1.218925139	1.114313148

CEL	0.001388198	TRUE	1.340804126	1.372356893
GJB2	0.001392775	TRUE	-1.550273551	-1.186006894
TNFRSF12A	0.001396515	TRUE	-2.341633739	-1.233750779
HSPA8	0.001404473	TRUE	-1.166754211	-1.11439866
DBF4B	0.001404895	TRUE	-1.232766185	-1.101196728
FPGS	0.001405808	TRUE	-1.208388841	-1.142723125
TAF3	0.001407922	TRUE	-1.202313036	-1.135742577
DPP3	0.00141076	TRUE	-1.092294726	-1.216525353
SENP5	0.001414698	TRUE	-1.096285358	-1.1546162
TGFBR2	0.001417222	TRUE	-1.183852733	-1.123351494
ZNF1	0.001418503	TRUE	-1.112638278	-1.150952746
TIMM50	0.001421477	TRUE	-1.31894106	-1.091943231
C19orf33	0.00143348	TRUE	-1.342742384	-1.143809224
IFNGR1	0.001436703	TRUE	1.226814535	1.498257433
TMPRSS11A	0.001444316	TRUE	1.466246047	1.273259802
CCDC86	0.001446269	TRUE	-1.311432264	-1.122974073
RPF1	0.001450566	TRUE	-1.133087226	-1.161898333
MB21D1	0.001451706	TRUE	-1.339010707	-1.241961728
MBOAT7	0.001452158	TRUE	-1.269807925	-1.277562324
NAB1	0.001460516	TRUE	1.185582643	1.28151164
FAM46B	0.001472671	TRUE	-1.414795759	-1.649355142
AMD1	0.001476467	TRUE	-1.251899882	-1.214332406
TUFT1	0.001477703	TRUE	1.140963355	1.137466277
KIAA1109	0.001481974	TRUE	1.245692252	1.092931675
GLTPD1	0.001486466	TRUE	-1.177801124	-1.21321892
GABPB1	0.001487898	TRUE	-1.216401676	-1.140353284
DUOXA1	0.001489659	TRUE	1.151324789	1.156810917
LYRM1	0.001497446	TRUE	-1.269402804	-1.418898328
FTSJ3	0.001498784	TRUE	-1.20521071	-1.169594844
IL20RB	0.001503662	TRUE	-1.184112697	-1.762295872
RAPGEFL1	0.001508814	TRUE	1.237370564	1.586575314
MSN	0.001522687	TRUE	-1.23313557	-1.419859376
TUBA1B	0.001527054	TRUE	-1.505878133	-1.309378629
ILK	0.001527135	TRUE	-1.336420855	-1.091769677
MFSD4	0.001534739	TRUE	1.643016039	1.231230696
SSX2IP	0.001534995	TRUE	-1.207673933	-1.346228866
E2F8	0.00154308	TRUE	-1.262078211	-1.161808004
PHLDA1	0.001544646	TRUE	-1.2224323	-1.138535969
RAB38	0.001547491	TRUE	-1.280250989	-1.140434634
FTSJ1	0.001548145	TRUE	-1.317200679	-1.097254255
CHMP1B	0.001551715	TRUE	1.111469325	1.240296725
SCARNA9	0.001560804	TRUE	2.159395854	1.530425976
ATG16L1	0.001561655	TRUE	-1.103690792	-1.23444781
AIM2	0.001562325	TRUE	-1.176411052	-1.633801341

UBL4B	0.001564197	TRUE	1.100648817	1.159740464
DHX37	0.001564566	TRUE	-1.34013498	-1.179388567
FLJ14186	0.001564729	TRUE	1.80047719	1.317123866
C1RL	0.001566619	TRUE	1.381145527	1.147127438
GPX2	0.001572546	TRUE	1.287491544	1.146209418
TM4SF1	0.001579043	TRUE	1.327555262	1.469193589
ZC3H6	0.001586275	TRUE	1.323810527	1.369627583
NKX3-1	0.001594272	TRUE	-1.421848291	-1.099355435
TRAM2	0.001595858	TRUE	-1.235538085	-2.701319124
ZBTB2	0.001600866	TRUE	-1.274403875	-1.280707866
POMP	0.001601396	TRUE	-1.292431582	-1.115094405
GSPT1	0.001606404	TRUE	-1.223006456	-1.077711489
HIST1H2BC	0.001608078	TRUE	-1.255272041	-1.287529045
ECD	0.001608965	TRUE	-1.172017589	-1.127102234
PHF15	0.001610779	TRUE	-1.288074551	-1.195964193
PCNT	0.001611838	TRUE	1.115459949	1.1496592
NUFIP1	0.001619404	TRUE	-1.220619176	-1.265636262
PSMA2	0.00162153	TRUE	-1.28741315	-1.116562835
SNRPD2	0.001623559	TRUE	-1.189800056	-1.07051603
MTUS1	0.001634375	TRUE	1.249070825	1.219192877
ECHDC2	0.001635451	TRUE	1.179462392	1.359621033
CHD3	0.001638785	TRUE	1.458033792	1.102622393
PPP3CA	0.001639156	TRUE	-1.10324315	-1.101903138
SEPW1	0.001640865	TRUE	-1.519620583	-1.1050454
SMG1P1	0.001642851	TRUE	1.378948163	1.284892531
CAMLG	0.001643155	TRUE	1.162277848	1.186139956
ABCE1	0.001645522	TRUE	-1.276707136	-1.170774229
TRIM24	0.0016482	TRUE	1.184551446	1.287662421
MXRA5	0.001651249	TRUE	-2.155046346	-1.212587055
LYRM4	0.0016521	TRUE	-1.191505186	-1.255715303
THRA	0.001656766	TRUE	1.179557849	1.38595627
TMEM141	0.001659966	TRUE	1.226407223	1.129469963
PSMB9	0.001660134	TRUE	-1.104367265	-1.362472407
CASP2	0.001663229	TRUE	-1.199424619	-1.189035551
GTF3C1	0.001664223	TRUE	-1.166259268	-1.074307839
NRG1	0.001664435	TRUE	-1.746382495	-1.203422955
ACAA2	0.001679736	TRUE	1.122078567	1.511711127
HEXB	0.001680107	TRUE	-1.127682645	-1.229744367
CBFA2T2	0.00168061	TRUE	1.475096054	1.115874886
HIST1H3J	0.001682296	TRUE	-1.333463136	-1.177663691
SF3B4	0.001685292	TRUE	-1.207630189	-1.329891045
MRT04	0.00169116	TRUE	-1.363927364	-1.185285641
TRIM32	0.001691549	TRUE	-1.196023348	-1.257436376
TMED4	0.001694386	TRUE	1.102334908	1.158585429

GOLGA6L9	0.001694958	TRUE	1.475971347	1.179278772
CSTF2	0.001696428	TRUE	-1.451104436	-1.162140154
MCM2	0.001697398	TRUE	-1.171806758	-1.187694795
RFC1	0.001699054	TRUE	-1.143029942	-1.105130838
TANC2	0.001703977	TRUE	-1.307225034	-1.197072427
TBC1D3F	0.001704152	TRUE	1.17226144	1.243354088
SS18	0.001705882	TRUE	-1.072729504	-1.076871499
BACE1-AS	0.001711884	TRUE	1.381616901	1.245603539
LOC100506178	0.001714927	TRUE	-1.165856211	-1.367922067
KLF11	0.001726258	TRUE	-1.454282236	-1.17097328
DDR1	0.001727243	TRUE	1.10983549	1.244166998
SEZ6L2	0.00173243	TRUE	1.137640807	1.131144143
CAMK1D	0.001733158	TRUE	1.490012241	1.198314832
VPS13A	0.001737815	TRUE	1.280915662	1.199477
LPIN2	0.001740617	TRUE	-1.194713542	-1.592150915
RICTOR	0.001742831	TRUE	1.126294017	1.084626589
ASUN	0.001743114	TRUE	-1.210143274	-1.095927995
POLR2J2	0.001744418	TRUE	1.168729181	1.51187421
DDX18	0.00174642	TRUE	-1.180665036	-1.083950627
NAIP	0.001754661	TRUE	1.519860443	1.263967574
MAK16	0.001780911	TRUE	-1.332179163	-1.145527748
RBM22	0.001782112	TRUE	-1.114030193	-1.177584253
BCAR1	0.001785618	TRUE	-1.252161402	-1.494904572
ARSI	0.001787443	TRUE	-1.971970524	-1.26329965
YDJC	0.001791405	TRUE	-1.233558229	-1.126383896
HERC6	0.001794875	TRUE	-1.214584305	-1.293875966
RPF2	0.001803664	TRUE	-1.229345839	-1.105119582
FAM19A3	0.001806276	TRUE	-1.507746138	-1.230062895
ECM2	0.001808656	TRUE	-1.317618682	-1.207004547
CENPL	0.001816082	TRUE	-1.283186906	-1.281818182
NGF	0.001819218	TRUE	-1.857263836	-1.189445563
FAM168A	0.001832311	TRUE	1.409268783	1.142975315
PIGW	0.00183746	TRUE	-1.23160181	-1.285592524
ENTPD6	0.001838015	TRUE	-1.095562629	-1.139383141
DEFB109P1	0.001842684	TRUE	-1.166430883	-1.101038234
CD59	0.001855089	TRUE	1.206591282	1.160892118
SELT	0.001860183	TRUE	-1.183195816	-1.073168366
SRD5A3	0.001861031	TRUE	1.087791906	1.349127008
CDY2A	0.001863158	TRUE	-1.509110178	-1.386819522
HLA-DRA	0.001875278	TRUE	3.392956715	1.502073608
RAB31	0.00187611	TRUE	-1.123412358	-1.117950864
MGAT2	0.001877608	TRUE	-1.163717111	-1.138087572
NR2C2AP	0.001878535	TRUE	-1.273546491	-1.288206742
REL	0.001879293	TRUE	1.122486639	1.247730276

FTH1	0.001887898	TRUE	1.515797787	1.183563924
AMIGO2	0.0018889	TRUE	-1.370059748	-2.654541156
PDGFB	0.001895263	TRUE	-1.30514377	-1.145577838
PCYT1B	0.001895392	TRUE	-1.687008186	-1.319150183
KIF13B	0.001904202	TRUE	1.154246125	1.275083274
IL6ST	0.001909535	TRUE	-1.097519898	-1.49688535
PHLDB2	0.001912044	TRUE	-1.52103877	-1.187214728
TTI2	0.001915738	TRUE	-1.192488871	-1.150062302
LOC100505769	0.001920731	TRUE	1.216849037	1.793648665
LOC554223	0.001928648	TRUE	-1.244880047	-1.104705254
ACSL4	0.001932316	TRUE	-1.196418266	-1.566722851
DENND4A	0.001937241	TRUE	1.22788202	1.074825569
MED12	0.001940255	TRUE	1.175610128	1.189952731
LOC440434	0.001944679	TRUE	1.417685291	1.538107228
CHTF8	0.001944822	TRUE	-1.159554928	-1.10619544
ITPR2	0.001947595	TRUE	-1.267331222	-1.201172766
NXT1	0.001948121	TRUE	-1.3153281	-1.268249653
EIF4E3	0.001950195	TRUE	1.24483531	1.354018173
SLC44A1	0.001953701	TRUE	1.091772711	1.40607191
LANCL1	0.00196403	TRUE	1.126603435	1.24952106
GTF2H1	0.001967902	TRUE	-1.077663498	-1.165380412
C12orf59	0.001973807	TRUE	-4.462578882	-1.351332975
CREB3L2	0.00199343	TRUE	1.177117834	1.340860052
ZWINT	0.001995665	TRUE	-1.079439671	-1.158654893
AP2S1	0.001996914	TRUE	-1.215380118	-1.105028331
SPIRE2	0.001998905	TRUE	1.179102772	1.342107252
RBBP9	0.002000119	TRUE	-1.146073802	-1.196902189
FARSB	0.002003137	TRUE	-1.205994364	-1.100465177
GOT1	0.002005937	TRUE	-1.128530028	-1.198985205
RPUSD1	0.00201212	TRUE	-1.333890094	-1.23427085
BCAS1	0.002016284	TRUE	1.21686995	2.281925522
THRB	0.002017064	TRUE	1.28056743	1.137884719
STRN3	0.002021722	TRUE	-1.086980717	-1.264304572
SAMD7	0.002024152	TRUE	-1.146964707	-1.194701411
NRAS	0.002025715	TRUE	-1.155318164	-1.066594519
C10orf47	0.002026082	TRUE	-1.183113047	-1.277951478
WDR12	0.002029242	TRUE	-1.166794406	-1.093704268
BOK	0.002033838	TRUE	-1.245632077	-1.183243098
CEP76	0.002038679	TRUE	-1.176622723	-1.173187332
MARVELD2	0.002038922	TRUE	-1.310658671	-1.147250866
LOC344887	0.002041176	TRUE	1.496098538	1.173339399
FAM222A	0.002044775	TRUE	-1.167014202	-1.207788541
SCARNA9L	0.00205073	TRUE	1.217027797	1.320618211
ZNF750	0.002051615	TRUE	1.254607421	1.563344097

DNAJC11	0.002052131	TRUE	-1.142415932	-1.138009672
DHX9	0.00205335	TRUE	-1.067735008	-1.155838053
PGAM1	0.00205944	TRUE	-1.402702428	-1.145015809
RAD23B	0.00206069	TRUE	-1.052766468	-1.144559637
CDK5RAP3	0.002062668	TRUE	1.158793292	1.127149198
C6orf48	0.002064983	TRUE	1.349574988	1.115607203
BDKRB2	0.002070944	TRUE	-1.839552791	-1.168585584
IL6R	0.002073781	TRUE	-1.613502897	-1.631757591
SPAG16	0.00207774	TRUE	1.15167729	1.49652797
HIST1H3I	0.002085524	TRUE	-1.101093387	-1.040258483
ANKHD1- EIF4EBP3	0.002086012	TRUE	1.169884293	1.058190366
MUT	0.002094237	TRUE	1.117245853	1.178885859
GCNT4	0.002100862	TRUE	-1.361015306	-1.463133484
PHF5A	0.002101862	TRUE	-1.329219151	-1.128645948
ZNF846	0.002101903	TRUE	1.302815936	1.09906791
DNA2	0.002110724	TRUE	-1.10717826	-1.243066418
NOC3L	0.002122419	TRUE	-1.344916592	-1.255595288
SGK196	0.002124806	TRUE	-1.143762307	-1.055077789
KCNN4	0.00212935	TRUE	-1.165088533	-1.470899749
MBOAT2	0.002130308	TRUE	-1.527001782	-1.099922551
CCDC127	0.002130445	TRUE	1.102536654	1.265324461
GIPC1	0.002132464	TRUE	-1.265939656	-1.100917231
NRG4	0.002144277	TRUE	-1.806812138	-1.229129855
SLC46A1	0.002145612	TRUE	-1.234678001	-2.055444891
HMOX2	0.002149694	TRUE	-1.209511061	-1.245151881
TNFRSF9	0.002151461	TRUE	-3.696606898	-1.348722585
FAM203A	0.002158012	TRUE	-1.134403819	-1.076893547
BCL7B	0.002184737	TRUE	-1.313308379	-1.087795697
MRPL18	0.002191749	TRUE	-1.198455694	-1.15546227
DICER1	0.002194187	TRUE	1.087241442	1.056457945
DDX60	0.002199101	TRUE	-1.249212937	-1.121971114
LOC100499467	0.002201694	TRUE	1.19716327	2.258450783
CYP4F3	0.002215465	TRUE	1.377293367	2.068479422
DCDC1	0.002218499	TRUE	1.552188768	1.239102932
CDR2	0.002221049	TRUE	-1.624659354	-1.122050251
AGFG1	0.002221564	TRUE	-1.185567425	-1.090608332
CAMSAP2	0.002223147	TRUE	-1.063866289	-1.110574929
DDX52	0.00222489	TRUE	-1.197720554	-1.087266256
MAMLD1	0.002232412	TRUE	-1.118988164	-1.311351969
PDIA5	0.00224384	TRUE	-1.226478628	-1.195226001
PFKP	0.002244232	TRUE	-1.134523211	-1.209129111
KIF18A	0.002245181	TRUE	-1.085760013	-1.17937557
IFT57	0.002245986	TRUE	-1.192021015	-1.170468386

SART1	0.002249354	TRUE	-1.078145098	-1.103160366
RN5S104	0.002254274	TRUE	-1.118190375	-1.124513105
IGFBP6	0.002255934	TRUE	-2.151902836	-1.14926457
NBPF24	0.002257625	TRUE	1.40727203	1.181699558
ITGA11	0.002263489	TRUE	1.129921048	1.191949199
ZFP42	0.002265391	TRUE	-1.144515741	-1.401934812
PRKAR1B	0.002265725	TRUE	-1.297097788	-1.251690115
LMNB2	0.002266644	TRUE	-1.145498067	-1.122192012
SOX21-AS1	0.002272671	TRUE	1.516658148	1.161536697
GMNN	0.002277658	TRUE	-1.394830351	-1.2178873
LOC100506258	0.002281291	TRUE	1.124551789	1.217540745
GPRC5B	0.002291121	TRUE	-1.48442547	-1.15520556
FZD2	0.002291203	TRUE	-1.173954957	-1.983459379
AMOTL2	0.002291759	TRUE	-1.31322146	-1.129505047
CDCA5	0.002292976	TRUE	-1.139114704	-1.27207661
HK1	0.002308038	TRUE	1.104431342	1.112554287
KLK5	0.002310367	TRUE	-3.44621433	-1.269083517
PPAT	0.002310672	TRUE	-1.210088781	-1.179118187
CRNDE	0.002312384	TRUE	1.339592474	1.436760647
ZNF238	0.002312966	TRUE	1.126829959	1.363241735
CELA1	0.0023271	TRUE	1.241493414	1.099401734
ARHGEF3	0.002338956	TRUE	-1.405865502	-1.109517764
UTRN	0.00234781	TRUE	1.143030417	1.192591832
PSMB7	0.002356647	TRUE	-1.215839245	-1.180231502
CLCF1	0.002366559	TRUE	-1.387492113	-1.211882572
MAP3K14	0.002369572	TRUE	-1.20011968	-1.252290466
GYS1	0.002373173	TRUE	-1.407726583	-1.201935672
SCARA3	0.002380121	TRUE	-1.161514245	-1.490131153
GET4	0.002382259	TRUE	-1.089864812	-1.119664475
GIT1	0.002383078	TRUE	-1.147907731	-1.16428397
ZMYM2-IT1	0.002383632	TRUE	1.382656396	1.516026909
ARMCX5-GPRASP2	0.002389738	TRUE	-1.170102188	-1.221563328
ERP27	0.002390417	TRUE	-1.340553883	-1.619644007
ATAD2	0.002390747	TRUE	-1.100247633	-1.116193715
DDX24	0.002390752	TRUE	-1.13489437	-1.122124321
GCNT2	0.002392403	TRUE	1.203843067	1.186978527
PPIP5K1	0.002412119	TRUE	1.201660985	1.100468453
CHMP7	0.00242197	TRUE	-1.108268488	-1.17284439
TPD52L2	0.002430858	TRUE	-1.362425014	-1.079315593
SLC25A19	0.002431575	TRUE	-1.642664601	-1.162905665
TSTD1	0.002431678	TRUE	1.177143875	1.188517442
DBN1	0.002433027	TRUE	-1.1149707	-1.402299193
FAM111B	0.002433605	TRUE	-1.170432276	-1.203789251

PAICS	0.002437675	TRUE	-1.267139331	-1.069742931
CDIPT	0.002437713	TRUE	1.199036694	1.125028368
NRARP	0.00245383	TRUE	1.176614385	2.57566935
PLS3	0.002463006	TRUE	-1.10673588	-1.102785943
CIRBP	0.002465042	TRUE	1.345853159	1.148189191
DDX60L	0.002466361	TRUE	-1.116488356	-1.649649911
ARPP19	0.00246997	TRUE	-1.082051199	-1.092981974
FBN2	0.002475414	TRUE	-1.920316276	-1.193015985
TNKS	0.002485846	TRUE	1.765935041	1.413357389
LRRC37A2	0.002487235	TRUE	1.370565188	1.169556702
ALDH1L1	0.002496596	TRUE	1.138416575	1.201907399
FAR2	0.002498042	TRUE	-1.419959775	-1.152290665
FZD10	0.002504277	TRUE	1.206910044	1.349591423
LOC728606	0.002517025	TRUE	-1.22416332	-1.175778607
NABP2	0.002517175	TRUE	-1.383018175	-1.131442787
NPIPL3	0.00252144	TRUE	1.395706503	1.270364901
RNF168	0.002523641	TRUE	1.114028918	1.070066232
KISS1	0.00252521	TRUE	-1.170128188	-2.49035286
MON2	0.002526281	TRUE	1.148741317	1.181160259
SPHK1	0.00252676	TRUE	-1.206943679	-1.145342787
SCAPER	0.002538495	TRUE	1.246713199	1.209605425
VGLL1	0.002539538	TRUE	-1.855396271	-1.15455075
TSPAN31	0.002547524	TRUE	1.399464065	1.139060721
LOC257396	0.002549042	TRUE	-1.233191072	-1.164321232
CELSR2	0.002564932	TRUE	1.098233224	1.510270021
CD27-AS1	0.002569054	TRUE	1.192694228	1.22525111
MYO5B	0.002570386	TRUE	1.217441455	1.302003298
TAP2	0.002572939	TRUE	-1.230357542	-1.161281066
DLGAP5	0.002573185	TRUE	-1.107102838	-1.103633439
ZFC3H1	0.002585062	TRUE	1.143696459	1.147895022
GPT2	0.002588037	TRUE	-1.144757003	-1.214038067
GARS	0.002593585	TRUE	-1.070619878	-1.090106976
PAK1	0.00259737	TRUE	1.174139241	1.282416819
ULBP3	0.002613593	TRUE	-1.351813499	-1.278702364
FLJ35390	0.002614073	TRUE	1.241784326	1.1604831
SERPINF1	0.002616824	TRUE	1.728826262	1.198599959
PSMD11	0.002619152	TRUE	-1.343163299	-1.102540213
HBEGF	0.002619748	TRUE	-1.441997294	-1.722791715
ABCA4	0.002642477	TRUE	1.095567231	1.270634246
UBR7	0.002643359	TRUE	-1.238384454	-1.148189901
SUPT5H	0.002647834	TRUE	-1.185310729	-1.092536255
ICAM1	0.002648618	TRUE	-1.851094079	-1.180240815
SARNP	0.002654577	TRUE	-1.12116317	-1.127744752
BSG	0.002665114	TRUE	-1.076064213	-1.122722406

PII5	0.002695354	TRUE	1.342300272	1.12681082
SLC9A2	0.002696376	TRUE	-1.262401045	-1.294304766
BCL6	0.002698801	TRUE	1.612769819	1.492786603
PCNA-AS1	0.00269972	TRUE	-1.310258938	-1.101888765
GSN-AS1	0.002706553	TRUE	1.190654083	1.296110839
PTGFRN	0.002708448	TRUE	-1.099257007	-1.304834208
EIF1AD	0.002714002	TRUE	-1.424563852	-1.159882229
IL15RA	0.002723342	TRUE	-1.246606873	-1.207906555
POLA2	0.0027234	TRUE	-1.120640471	-1.130819211
PKM	0.002729077	TRUE	-1.242955761	-1.095233742
ANKRD18A	0.002730139	TRUE	1.447504023	1.205503467
DHCR7	0.002732832	TRUE	-1.352562039	-1.099655764
CARD6	0.002735661	TRUE	-1.405273853	-1.106023004
PFN2	0.002735971	TRUE	-1.108852942	-1.324108867
CDC123	0.00273916	TRUE	-1.112343497	-1.091116752
GTF2E1	0.002741587	TRUE	-1.249261636	-1.10088464
LOC100289019	0.002746406	TRUE	1.687012677	1.126432613
BIVM-ERCC5	0.002748825	TRUE	1.086643622	1.193060427
ATP8B2	0.002760932	TRUE	-1.429907169	-1.160025975
CCNB1	0.002765899	TRUE	-1.122703287	-1.13803194
ACOT2	0.002768714	TRUE	-1.189366492	-1.629533525
CCT3	0.002772158	TRUE	-1.157293809	-1.071512655
CXCL1	0.002784748	TRUE	1.193737939	2.078109947
RN7SK	0.002785229	TRUE	1.275156378	1.126100474
SGTA	0.00279075	TRUE	-1.244558614	-1.069019178
NACC1	0.002794968	TRUE	-1.386096742	-1.224529986
LOC100652992	0.002797113	TRUE	1.421005768	1.212574119
SUDS3	0.002799459	TRUE	1.227098702	1.118632693
SCARNA27	0.002805637	TRUE	1.239233805	1.319997957
GCFC2	0.00280636	TRUE	-1.155049168	-1.146660982
SNRNP40	0.002817561	TRUE	-1.115553739	-1.151854133
GLS2	0.002820875	TRUE	1.243205439	1.222093362
FRY-AS1	0.00282321	TRUE	1.43902438	1.089422301
SNX7	0.002831562	TRUE	-1.312775495	-1.362793439
EIF2AK4	0.002832392	TRUE	-1.162871454	-1.234870388
MYT1L	0.002835832	TRUE	1.165928009	1.1098912
DNAJC4	0.002847734	TRUE	1.383735782	1.19224049
NAGS	0.002855775	TRUE	-1.116907005	-1.202224476
VAMP2	0.002856759	TRUE	1.183496157	1.096094383
APPL2	0.002860204	TRUE	1.112933131	1.146374826
LAMB2	0.002871771	TRUE	1.472150566	1.173650715
SRPX	0.002876775	TRUE	-1.578515077	-1.149005227
ANKRD10-IT1	0.002882154	TRUE	2.190458821	1.346461716
CTNBNL1	0.002889617	TRUE	-1.1930241	-1.105663299

LOC643837	0.002890426	TRUE	-1.225685934	-1.140920259
LIMCH1	0.002909008	TRUE	1.114587654	1.735944258
CXorf23	0.002910325	TRUE	1.216649276	1.110283963
SLC27A2	0.002928456	TRUE	1.382945581	1.107595642
FASN	0.002929361	TRUE	-1.323272797	-1.149428352
C17orf28	0.002935067	TRUE	1.387421459	1.13643974
MAP2K6	0.002937166	TRUE	1.484045831	1.218326397
GALNT3	0.002939096	TRUE	-1.154176915	-1.222822213
DSCC1	0.00294281	TRUE	-1.39931163	-1.173490177
RNPEP	0.002956789	TRUE	-1.073997946	-1.066248838
WDFY1	0.00296533	TRUE	1.05833967	1.119753887
EZH1	0.002967625	TRUE	1.458264596	1.158284663
PSMC2	0.002971222	TRUE	-1.254788	-1.093191446
TPX2	0.002973191	TRUE	-1.209193054	-1.06619505
GOLM1	0.002978609	TRUE	-1.257087057	-1.149576236
SLC35B4	0.002994509	TRUE	-1.287738815	-1.175406287
UNC5B	0.002999856	TRUE	1.402450814	1.186394749
STAG2	0.003009528	TRUE	1.068595927	1.082226979
IFT81	0.003015101	TRUE	1.108790228	1.311488189
C12orf57	0.00303509	TRUE	1.170580763	1.162838655
MBNL2	0.003036181	TRUE	-1.238289448	-1.063536153
SAP30BP	0.003042976	TRUE	-1.17661259	-1.092405533
PINX1	0.003048383	TRUE	-1.421303662	-1.172331129
POP4	0.003049721	TRUE	-1.191528888	-1.097556366
BARD1	0.003049879	TRUE	-1.154652812	-1.112292012
AP3D1	0.0030509	TRUE	-1.162894145	-1.074088895
FAM203B	0.003052782	TRUE	-1.110156315	-1.087277278
CCP110	0.003066282	TRUE	-1.120106405	-1.095360432
BTG1	0.00307616	TRUE	1.084299393	1.298566002
OPN3	0.003091637	TRUE	-1.378527457	-1.187582613
MRPS23	0.003092511	TRUE	-1.300815737	-1.10542628
SPRR2E	0.003107085	TRUE	1.098568851	1.143803489
LOC100288160	0.003138126	TRUE	-1.14559791	-1.12753567
SPPL2B	0.003141676	TRUE	1.325435916	1.281562095
UXS1	0.003144896	TRUE	-1.068649301	-1.170440854
KIAA0226	0.003144912	TRUE	-1.158831682	-1.120836558
ANKRD5	0.003145151	TRUE	-1.200251027	-1.16101368
RIT1	0.003147678	TRUE	1.208134711	1.14476044
TNFRSF10D	0.003151111	TRUE	-1.539228053	-1.275111909
LOC100190986	0.003169444	TRUE	1.660177527	1.724934623
MAP3K7	0.003171607	TRUE	-1.082181618	-1.045339693
ZNF619	0.003173685	TRUE	-1.180786096	-1.168204128
EREG	0.003182918	TRUE	-1.931121423	-1.461798475
DDB2	0.003185302	TRUE	-1.12304318	-1.325501907

FAM169A	0.003195057	TRUE	-1.17217684	-2.995086784
NRF1	0.003201971	TRUE	-1.098196536	-1.154305657
EIF4G3	0.003202984	TRUE	1.106385013	1.065194481
GNG12	0.003203886	TRUE	-1.106649321	-1.24716913
CYB5R4	0.003210069	TRUE	-1.212716969	-1.104555573
HMGA1P4	0.003215476	TRUE	1.406157001	1.272746004
ACLY	0.003221855	TRUE	-1.287566089	-1.041224964
ZNF689	0.003222958	TRUE	-1.265275331	-1.479481504
NBPF11	0.003223878	TRUE	1.336698773	1.171242874
CEBPA	0.003243341	TRUE	1.310685413	1.218178143
ATP6V1B2	0.003243559	TRUE	-1.161813572	-1.044054719
XRCC6BP1	0.003244666	TRUE	-1.074312058	-1.105370208
PLS1	0.003253141	TRUE	-1.241215571	-1.210463275
FER	0.003261466	TRUE	-1.071336909	-1.337982093
RPL13AP20	0.003272268	TRUE	1.192903444	1.125402977
SNAPIN	0.003274536	TRUE	-1.159368136	-1.140680064
MRPL15	0.003279463	TRUE	-1.086250246	-1.232302451
CNDP2	0.003289038	TRUE	-1.365562389	-1.132041221
PROS1	0.003289229	TRUE	-1.285737913	-1.30550612
LOC415056	0.003306014	TRUE	1.159801921	1.122750371
LOC100133669	0.003314445	TRUE	-1.178793239	-2.018987125
KPNB1	0.003331162	TRUE	-1.071652363	-1.160201966
PTHLH	0.003333005	TRUE	-2.3633521	-1.184768222
LOC100507199	0.003336311	TRUE	1.322883461	1.115190706
PION	0.003336927	TRUE	1.333610517	1.266179329
AURKA	0.003337368	TRUE	-1.354457355	-1.110315613
AKAP13	0.003370835	TRUE	1.087849728	1.506385185
GSK3B	0.003379306	TRUE	-1.106976598	-1.873139921
CDKN2AIPNL	0.003380381	TRUE	-1.248592737	-1.248643063
TLR4	0.003386971	TRUE	-1.106566678	-1.520068773
ZNF740	0.003397391	TRUE	1.164516484	1.175504417
DKC1	0.003406962	TRUE	-1.202241275	-1.114876953
GDF11	0.003425076	TRUE	-1.134603411	-1.231346233
ANKRD27	0.003442147	TRUE	-1.276613363	-1.069970688
PSMB3	0.003445408	TRUE	-1.244923217	-1.062206844
NIPSNAP1	0.00344725	TRUE	1.097781127	1.284449757
PSMB5	0.003449801	TRUE	-1.172084358	-1.075886941
KPNA4	0.003458955	TRUE	-1.170024011	-1.208324225
BCAR3	0.003462363	TRUE	-1.255888709	-1.297509566
LOC100506804	0.003463584	TRUE	1.202009396	1.168048552
APOD	0.003476295	TRUE	1.367718163	1.472172658
CA11	0.003479881	TRUE	1.289543166	1.177581642
CLDN7	0.003483401	TRUE	-1.190980605	-1.054353195
C20orf72	0.00348514	TRUE	-1.116330284	-1.14895433

THUMPD3	0.003490639	TRUE	-1.130637291	-1.120661977
CLDN1	0.003503503	TRUE	1.106736677	1.79761982
TMEM48	0.003504059	TRUE	-1.213399131	-1.085692405
S100A8	0.003513288	TRUE	1.292746638	1.751789617
FKBP5	0.00351514	TRUE	-1.378728917	-1.140475381
C1orf21	0.003515416	TRUE	-1.203666892	-1.470173521
TTF2	0.003519936	TRUE	-1.122876679	-1.218695481
ZNF563	0.003522237	TRUE	-1.303223629	-1.309231386
RBBP7	0.003529097	TRUE	1.119974572	1.080114075
SCN8A	0.003530101	TRUE	1.308399796	1.208781854
PIP4K2C	0.003543426	TRUE	-1.20226338	-1.152433726
CYTH1	0.003551255	TRUE	1.283807985	1.090690449
RAB8A	0.003555313	TRUE	-1.133348787	-1.066929524
MAPK6	0.003560525	TRUE	-1.297845976	-1.077482136
PACSIN3	0.003564382	TRUE	-1.209624035	-1.260059526
C17orf53	0.00357018	TRUE	-1.254742787	-1.172815706
FLG-AS1	0.00357038	TRUE	1.218543112	2.096552226
CLINT1	0.003574341	TRUE	1.201878826	1.093476115
CD9	0.003579104	TRUE	1.291114621	1.095622778
RORB	0.003581996	TRUE	2.305520197	1.156790204
CCL5	0.003586256	TRUE	-1.138367565	-1.244396278
TRIM4	0.00358752	TRUE	1.256453563	1.176156361
UBR3	0.003600691	TRUE	1.074661666	1.088516128
EFNB2	0.003609829	TRUE	-1.887020609	-1.212295967
MYCBP2	0.00361039	TRUE	1.10358465	1.17444841
PDIA6	0.003611713	TRUE	-1.077698433	-1.188663018
VDR	0.003612768	TRUE	-1.480292037	-1.197292697
BOLA2	0.003616414	TRUE	-1.359190005	-1.107851369
BCL10	0.003617988	TRUE	-1.097934199	-1.268327415
LAPTM4A	0.003623557	TRUE	1.079062036	1.142991613
VAMP5	0.003636687	TRUE	-1.14357966	-1.170539614
STIP1	0.00363671	TRUE	-1.097230887	-1.114602272
CBLB	0.003636926	TRUE	1.444981564	1.239025545
C18orf25	0.003640532	TRUE	-1.093637814	-1.225321085
DOCK9	0.003656273	TRUE	1.286139874	1.091243829
AIFM2	0.003657111	TRUE	-1.236242592	-1.157700853
MED8	0.003664012	TRUE	-1.360762755	-1.120778643
MIG7	0.00366875	TRUE	-1.279347539	-4.405221919
SIPA1L2	0.003689658	TRUE	1.88251308	1.133681836
ITGB1	0.003690357	TRUE	-1.172624678	-1.145337663
CHAMP1	0.003701113	TRUE	-1.134070527	-1.339542844
MGC2752	0.003705642	TRUE	-1.155335628	-1.05803155
LOC100506136	0.003712409	TRUE	-1.316972579	-1.213485438
FAM63A	0.003715406	TRUE	1.202699844	1.197762985

MICAL2	0.003716035	TRUE	-1.170288627	-1.283499311
SNX29P2	0.003723391	TRUE	1.751767962	1.683325307
ARAP3	0.003725809	TRUE	-1.173884988	-1.094235587
GBE1	0.00374762	TRUE	-1.270623414	-1.25934132
FGFR1OP	0.003771042	TRUE	-1.228498117	-1.093366926
TBP	0.003772004	TRUE	-1.207969848	-1.151420835
UBL4A	0.003788764	TRUE	-1.373996656	-1.080844233
HECW1	0.003788943	TRUE	-1.185810207	-1.107417142
AJUBA	0.003794642	TRUE	-1.095946407	-1.97432583
MAOB	0.003800504	TRUE	-2.459902328	-1.177104216
HIST1H1A	0.003803799	TRUE	-1.39855425	-1.143097135
LOC440944	0.003804632	TRUE	1.149577821	1.103192592
FAM13B	0.003806342	TRUE	1.100594453	1.153880883
MAP3K5	0.003809359	TRUE	1.544726089	1.11024421
GUF1	0.003815355	TRUE	-1.164865929	-1.126860662
IGLJ5	0.003817595	TRUE	1.428029229	1.637252849
TMEM209	0.003834483	TRUE	-1.137301411	-1.12152051
PNP	0.003852553	TRUE	-1.347254186	-1.078097371
RHOBTB3	0.003858956	TRUE	1.215926571	1.397818569
QRSL1	0.003859864	TRUE	-1.138259386	-1.132257384
ZMPSTE24	0.00387697	TRUE	-1.223495418	-1.07050938
KRT18	0.003886966	TRUE	-1.117948851	-1.292367582
OSGIN1	0.003892182	TRUE	1.201611666	1.132394157
ZBTB44	0.00389521	TRUE	1.135579315	1.204476297
AOX1	0.003901165	TRUE	-1.611822784	-1.10504109
EHHADH	0.003902219	TRUE	1.140698062	1.229721705
FAM171B	0.003902872	TRUE	1.143958219	1.560654613
C11orf82	0.00390619	TRUE	-1.370248264	-1.109295697
C3orf26	0.003907069	TRUE	-1.13438655	-1.114804842
HIST1H2BB	0.003911526	TRUE	-1.505613308	-1.329101468
USP6NL	0.003919954	TRUE	-1.084426821	-1.291945527
HUS1	0.003926221	TRUE	-1.151164774	-1.135031706
ENTPD7	0.003932098	TRUE	-1.428519867	-1.087591361
PNPT1	0.003933864	TRUE	-1.185267731	-1.174778542
RNF26	0.003934775	TRUE	-1.320173515	-1.203379748
INPP5F	0.003935839	TRUE	-1.134769168	-1.254914581
3-Sep	0.003940891	TRUE	-1.182771003	-1.200939826
GPR132	0.003957742	TRUE	1.400114335	1.234411717
C12orf75	0.003970048	TRUE	-1.086323232	-1.190054464
MRPL40	0.003979484	TRUE	-1.255231168	-1.08716925
NLRP6	0.003980402	TRUE	-1.221828347	-1.304519361
ZNF695	0.003981614	TRUE	-1.293683596	-1.23745659
LMAN2	0.003998222	TRUE	-1.080632128	-1.087144156
AP1M1	0.004029601	TRUE	-1.363355121	-1.100194177

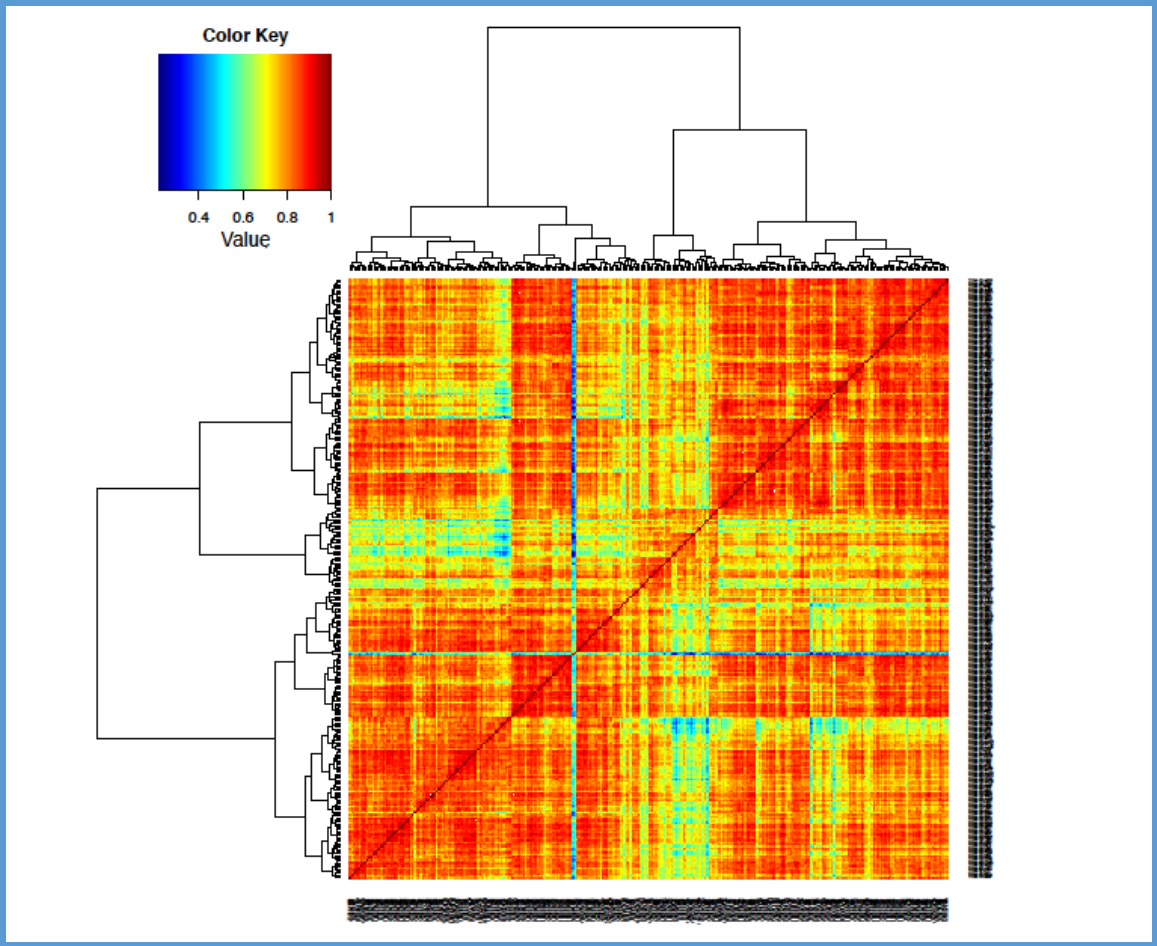
LOC100128281	0.00403143	TRUE	1.242251371	1.650789252
NCOA5	0.004032154	TRUE	-1.082084766	-1.124284531
C1orf106	0.004038427	TRUE	-1.08549052	-1.06583896
DDX10	0.0040408	TRUE	-1.113859545	-1.153509504
EFNB1	0.004041008	TRUE	-1.616562135	-1.19028385
AFAP1-AS1	0.004041949	TRUE	-1.286392993	-1.054473916
SCYL3	0.004050677	TRUE	1.176236419	1.161588912
TMEM170A	0.004053174	TRUE	-1.160372899	-1.18251556
RPS6KC1	0.00405863	TRUE	-1.095497802	-1.195345157
PDDC1	0.004061403	TRUE	1.143999932	1.125551116
C19orf53	0.004081333	TRUE	-1.25015655	-1.062390496
PUS7	0.004081597	TRUE	-1.259396921	-1.084624549
LOC100131541	0.004083052	TRUE	1.147725622	1.854010116
KITLG	0.004087722	TRUE	1.164992545	1.329053537
MYCL1	0.004096679	TRUE	1.178075883	1.642415235
MSX1	0.004108082	TRUE	-1.208747162	-1.217716168
MIR548AL	0.004110371	TRUE	1.339608071	1.92724487
IL23A	0.004118789	TRUE	-1.146075704	-1.465917073
B4GALT1	0.004119083	TRUE	-1.107250234	-1.839768256
ZNF101	0.004119494	TRUE	-1.17114352	-1.271362587
FAM43A	0.004119688	TRUE	1.264085829	1.50038922
METTL5	0.004123839	TRUE	-1.159113814	-1.14879745
SAMM50	0.004126289	TRUE	-1.158837606	-1.075291039
TRIM52	0.004128557	TRUE	1.490052902	1.199511002
CAMK2N1	0.004152479	TRUE	-1.293968882	-1.087356902
TMEM194A	0.004154253	TRUE	-1.298127409	-1.133182897
PCDH20	0.004173266	TRUE	1.159817835	1.098041328
PPFIBP2	0.004177304	TRUE	1.237825081	1.116166451
NDRG2	0.004178598	TRUE	1.091359315	1.419668742
EDC3	0.00419786	TRUE	1.086870931	1.22488415
GABRP	0.004203632	TRUE	2.02207947	1.111175515
AKIRIN2	0.004204103	TRUE	-1.260933636	-1.086567092
HAGH	0.004208016	TRUE	1.148645506	1.292064291
NBPF10	0.004211205	TRUE	1.404516994	1.179842423
MRPS34	0.004224818	TRUE	-1.322273042	-1.050062031
SEC23B	0.004233923	TRUE	-1.100206141	-1.060205693
IL1RAP	0.004236118	TRUE	1.193526574	1.502868998
BZW1	0.00424065	TRUE	-1.25824909	-1.191338958
KIAA1217	0.00424126	TRUE	1.154905573	1.180003245
ARRDC4	0.004248674	TRUE	1.311793217	1.434698824
LOC440149	0.004249805	TRUE	-1.2207115	-1.166280647
PLEKHA5	0.004255251	TRUE	1.379652685	1.070696468
VTRNA1-3	0.004264186	TRUE	-2.691442655	-1.404992161
FEZ2	0.004269765	TRUE	1.2090904	1.090259907

CALR	0.004274298	TRUE	-1.036209647	-1.173903819
SLC20A1	0.004285127	TRUE	-1.658305212	-1.17930484
NRP2	0.004288149	TRUE	-1.078444916	-1.365922441
C9orf64	0.004290423	TRUE	-1.195049481	-1.164332532
TCEANC	0.00429656	TRUE	1.243734509	1.217387746
KIF5B	0.004300333	TRUE	-1.036819922	-1.065551353
OMA1	0.004308375	TRUE	1.176422581	1.137270104
SLC45A3	0.004310858	TRUE	-1.213001219	-1.643509122
IQSEC2	0.004313657	TRUE	1.157784395	1.173756915
ATG4A	0.00431996	TRUE	-1.402823052	-1.047225577
LOH12CR1	0.004324276	TRUE	1.300008831	1.159797241
YPEL3	0.004326632	TRUE	1.189489686	1.350877956
DKFZP434I0714	0.004330564	TRUE	1.14384037	1.169318974
SHCBP1	0.004332587	TRUE	-1.275325063	-1.057083158
GIGYF1	0.004342846	TRUE	1.376004176	1.088944141
BCL2L1	0.004343814	TRUE	-1.184137972	-1.32827688
ACSL3	0.004353056	TRUE	-1.165582627	-1.223124442
NFKBIB	0.004355086	TRUE	-1.269397039	-1.104230169
ZHX2	0.004365018	TRUE	-1.093884074	-1.210641632
RBM27	0.004375577	TRUE	-1.083589628	-1.136797624
RAP1GDS1	0.004390651	TRUE	-1.339744051	-1.119818895
WISP2	0.00439078	TRUE	1.123830228	1.110013828
RECQL4	0.004392177	TRUE	-1.104963093	-1.223264795
COL6A5	0.004399322	TRUE	1.119740619	1.124218203
RNF185	0.004406729	TRUE	-1.233341435	-1.141333983
CHKB-CPT1B	0.004410121	TRUE	1.315946345	1.153855919
LOC100130691	0.004410603	TRUE	1.229944632	1.152289363
PLD6	0.004427323	TRUE	-1.194057386	-1.477129885
EZR	0.004431593	TRUE	-1.155397527	-1.079645239
DDAH2	0.004454441	TRUE	-1.127709588	-1.135148666
TTC3P1	0.004454853	TRUE	1.153668744	1.240291044
JOSD1	0.004455513	TRUE	-1.105060033	-1.174153892
SLMAP	0.004473647	TRUE	-1.083532819	-1.079570575
XYLT2	0.004475296	TRUE	-1.088270218	-1.226456577
EBNA1BP2	0.004481313	TRUE	-1.316743421	-1.062543118
C1orf135	0.004481411	TRUE	-1.177852784	-1.458163002
FANCI	0.004490913	TRUE	-1.172429925	-1.164778746
CHD6	0.004495298	TRUE	1.42458742	1.088147242
CMTM1	0.004502117	TRUE	-1.076498425	-1.28792458
MIR27B	0.004502838	TRUE	2.670782417	1.365566985
ILF2	0.004504118	TRUE	-1.140385878	-1.043763047
TBC1D3	0.004505459	TRUE	1.113248061	1.248940488
KLRAP1	0.004522846	TRUE	1.12535877	1.226925478
HSD11B2	0.004523267	TRUE	-1.261739246	-1.188009278

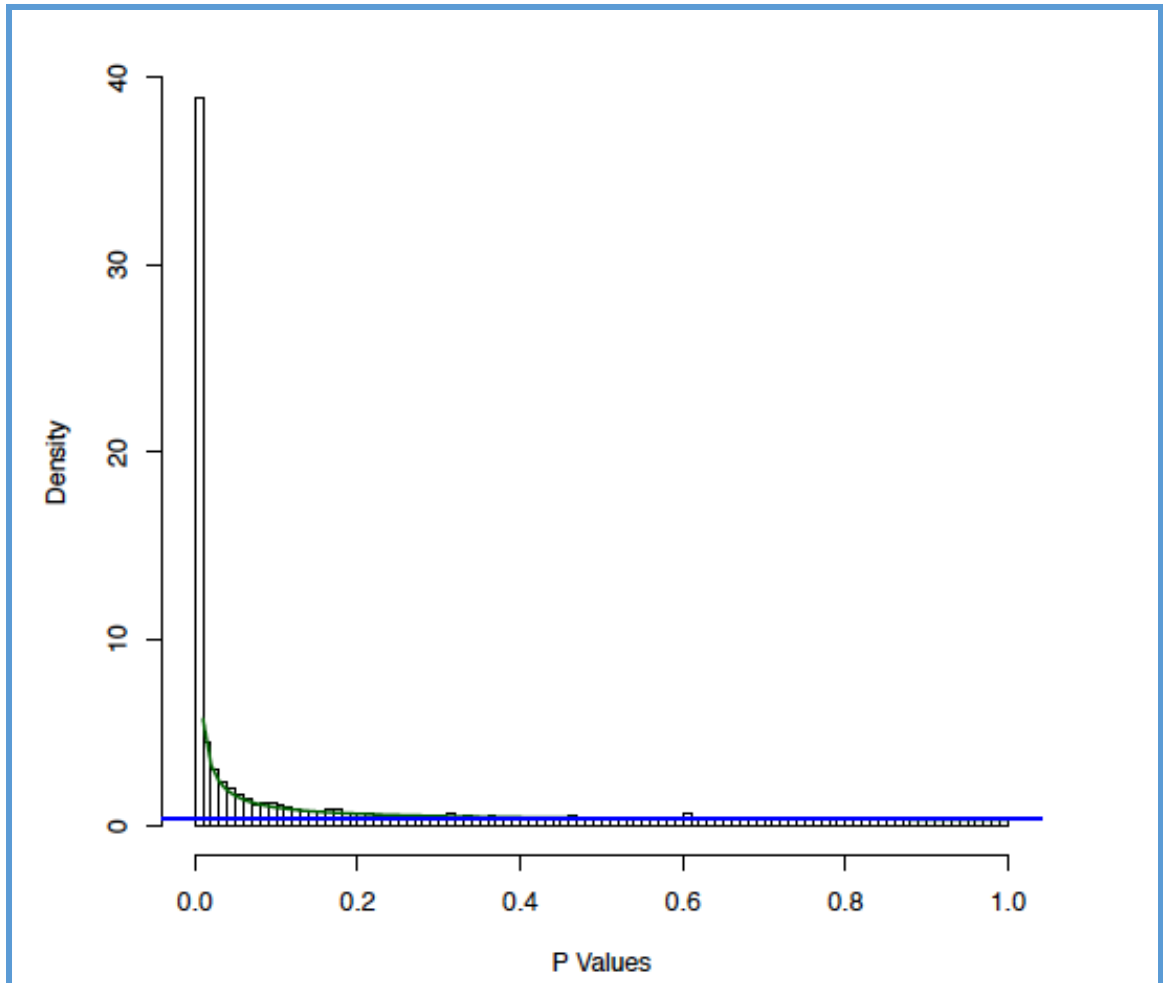
CXXC1	0.004531646	TRUE	-1.287278235	-1.132789803
MUC20	0.004537564	TRUE	1.231221954	1.184016722
WNT2B	0.004538284	TRUE	1.251165848	1.099220242
KBTBD8	0.004545545	TRUE	-1.535118546	-1.14084761
EXT2	0.004545622	TRUE	-1.30540718	-1.082640676
HNRNPAB	0.004550528	TRUE	-1.115828718	-1.076557718
ETS2	0.004552425	TRUE	-1.059699545	-1.231031698
SYNJ2	0.004552862	TRUE	-1.291958383	-1.0921503
SEC22C	0.004563696	TRUE	-1.20404925	-1.140364763
CWF19L1	0.004565285	TRUE	-1.212187418	-1.07267011
ANXA5	0.00457023	TRUE	-1.091983605	-1.213170894
TIMM10	0.004574681	TRUE	-1.340203967	-1.11379973
C18orf62	0.004586677	TRUE	-1.271028807	-1.131889082
LOC100289488	0.004590148	TRUE	1.126349835	1.355924183
C21orf59	0.004596453	TRUE	-1.16881241	-1.093295821
ICK	0.004614763	TRUE	1.461220094	1.099171058
ATP5D	0.004618436	TRUE	1.084637415	1.129080916
PBK	0.004621447	TRUE	-1.343428961	-1.126106391
IL31RA	0.004632518	TRUE	-1.334591948	-1.177130315
C10orf55	0.004635059	TRUE	-1.588741751	-1.263536559
MEIS2	0.004636792	TRUE	1.303565578	1.155966099
ELOVL5	0.004656555	TRUE	-1.113404365	-1.146743145
ORC2	0.004657139	TRUE	-1.098404106	-1.124633289
SERPINB4	0.004666116	TRUE	-1.91972371	-1.188959179
EFTUD2	0.004667626	TRUE	-1.151727994	-1.054101369
PDGFA	0.004670081	TRUE	-1.126481472	-1.895154465
CITED4	0.004670944	TRUE	1.167312628	1.175944667
RALGDS	0.004676469	TRUE	1.081375279	1.178787196
SCD	0.004678316	TRUE	-1.940549062	-1.106325896
BYSL	0.004682591	TRUE	-1.304399026	-1.242852341
CENPE	0.004691311	TRUE	-1.232118565	-1.089289318
ZNF652	0.00469199	TRUE	1.152234876	1.166833979
FXR2	0.004708679	TRUE	-1.357534561	-1.109798205
FAM135A	0.004717198	TRUE	1.245677615	1.089870396
PTPRG	0.004718958	TRUE	-1.114649335	-1.566001932
KREMEN2	0.004721884	TRUE	-1.397514352	-1.134617164
BRWD1	0.004728881	TRUE	1.12386667	1.124005633
LOC100507431	0.004729159	TRUE	-1.21609888	-1.214917183
NCAPD3	0.004737876	TRUE	-1.226685884	-1.076695166
TNC	0.004741788	TRUE	-6.6766172	-1.240216628
TPM4	0.004743035	TRUE	-1.306180835	-1.061591712
DPAGT1	0.004747405	TRUE	-1.241776712	-1.162593768
B4GALT6	0.004750404	TRUE	-1.461606731	-1.497859073
MAPRE2	0.004759408	TRUE	-1.407919846	-1.309954402

CD164	0.004764811	TRUE	1.216611369	1.073062693
EXOC4	0.004769298	TRUE	1.139572044	1.055550076
CST5	0.004772751	TRUE	-1.217518515	-1.425639003
SIAH2	0.004776657	TRUE	-1.153068428	-1.144330104
TRMT1	0.004780995	TRUE	-1.245092095	-1.123824371
TMED1	0.004784666	TRUE	-1.171662031	-1.100043077
PRKCH	0.004790524	TRUE	1.174798921	1.049270173
BEND3	0.004793051	TRUE	-1.261956531	-1.213828255
PAIP2B	0.004793439	TRUE	1.384374543	1.261033303
GCC2	0.004812118	TRUE	1.100738747	1.197230534
LOC100170939	0.004834272	TRUE	1.81936338	1.344978625
CLK2	0.004849416	TRUE	1.223342836	1.118383522
POLR1A	0.004854934	TRUE	-1.096706765	-1.069029034

Appendix 2: Correlation heat-map in the Oral Cavity group



Appendix 3: Histogram of p-values testing Cluster 1 versus Cluster 2 in the Oral Cavity group



Appendix 4: Ingenuity Pathway Analysis of significantly modulated pathways after NOTCH activation by Jagged1 in cell lines

	Functions	P-value	# Molecules
Cellular Movement			48
	cell movement of tumor cell lines	4.79E-13	30
	migration of tumor cell lines	9.92E-13	27
	cell movement	2.72E-12	47
	invasion of tumor cell lines	6.64E-11	24
	migration of cells	6.65E-11	42
	invasion of cells	1.63E-10	27
	cell movement of brain cancer cell lines	4.48E-10	11
	migration of tumor cells	2.26E-09	13
	migration of endothelial cells	6.04E-09	15
	cell movement of fibroblast cell lines	6.87E-09	11
	migration of brain cancer cell lines	2.66E-08	9
	migration of cancer cells	4.13E-08	11
	migration of fibroblast cell lines	1.12E-07	9
	homing	1.45E-07	18
	homing of cells	4.80E-07	17
	chemotaxis	1.71E-06	16
	invasion of tumor cells	2.28E-06	9
	cell movement of tumor cells	2.47E-06	9
	migration of sarcoma cell lines	3.81E-06	6
	invasion of carcinoma cell lines	4.70E-06	9
	chemotaxis of cells	5.22E-06	15
	leukocyte migration	6.30E-06	20
	invasion of breast cancer cell lines	7.09E-06	10
	cell movement of phagocytes	8.92E-06	15
	invasion of squamous cell carcinoma cell lines	1.24E-05	5
	migration of endothelial cell lines	1.33E-05	6
	dissemination of cells	2.26E-05	5
	invasion of prostate cancer cell lines	2.81E-05	6
	cell movement of leukocytes	4.66E-05	17
	cellular infiltration	5.76E-05	12
	dissemination of tumor cells	7.25E-05	3
	migration of skin cancer cell lines	8.89E-05	3
	migration of keratinocytes	8.90E-05	5

	invasion of ovarian cancer cell lines	1.13E-04	4
	invasion of glioma cells	1.29E-04	3
	cell movement of myeloid cells	1.30E-04	13
	migration of connective tissue cells	1.41E-04	7
	recruitment of neutrophils	1.69E-04	7
	invasion of brain cancer cell lines	1.80E-04	5
	movement of endometrial stromal cells	1.83E-04	2
	migration of breast cancer cell lines	2.09E-04	8
	recruitment of phagocytes	2.14E-04	8
	cell movement of pancreatic cancer cell lines	2.15E-04	4
	migration of kidney cell lines	2.19E-04	5
	cell movement of neuroglia	2.64E-04	5
	migration of mesenchymal stem cells	2.73E-04	3
	cell movement of cancer cells	2.83E-04	6
	cell movement of epithelial cells	2.83E-04	6
	migration of smooth muscle cells	2.93E-04	6
	cellular infiltration by leukocytes	3.55E-04	10
	transmigration of myeloid cells	3.94E-04	4
	migration of phagocytes	4.89E-04	8
	migration of myeloid cells	5.76E-04	6
	migration of cervical cancer cell lines	7.73E-04	4
	migration of neuroglia	7.73E-04	4
	migration of bone cancer cell lines	8.09E-04	3
	cell movement of embryonic cells	9.18E-04	5
	cell movement of granulocytes	1.03E-03	9
	transmigration of phagocytes	1.04E-03	4
	intravasation of cells	1.08E-03	2
	migration of embryonic cell lines	1.19E-03	4
	cell movement of bladder cancer cell lines	1.23E-03	3
	invasion of endothelial cells	1.23E-03	3
Cellular Growth and Proliferation			64
	proliferation of cells	3.95E-11	62
	proliferation of tumor cells	1.02E-10	20
	proliferation of tumor cell lines	5.32E-10	36

	proliferation of cancer cells	2.03E-07	14
	proliferation of epithelial cells	3.96E-07	16
	proliferation of connective tissue cells	1.21E-06	17
	proliferation of ovarian cancer cell lines	1.51E-06	8
	proliferation of muscle cells	1.62E-06	13
	proliferation of smooth muscle cells	3.21E-06	11
	proliferation of blood cells	3.65E-06	20
	proliferation of immune cells	5.35E-06	19
	proliferation of endothelial cells	8.11E-06	11
	formation of connective tissue cells	8.46E-06	9
	proliferation of lymphocytes	2.26E-05	17
	colony formation	2.93E-05	14
	inhibition of cells	3.70E-05	7
	proliferation of prostate cancer cell lines	3.90E-05	10
	proliferation of mammary tumor cells	6.16E-05	5
	proliferation of lung cancer cell lines	7.39E-05	9
	expansion of neutrophils	9.16E-05	2
	proliferation of carcinoma cell lines	1.23E-04	11
	formation of cells	1.26E-04	19
	proliferation of fibroblasts	1.53E-04	10
	proliferation of brain cancer cell lines	2.45E-04	7
	proliferation of neuronal cells	2.60E-04	13
	proliferation of keratinocytes	3.56E-04	6
	growth of neurites	4.20E-04	11
	formation of colony forming unit osteoblasts	4.53E-04	2
	colony formation of tumor cell lines	4.89E-04	8
	inhibition of mononuclear leukocytes	5.93E-04	4
	colony formation of cells	7.46E-04	11
	proliferation of fibroblast cell lines	7.64E-04	10
	formation of osteoclasts	8.01E-04	5
	outgrowth of cells	9.31E-04	10
Cell Death and Survival			59

	cell viability	7.12E-11	34
	cell survival	1.10E-10	35
	necrosis	7.22E-10	48
	cell viability of tumor cell lines	5.06E-08	22
	cell death	7.44E-08	52
	cell death of tumor cell lines	2.68E-07	31
	apoptosis	5.44E-07	43
	necrosis of epithelial tissue	1.09E-06	17
	cell viability of endothelial cells	1.49E-06	6
	apoptosis of pericytes	1.05E-05	4
	apoptosis of tumor cell lines	1.07E-05	24
	cell death of tumor	1.30E-05	12
	cell death of muscle cells	1.78E-05	11
	apoptosis of muscle cell lines	2.64E-05	5
	apoptosis of heart cell lines	2.89E-05	4
	repopulation of fibroblasts	3.06E-05	2
	cell death of tumor cells	5.09E-05	11
	anoikis	5.39E-05	6
	apoptosis of tumor cells	1.23E-04	9
	apoptosis of endothelial cells	1.59E-04	7
	apoptosis of hepatic stellate cells	2.07E-04	3
	cell death of epithelial cells	2.15E-04	12
	anoikis of tumor cell lines	2.15E-04	4
	cell viability of carcinoma cell lines	2.39E-04	6
	apoptosis of muscle cells	3.21E-04	8
	cell viability of prostate cancer cell lines	4.19E-04	4
	permeability of endothelial cell lines	4.44E-04	3
	cell death of lymphatic system cells	5.58E-04	5
	cell viability of leukemia cell lines	5.93E-04	4
	killing of lung cancer cell lines	6.32E-04	2
	apoptosis of mammary tumor cells	7.38E-04	3
	cell viability of kidney cell lines	8.13E-04	4
	cell death of immune cells	1.04E-03	13
Cellular Development			62
	proliferation of tumor cells	1.02E-10	20
	proliferation of tumor cell lines	5.32E-10	36
	differentiation of cells	1.42E-08	42
	endothelial cell development	1.34E-07	14

	proliferation of cancer cells	2.03E-07	14
	proliferation of ovarian cancer cell lines	1.51E-06	8
	proliferation of muscle cells	1.62E-06	13
	proliferation of smooth muscle cells	3.21E-06	11
	proliferation of blood cells	3.65E-06	20
	proliferation of immune cells	5.35E-06	19
	tubulation of endothelial cells	6.01E-06	7
	proliferation of endothelial cells	8.11E-06	11
	proliferation of lymphocytes	2.26E-05	17
	tubulation of endothelial progenitor cells	3.55E-05	3
	differentiation of epithelial tissue	3.62E-05	11
	proliferation of prostate cancer cell lines	3.90E-05	10
	differentiation of epithelial cells	5.11E-05	10
	proliferation of mammary tumor cells	6.16E-05	5
	differentiation of tumor cell lines	6.17E-05	11
	proliferation of lung cancer cell lines	7.39E-05	9
	expansion of neutrophils	9.16E-05	2
	development of connective tissue cells	9.57E-05	8
	proliferation of carcinoma cell lines	1.23E-04	11
	proliferation of fibroblasts	1.53E-04	10
	differentiation of connective tissue cells	2.38E-04	14
	proliferation of brain cancer cell lines	2.45E-04	7
	proliferation of neuronal cells	2.60E-04	13
	differentiation of connective tissue	2.94E-04	15
	proliferation of keratinocytes	3.56E-04	6
	growth of neurites	4.20E-04	11
	hematopoiesis of bone marrow cells	4.44E-04	3
	formation of colony forming unit osteoblasts	4.53E-04	2
	differentiation of osteoblasts	5.29E-04	8
	differentiation of bone cells	5.43E-04	10
	proliferation of fibroblast cell lines	7.64E-04	10
	formation of osteoclasts	8.01E-04	5

	onset of differentiation of cells	8.39E-04	2
	differentiation of skin	9.61E-04	6
Cell-To-Cell Signaling and Interaction			41
	adhesion of tumor cell lines	8.05E-10	15
	cell-cell adhesion	1.01E-06	10
	attachment of tumor cell lines	3.11E-06	5
	activation of cells	3.11E-06	22
	adhesion of epithelial cells	4.32E-06	7
	binding of cells	7.29E-06	14
	adhesion of kidney cell lines	7.63E-06	5
	adhesion of embryonic cells	1.36E-05	5
	adhesion of mesothelial cells	3.06E-05	2
	activation of blood cells	3.29E-05	17
	binding of endothelial cells	3.29E-05	6
	adhesion of embryonic cell lines	3.69E-05	4
	activation of leukocytes	5.00E-05	16
	adhesion of melanoma cell lines	5.78E-05	4
	adhesion of blood cells	5.83E-05	11
	adhesion of epithelial cell lines	7.83E-05	4
	cell-cell adhesion of embryonic cell lines	9.16E-05	2
	attachment of cells	1.67E-04	6
	recruitment of neutrophils	1.69E-04	7
	activation of T lymphocytes	1.78E-04	10
	adhesion of muscle cells	1.78E-04	3
	cell-cell adhesion of epithelial cell lines	1.83E-04	2
	recruitment of phagocytes	2.14E-04	8
	aggregation of myoblasts	3.03E-04	2
	activation of lymphocytes	4.08E-04	11
	phagocytosis of cells	4.41E-04	8
	cell-cell adhesion of kidney cell lines	4.53E-04	2
	cell-cell adhesion of leukocytes	5.50E-04	3
	activation of endothelial cells	5.61E-04	4
	adhesion of fibrosarcoma cell lines	6.32E-04	2
	adhesion of stomach cancer cell lines	6.32E-04	2
	phagocytosis of leukemia cell lines	8.83E-04	3
	adhesion of endothelial cell lines	9.62E-04	3
	adhesion of carcinoma cell lines	1.13E-03	3

Bibliography

- Aberle, H., Schwartz, H., & Kemler, R. (1996). Cadherin-catenin complex: protein interactions and their implications for cadherin function. *J Cell Biochem*, 61(4), 514-523. doi: 10.1002/(SICI)1097-4644(19960616)61:4<514::AID-JCB4>3.0.CO;2-R
- Agrawal, N., Frederick, M. J., Pickering, C. R., Bettegowda, C., Chang, K., Li, R. J., . . . Myers, J. N. (2011). Exome sequencing of head and neck squamous cell carcinoma reveals inactivating mutations in NOTCH1. *Science*, 333(6046), 1154-1157. doi: 10.1126/science.1206923
- Alcolea, M. P., Greulich, P., Wabik, A., Frede, J., Simons, B. D., & Jones, P. H. (2014). Differentiation imbalance in single oesophageal progenitor cells causes clonal immortalization and field change. *Nat Cell Biol*, 16(6), 615-622. doi: 10.1038/ncb2963
- Ambler, C. A., & Maatta, A. (2009). Epidermal stem cells: location, potential and contribution to cancer. *J Pathol*, 217(2), 206-216. doi: 10.1002/path.2468
- Ambrosch, P. (2007). The role of laser microsurgery in the treatment of laryngeal cancer. *Curr Opin Otolaryngol Head Neck Surg*, 15(2), 82-88. doi: 10.1097/MOO.0b013e3280147336
- Argiris, A., Karamouzis, M. V., Raben, D., & Ferris, R. L. (2008). Head and neck cancer. *Lancet*, 371(9625), 1695-1709. doi: 10.1016/S0140-6736(08)60728-X
- Artavanis-Tsakonas, S., Rand, M. D., & Lake, R. J. (1999). Notch signaling: cell fate control and signal integration in development. *Science*, 284(5415), 770-776.
- Axelrod, H., & Pienta, K. J. (2014). Axl as a mediator of cellular growth and survival. *Oncotarget*, 5(19), 8818-8852.

- Balint, K., Xiao, M., Pinnix, C. C., Soma, A., Veres, I., Juhasz, I., . . . Liu, Z. J. (2005). Activation of Notch1 signaling is required for beta-catenin-mediated human primary melanoma progression. *J Clin Invest*, 115(11), 3166-3176. doi: 10.1172/JCI25001
- Barth, P. J., Schenck zu Schweinsberg, T., Ramaswamy, A., & Moll, R. (2004). CD34+ fibrocytes, alpha-smooth muscle antigen-positive myofibroblasts, and CD117 expression in the stroma of invasive squamous cell carcinomas of the oral cavity, pharynx, and larynx. *Virchows Arch*, 444(3), 231-234. doi: 10.1007/s00428-003-0965-1
- Bartolomei, M. S., Webber, A. L., Brunkow, M. E., & Tilghman, S. M. (1993). Epigenetic mechanisms underlying the imprinting of the mouse H19 gene. *Genes Dev*, 7(9), 1663-1673.
- Belandia, B., Powell, S. M., Garcia-Pedrero, J. M., Walker, M. M., Bevan, C. L., & Parker, M. G. (2005). Hey1, a mediator of notch signaling, is an androgen receptor corepressor. *Mol Cell Biol*, 25(4), 1425-1436. doi: 10.1128/MCB.25.4.1425-1436.2005
- Ben-Batalla, I., Schultze, A., Wroblewski, M., Erdmann, R., Heuser, M., Waizenegger, J. S., . . . Loges, S. (2013). Axl, a prognostic and therapeutic target in acute myeloid leukemia mediates paracrine crosstalk of leukemia cells with bone marrow stroma. *Blood*, 122(14), 2443-2452. doi: 10.1182/blood-2013-03-491431
- Berclaz, G., Altermatt, H. J., Rohrbach, V., Kieffer, I., Dreher, E., & Andres, A. C. (2001). Estrogen dependent expression of the receptor tyrosine kinase axl in normal and malignant human breast. *Ann Oncol*, 12(6), 819-824.

- Blanpain, C., & Fuchs, E. (2006). Epidermal stem cells of the skin. *Annu Rev Cell Dev Biol*, 22, 339-373. doi: 10.1146/annurev.cellbio.22.010305.104357
- Blanpain, C., & Fuchs, E. (2009). Epidermal homeostasis: a balancing act of stem cells in the skin. *Nat Rev Mol Cell Biol*, 10(3), 207-217. doi: 10.1038/nrm2636
- Blanpain, C., Lowry, W. E., Pasolli, H. A., & Fuchs, E. (2006). Canonical notch signaling functions as a commitment switch in the epidermal lineage. *Genes Dev*, 20(21), 3022-3035. doi: 10.1101/gad.1477606
- Blot, W. J., McLaughlin, J. K., Winn, D. M., Austin, D. F., Greenberg, R. S., Preston-Martin, S., . . . Fraumeni, J. F., Jr. (1988). Smoking and drinking in relation to oral and pharyngeal cancer. *Cancer Res*, 48(11), 3282-3287.
- Bonner, J. A., Harari, P. M., Giral, J., Cohen, R. B., Jones, C. U., Sur, R. K., . . . Ang, K. K. (2010). Radiotherapy plus cetuximab for locoregionally advanced head and neck cancer: 5-year survival data from a phase 3 randomised trial, and relation between cetuximab-induced rash and survival. *Lancet Oncol*, 11(1), 21-28. doi: 10.1016/S1470-2045(09)70311-0
- Boschelli, D. H., Barrios Sosa, A. C., Golas, J. M., & Boschelli, F. (2007). Inhibition of Src kinase activity by 7-ethynyl-4-phenylamino-3-quinolinecarbonitriles: identification of SKS-927. *Bioorg Med Chem Lett*, 17(5), 1358-1361. doi: 10.1016/j.bmcl.2006.11.077
- Boschelli, D. H., Wang, Y. D., Ye, F., Wu, B., Zhang, N., Dutia, M., . . . Boschelli, F. (2001). Synthesis and Src kinase inhibitory activity of a series of 4-phenylamino-3-quinolinecarbonitriles. *J Med Chem*, 44(5), 822-833.

- Bose, R., Molina, H., Patterson, A. S., Bitok, J. K., Periaswamy, B., Bader, J. S., . . . Cole, P. A. (2006). Phosphoproteomic analysis of Her2/neu signaling and inhibition. *Proc Natl Acad Sci U S A*, 103(26), 9773-9778. doi: 10.1073/pnas.0603948103
- Boyle, J. O., Hakim, J., Koch, W., van der Riet, P., Hruban, R. H., Roa, R. A., . . . Sidransky, D. (1993). The incidence of p53 mutations increases with progression of head and neck cancer. *Cancer Res*, 53(19), 4477-4480.
- Brand, T. M., Iida, M., Stein, A. P., Corrigan, K. L., Braverman, C. M., Coan, J. P., . . . Wheeler, D. L. (2015). AXL Is a Logical Molecular Target in Head and Neck Squamous Cell Carcinoma. *Clin Cancer Res*, 21(11), 2601-2612. doi: 10.1158/1078-0432.CCR-14-2648
- Bray, F., Sankila, R., Ferlay, J., & Parkin, D. M. (2002). Estimates of cancer incidence and mortality in Europe in 1995. *Eur J Cancer*, 38(1), 99-166.
- Bray, S. J. (2006). Notch signalling: a simple pathway becomes complex. *Nat Rev Mol Cell Biol*, 7(9), 678-689. doi: 10.1038/nrm2009
- Burridge, K., Chrzanowska-Wodnicka, M., & Zhong, C. (1997). Focal adhesion assembly. *Trends Cell Biol*, 7(9), 342-347. doi: 10.1016/S0962-8924(97)01127-6
- Byers, L. A., Diao, L., Wang, J., Saintigny, P., Girard, L., Peyton, M., . . . Heymach, J. V. (2013). An epithelial-mesenchymal transition gene signature predicts resistance to EGFR and PI3K inhibitors and identifies Axl as a therapeutic target for overcoming EGFR inhibitor resistance. *Clin Cancer Res*, 19(1), 279-290. doi: 10.1158/1078-0432.CCR-12-1558

- Califano, J., van der Riet, P., Westra, W., Nawroz, H., Clayman, G., Piantadosi, S., . . . Sidransky, D. (1996). Genetic progression model for head and neck cancer: implications for field cancerization. *Cancer Res*, 56(11), 2488-2492.
- Califano, J., Westra, W. H., Meininger, G., Corio, R., Koch, W. M., & Sidransky, D. (2000). Genetic progression and clonal relationship of recurrent premalignant head and neck lesions. *Clin Cancer Res*, 6(2), 347-352.
- Camenisch, T. D., Koller, B. H., Earp, H. S., & Matsushima, G. K. (1999). A novel receptor tyrosine kinase, Mer, inhibits TNF- α production and lipopolysaccharide-induced endotoxic shock. *J Immunol*, 162(6), 3498-3503.
- Cao, C., Chen, Y., Masood, R., Sinha, U. K., & Kobiak, A. (2012). α -Catulin marks the invasion front of squamous cell carcinoma and is important for tumor cell metastasis. *Mol Cancer Res*, 10(7), 892-903. doi: 10.1158/1541-7786.MCR-12-0169
- Carlone, D. L., Lee, J. H., Young, S. R., Dobrota, E., Butler, J. S., Ruiz, J., & Skalik, D. G. (2005). Reduced genomic cytosine methylation and defective cellular differentiation in embryonic stem cells lacking CpG binding protein. *Mol Cell Biol*, 25(12), 4881-4891. doi: 10.1128/MCB.25.12.4881-4891.2005
- Castella, P., Sawai, S., Nakao, K., Wagner, J. A., & Caudy, M. (2000). HES-1 repression of differentiation and proliferation in PC12 cells: role for the helix 3-helix 4 domain in transcription repression. *Mol Cell Biol*, 20(16), 6170-6183.
- Castro, N. P., Fedorova-Abrams, N. D., Merchant, A. S., Rangel, M. C., Nagaoka, T., Karasawa, H., . . . Salomon, D. S. (2015). Cripto-1 as a novel therapeutic target for triple negative breast cancer. *Oncotarget*, 6(14), 11910-11929.

- Cerchia, L., Esposito, C. L., Camorani, S., Rienzo, A., Stasio, L., Insabato, L., . . . de Franciscis, V. (2012). Targeting Axl with an high-affinity inhibitory aptamer. *Mol Ther*, 20(12), 2291-2303. doi: 10.1038/mt.2012.163
- Chen, C., Liu, Y., Rappaport, A. R., Kitzing, T., Schultz, N., Zhao, Z., . . . Lowe, S. W. (2014). MLL3 is a haploinsufficient 7q tumor suppressor in acute myeloid leukemia. *Cancer Cell*, 25(5), 652-665. doi: 10.1016/j.ccr.2014.03.016
- Chen, P. M., Yen, C. C., Wang, W. S., Lin, Y. J., Chu, C. J., Chiou, T. J., . . . Yang, M. H. (2008). Down-regulation of Notch-1 expression decreases PU.1-mediated myeloid differentiation signaling in acute myeloid leukemia. *Int J Oncol*, 32(6), 1335-1341.
- Chen, S., Sanjana, N. E., Zheng, K., Shalem, O., Lee, K., Shi, X., . . . Sharp, P. A. (2015). Genome-wide CRISPR screen in a mouse model of tumor growth and metastasis. *Cell*, 160(6), 1246-1260. doi: 10.1016/j.cell.2015.02.038
- Chu, J., Jeffries, S., Norton, J. E., Capobianco, A. J., & Bresnick, E. H. (2002). Repression of activator protein-1-mediated transcriptional activation by the Notch-1 intracellular domain. *J Biol Chem*, 277(9), 7587-7597. doi: 10.1074/jbc.M111044200
- Colevas, A. D. (2006). Chemotherapy options for patients with metastatic or recurrent squamous cell carcinoma of the head and neck. *J Clin Oncol*, 24(17), 2644-2652. doi: 10.1200/JCO.2005.05.3348
- Cordle, J., Johnson, S., Tay, J. Z., Roversi, P., Wilkin, M. B., de Madrid, B. H., . . . Handford, P. A. (2008). A conserved face of the Jagged/Serrate DSL domain is

- involved in Notch trans-activation and cis-inhibition. *Nat Struct Mol Biol*, 15(8), 849-857. doi: 10.1038/nsmb.1457
- D'Alfonso, T. M., Hannah, J., Chen, Z., Liu, Y., Zhou, P., & Shin, S. J. (2014). Axl receptor tyrosine kinase expression in breast cancer. *J Clin Pathol*, 67(8), 690-696. doi: 10.1136/jclinpath-2013-202161
- D'Souza, B., Miyamoto, A., & Weinmaster, G. (2008). The many facets of Notch ligands. *Oncogene*, 27(38), 5148-5167. doi: 10.1038/onc.2008.229
- D'Souza, G., & Dempsey, A. (2011). The role of HPV in head and neck cancer and review of the HPV vaccine. *Prev Med*, 53 Suppl 1, S5-S11. doi: 10.1016/j.ypmed.2011.08.001
- D'Souza, G., Kreimer, A. R., Viscidi, R., Pawlita, M., Fakhry, C., Koch, W. M., . . . Gillison, M. L. (2007). Case-control study of human papillomavirus and oropharyngeal cancer. *N Engl J Med*, 356(19), 1944-1956. doi: 10.1056/NEJMoa065497
- Dai, M. Y., Fang, F., Zou, Y., Yi, X., Ding, Y. J., Chen, C., . . . Chen, S. M. (2015). Downregulation of Notch1 induces apoptosis and inhibits cell proliferation and metastasis in laryngeal squamous cell carcinoma. *Oncol Rep*. doi: 10.3892/or.2015.4274
- de La Coste, A., Six, E., Fazilleau, N., Mascarell, L., Legrand, N., Mailhe, M. P., . . . Freitas, A. A. (2005). In vivo and in absence of a thymus, the enforced expression of the Notch ligands delta-1 or delta-4 promotes T cell development with specific unique effects. *J Immunol*, 174(5), 2730-2737.

- Demehri, S., & Kopan, R. (2009). Notch signaling in bulge stem cells is not required for selection of hair follicle fate. *Development*, 136(6), 891-896. doi: 10.1242/dev.030700
- Demehri, S., Liu, Z., Lee, J., Lin, M. H., Crosby, S. D., Roberts, C. J., . . . Kopan, R. (2008). Notch-deficient skin induces a lethal systemic B-lymphoproliferative disorder by secreting TSLP, a sentinel for epidermal integrity. *PLoS Biol*, 6(5), e123. doi: 10.1371/journal.pbio.0060123
- Demehri, S., Turkoz, A., & Kopan, R. (2009). Epidermal Notch1 loss promotes skin tumorigenesis by impacting the stromal microenvironment. *Cancer Cell*, 16(1), 55-66. doi: 10.1016/j.ccr.2009.05.016
- Demokan, S., Chuang, A., Suoglu, Y., Ulsan, M., Yalniz, Z., Califano, J. A., & Dalay, N. (2012). Promoter methylation and loss of p16(INK4a) gene expression in head and neck cancer. *Head Neck*, 34(10), 1470-1475. doi: 10.1002/hed.21949
- Devgan, V., Mammucari, C., Millar, S. E., Briskin, C., & Dotto, G. P. (2005). p21WAF1/Cip1 is a negative transcriptional regulator of Wnt4 expression downstream of Notch1 activation. *Genes Dev*, 19(12), 1485-1495. doi: 10.1101/gad.341405
- Dotto, G. P. (2008). Notch tumor suppressor function. *Oncogene*, 27(38), 5115-5123. doi: 10.1038/onc.2008.225
- Dunne, P. D., McArt, D. G., Blayney, J. K., Kalimutho, M., Greer, S., Wang, T., . . . Van Schaeybroeck, S. (2014). AXL is a key regulator of inherent and chemotherapy-induced invasion and predicts a poor clinical outcome in early-stage colon cancer. *Clin Cancer Res*, 20(1), 164-175. doi: 10.1158/1078-0432.CCR-13-1354

- Efimova, T., LaCelle, P., Welter, J. F., & Eckert, R. L. (1998). Regulation of human involucrin promoter activity by a protein kinase C, Ras, MEKK1, MEK3, p38/RK, AP1 signal transduction pathway. *J Biol Chem*, 273(38), 24387-24395.
- Egloff, A. M., & Grandis, J. R. (2012). Molecular pathways: context-dependent approaches to Notch targeting as cancer therapy. *Clin Cancer Res*, 18(19), 5188-5195. doi: 10.1158/1078-0432.CCR-11-2258
- Ellisen, L. W., Bird, J., West, D. C., Soreng, A. L., Reynolds, T. C., Smith, S. D., & Sklar, J. (1991). TAN-1, the human homolog of the *Drosophila* notch gene, is broken by chromosomal translocations in T lymphoblastic neoplasms. *Cell*, 66(4), 649-661.
- Fabbri, G., Rasi, S., Rossi, D., Trifonov, V., Khiabani, H., Ma, J., . . . Gaidano, G. (2011). Analysis of the chronic lymphocytic leukemia coding genome: role of NOTCH1 mutational activation. *J Exp Med*, 208(7), 1389-1401. doi: 10.1084/jem.20110921
- Fabian, A., Barok, M., Vereb, G., & Szollosi, J. (2009). Die hard: are cancer stem cells the Bruce Willises of tumor biology? *Cytometry A*, 75(1), 67-74. doi: 10.1002/cyto.a.20690
- Fan, L. C., Chiang, W. F., Liang, C. H., Tsai, Y. T., Wong, T. Y., Chen, K. C., . . . Chen, Y. L. (2011). alpha-Catulin knockdown induces senescence in cancer cells. *Oncogene*, 30(23), 2610-2621. doi: 10.1038/onc.2010.637
- Fischer, A., Klattig, J., Kneitz, B., Diez, H., Maier, M., Holtmann, B., . . . Gessler, M. (2005). Hey basic helix-loop-helix transcription factors are repressors of GATA4

- and GATA6 and restrict expression of the GATA target gene ANF in fetal hearts. *Mol Cell Biol*, 25(20), 8960-8970. doi: 10.1128/MCB.25.20.8960-8970.2005
- Fleuren, E. D., Hillebrandt-Roeffen, M. H., Flucke, U. E., Te Loo, D. M., Boerman, O. C., van der Graaf, W. T., & Versleijen-Jonkers, Y. M. (2014). The role of AXL and the in vitro activity of the receptor tyrosine kinase inhibitor BGB324 in Ewing sarcoma. *Oncotarget*, 5(24), 12753-12768.
- Flores, A. N., McDermott, N., Meunier, A., & Marignol, L. (2014). NUMB inhibition of NOTCH signalling as a therapeutic target in prostate cancer. *Nat Rev Urol*, 11(9), 499-507. doi: 10.1038/nrurol.2014.195
- Foulkes, W. D., Brunet, J. S., Sieh, W., Black, M. J., Shenouda, G., & Narod, S. A. (1996). Familial risks of squamous cell carcinoma of the head and neck: retrospective case-control study. *BMJ*, 313(7059), 716-721.
- Fridell, Y. W., Jin, Y., Quilliam, L. A., Burchert, A., McCloskey, P., Spizz, G., . . . Liu, E. T. (1996). Differential activation of the Ras/extracellular-signal-regulated protein kinase pathway is responsible for the biological consequences induced by the Axl receptor tyrosine kinase. *Mol Cell Biol*, 16(1), 135-145.
- Frise, E., Knoblich, J. A., Younger-Shepherd, S., Jan, L. Y., & Jan, Y. N. (1996). The Drosophila Numb protein inhibits signaling of the Notch receptor during cell-cell interaction in sensory organ lineage. *Proc Natl Acad Sci U S A*, 93(21), 11925-11932.
- Fuchs, E., & Raghavan, S. (2002). Getting under the skin of epidermal morphogenesis. *Nat Rev Genet*, 3(3), 199-209. doi: 10.1038/nrg758

- Gallahan, D., Kozak, C., & Callahan, R. (1987). A new common integration region (int-3) for mouse mammary tumor virus on mouse chromosome 17. *J Virol*, 61(1), 218-220.
- Georgia, S., Soliz, R., Li, M., Zhang, P., & Bhushan, A. (2006). p57 and Hes1 coordinate cell cycle exit with self-renewal of pancreatic progenitors. *Dev Biol*, 298(1), 22-31. doi: 10.1016/j.ydbio.2006.05.036
- Giles, K. M., Kalinowski, F. C., Candy, P. A., Epis, M. R., Zhang, P. M., Redfern, A. D., . . . Leedman, P. J. (2013). Axl mediates acquired resistance of head and neck cancer cells to the epidermal growth factor receptor inhibitor erlotinib. *Mol Cancer Ther*, 12(11), 2541-2558. doi: 10.1158/1535-7163.MCT-13-0170
- Gjerdrum, C., Tiron, C., Hoiby, T., Stefansson, I., Haugen, H., Sandal, T., . . . Lorens, J. B. (2010). Axl is an essential epithelial-to-mesenchymal transition-induced regulator of breast cancer metastasis and patient survival. *Proc Natl Acad Sci U S A*, 107(3), 1124-1129. doi: 10.1073/pnas.0909333107
- Gould, F., Harrison, S. M., Hewitt, E. W., & Whitehouse, A. (2009). Kaposi's sarcoma-associated herpesvirus RTA promotes degradation of the Hey1 repressor protein through the ubiquitin proteasome pathway. *J Virol*, 83(13), 6727-6738. doi: 10.1128/JVI.00351-09
- Graham, D. K., Dawson, T. L., Mullaney, D. L., Snodgrass, H. R., & Earp, H. S. (1994). Cloning and mRNA expression analysis of a novel human protooncogene, c-mer. *Cell Growth Differ*, 5(6), 647-657.

- Graham, D. K., DeRyckere, D., Davies, K. D., & Earp, H. S. (2014). The TAM family: phosphatidylserine sensing receptor tyrosine kinases gone awry in cancer. *Nat Rev Cancer*, 14(12), 769-785.
- Grandis, J. R., & Tweardy, D. J. (1993). Elevated levels of transforming growth factor alpha and epidermal growth factor receptor messenger RNA are early markers of carcinogenesis in head and neck cancer. *Cancer Res*, 53(15), 3579-3584.
- Gschwind, A., Fischer, O. M., & Ullrich, A. (2004). The discovery of receptor tyrosine kinases: targets for cancer therapy. *Nat Rev Cancer*, 4(5), 361-370. doi: 10.1038/nrc1360
- Ha, P. K., Benoit, N. E., Yochem, R., Sciubba, J., Zahurak, M., Sidransky, D., . . . Califano, J. (2003). A transcriptional progression model for head and neck cancer. *Clin Cancer Res*, 9(8), 3058-3064.
- Hadland, B. K., Manley, N. R., Su, D., Longmore, G. D., Moore, C. L., Wolfe, M. S., . . . Kopan, R. (2001). Gamma -secretase inhibitors repress thymocyte development. *Proc Natl Acad Sci U S A*, 98(13), 7487-7491. doi: 10.1073/pnas.131202798
- Hafizi, S., & Dahlback, B. (2006). Gas6 and protein S. Vitamin K-dependent ligands for the Axl receptor tyrosine kinase subfamily. *FEBS J*, 273(23), 5231-5244. doi: 10.1111/j.1742-4658.2006.05529.x
- Haines, N., & Irvine, K. D. (2003). Glycosylation regulates Notch signalling. *Nat Rev Mol Cell Biol*, 4(10), 786-797. doi: 10.1038/nrm1228
- Hallahan, A. R., Pritchard, J. I., Hansen, S., Benson, M., Stoeck, J., Hatton, B. A., . . . Olson, J. M. (2004). The SmoA1 mouse model reveals that notch signaling is

- critical for the growth and survival of sonic hedgehog-induced medulloblastomas. *Cancer Res*, 64(21), 7794-7800. doi: 10.1158/0008-5472.CAN-04-1813
- Han, H., Tanigaki, K., Yamamoto, N., Kuroda, K., Yoshimoto, M., Nakahata, T., . . . Honjo, T. (2002). Inducible gene knockout of transcription factor recombination signal binding protein-J reveals its essential role in T versus B lineage decision. *Int Immunol*, 14(6), 637-645.
- Han, J., Tian, R., Yong, B., Luo, C., Tan, P., Shen, J., & Peng, T. (2013). Gas6/Axl mediates tumor cell apoptosis, migration and invasion and predicts the clinical outcome of osteosarcoma patients. *Biochem Biophys Res Commun*, 435(3), 493-500. doi: 10.1016/j.bbrc.2013.05.019
- Hanahan, D., & Weinberg, R. A. (2011). Hallmarks of cancer: the next generation. *Cell*, 144(5), 646-674. doi: 10.1016/j.cell.2011.02.013
- Hartman, J., Muller, P., Foster, J. S., Wimalasena, J., Gustafsson, J. A., & Strom, A. (2004). HES-1 inhibits 17beta-estradiol and heregulin-beta1-mediated upregulation of E2F-1. *Oncogene*, 23(54), 8826-8833. doi: 10.1038/sj.onc.1208139
- Hashibe, M., Boffetta, P., Zaridze, D., Shangina, O., Szeszenia-Dabrowska, N., Mates, D., . . . Brennan, P. (2006). Evidence for an important role of alcohol- and aldehyde-metabolizing genes in cancers of the upper aerodigestive tract. *Cancer Epidemiol Biomarkers Prev*, 15(4), 696-703. doi: 10.1158/1055-9965.EPI-05-0710
- Heckl, D., Kowalczyk, M. S., Yudovich, D., Belizaire, R., Puram, R. V., McConkey, M. E., . . . Ebert, B. L. (2014). Generation of mouse models of myeloid malignancy

- with combinatorial genetic lesions using CRISPR-Cas9 genome editing. *Nat Biotechnol*, 32(9), 941-946. doi: 10.1038/nbt.2951
- Heisig, J., Weber, D., Englberger, E., Winkler, A., Kneitz, S., Sung, W. K., . . . Gessler, M. (2012). Target gene analysis by microarrays and chromatin immunoprecipitation identifies HEY proteins as highly redundant bHLH repressors. *PLoS Genet*, 8(5), e1002728. doi: 10.1371/journal.pgen.1002728
- Hobbs, C. G., Sterne, J. A., Bailey, M., Heyderman, R. S., Birchall, M. A., & Thomas, S. J. (2006). Human papillomavirus and head and neck cancer: a systematic review and meta-analysis. *Clin Otolaryngol*, 31(4), 259-266. doi: 10.1111/j.1749-4486.2006.01246.x
- Hoffmann, K., Matthes, U., Stucker, M., Segerling, M., & Altmeyer, P. (1990). [1989 Bochum health education program for malignant melanoma]. *Offentl Gesundheitswes*, 52(1), 9-13.
- Hogg, R. P., Honorio, S., Martinez, A., Agathangelou, A., Dallol, A., Fullwood, P., . . . Latif, F. (2002). Frequent 3p allele loss and epigenetic inactivation of the RASSF1A tumour suppressor gene from region 3p21.3 in head and neck squamous cell carcinoma. *Eur J Cancer*, 38(12), 1585-1592.
- Holland, S. J., Pan, A., Franci, C., Hu, Y., Chang, B., Li, W., . . . Hitoshi, Y. (2010). R428, a selective small molecule inhibitor of Axl kinase, blocks tumor spread and prolongs survival in models of metastatic breast cancer. *Cancer Res*, 70(4), 1544-1554. doi: 10.1158/0008-5472.CAN-09-2997
- Holland, S. J., Powell, M. J., Franci, C., Chan, E. W., Frieri, A. M., Atchison, R. E., . . . Lorens, J. B. (2005). Multiple roles for the receptor tyrosine kinase axl in tumor

- formation. *Cancer Res*, 65(20), 9294-9303. doi: 10.1158/0008-5472.CAN-05-0993
- Hong, C. C., Lay, J. D., Huang, J. S., Cheng, A. L., Tang, J. L., Lin, M. T., . . . Chuang, S. E. (2008). Receptor tyrosine kinase AXL is induced by chemotherapy drugs and overexpression of AXL confers drug resistance in acute myeloid leukemia. *Cancer Lett*, 268(2), 314-324. doi: 10.1016/j.canlet.2008.04.017
- Hozumi, K., Abe, N., Chiba, S., Hirai, H., & Habu, S. (2003). Active form of Notch members can enforce T lymphopoiesis on lymphoid progenitors in the monolayer culture specific for B cell development. *J Immunol*, 170(10), 4973-4979.
- Huang, M., Rigby, A. C., Morelli, X., Grant, M. A., Huang, G., Furie, B., . . . Furie, B. C. (2003). Structural basis of membrane binding by Gla domains of vitamin K-dependent proteins. *Nat Struct Biol*, 10(9), 751-756. doi: 10.1038/nsb971
- Jaleco, A. C., Neves, H., Hooijberg, E., Gameiro, P., Clode, N., Haury, M., . . . Parreira, L. (2001). Differential effects of Notch ligands Delta-1 and Jagged-1 in human lymphoid differentiation. *J Exp Med*, 194(7), 991-1002.
- Janes, S. M., & Watt, F. M. (2006). New roles for integrins in squamous-cell carcinoma. *Nat Rev Cancer*, 6(3), 175-183. doi: 10.1038/nrc1817
- Janssens, B., Staes, K., & van Roy, F. (1999). Human alpha-catulin, a novel alpha-catenin-like molecule with conserved genomic structure, but deviating alternative splicing. *Biochim Biophys Acta*, 1447(2-3), 341-347.
- Jin, S., Mutvei, A. P., Chivukula, I. V., Andersson, E. R., Ramskold, D., Sandberg, R., . . . Lendahl, U. (2013). Non-canonical Notch signaling activates IL-6/JAK/STAT

- signaling in breast tumor cells and is controlled by p53 and IKK α /IKK β .
Oncogene, 32(41), 4892-4902. doi: 10.1038/onc.2012.517
- Kagawa, S., Natsuizaka, M., Whelan, K. A., Facompre, N., Naganuma, S., Ohashi, S., . . . Nakagawa, H. (2015). Cellular senescence checkpoint function determines differential Notch1-dependent oncogenic and tumor-suppressor activities.
Oncogene, 34(18), 2347-2359. doi: 10.1038/onc.2014.169
- Kageyama, R., Ohtsuka, T., Hatakeyama, J., & Ohsawa, R. (2005). Roles of bHLH genes in neural stem cell differentiation. *Exp Cell Res*, 306(2), 343-348. doi: 10.1016/j.yexcr.2005.03.015
- Kannan, S., Fang, W., Song, G., Mullighan, C. G., Hammitt, R., McMurray, J., & Zweidler-McKay, P. A. (2011). Notch/HES1-mediated PARP1 activation: a cell type-specific mechanism for tumor suppression. *Blood*, 117(10), 2891-2900. doi: 10.1182/blood-2009-12-253419
- Kannan, S., Sutphin, R. M., Hall, M. G., Golfman, L. S., Fang, W., Nolo, R. M., . . . Zweidler-McKay, P. A. (2013). Notch activation inhibits AML growth and survival: a potential therapeutic approach. *J Exp Med*, 210(2), 321-337. doi: 10.1084/jem.20121527
- Karamouzis, M. V., Grandis, J. R., & Argiris, A. (2007). Therapies directed against epidermal growth factor receptor in aerodigestive carcinomas. *JAMA*, 298(1), 70-82. doi: 10.1001/jama.298.1.70
- Katoh, M., & Katoh, M. (2007). Integrative genomic analyses on HES/HEY family: Notch-independent HES1, HES3 transcription in undifferentiated ES cells, and

- Notch-dependent HES1, HES5, HEY1, HEY2, HEYL transcription in fetal tissues, adult tissues, or cancer. *Int J Oncol*, 31(2), 461-466.
- Keating, A. K., Kim, G. K., Jones, A. E., Donson, A. M., Ware, K., Mulcahy, J. M., . . . Graham, D. K. (2010). Inhibition of Mer and Axl receptor tyrosine kinases in astrocytoma cells leads to increased apoptosis and improved chemosensitivity. *Mol Cancer Ther*, 9(5), 1298-1307. doi: 10.1158/1535-7163.MCT-09-0707
- Keri, G., Szekelyhidi, Z., Banhegyi, P., Varga, Z., Hegymegi-Barakonyi, B., Szantai-Kis, C., . . . Orfi, L. (2005). Drug discovery in the kinase inhibitory field using the Nested Chemical Library technology. *Assay Drug Dev Technol*, 3(5), 543-551. doi: 10.1089/adt.2005.3.543
- Keyes, W. M., Wu, Y., Vogel, H., Guo, X., Lowe, S. W., & Mills, A. A. (2005). p63 deficiency activates a program of cellular senescence and leads to accelerated aging. *Genes Dev*, 19(17), 1986-1999. doi: 10.1101/gad.342305
- King, K. E., Ponnamperna, R. M., Yamashita, T., Tokino, T., Lee, L. A., Young, M. F., & Weinberg, W. C. (2003). deltaNp63alpha functions as both a positive and a negative transcriptional regulator and blocks in vitro differentiation of murine keratinocytes. *Oncogene*, 22(23), 3635-3644. doi: 10.1038/sj.onc.1206536
- Kobayashi, T., & Kageyama, R. (2014). Expression dynamics and functions of Hes factors in development and diseases. *Curr Top Dev Biol*, 110, 263-283. doi: 10.1016/B978-0-12-405943-6.00007-5
- Kobayashi, T., Mizuno, H., Imayoshi, I., Furusawa, C., Shirahige, K., & Kageyama, R. (2009). The cyclic gene Hes1 contributes to diverse differentiation responses of embryonic stem cells. *Genes Dev*, 23(16), 1870-1875. doi: 10.1101/gad.1823109

- Kode, A., Manavalan, J. S., Mosialou, I., Bhagat, G., Rathinam, C. V., Luo, N., . . .
- Kousteni, S. (2014). Leukaemogenesis induced by an activating beta-catenin mutation in osteoblasts. *Nature*, *506*(7487), 240-244. doi: 10.1038/nature12883
- Kojc, N., Zidar, N., Vodopivec, B., & Gale, N. (2005). Expression of CD34, alpha-smooth muscle actin, and transforming growth factor beta1 in squamous intraepithelial lesions and squamous cell carcinoma of the larynx and hypopharynx. *Hum Pathol*, *36*(1), 16-21. doi: 10.1016/j.humpath.2004.10.011
- Konski, A., Watkins-Bruner, D., Feigenberg, S., Hanlon, A., Kulkarni, S., Beck, J. R., . . .
- Pollack, A. (2006). Using decision analysis to determine the cost-effectiveness of intensity-modulated radiation therapy in the treatment of intermediate risk prostate cancer. *Int J Radiat Oncol Biol Phys*, *66*(2), 408-415. doi: 10.1016/j.ijrobp.2006.04.049
- Kopan, R., & Ilagan, M. X. (2009). The canonical Notch signaling pathway: unfolding the activation mechanism. *Cell*, *137*(2), 216-233. doi: 10.1016/j.cell.2009.03.045
- Kraman, M., & McCright, B. (2005). Functional conservation of Notch1 and Notch2 intracellular domains. *FASEB J*, *19*(10), 1311-1313. doi: 10.1096/fj.04-3407fje
- Kreimer, A. R., Clifford, G. M., Boyle, P., & Franceschi, S. (2005). Human papillomavirus types in head and neck squamous cell carcinomas worldwide: a systematic review. *Cancer Epidemiol Biomarkers Prev*, *14*(2), 467-475. doi: 10.1158/1055-9965.EPI-04-0551
- Kreiseder, B., Holper-Schichl, Y. M., Muellauer, B., Jacobi, N., Pretsch, A., Schmid, J. A., . . . Wiesner, C. (2015). Alpha-catulin contributes to drug-resistance of

- melanoma by activating NF-kappaB and AP-1. *PLoS One*, 10(3), e0119402. doi: 10.1371/journal.pone.0119402
- Kreiseder, B., Orel, L., Bujnow, C., Buschek, S., Pflueger, M., Schuett, W., . . . Wiesner, C. (2013). alpha-Catulin downregulates E-cadherin and promotes melanoma progression and invasion. *Int J Cancer*, 132(3), 521-530. doi: 10.1002/ijc.27698
- Kurokawa, A., Nagata, M., Kitamura, N., Noman, A. A., Ohnishi, M., Ohyama, T., . . . Surgery, G. (2008). Diagnostic value of integrin alpha3, beta4, and beta5 gene expression levels for the clinical outcome of tongue squamous cell carcinoma. *Cancer*, 112(6), 1272-1281. doi: 10.1002/cncr.23295
- Kurooka, H., Kuroda, K., & Honjo, T. (1998). Roles of the ankyrin repeats and C-terminal region of the mouse notch1 intracellular region. *Nucleic Acids Res*, 26(23), 5448-5455.
- Lai, C., & Lemke, G. (1991). An extended family of protein-tyrosine kinase genes differentially expressed in the vertebrate nervous system. *Neuron*, 6(5), 691-704.
- Le Borgne, R. (2006). Regulation of Notch signalling by endocytosis and endosomal sorting. *Curr Opin Cell Biol*, 18(2), 213-222. doi: 10.1016/j.ceb.2006.02.011
- Lee, C. H., Yen, C. Y., Liu, S. Y., Chen, C. K., Chiang, C. F., Shiah, S. G., . . . Shieh, Y. S. (2012). Axl is a prognostic marker in oral squamous cell carcinoma. *Ann Surg Oncol*, 19 Suppl 3, S500-508. doi: 10.1245/s10434-011-1985-8
- Lee, J. C., Smith, S. B., Watada, H., Lin, J., Scheel, D., Wang, J., . . . German, M. S. (2001). Regulation of the pancreatic pro-endocrine gene neurogenin3. *Diabetes*, 50(5), 928-936.

- Lefebvre, J. L. (2006). Laryngeal preservation in head and neck cancer: multidisciplinary approach. *Lancet Oncol*, 7(9), 747-755. doi: 10.1016/S1470-2045(06)70860-9
- Lefort, K., Mandinova, A., Ostano, P., Kolev, V., Calpini, V., Kolfschoten, I., . . . Dotto, G. P. (2007). Notch1 is a p53 target gene involved in human keratinocyte tumor suppression through negative regulation of ROCK1/2 and MRCKalpha kinases. *Genes Dev*, 21(5), 562-577. doi: 10.1101/gad.1484707
- Li, H., Wawrose, J. S., Gooding, W. E., Garraway, L. A., Lui, V. W., Peyser, N. D., & Grandis, J. R. (2014). Genomic analysis of head and neck squamous cell carcinoma cell lines and human tumors: a rational approach to preclinical model selection. *Mol Cancer Res*, 12(4), 571-582. doi: 10.1158/1541-7786.MCR-13-0396
- Li, L., & Clevers, H. (2010). Coexistence of quiescent and active adult stem cells in mammals. *Science*, 327(5965), 542-545. doi: 10.1126/science.1180794
- Li, L., & Neaves, W. B. (2006). Normal stem cells and cancer stem cells: the niche matters. *Cancer Res*, 66(9), 4553-4557. doi: 10.1158/0008-5472.CAN-05-3986
- Liang, C. H., Chiu, S. Y., Hsu, I. L., Wu, Y. Y., Tsai, Y. T., Ke, J. Y., . . . Hong, T. M. (2013). alpha-Catulin drives metastasis by activating ILK and driving an alphavbeta3 integrin signaling axis. *Cancer Res*, 73(1), 428-438. doi: 10.1158/0008-5472.CAN-12-2095
- Liao, W. R., Hsieh, R. H., Hsu, K. W., Wu, M. Z., Tseng, M. J., Mai, R. T., . . . Yeh, T. S. (2007). The CBF1-independent Notch1 signal pathway activates human c-myc expression partially via transcription factor YY1. *Carcinogenesis*, 28(9), 1867-1876. doi: 10.1093/carcin/bgm092

- Ling, L., Templeton, D., & Kung, H. J. (1996). Identification of the major autophosphorylation sites of Nyk/Mer, an NCAM-related receptor tyrosine kinase. *J Biol Chem*, 271(31), 18355-18362.
- Linger, R. M., Cohen, R. A., Cummings, C. T., Sather, S., Migdall-Wilson, J., Middleton, D. H., . . . Graham, D. K. (2013). Mer or Axl receptor tyrosine kinase inhibition promotes apoptosis, blocks growth and enhances chemosensitivity of human non-small cell lung cancer. *Oncogene*, 32(29), 3420-3431. doi: 10.1038/onc.2012.355
- Liu, E., Hjelle, B., & Bishop, J. M. (1988). Transforming genes in chronic myelogenous leukemia. *Proc Natl Acad Sci U S A*, 85(6), 1952-1956.
- Liu, Z. J., Xiao, M., Balint, K., Smalley, K. S., Brafford, P., Qiu, R., . . . Herlyn, M. (2006). Notch1 signaling promotes primary melanoma progression by activating mitogen-activated protein kinase/phosphatidylinositol 3-kinase-Akt pathways and up-regulating N-cadherin expression. *Cancer Res*, 66(8), 4182-4190. doi: 10.1158/0008-5472.CAN-05-3589
- Lobry, C., Oh, P., & Aifantis, I. (2011). Oncogenic and tumor suppressor functions of Notch in cancer: it's NOTCH what you think. *J Exp Med*, 208(10), 1931-1935. doi: 10.1084/jem.20111855
- Lu, J. G., Sun, Y. N., Wang, C., Jin de, J., & Liu, M. (2009). Role of the alpha v-integrin subunit in cell proliferation, apoptosis and tumor metastasis of laryngeal and hypopharyngeal squamous cell carcinomas: a clinical and in vitro investigation. *Eur Arch Otorhinolaryngol*, 266(1), 89-96. doi: 10.1007/s00405-008-0675-z

- Lubman, O. Y., Korolev, S. V., & Kopan, R. (2004). Anchoring notch genetics and biochemistry; structural analysis of the ankyrin domain sheds light on existing data. *Mol Cell*, 13(5), 619-626.
- Luo, B., Aster, J. C., Hasserjian, R. P., Kuo, F., & Sklar, J. (1997). Isolation and functional analysis of a cDNA for human Jagged2, a gene encoding a ligand for the Notch1 receptor. *Mol Cell Biol*, 17(10), 6057-6067.
- Mackiewicz, M., Huppi, K., Pitt, J. J., Dorsey, T. H., Ambs, S., & Caplen, N. J. (2011). Identification of the receptor tyrosine kinase AXL in breast cancer as a target for the human miR-34a microRNA. *Breast Cancer Res Treat*, 130(2), 663-679. doi: 10.1007/s10549-011-1690-0
- Malecki, M. J., Sanchez-Irizarry, C., Mitchell, J. L., Histen, G., Xu, M. L., Aster, J. C., & Blacklow, S. C. (2006). Leukemia-associated mutations within the NOTCH1 heterodimerization domain fall into at least two distinct mechanistic classes. *Mol Cell Biol*, 26(12), 4642-4651. doi: 10.1128/MCB.01655-05
- Manohar, A., Shome, S. G., Lamar, J., Stirling, L., Iyer, V., Pumiglia, K., & DiPersio, C. M. (2004). Alpha 3 beta 1 integrin promotes keratinocyte cell survival through activation of a MEK/ERK signaling pathway. *J Cell Sci*, 117(Pt 18), 4043-4054. doi: 10.1242/jcs.01277
- Mao, L., Fan, Y. H., Lotan, R., & Hong, W. K. (1996). Frequent abnormalities of FHIT, a candidate tumor suppressor gene, in head and neck cancer cell lines. *Cancer Res*, 56(22), 5128-5131.
- Maris, J. M., & Matthay, K. K. (1999). Molecular biology of neuroblastoma. *J Clin Oncol*, 17(7), 2264-2279.

- Mercher, T., Raffel, G. D., Moore, S. A., Cornejo, M. G., Baudry-Bluteau, D., Cagnard, N., . . . Gilliland, D. G. (2009). The OTT-MAL fusion oncogene activates RBPJ-mediated transcription and induces acute megakaryoblastic leukemia in a knockin mouse model. *J Clin Invest*, *119*(4), 852-864. doi: 10.1172/JCI35901
- Merdek, K. D., Nguyen, N. T., & Toksoz, D. (2004). Distinct activities of the alpha-catenin family, alpha-catenin and alpha-catenin, on beta-catenin-mediated signaling. *Mol Cell Biol*, *24*(6), 2410-2422.
- Meredith, S. D., Levine, P. A., Burns, J. A., Gaffey, M. J., Boyd, J. C., Weiss, L. M., . . . Williams, M. E. (1995). Chromosome 11q13 amplification in head and neck squamous cell carcinoma. Association with poor prognosis. *Arch Otolaryngol Head Neck Surg*, *121*(7), 790-794.
- Michalides, R., van Veelen, N., Hart, A., Loftus, B., Wientjens, E., & Balm, A. (1995). Overexpression of cyclin D1 correlates with recurrence in a group of forty-seven operable squamous cell carcinomas of the head and neck. *Cancer Res*, *55*(5), 975-978.
- Mills, A. A., Zheng, B., Wang, X. J., Vogel, H., Roop, D. R., & Bradley, A. (1999). p63 is a p53 homologue required for limb and epidermal morphogenesis. *Nature*, *398*(6729), 708-713. doi: 10.1038/19531
- Missero, C., Di Cunto, F., Kiyokawa, H., Koff, A., & Dotto, G. P. (1996). The absence of p21Cip1/WAF1 alters keratinocyte growth and differentiation and promotes ras-tumor progression. *Genes Dev*, *10*(23), 3065-3075.
- Mollard, A., Warner, S. L., Call, L. T., Wade, M. L., Bearss, J. J., Verma, A., . . . Bearss, D. J. (2011). Design, Synthesis and Biological Evaluation of a Series of Novel

- Axl Kinase Inhibitors. *ACS Med Chem Lett*, 2(12), 907-912. doi: 10.1021/ml200198x
- Moran-Crusio, K., Reavie, L., Shih, A., Abdel-Wahab, O., Ndiaye-Lobry, D., Lobry, C., . . . Levine, R. L. (2011). Tet2 loss leads to increased hematopoietic stem cell self-renewal and myeloid transformation. *Cancer Cell*, 20(1), 11-24. doi: 10.1016/j.ccr.2011.06.001
- Mudduluru, G., & Allgayer, H. (2008). The human receptor tyrosine kinase Axl gene--promoter characterization and regulation of constitutive expression by Sp1, Sp3 and CpG methylation. *Biosci Rep*, 28(3), 161-176. doi: 10.1042/BSR20080046
- Mudduluru, G., Ceppi, P., Kumarswamy, R., Scagliotti, G. V., Papotti, M., & Allgayer, H. (2011). Regulation of Axl receptor tyrosine kinase expression by miR-34a and miR-199a/b in solid cancer. *Oncogene*, 30(25), 2888-2899. doi: 10.1038/onc.2011.13
- Mudduluru, G., Leupold, J. H., Stroebel, P., & Allgayer, H. (2010). PMA up-regulates the transcription of Axl by AP-1 transcription factor binding to TRE sequences via the MAPK cascade in leukaemia cells. *Biol Cell*, 103(1), 21-33. doi: 10.1042/BC20100094
- Mudduluru, G., Vajkoczy, P., & Allgayer, H. (2010). Myeloid zinc finger 1 induces migration, invasion, and in vivo metastasis through Axl gene expression in solid cancer. *Mol Cancer Res*, 8(2), 159-169. doi: 10.1158/1541-7786.MCR-09-0326
- Munger, K., & Howley, P. M. (2002). Human papillomavirus immortalization and transformation functions. *Virus Res*, 89(2), 213-228.

- Murata, K., Hattori, M., Hirai, N., Shinozuka, Y., Hirata, H., Kageyama, R., . . . Minato, N. (2005). Hes1 directly controls cell proliferation through the transcriptional repression of p27Kip1. *Mol Cell Biol*, 25(10), 4262-4271. doi: 10.1128/MCB.25.10.4262-4271.2005
- Murugan, A. K., Hong, N. T., Fukui, Y., Munirajan, A. K., & Tsuchida, N. (2008). Oncogenic mutations of the PIK3CA gene in head and neck squamous cell carcinomas. *Int J Oncol*, 32(1), 101-111.
- Nagata, M., Noman, A. A., Suzuki, K., Kurita, H., Ohnishi, M., Ohyama, T., . . . Takagi, R. (2013). ITGA3 and ITGB4 expression biomarkers estimate the risks of locoregional and hematogenous dissemination of oral squamous cell carcinoma. *BMC Cancer*, 13, 410. doi: 10.1186/1471-2407-13-410
- Nakada, M., Nambu, E., Furuyama, N., Yoshida, Y., Takino, T., Hayashi, Y., . . . Hamada, J. I. (2013). Integrin alpha3 is overexpressed in glioma stem-like cells and promotes invasion. *Br J Cancer*, 108(12), 2516-2524. doi: 10.1038/bjc.2013.218
- Nakayama, K., Satoh, T., Igari, A., Kageyama, R., & Nishida, E. (2008). FGF induces oscillations of Hes1 expression and Ras/ERK activation. *Curr Biol*, 18(8), R332-334. doi: 10.1016/j.cub.2008.03.013
- Nicolas, M., Wolfer, A., Raj, K., Kummer, J. A., Mill, P., van Noort, M., . . . Radtke, F. (2003). Notch1 functions as a tumor suppressor in mouse skin. *Nat Genet*, 33(3), 416-421. doi: 10.1038/ng1099
- Nielsen-Preiss, S. M., Allen, M. P., Xu, M., Linseman, D. A., Pawlowski, J. E., Bouchard, R. J., . . . Wierman, M. E. (2007). Adhesion-related kinase induction of

migration requires phosphatidylinositol-3-kinase and ras stimulation of rac activity in immortalized gonadotropin-releasing hormone neuronal cells.

Endocrinology, 148(6), 2806-2814. doi: 10.1210/en.2007-0039

O'Bryan, J. P., Frye, R. A., Cogswell, P. C., Neubauer, A., Kitch, B., Prokop, C., . . . Liu, E. T. (1991). axl, a transforming gene isolated from primary human myeloid leukemia cells, encodes a novel receptor tyrosine kinase. *Mol Cell Biol*, 11(10), 5016-5031.

Ohashi, S., Natsuzaka, M., Yashiro-Ohtani, Y., Kalman, R. A., Nakagawa, M., Wu, L., . . . Nakagawa, H. (2010). NOTCH1 and NOTCH3 coordinate esophageal squamous differentiation through a CSL-dependent transcriptional network. *Gastroenterology*, 139(6), 2113-2123. doi: 10.1053/j.gastro.2010.08.040

Ohtsuka, T., Ishibashi, M., Gradwohl, G., Nakanishi, S., Guillemot, F., & Kageyama, R. (1999). Hes1 and Hes5 as notch effectors in mammalian neuronal differentiation. *EMBO J*, 18(8), 2196-2207. doi: 10.1093/emboj/18.8.2196

Okuyama, R., Tagami, H., & Aiba, S. (2008). Notch signaling: its role in epidermal homeostasis and in the pathogenesis of skin diseases. *J Dermatol Sci*, 49(3), 187-194. doi: 10.1016/j.jdermsci.2007.05.017

Paccez, J. D., Vasques, G. J., Correa, R. G., Vasconcellos, J. F., Duncan, K., Gu, X., . . . Zerbini, L. F. (2013). The receptor tyrosine kinase Axl is an essential regulator of prostate cancer proliferation and tumor growth and represents a new therapeutic target. *Oncogene*, 32(6), 689-698. doi: 10.1038/onc.2012.89

- Paccez, J. D., Vogelsang, M., Parker, M. I., & Zerbini, L. F. (2014). The receptor tyrosine kinase Axl in cancer: biological functions and therapeutic implications. *Int J Cancer*, 134(5), 1024-1033. doi: 10.1002/ijc.28246
- Papadimitrakopoulou, V. A., Izzo, J., Mao, L., Keck, J., Hamilton, D., Shin, D. M., . . . Hong, W. K. (2001). Cyclin D1 and p16 alterations in advanced premalignant lesions of the upper aerodigestive tract: role in response to chemoprevention and cancer development. *Clin Cancer Res*, 7(10), 3127-3134.
- Park, B., Nguyen, N. T., Dutt, P., Merdek, K. D., Bashar, M., Sterpetti, P., . . . Toksoz, D. (2002). Association of Lbc Rho guanine nucleotide exchange factor with alpha-catenin-related protein, alpha-catenin/CTNNAL1, supports serum response factor activation. *J Biol Chem*, 277(47), 45361-45370. doi: 10.1074/jbc.M202447200
- Park, J. T., Li, M., Nakayama, K., Mao, T. L., Davidson, B., Zhang, Z., . . . Wang, T. L. (2006). Notch3 gene amplification in ovarian cancer. *Cancer Res*, 66(12), 6312-6318. doi: 10.1158/0008-5472.CAN-05-3610
- Park, M., Yaich, L. E., & Bodmer, R. (1998). Mesodermal cell fate decisions in *Drosophila* are under the control of the lineage genes numb, Notch, and sanpodo. *Mech Dev*, 75(1-2), 117-126.
- Parsa, R., Yang, A., McKeon, F., & Green, H. (1999). Association of p63 with proliferative potential in normal and neoplastic human keratinocytes. *J Invest Dermatol*, 113(6), 1099-1105. doi: 10.1046/j.1523-1747.1999.00780.x
- Pear, W., Tang, Z., DeRocco, S., Allman, D., Hardy, R., Pui, J., . . . Kadesch, T. (1999). Consequences of Notch-mediated inhibition of the transcription factor E47. *Cold Spring Harb Symp Quant Biol*, 64, 33-38.

- Pear, W. S., Aster, J. C., Scott, M. L., Hasserjian, R. P., Soffer, B., Sklar, J., & Baltimore, D. (1996). Exclusive development of T cell neoplasms in mice transplanted with bone marrow expressing activated Notch alleles. *J Exp Med*, 183(5), 2283-2291.
- Pear, W. S., Miller, J. P., Xu, L., Pui, J. C., Soffer, B., Quackenbush, R. C., . . . Baltimore, D. (1998). Efficient and rapid induction of a chronic myelogenous leukemia-like myeloproliferative disease in mice receiving P210 bcr/abl-transduced bone marrow. *Blood*, 92(10), 3780-3792.
- Pellegrini, G., Dellambra, E., Golisano, O., Martinelli, E., Fantozzi, I., Bondanza, S., . . . De Luca, M. (2001). p63 identifies keratinocyte stem cells. *Proc Natl Acad Sci U S A*, 98(6), 3156-3161. doi: 10.1073/pnas.061032098
- Pfister, S., Przemeck, G. K., Gerber, J. K., Beckers, J., Adamski, J., & Hrabe de Angelis, M. (2003). Interaction of the MAGUK family member Acvrin1 and the cytoplasmic domain of the Notch ligand Delta1. *J Mol Biol*, 333(2), 229-235.
- Pickering, C. R., Zhang, J., Yoo, S. Y., Bengtsson, L., Moorthy, S., Neskey, D. M., . . . Frederick, M. J. (2013). Integrative genomic characterization of oral squamous cell carcinoma identifies frequent somatic drivers. *Cancer Discov*, 3(7), 770-781. doi: 10.1158/2159-8290.CD-12-0537
- Pickering, C. R., Zhou, J. H., Lee, J. J., Drummond, J. A., Peng, S. A., Saade, R. E., . . . Frederick, M. J. (2014). Mutational landscape of aggressive cutaneous squamous cell carcinoma. *Clin Cancer Res*, 20(24), 6582-6592. doi: 10.1158/1078-0432.CCR-14-1768
- Poeta, M. L., Manola, J., Goldenberg, D., Forastiere, A., Califano, J. A., Ridge, J. A., . . . Koch, W. M. (2009). The Ligamp TP53 Assay for Detection of Minimal Residual

- Disease in Head and Neck Squamous Cell Carcinoma Surgical Margins. *Clin Cancer Res*, 15(24), 7658-7665. doi: 10.1158/1078-0432.CCR-09-1433
- Prasad, D., Rothlin, C. V., Burrola, P., Burstyn-Cohen, T., Lu, Q., Garcia de Frutos, P., & Lemke, G. (2006). TAM receptor function in the retinal pigment epithelium. *Mol Cell Neurosci*, 33(1), 96-108. doi: 10.1016/j.mcn.2006.06.011
- Pries, R., Witkopf, N., Trenkle, T., Nitsch, S. M., & Wollenberg, B. (2008). Potential stem cell marker CD44 is constitutively expressed in permanent cell lines of head and neck cancer. *In Vivo*, 22(1), 89-92.
- Proia, N. K., Paszkiewicz, G. M., Nasca, M. A., Franke, G. E., & Pauly, J. L. (2006). Smoking and smokeless tobacco-associated human buccal cell mutations and their association with oral cancer--a review. *Cancer Epidemiol Biomarkers Prev*, 15(6), 1061-1077. doi: 10.1158/1055-9965.EPI-05-0983
- Proweller, A., Tu, L., Lepore, J. J., Cheng, L., Lu, M. M., Seykora, J., . . . Parmacek, M. S. (2006). Impaired notch signaling promotes de novo squamous cell carcinoma formation. *Cancer Res*, 66(15), 7438-7444. doi: 10.1158/0008-5472.CAN-06-0793
- Pui, J. C., Allman, D., Xu, L., DeRocco, S., Karnell, F. G., Bakkour, S., . . . Pear, W. S. (1999). Notch1 expression in early lymphopoiesis influences B versus T lineage determination. *Immunity*, 11(3), 299-308.
- Qi, R., An, H., Yu, Y., Zhang, M., Liu, S., Xu, H., . . . Cao, X. (2003). Notch1 signaling inhibits growth of human hepatocellular carcinoma through induction of cell cycle arrest and apoptosis. *Cancer Res*, 63(23), 8323-8329.

- Radtke, F., Wilson, A., Mancini, S. J., & MacDonald, H. R. (2004). Notch regulation of lymphocyte development and function. *Nat Immunol*, 5(3), 247-253. doi: 10.1038/ni1045
- Rampal, R., Luther, K. B., & Haltiwanger, R. S. (2007). Notch signaling in normal and disease States: possible therapies related to glycosylation. *Curr Mol Med*, 7(4), 427-445.
- Ranganathan, P., Weaver, K. L., & Capobianco, A. J. (2011). Notch signalling in solid tumours: a little bit of everything but not all the time. *Nat Rev Cancer*, 11(5), 338-351. doi: 10.1038/nrc3035
- Rangarajan, A., Talora, C., Okuyama, R., Nicolas, M., Mammucari, C., Oh, H., . . . Dotto, G. P. (2001). Notch signaling is a direct determinant of keratinocyte growth arrest and entry into differentiation. *EMBO J*, 20(13), 3427-3436. doi: 10.1093/emboj/20.13.3427
- Rankin, E. B., Fuh, K. C., Taylor, T. E., Krieg, A. J., Musser, M., Yuan, J., . . . Giaccia, A. J. (2010). AXL is an essential factor and therapeutic target for metastatic ovarian cancer. *Cancer Res*, 70(19), 7570-7579. doi: 10.1158/0008-5472.CAN-10-1267
- Reed, A. L., Califano, J., Cairns, P., Westra, W. H., Jones, R. M., Koch, W., . . . Sidransky, D. (1996). High frequency of p16 (CDKN2/MTS-1/INK4A) inactivation in head and neck squamous cell carcinoma. *Cancer Res*, 56(16), 3630-3633.
- Reedijk, M., Odorcic, S., Chang, L., Zhang, H., Miller, N., McCready, D. R., . . . Egan, S. E. (2005). High-level coexpression of JAG1 and NOTCH1 is observed in human

- breast cancer and is associated with poor overall survival. *Cancer Res*, 65(18), 8530-8537. doi: 10.1158/0008-5472.CAN-05-1069
- Reynolds, T. C., Smith, S. D., & Sklar, J. (1987). Analysis of DNA surrounding the breakpoints of chromosomal translocations involving the beta T cell receptor gene in human lymphoblastic neoplasms. *Cell*, 50(1), 107-117.
- Richer, J. K., Jacobsen, B. M., Manning, N. G., Abel, M. G., Wolf, D. M., & Horwitz, K. B. (2002). Differential gene regulation by the two progesterone receptor isoforms in human breast cancer cells. *J Biol Chem*, 277(7), 5209-5218. doi: 10.1074/jbc.M110090200
- Rochlitz, C., Lohri, A., Bacchi, M., Schmidt, M., Nagel, S., Fopp, M., . . . Neubauer, A. (1999). Axl expression is associated with adverse prognosis and with expression of Bcl-2 and CD34 in de novo acute myeloid leukemia (AML): results from a multicenter trial of the Swiss Group for Clinical Cancer Research (SAKK). *Leukemia*, 13(9), 1352-1358.
- Rothenberg, S. M., & Ellisen, L. W. (2012). The molecular pathogenesis of head and neck squamous cell carcinoma. *J Clin Invest*, 122(6), 1951-1957.
- Ruan, G. X., & Kazlauskas, A. (2013). Lactate engages receptor tyrosine kinases Axl, Tie2, and vascular endothelial growth factor receptor 2 to activate phosphoinositide 3-kinase/Akt and promote angiogenesis. *J Biol Chem*, 288(29), 21161-21172. doi: 10.1074/jbc.M113.474619
- Rubin Grandis, J., Melhem, M. F., Gooding, W. E., Day, R., Holst, V. A., Wagener, M. M., . . . Tweardy, D. J. (1998). Levels of TGF- α and EGFR protein in head

- and neck squamous cell carcinoma and patient survival. *J Natl Cancer Inst*, 90(11), 824-832.
- Rudiger, M. (1998). Vinculin and alpha-catenin: shared and unique functions in adherens junctions. *Bioessays*, 20(9), 733-740. doi: 10.1002/(SICI)1521-1878(199809)20:9<733::AID-BIES6>3.0.CO;2-H
- Sano, D., Xie, T. X., Ow, T. J., Zhao, M., Pickering, C. R., Zhou, G., . . . Myers, J. N. (2011). Disruptive TP53 mutation is associated with aggressive disease characteristics in an orthotopic murine model of oral tongue cancer. *Clin Cancer Res*, 17(21), 6658-6670. doi: 10.1158/1078-0432.CCR-11-0046
- Santolini, E., Puri, C., Salcini, A. E., Gagliani, M. C., Pelicci, P. G., Tacchetti, C., & Di Fiore, P. P. (2000). Numb is an endocytic protein. *J Cell Biol*, 151(6), 1345-1352.
- Sasai, Y., Kageyama, R., Tagawa, Y., Shigemoto, R., & Nakanishi, S. (1992). Two mammalian helix-loop-helix factors structurally related to Drosophila hairy and Enhancer of split. *Genes Dev*, 6(12B), 2620-2634.
- Sasaki, T., Knyazev, P. G., Clout, N. J., Cheburkin, Y., Gohring, W., Ulrich, A., . . . Hohenester, E. (2006). Structural basis for Gas6-Axl signalling. *EMBO J*, 25(1), 80-87. doi: 10.1038/sj.emboj.7600912
- Schroeder, T., & Just, U. (2000). mNotch1 signaling reduces proliferation of myeloid progenitor cells by altering cell-cycle kinetics. *Exp Hematol*, 28(11), 1206-1213.
- Schultz, D. C., Vanderveer, L., Buetow, K. H., Boente, M. P., Ozols, R. F., Hamilton, T. C., & Godwin, A. K. (1995). Characterization of chromosome 9 in human ovarian neoplasia identifies frequent genetic imbalance on 9q and rare alterations involving 9p, including CDKN2. *Cancer Res*, 55(10), 2150-2157.

- Shalem, O., Sanjana, N. E., Hartenian, E., Shi, X., Scott, D. A., Mikkelsen, T. S., . . . Zhang, F. (2014). Genome-scale CRISPR-Cas9 knockout screening in human cells. *Science*, 343(6166), 84-87. doi: 10.1126/science.1247005
- Shieh, Y. S., Lai, C. Y., Kao, Y. R., Shiah, S. G., Chu, Y. W., Lee, H. S., & Wu, C. W. (2005). Expression of axl in lung adenocarcinoma and correlation with tumor progression. *Neoplasia*, 7(12), 1058-1064.
- Shiozawa, Y., Pedersen, E. A., Patel, L. R., Ziegler, A. M., Havens, A. M., Jung, Y., . . . Taichman, R. S. (2010). GAS6/AXL axis regulates prostate cancer invasion, proliferation, and survival in the bone marrow niche. *Neoplasia*, 12(2), 116-127.
- Slaughter, D. P., Southwick, H. W., & Smejkal, W. (1953). Field cancerization in oral stratified squamous epithelium; clinical implications of multicentric origin. *Cancer*, 6(5), 963-968.
- Slebos, R. J., Yi, Y., Ely, K., Carter, J., Evjen, A., Zhang, X., . . . Chung, C. H. (2006). Gene expression differences associated with human papillomavirus status in head and neck squamous cell carcinoma. *Clin Cancer Res*, 12(3 Pt 1), 701-709. doi: 10.1158/1078-0432.CCR-05-2017
- Song, X., Wang, H., Logsdon, C. D., Rashid, A., Fleming, J. B., Abbruzzese, J. L., . . . Wang, H. (2011). Overexpression of receptor tyrosine kinase Axl promotes tumor cell invasion and survival in pancreatic ductal adenocarcinoma. *Cancer*, 117(4), 734-743. doi: 10.1002/cncr.25483
- Song, X., Xia, R., Li, J., Long, Z., Ren, H., Chen, W., & Mao, L. (2014). Common and complex Notch1 mutations in Chinese oral squamous cell carcinoma. *Clin Cancer Res*, 20(3), 701-710. doi: 10.1158/1078-0432.CCR-13-1050

- Sriuranpong, V., Borges, M. W., Ravi, R. K., Arnold, D. R., Nelkin, B. D., Baylin, S. B., & Ball, D. W. (2001). Notch signaling induces cell cycle arrest in small cell lung cancer cells. *Cancer Res*, 61(7), 3200-3205.
- Stanley, P. (2007). Regulation of Notch signaling by glycosylation. *Curr Opin Struct Biol*, 17(5), 530-535. doi: 10.1016/j.sbi.2007.09.007
- Stitt, T. N., Conn, G., Gore, M., Lai, C., Bruno, J., Radziejewski, C., . . . et al. (1995). The anticoagulation factor protein S and its relative, Gas6, are ligands for the Tyro 3/Axl family of receptor tyrosine kinases. *Cell*, 80(4), 661-670.
- Stransky, N., Egloff, A. M., Tward, A. D., Kostic, A. D., Cibulskis, K., Sivachenko, A., . . . Grandis, J. R. (2011). The mutational landscape of head and neck squamous cell carcinoma. *Science*, 333(6046), 1157-1160. doi: 10.1126/science.1208130
- Sun, W., Gaykalova, D. A., Ochs, M. F., Mambo, E., Arnaoutakis, D., Liu, Y., . . . Califano, J. A. (2014). Activation of the NOTCH pathway in head and neck cancer. *Cancer Res*, 74(4), 1091-1104. doi: 10.1158/0008-5472.CAN-13-1259
- Takata, T., & Ishikawa, F. (2003). Human Sir2-related protein SIRT1 associates with the bHLH repressors HES1 and HEY2 and is involved in HES1- and HEY2-mediated transcriptional repression. *Biochem Biophys Res Commun*, 301(1), 250-257.
- Talora, C., Sgroi, D. C., Crum, C. P., & Dotto, G. P. (2002). Specific down-modulation of Notch1 signaling in cervical cancer cells is required for sustained HPV-E6/E7 expression and late steps of malignant transformation. *Genes Dev*, 16(17), 2252-2263. doi: 10.1101/gad.988902
- Tan, E. L., Selvaratnam, G., Kananathan, R., & Sam, C. K. (2006). Quantification of Epstein-Barr virus DNA load, interleukin-6, interleukin-10, transforming growth

- factor-beta1 and stem cell factor in plasma of patients with nasopharyngeal carcinoma. *BMC Cancer*, 6, 227. doi: 10.1186/1471-2407-6-227
- TCGA Releases Head and Neck Cancer Data. (2015). *Cancer Discov*, 5(4), 340-341. doi: 10.1158/2159-8290.CD-NB2015-024
- Thariat, J., Vignot, S., Lapierre, A., Falk, A. T., Guigay, J., Van Obberghen-Schilling, E., & Milano, G. (2015). Integrating genomics in head and neck cancer treatment: Promises and pitfalls. *Crit Rev Oncol Hematol*, 95(3), 397-406. doi: 10.1016/j.critrevonc.2015.03.005
- Thomas, M. M., Zhang, Y., Mathew, E., Kane, K. T., Maillard, I., & Pasca di Magliano, M. (2014). Epithelial Notch signaling is a limiting step for pancreatic carcinogenesis. *BMC Cancer*, 14, 862. doi: 10.1186/1471-2407-14-862
- Thomson, J. A., Itskovitz-Eldor, J., Shapiro, S. S., Waknitz, M. A., Swiergiel, J. J., Marshall, V. S., & Jones, J. M. (1998). Embryonic stem cell lines derived from human blastocysts. *Science*, 282(5391), 1145-1147.
- Torre, L. A., Bray, F., Siegel, R. L., Ferlay, J., Lortet-Tieulent, J., & Jemal, A. (2015). Global cancer statistics, 2012. *CA Cancer J Clin*, 65(2), 87-108. doi: 10.3322/caac.21262
- Trizna, Z., & Schantz, S. P. (1992). Hereditary and environmental factors associated with risk and progression of head and neck cancer. *Otolaryngol Clin North Am*, 25(5), 1089-1103.
- Tsukumo, S., Hirose, K., Maekawa, Y., Kishihara, K., & Yasutomo, K. (2006). Lunatic fringe controls T cell differentiation through modulating notch signaling. *J Immunol*, 177(12), 8365-8371.

- Tuyns, A. J., Esteve, J., Raymond, L., Berrino, F., Benhamou, E., Blanchet, F., . . . et al. (1988). Cancer of the larynx/hypopharynx, tobacco and alcohol: IARC international case-control study in Turin and Varese (Italy), Zaragoza and Navarra (Spain), Geneva (Switzerland) and Calvados (France). *Int J Cancer*, 41(4), 483-491.
- Uemura, T., Shepherd, S., Ackerman, L., Jan, L. Y., & Jan, Y. N. (1989). numb, a gene required in determination of cell fate during sensory organ formation in *Drosophila* embryos. *Cell*, 58(2), 349-360.
- Valverde, P. (2005). Effects of Gas6 and hydrogen peroxide in Axl ubiquitination and downregulation. *Biochem Biophys Res Commun*, 333(1), 180-185. doi: 10.1016/j.bbrc.2005.05.086
- van der Riet, P., Nawroz, H., Hruban, R. H., Corio, R., Tokino, K., Koch, W., & Sidransky, D. (1994). Frequent loss of chromosome 9p21-22 early in head and neck cancer progression. *Cancer Res*, 54(5), 1156-1158.
- Vaughan, C. A., Singh, S., Windle, B., Yeudall, W. A., Frum, R., Grossman, S. R., . . . Deb, S. (2012). Gain-of-Function Activity of Mutant p53 in Lung Cancer through Up-Regulation of Receptor Protein Tyrosine Kinase Axl. *Genes Cancer*, 3(7-8), 491-502. doi: 10.1177/1947601912462719
- Viatour, P., Ehmer, U., Saddic, L. A., Dorrell, C., Andersen, J. B., Lin, C., . . . Sage, J. (2011). Notch signaling inhibits hepatocellular carcinoma following inactivation of the RB pathway. *J Exp Med*, 208(10), 1963-1976. doi: 10.1084/jem.20110198

- Vilimas, T., Mascarenhas, J., Palomero, T., Mandal, M., Buonamici, S., Meng, F., . . . Aifantis, I. (2007). Targeting the NF-kappaB signaling pathway in Notch1-induced T-cell leukemia. *Nat Med*, 13(1), 70-77. doi: 10.1038/nm1524
- Visan, I., Tan, J. B., Yuan, J. S., Harper, J. A., Koch, U., & Guidos, C. J. (2006). Regulation of T lymphopoiesis by Notch1 and Lunatic fringe-mediated competition for intrathymic niches. *Nat Immunol*, 7(6), 634-643. doi: 10.1038/nl1345
- Vuoriluoto, K., Haugen, H., Kiviluoto, S., Mpindi, J. P., Nevo, J., Gjerdrum, C., . . . Ivaska, J. (2011). Vimentin regulates EMT induction by Slug and oncogenic H-Ras and migration by governing Axl expression in breast cancer. *Oncogene*, 30(12), 1436-1448. doi: 10.1038/onc.2010.509
- Wang, X., Chen, X., Fang, J., & Yang, C. (2013). Overexpression of both VEGF-A and VEGF-C in gastric cancer correlates with prognosis, and silencing of both is effective to inhibit cancer growth. *Int J Clin Exp Pathol*, 6(4), 586-597.
- Watt, F. M., Estrach, S., & Ambler, C. A. (2008). Epidermal Notch signalling: differentiation, cancer and adhesion. *Curr Opin Cell Biol*, 20(2), 171-179. doi: 10.1016/j.ceb.2008.01.010
- Weber, D., Wiese, C., & Gessler, M. (2014). Hey bHLH transcription factors. *Curr Top Dev Biol*, 110, 285-315. doi: 10.1016/B978-0-12-405943-6.00008-7
- Weijzen, S., Rizzo, P., Braid, M., Vaishnav, R., Jonkheer, S. M., Zlobin, A., . . . Miele, L. (2002). Activation of Notch-1 signaling maintains the neoplastic phenotype in human Ras-transformed cells. *Nat Med*, 8(9), 979-986. doi: 10.1038/nm754

- Weng, A. P., Ferrando, A. A., Lee, W., Morris, J. P. t., Silverman, L. B., Sanchez-Irizarry, C., . . . Aster, J. C. (2004). Activating mutations of NOTCH1 in human T cell acute lymphoblastic leukemia. *Science*, 306(5694), 269-271. doi: 10.1126/science.1102160
- Wiesner, C., Winsauer, G., Resch, U., Hoeth, M., Schmid, J. A., van Hengel, J., . . . de Martin, R. (2008). Alpha-catulin, a Rho signalling component, can regulate NF-kappaB through binding to IKK-beta, and confers resistance to apoptosis. *Oncogene*, 27(15), 2159-2169. doi: 10.1038/sj.onc.1210863
- Wimmel, A., Glitz, D., Kraus, A., Roeder, J., & Schuermann, M. (2001). Axl receptor tyrosine kinase expression in human lung cancer cell lines correlates with cellular adhesion. *Eur J Cancer*, 37(17), 2264-2274.
- Wolfe, M. S., & Kopan, R. (2004). Intramembrane proteolysis: theme and variations. *Science*, 305(5687), 1119-1123. doi: 10.1126/science.1096187
- Wu, J., & Bresnick, E. H. (2007). Bare rudiments of notch signaling: how receptor levels are regulated. *Trends Biochem Sci*, 32(10), 477-485. doi: 10.1016/j.tibs.2007.09.002
- Xiang, Y., Qin, X. Q., Liu, H. J., Tan, Y. R., Liu, C., & Liu, C. X. (2012). Identification of transcription factors regulating CTNNAL1 expression in human bronchial epithelial cells. *PLoS One*, 7(2), e31158. doi: 10.1371/journal.pone.0031158
- Yamamoto, S., Charng, W. L., & Bellen, H. J. (2010). Endocytosis and intracellular trafficking of Notch and its ligands. *Curr Top Dev Biol*, 92, 165-200. doi: 10.1016/S0070-2153(10)92005-X

- Yan, B., Raben, N., & Plotz, P. H. (2002). Hes-1, a known transcriptional repressor, acts as a transcriptional activator for the human acid alpha-glucosidase gene in human fibroblast cells. *Biochem Biophys Res Commun*, 291(3), 582-587. doi: 10.1006/bbrc.2002.6483
- Yang, A., Schweitzer, R., Sun, D., Kaghad, M., Walker, N., Bronson, R. T., . . . McKeon, F. (1999). p63 is essential for regenerative proliferation in limb, craniofacial and epithelial development. *Nature*, 398(6729), 714-718. doi: 10.1038/19539
- Ye, X., Li, Y., Stawicki, S., Couto, S., Eastham-Anderson, J., Kallop, D., . . . Pei, L. (2010). An anti-Axl monoclonal antibody attenuates xenograft tumor growth and enhances the effect of multiple anticancer therapies. *Oncogene*, 29(38), 5254-5264. doi: 10.1038/onc.2010.268
- Yoshiura, S., Ohtsuka, T., Takenaka, Y., Nagahara, H., Yoshikawa, K., & Kageyama, R. (2007). Ultradian oscillations of Stat, Smad, and Hes1 expression in response to serum. *Proc Natl Acad Sci U S A*, 104(27), 11292-11297. doi: 10.1073/pnas.0701837104
- Yu, X., Alder, J. K., Chun, J. H., Friedman, A. D., Heimfeld, S., Cheng, L., & Civin, C. I. (2006). HES1 inhibits cycling of hematopoietic progenitor cells via DNA binding. *Stem Cells*, 24(4), 876-888. doi: 10.1634/stemcells.2005-0598
- Zage, P. E., Nolo, R., Fang, W., Stewart, J., Garcia-Manero, G., & Zweidler-McKay, P. A. (2012). Notch pathway activation induces neuroblastoma tumor cell growth arrest. *Pediatr Blood Cancer*, 58(5), 682-689. doi: 10.1002/pbc.23202
- Zhang, J. S., Nelson, M., Wang, L., Liu, W., Qian, C. P., Shridhar, V., . . . Smith, D. I. (1998). Identification and chromosomal localization of CTNNAL1, a novel

- protein homologous to alpha-catenin. *Genomics*, 54(1), 149-154. doi: 10.1006/geno.1998.5458
- Zhang, Y. X., Knyazev, P. G., Cheburkin, Y. V., Sharma, K., Knyazev, Y. P., Orfi, L., . . . Ullrich, A. (2008). AXL is a potential target for therapeutic intervention in breast cancer progression. *Cancer Res*, 68(6), 1905-1915. doi: 10.1158/0008-5472.CAN-07-2661
- Zhang, Z., Lee, J. C., Lin, L., Olivas, V., Au, V., LaFramboise, T., . . . Bivona, T. G. (2012). Activation of the AXL kinase causes resistance to EGFR-targeted therapy in lung cancer. *Nat Genet*, 44(8), 852-860. doi: 10.1038/ng.2330
- Zhang, Z., Yang, X. F., Huang, K. Q., Ren, L., Zhao, S., Gou, W. F., . . . Zheng, H. C. (2015). The upregulated alpha-catulin expression was involved in head-neck squamous cell carcinogenesis by promoting proliferation, migration, invasion, and epithelial to mesenchymal transition. *Tumour Biol*. doi: 10.1007/s13277-015-3901-5
- Zhao, M., Sano, D., Pickering, C. R., Jasser, S. A., Henderson, Y. C., Clayman, G. L., . . . Myers, J. N. (2011). Assembly and initial characterization of a panel of 85 genomically validated cell lines from diverse head and neck tumor sites. *Clin Cancer Res*, 17(23), 7248-7264. doi: 10.1158/1078-0432.CCR-11-0690
- Zhu, W. G., Srinivasan, K., Dai, Z., Duan, W., Druhan, L. J., Ding, H., . . . Otterson, G. A. (2003). Methylation of adjacent CpG sites affects Sp1/Sp3 binding and activity in the p21(Cip1) promoter. *Mol Cell Biol*, 23(12), 4056-4065.
- Zweidler-McKay, P. A., He, Y., Xu, L., Rodriguez, C. G., Karnell, F. G., Carpenter, A. C., . . . Pear, W. S. (2005). Notch signaling is a potent inducer of growth arrest

and apoptosis in a wide range of B-cell malignancies. *Blood*, 106(12), 3898-3906.

doi: 10.1182/blood-2005-01-0355

Vita

Shhyam Moorthy was born in India to Mr. Srinivasan Moorthy and Mrs. Padma Moorthy on May 7th, 1988. He grew up in Dubai, U.A.E, where he completed his schooling at the Indian High School in 2006. He then went to college at Louisiana State University, Baton Rouge, LA where he majored in Biological Sciences and minored in Chemistry and Math. At LSU, he pursued his Undergraduate Honors thesis awarded by the Howard Hughes Medical Institute (HHMI) under the mentorship of Dr. Steven Hand. He also pursued a summer internship awarded by HHMI at the University of Florida, Gainesville, FL under the mentorship of Dr. David Julian. He graduated from the LSU *Honors* College in 2010 with a *Cum Laude* after completion of his Undergraduate Honors thesis titled “The role of trehalose in conferring freeze tolerance to human hepatoma cells”. He then entered The University of Texas Graduate School of Biomedical Sciences, Houston, TX in August 2010. He joined the lab of Dr. Jeffrey Myers in May 2011 where he investigated the role of NOTCH signaling in suppressing tumor growth of Head and Neck Squamous Cell Carcinoma (HNSCC).